Development of Ca-based catalytic systems for the selective polymerization of glycerol

Negisa Ebadi Pour

CENTRALE LILLE

THÈSE

Présentée en vue

d'obtenir le grade de

DOCTEUR

En

Spécialité : Molécules et Matière Condensée

Par

Negisa EBADI POUR

DOCTORAT DÉLIVRÉ PAR CENTRALE LILLE

Development of Ca-based catalytic systems for the selective polymerization of glycerol

Développement de systèmes catalytiques à base de Ca pour la polymérisation sélective de glycérol

Soutenue **le 8 Novembre 2021** devant le jury d'examen :

Président :	**Véronique NARDELLO-RATAJ**	Professeure, Centrale Lille
Rapporteur :	**Sandrine BOUQUILLON**	Professeure, Université de Reims Champagne-Ardenne
Rapporteur :	**Pedro MAIRELES-TORRES**	Professeur, Université de Malaga
Membre :	**Karine DE OLIVEIRA VIGIER**	Professeure, Université de Poitiers
Membre :	**Benjamin KATRYNIOK**	Maître de Conférences, Centrale Lille
Directeur de thèse :	**Sébastien PAUL**	Professeur, Centrale Lille
Co-directeur :	**Franck DUMEIGNIL**	Professeur, Université de Lille

Thèse préparée dans le laboratoire UCCS

Ecole Doctorale SMRE

centralelille

Acknowledgements

Firstly I would like to thank my supervisors Prof. Sébastien Paul and Prof. Franck Dumeignil for having given me a chance to do my doctoral studies in their group. They gave me tremendous academic support, constant encouragement and kept me on the right track during the entire period of my PhD project.

I am also grateful to Dr. Benjamin Katryniok for his invaluable support, suggestion and discussion that we have shared during the period of my PhD project.

Special thanks to Dr. Christophe Flahaut, Dr. Egon Heuson and Dr. Barbara Deracinois who helped me to learn more about the ESI-MS and MALDI.

I would like to thank our technical staff (engineers and technicians), Joelle Thriot who kindly helped me to do XRD, IR and ICP analysis; Svetlana Heyte for helping me to use SPR reactor; Johann Jezequel who performed the BET analyses and kindly helped me whenever I faced technical problems.

I am thankful to Olivier Gardoll for helping me to perform the TGA/DTA and Pardis Simon who performed the XPS analyses.

I wish to extend a warm thanks to the committee members: Prof. Sandrine Bouquillon, Prof. Pedro Maireles-Torres, Prof. Karine De Oliveira Vigier and Prof. Véronique Nardello-Rataj for the great suggestions and scientific discussions.

I would like to thank all my great colleagues in UCCS: Li, Flora, Beatriz, Antoine, Roxane, Karen, Nathalie and … for their help, support and friendship which made my research a rewarding experience.

Last, but far from least, thank you to my family and friends for their sincere love and support.

SYMBOLS AND ABBREVIATIONS

BET	Brunauer-Emmett-Teller
CaDG	Calcium diglyceroxide
CaG	Calcium mono glyceroxide
ESI-MS	Electrospray ionization mass spectrometry
GC	Gas chromatography
HAp	Hydroxyapatite
HAp-S	Stoichiometric hydroxyapatite
HAp-D	Deficient hydroxyapatite
HAp-R	Ca-rich hydroxyapatite
HAp-CP	P123-hydroxyapatite
HAp-CO	Carbonated hydroxyapatite
HBPG	Hyperbranched polyglycerol
HPLC	High performance liquid chromatography
ICP-OES	Inductively coupled plasma-optic emission spectroscopy
IR	Infrared spectroscopy
MALDI	Matrix-assisted laser desorption ionization
MAS	Magic angle spinning
PG	Polyglycerol
PG2	Diglycerol
PG3	Triglycerol
RI	Refractive index
SEC	Size exclusion chromatography
SEM	Scanning electron microscopy
SS NMR	Solid state nuclear magnetic resonance
TGA-DSC	Thermal Gravimetric Analysis-Differential Scanning Calorimetry
XPS	X-ray Photoelectron Spectroscopy
XRD	X-Ray diffraction patterns

Contents

List of Figures

List of Schemes

List of Tables

Abstract

Polyglycerols (PGs) are biocompatible and highly functional polyols with a wide range of applications in many industries. About 50% of the demand in PGs concerns di- and tri-glycerol (PG2-3), mainly for cosmetics, and the other 50% tetra- to deca-glycerol (PG4-10), mainly for food industry.

The increase of the demand for bio-based PGs encourages researchers to develop new catalytic systems for glycerol polymerization. In the last two decades, much attention was paid to alkaline earth oxides-based catalysts, particularly Ca-based catalysts, due to their high catalytic performances, their wide availability and the absence of any toxicity. However, Ca-based catalysts showed, up to now, a moderate selectivity to PG2-3 or to PG4-10. Another issue for heterogenous catalytic systems, which is unsolved so far, is their instability due to partial dissolution in the reaction medium. Thus, the purpose of this PhD is to develop Ca-based heterogeneous catalysts which are stable, highly active to convert glycerol and highly selective, either to PG2-3 or to PG4-10.

First, we investigated for this reaction calcium diglyceroxide (CaDG) and other Ca-based catalysts including CaO, $Ca(OH)_2$ and $CaCO_3$. The catalysts were analyzed by XRD, solid-state ^{13}C-NMR and TGA-DSC analyses. XRD evidenced the presence of calcium glycerolate (CaG) in the spent catalysts when starting from CaO, $Ca(OH)_2$ and CaDG. This was corroborated by TGA-DSC results. Further, the ^{13}C-NMR results showed that CaG is a mixture of its linear form $Ca(C_3H_7O_3)$ and its cyclic-branched form $Ca(C_3H_6O_3)$. As a main outcome, we showed that CaG is the actual *solid* active phase, which is formed *in situ* from CaO, $Ca(OH)_2$ or CaDG playing the role of catalyst precursors. Two mechanisms for the CaG formation were proposed: *a)* the dissolution of CaO and $Ca(OH)_2$, the formation of CaG and its precipitation followed by crystallization and *b)* the formation of CaDG and its gradual decomposition to CaG.

Since CaDG is directly converted to CaG and a glyceroxide ion during the reaction, the effect of operating conditions on the catalytic performances, including the temperature, the amount of CaDG used, the reaction time and the presence of water, was investigated. The reaction products were analysed by electron spray ionization-mass spectrometry (ESI-MS). CaDG showed the highest selectivity to PG4-10 (84%) at a glycerol conversion of 70%, at 245 °C in the presence of 3.5 mol.% of catalyst after 22 h of reaction. However, the ICP analysis of the reaction medium showed that 70 % of CaDG was dissolved in the liquid phase under these conditions. Still, considering the low cost, the absence of any toxicity and the high selectivity to PG4-10 of CaDG, this species is considered as a promising catalyst for glycerol polymerization.

To try to develop a selective catalytic system for PG2-3, several calcium hydroxyapatite (HAp)-based catalysts have been synthetized, characterized and tested for glycerol polymerization reaction. These catalysts were divided in three groups; *i)* Ca-based HAps including Ca-deficient, stochiometric

and Ca-rich HAps, *ii)* HAp enriched with CaO (CaO supported on HAp) and *iii)* carbonated HAp. The catalysts were characterized by XRD, IR, XPS, TGA-DSC and ICP-OES analyses. Among them the stochiometric HAp with a Ca/P ratio of 1.67 was highly selective to PG3 (100%) at 15% glycerol conversion. Moreover, rich-HAp with a Ca/P ratio of 1.78 and 5wt.% CaO/HAp catalysts also exhibited a high selectivity to PG2-3, 88% (at 27% conversion) and 67 % (at 23% conversion), respectively, at 245 °C after 8 h of reaction in the presence 0.5 mol.% of catalyst. Most importantly, these heterogeneous catalysts were highly stable under reaction conditions as shown by ICP-OES analyses (less than 5 % of Ca leaching). In contrast, the carbonated-HAps showed a very low catalytic activity (below 6% of glycerol conversion). Finally, we proved that HAps can be deactivated by the presence of water and polymers.

Résumé en français

Ces dernières années, pour faire face aux problèmes environnementaux, la production de biodiesel a été encouragée avec, pour conséquence, une augmentation significative de la disponibilité du glycérol comme coproduit. Par conséquent, la valorisation du glycérol pourrait contribuer à soutenir l'économie de la chaîne de valeur du biodiesel à condition que des produits chimiques à haute valeur ajoutée tels que les polyglycérols puissent être produits.

En effet, les polyglycérols (PGs) sont des polyols biocompatibles présentant de nombreuses applications industrielles, notamment dans les secteurs cosmétique, biomédical et alimentaire. Environ 50 % de la demande concerne le di- et le tri-glycérol (PG2-3), principalement pour les cosmétiques, et les autres 50 % la fraction tétra- à déca-glycérol (PG4-10), principalement pour l'industrie alimentaire.

Cependant, les méthodes industrielles actuelles de production de PGs, comme l'hydrolyse basique de l'épichlorhydrine, présentent de nombreux inconvénients, tels que l'utilisation de matières premières toxiques et cancérigènes, une faible sélectivité conduisant à de nombreux sous-produits. Par ailleurs, l'utilisation d'un catalyseur homogène alcalin fort dans ces procédés pour convertir directement le glycérol en PGs, présente également plusieurs inconvénients : la réaction rapide entraîne une difficulté à contrôler le degré de polymérisation et le catalyseur homogène ne peut pas être récupéré du milieu réactionnel.

Ces inconvénients couplés à la croissance de la demande en PGs biosourcés incitent les chercheurs à développer de nouveaux catalyseurs hétérogènes pour la polymérisation du glycérol. Au cours des deux dernières décennies, une grande attention a été accordée aux systèmes à base de Ca, en raison de leurs bonnes performances catalytiques, de leur grande disponibilité, de leur faible coût et de l'absence de toxicité. Toutefois, ces catalyseurs présentent jusqu'alors une sélectivité modérée. Un autre problème des catalyseurs hétérogènes, non résolu à ce jour, est lié à leur instabilité due à une dissolution partielle dans le milieu réactionnel. Outre le catalyseur, les conditions opérationnelles telles que la température, la quantité de catalyseur, l'atmosphère et le temps de réaction jouent un rôle très important sur la conversion du glycérol et le degré de polymérisation.

Ainsi, l'objectif de cette thèse est de développer un catalyseur hétérogène à base de Ca qui soit stable, hautement actif pour convertir le glycérol et hautement sélectif, soit en PG2-3, soit en PG4-10 ; et d'optimiser les conditions de sa mise en œuvre en réaction.

La polymérisation du glycérol peut conduire à des mélanges complexes de PGs contenant des isomères linéaires, ramifiés et cycliques. L'augmentation du degré de polymérisation conduit à des mélanges de plus en plus complexes. Ainsi, la caractérisation et l'analyse de tels mélanges, même si elles sont cruciales pour évaluer les performances des procédés catalytiques étudiés, sont très difficiles et nécessitent généralement la combinaison de plusieurs techniques de séparation et d'analyse. Ainsi,

un autre objectif de cette thèse est d'améliorer les techniques d'analyse des PGs.

Pour identifier la meilleure méthode analytique pour caractériser les PGs, plusieurs techniques ont été utilisées, telles que la chromatographie liquide à haute performance (HPLC), la chromatographie d'exclusion stérique (SEC), la résonance magnétique nucléaire (RMN), l'ionisation par électronébuliseur couplée à la spectrométrie de masse (ESI-MS) et la désorption-ionisation laser assistée par matrice (MALDI-ToF). Les résultats ont révélé que la séparation de tous les PGs n'est pas possible par les méthodes de chromatographie liquide, ni par HPLC, ni par analyse SEC. De plus, la RMN n'est pas informative dans le cas d'un mélange de PGs. L'ESI-MS, en tant que technique d'ionisation douce, a confirmé que les échantillons de PGs sont un mélange de PGs non-cycliques (linéaires ou ramifiés) et cycliques, sur la base de la masse exacte du polymère, alors que, le MALDI-ToF, n'est pas capable de détecter le polymère en dessous du pentaglycérol (PG5). Ainsi, la technique ESI-MS a été choisie comme la meilleure technique analytique pour identifier les PGs.

Nous avons d'abord étudié en tant que catalyseurs pour la réaction de polymérisation du glycérol le diglycéroxyde de Ca (CaDG), CaO, $Ca(OH)_2$ et $CaCO_3$. Les catalyseurs ont été analysés par DRX, RMN du ^{13}C à l'état solide et ATG-ACD. La DRX a montré la présence, après test, de glycérolate de calcium (CaG) dans les catalyseurs dérivés de CaO, $Ca(OH)_2$ et de CaDG. Ceci a été corroboré par les résultats des analyses ATG-ACD. La RMN du ^{13}C a montré que le CaG est un mélange de ses formes linéaire $Ca(C_3H_7O_3)$ et cyclique ramifiée $Ca(C_3H_6O_3)$. Le CaG est la phase active solide réelle qui est formée *in situ* à partir de CaO, de $Ca(OH)_2$ ou de CaDG, précurseurs du catalyseur. Deux mécanismes de formation de CaG sont proposés : a) dissolution de CaO et de $Ca(OH)_2$, suivie de la formation de CaG et de sa précipitation/cristallisation et b) formation de CaDG et décomposition progressive en CaG.

Dans le premier mécanisme, le CaG est formé à partir de CaO ou $Ca(OH)_2$ par une dissolution du précurseur, sa conversion en phase liquide suivie d'une étape de précipitation qui permet au CaG de cristalliser finalement. Dans le deuxième mécanisme proposé, le CaDG commence à être formé lorsque le CaO et le glycérol sont chauffés à 80 °C. Ensuite, une augmentation supplémentaire de la température du mélange réactionnel jusqu'à 180 °C provoque la décomposition du CaDG en CaG, Dans les deux mécanismes, les ions Ca et glycéroxyde sont formés comme intermédiaires et cependant, il faut noter que les ions CaG et glycéroxyde participent tous à la formation du polyglycérols.

CaDG étant directement converti en CaG et en ion glycéroxyde pendant la réaction, il peut promouvoir la formation des PGs. Ainsi, l'effet sur les performances catalytiques de la température de réaction, la quantité de catalyseur, le temps de réaction et la présence d'eau, a été étudié. Les produits de la réaction ont été analysés par spectrométrie de masse (ESI-MS). Le CaDG a montré la plus grande sélectivité en PG4-10 (84%) à 70% de conversion du glycérol, à 245 °C après 22 h de réaction

en présence de 3.5 mol.% de catalyseur. Cependant, l'analyse ICP du milieu réactionnel a montré que 70% du CaDG était alors en phase liquide. Néanmoins, en raison du faible coût, de l'absence de toxicité et de la très haute sélectivité en PG4-10, le CaDG peut être considéré comme un catalyseur prometteur pour la polymérisation du glycérol.

Enfin, pour tenter de développer un système sélectif pour la production de PG2-3, des catalyseurs à base d'hydroxyapatite de calcium (HAp) ont été synthétisés, caractérisés et testés. En effet, les hydroxyapatites présentent des propriétés intéressantes, telles qu'une grande stabilité thermique, une solubilité dans l'eau très limitée et une insolubilité dans les solutions alcalines. Ils sont divisés en trois groupes : *i)* les HAp déficientes (HAp-D), stochiométriques (HAp-S) et riches en Ca (HAp-R), *ii)* les HAp enrichies en CaO (CaO supporté sur HAp) et *iii)* les HAp carbonatées. Tous ces solides ont été caractérisés par DRX, IR, XPS, ATG-ACD et ICP-OES.

Pour le premier groupe (HAp-S, HAp-D et HAp-R), la formation de structures d'hydroxyapatite de calcium est confirmée et aucune autre phase cristalline n'a été observée par XRD. De plus, les spectres IR ont montré les pics caractéristiques de l'hydroxyapatite incluant les groupes hydroxyle et phosphate pour tous les HAps. En plus de cela, la présence de groupes carbonés a été observée. Les spectres XPS pour HAp-D, HAp-S et HAp-R ont confirmé que moins de Ca était exposé à la surface de ces catalyseurs calcinés par rapport à leur coeur, ce qui peut être dû à la formation de carbonate. En termes d'activité catalytique, l'HAp stochiométrique (rapport Ca/P=1,67) s'est montrée hautement sélective en PG3 (100%) à 15% de conversion du glycérol.

Pour le deuxième groupe, les résultats de la XRD ont confirmé la présence de CaO dans les catalyseurs CaO/HAp à 10 et 30 % en poids, tandis que pour le catalyseur CaO/HAp à 5 % en poids, seuls les pics caractéristiques de l'hydroxyapatite ont été observés. De plus, l'analyse élémentaire de ces catalyseurs réalisée par ICP-OES a confirmé des rapports Ca/P plus élevés qu'attendus en théorie. L'HAp riche en Ca (rapport Ca/P=1,78) et le catalyseur à 5% poids de CaO sur HAp ont présenté une sélectivité élevée en PG2-3 à 245 °C après 8 h en présence de 0,5% molaire de catalyseur : 88 % et 67% (à 27% et 23% de conversion), respectivement. Plus important, ces catalyseurs sont très stables dans les conditions de réaction (moins de 5% de lixiviation du Ca).

Au contraire, les HAps carbonatées ont une très faible activité. Ainsi, sur la base de nos résultats, nous avons proposé et examiné trois mécanismes qui pourraient expliquer la désactivation du catalyseur : i) le dépôt physique de PGs à sa surface, ii) la désactivation par l'eau et iii) la chimisorption des polymères PGs sur les sites catalytiques. Finalement, les résultats ont suggéré que les HAps étaient principalement désactivés par la présence de PGs et d'eau pendant la réaction de polymérisation du glycérol.

General introduction

In the last years, in view of the environmental issues faced by humanity, the use of biofuels has been favoured with the idea of limiting the neat emissions of greenhouse gases and, hence, the global warming effect. In that frame, biodiesel production has been promoted with, as a consequence, a significant increase in glycerol availability. Indeed, biodiesel (fatty acid methyl esters) is produced by the triglycerides transesterification process which yields glycerol as a co-product (*ca.* 100 kg of glycerol per ton of biodiesel). The crude glycerol production is estimated to reach 4 billion litres by 2026 (Figure 1) [1]. Even if the development of the biodiesel industry seems to be slowed down due to recent political decisions in Europe, this sector still generates and will generate in the coming years a huge glut of glycerol, which must be valorised to help sustaining the economy of the whole biodiesel value chain. Of course, the higher the economic value of the chemicals derived from glycerol, the better.

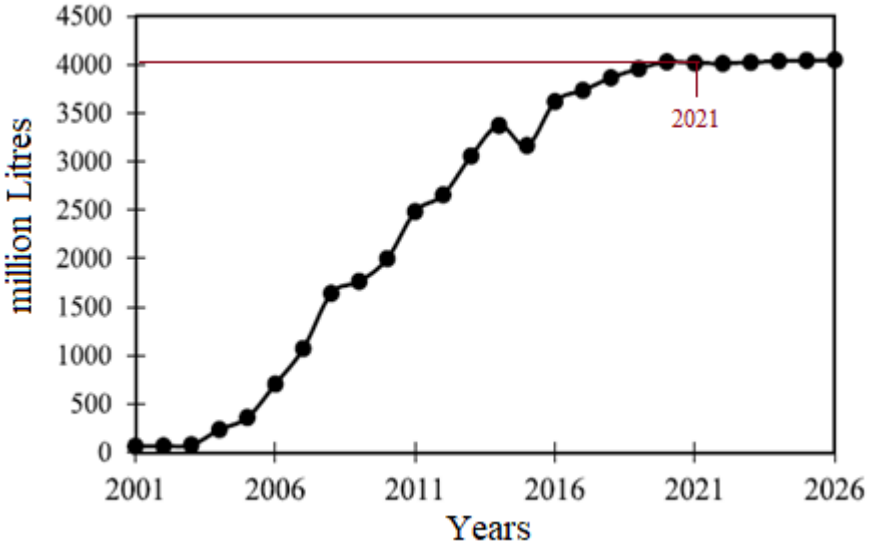

Figure 1. Past evolution and prediction of the worldwide glycerol production [1], where the brown line indicates the glycerol production at the moment (2021).

In that context, polyglycerols (PGs) are among the most interesting candidates. Indeed, these polymers have demonstrated excellent biocompatibility and have many direct applications in pharmacy and food sectors. Chemicals manufacturers also utilize PGs as intermediates for obtaining other molecules, such as PGs esters, with a global market size of USD 1.91 billion in 2017 [2]. Considering the large diversity of final applications (emulsifiers, stabilizers, antimicrobial agent, cosmetics, etc.) a drastic increase in the production of PGs is expected with a global market of USD 5.52 billion for 700 kt envisioned for 2022 (Figure 2). 52% of the market demand is for PG2 and PG3 and 48% for PG4 to PG10 (further noted PG4+).

While polyglycerols are currently produced from biosourced epichlorohydrin (Epicerol®), the change in the customers' demand, more particularly in the cosmetic and food sectors, require products derived from nontoxic and, preferably, natural ingredients. This strongly encourages the manufacturers to produce PGs directly from biosourced glycerol. Currently, in Europe, manufacturers such as Solvay, Lonza and, recently, Spiga Nord produce PGs from refined glycerol deriving from the biodiesel and oleochemicals industries [3].

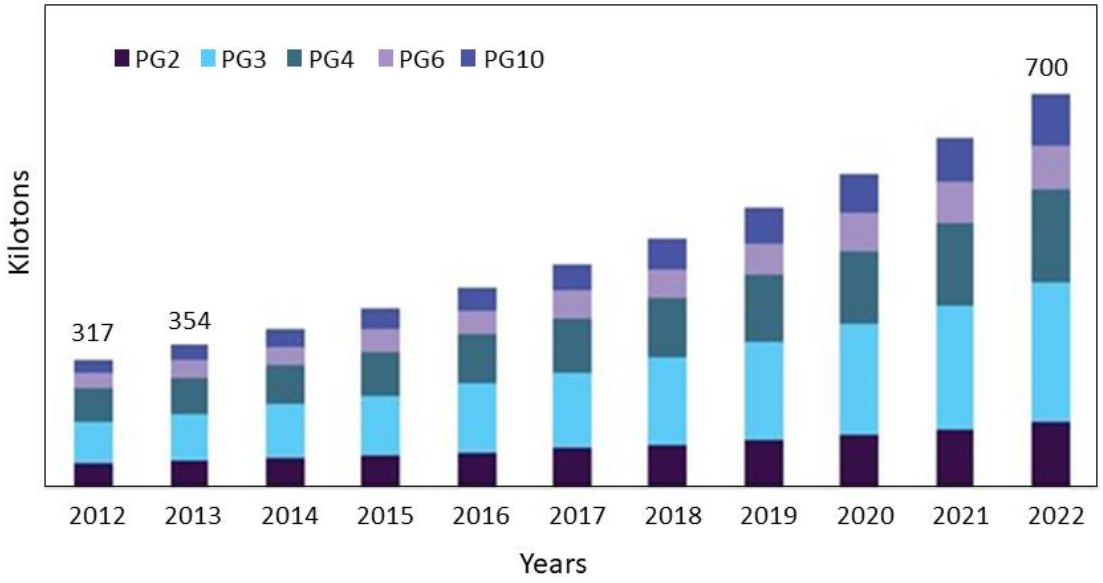

Figure 2. Polyglycerols global market demand for diglycerol (PG2), triglycerol (PG3), hexaglycerol (PG6) and decaglycerol (PG10) [2].

Polyglycerols manufacturers nowadays focus on two methods of production. First, the basic hydrolysis of epichlorohydrin and glycerol, with the strong disadvantage of using highly toxic and carcinogenic raw material (epichlorohydrin) [4]. The second method consists on the direct polymerization of glycerol in the presence of a strong homogeneous base, such as NaOH and KOH (see details in Section 1.3 of Chapter 1). Although the raw material, glycerol, is here non-toxic, the homogeneous catalysts used cannot be recovered from the medium after reaction, which is the main drawback of this method.

Besides these methods, several types of catalysts have been reported in the literature to polymerize glycerol, including strong acids [5–7], alkali-modified zeolites [8, 9], bulk or supported alkaline oxides [10–13], alkaline carbonate and hydroxide [12, 14–16] and impregnated basic mesoporous solids [17]. Among them, alkaline heterogenous catalysts have several advantages over the other, including higher selectivity to PGs and their absence of corrosiveness. Particularly, CaO-based catalysts, due to their large availability, lower cost and absence of toxicity in the case of leaching in the reaction medium, attracted the interest of many research groups [10, 11, 13, 18–21].

However, there is a lack of information on many aspects, such as the reaction mechanism and PGs characterizations. These points represent to date a critical gap in knowledge. Moreover, the partial or total dissolution of this type of catalyst in glycerol and, *e.g.*, the formation of colloidal $Ca(OH)_2$ from CaO-based catalysts, are still an issue to be solved. Therefore, it is crucial to develop new catalysts to try to overcome this issue and to improve the catalytic activity and selectivity while keeping the catalysts stable under reaction conditions.

Considering the current aforementioned limitations, the general objectives of this thesis are: *(i) to* develop Ca-based heterogeneous catalytic systems for the selective polymerization of glycerol; *(ii)* to study the influence of various parameters such as temperature, catalyst concentration and reaction time on the conversion and degree of polymerization of glycerol; *(iii)* to understand the mechanism of glycerol polymerization on Ca-based catalysts; and, in parallel, *(iv)* to develop a reliable analytical method procedure for characterizing polyglycerols.

Thus, in Chapter 1, a bibliographical study will focus on: *(i)* the PGs applications; *(ii)* the catalytic systems that have been developed previously to promote glycerol polymerisation; *(iii)* summing up their advantages and disadvantages, particularly concerning the catalyst stability; *(iv)* discussing the mechanism proposed and, finally, *(v)* describing the factors influencing the polymerization reaction. In Chapter 2, catalysts preparation, characterisation techniques, analytical methods and set-ups and procedures used for catalytic tests will be described. Then, Chapters 3 and 4 will focus on the development of two types of potential catalytic systems for glycerol polymerization: calcium glyceroxides and calcium hydroxyapatites, respectively. In Chapter 3, first the catalytic performances of calcium glyceroxides and the catalysts characterization will be investigated. Then, the mechanism of active phase genesis and, consequently, of the PGs formation will be proposed. Finally, the effect of the operating conditions on the catalytic performances and stability of the catalysts will be studied. In Chapter 4, calcium-based hydroxyapatites, as other potential catalysts for glycerol polymerization, will be studied. In that frame, several catalysts were prepared, characterized and tested and a tentative mechanism is proposed to explain their deactivation. This thesis will be finally closed by final conclusions and a few perspectives.

References

[1] Chong, C. C.; Aqsha, A.; Ayoub, M.; Sajid, M.; Abdullah, A. Z.; Yusup, S.; Abdullah, B. A Review over the Role of Catalysts for Selective Short-Chain Polyglycerol Production from Biodiesel Derived Waste Glycerol. Environ. Technol. Innov., 2020, 19, 100859. https://doi.org/10.1016/j.eti.2020.100859.

[2] Polyglycerol Market Size https://www.grandviewresearch.com/industry-analysis/polyglycerol-market (accessed May 5, 2020).

[3] Ciriminna, R.; Katryniok, B.; Paul, S.; Dumeignil, F.; Pagliaro, M. Glycerol-Derived Renewable Polyglycerols: A Class of Versatile Chemicals of Wide Potential Application. Org. Process Res. Dev., 2015, 19 (7), 748–754. https://doi.org/10.1021/op500313x.

[4] Gholami, Z.; Abdullah, A. Z.; Lee, K.-T. Dealing with the Surplus of Glycerol Production from Biodiesel Industry through Catalytic Upgrading to Polyglycerols and Other Value-Added Products. Renew. Sustain. Energy Rev., 2014, 39, 327–341. https://doi.org/10.1016/j.rser.2014.07.092.

[5] Sayoud, N.; De Oliveira Vigier, K.; Cucu, T.; De Meulenaer, B.; Fan, Z.; Lai, J.; Clacens, J.-M.; Liebens, A.; Jérôme, F. Homogeneously-Acid Catalyzed Oligomerization of Glycerol. Green Chem., 2015, 17 (8), 4307–4314. https://doi.org/10.1039/C5GC01020A.

[6] Salehpour, S.; Dubé, M. A. Towards the Sustainable Production of Higher-Molecular-Weight Polyglycerol. Macromol. Chem. Phys., 2011, 212 (12), 1284–1293. https://doi.org/10.1002/macp.201100064.

[7] Medeiros, M. A.; Araujo, M. H.; Augusti, R.; Oliveira, L. C. A. de; Lago, R. M. Acid-Catalyzed Oligomerization of Glycerol Investigated by Electrospray Ionization Mass Spectrometry. J. Braz. Chem. Soc., 2009, 20 (9), 1667–1673. https://doi.org/10.1590/S0103-50532009000900015.

[8] Krisnandi, Y. K.; Eckelt, R.; Schneider, M.; Martin, A.; Richter, M. Glycerol Upgrading over Zeolites by Batch-Reactor Liquid-Phase Oligomerization: Heterogeneous versus Homogeneous Reaction. ChemSusChem, 2008, 1 (10), 835–844. https://doi.org/10.1002/cssc.200800128.

[9] Harris, E. G.; Hees, U.; Bunte, R.; Hachgenei, J. W.; Kuhm, P. Process for the Production of Oligoglycerol Mixtures of Increased Diglycerol Content. US5349094A, September 20, 1994.

[10] Barros, F. J. S.; Moreno-Tost, R.; Cecilia, J. A.; Ledesma-Muñoz, A. L.; de Oliveira, L. C. C.; Luna, F. M. T.; Vieira, R. S. Glycerol Oligomers Production by Etherification Using Calcined Eggshell as Catalyst. Mol. Catal., 2017, 433, 282–290. https://doi.org/10.1016/j.mcat.2017.02.030.

[11] Ruppert, A. M.; Meeldijk, J. D.; Kuipers, B. W. M.; Erné, B. H.; Weckhuysen, B. M. Glycerol Etherification over Highly Active CaO-Based Materials: New Mechanistic Aspects and Related Colloidal Particle Formation. Chem. - Eur. J., 2008, 14 (7), 2016–2024. https://doi.org/10.1002/chem.200701757.

[12] Ayoub, M.; Khayoon, M. S.; Abdullah, A. Z. Synthesis of Oxygenated Fuel Additives via the Solventless Etherification of Glycerol. Bioresour. Technol., 2012, 112, 308–312. https://doi.org/10.1016/j.biortech.2012.02.103.

[13] Kirby, F.; Nieuwelink, A.-E.; Kuipers, B. W. M.; Kaiser, A.; Bruijnincx, P. C. A.; Weckhuysen, B. M. CaO as Drop-In Colloidal Catalysts for the Synthesis of Higher Polyglycerols. Chem. - Eur. J., 2015, 21 (13), 5101–5109. https://doi.org/10.1002/chem.201405906.

[14] Richter, M.; Krisnandi, Y.; Eckelt, R.; Martin, A. Homogeneously Catalyzed Batch Reactor Glycerol Etherification by $CsHCO_3$. Catal. Commun., 2008, 9 (11–12), 2112–2116. https://doi.org/10.1016/j.catcom.2008.04.007.

[15] Garti, N.; Aserin, A.; Zaidman, B. Polyglycerol Esters: Optimization and Techno-Economic Evaluation. J. Am. Oil Chem. Soc., 1981, 58 (9), 878–883. https://doi.org/10.1007/BF02672963.

[16] Lemke, D. W. Processes for Preparing Linear Polyglycerols and Polyglycerol Esters. US6620904B2, 2003.

[17] Clacens, J.-M.; Pouilloux, Y.; Barrault, J. Selective Etherification of Glycerol to Polyglycerols over Impregnated Basic MCM-41 Type Mesoporous Catalysts. Appl. Catal. Gen., 2002, 227 (1–2), 181–190. https://doi.org/10.1016/S0926-860X(01)00920-6.

[18] Barros, F. J. S.; Cecilia, J. A.; Moreno-Tost, R.; de Oliveira, M. F.; Rodríguez-Castellón, E.; Luna, F. M. T.; Vieira, R. S. Glycerol Oligomerization Using Low Cost Dolomite Catalyst. Waste Biomass Valorization, 2018. https://doi.org/10.1007/s12649-018-0477-5.

[19] Nieuwelink, A.-E. CaO/CNF for the Oligomerization of Glycerol. Master thesis, Utrecht University, Department of Chemistry, 2015.

[20] Gholami, Z.; Abdullah, A. Z.; Lee, K.-T. Selective Etherification of Glycerol over Heterogeneous Mixed Oxide Catalyst: Optimization of Reaction Parameters. Chem. Eng. Sci., 2013, 1 (4), 79–86. https://doi.org/10.12691/ces-1-4-6.

[21] Gholami, Z.; Abdullah, A. Z.; Lee, K. T. Heterogeneously Catalyzed Etherification of Glycerol to Diglycerol over Calcium–Lanthanum Oxide Supported on MCM-41: A Heterogeneous Basic Catalyst. Appl. Catal. Gen., 2014, 479, 76–86. https://doi.org/10.1016/j.apcata.2014.04.024.

Chapter 1

Bibliography

*The content of this chapter has been published as a review: N. Ebadipour, S. Paul, B. Katryniok, F. Dumeignil, Alkaline-Based Catalysts for Glycerol Polymerization Reaction: A Review, Catalysts, 10 (**2020**) 1021.*

1.1 Introduction

Polyglycerols (PGs) are water soluble, biocompatible and highly functional materials, which makes them very interesting in many applications including cosmetics, food, polymers and plastic industries [1–5]. In the current market, di-, tri-, tetra-, penta-, hexa- and deca-glycerols are the most demanded PGs [2, 4].

The various applications of PGs depend on their degree of polymerization, number of hydroxyl groups, structure and properties such as viscosity and functionality. Hydroxyl functionality refers to the number of OH groups (primary and secondary groups) per molecule that make them reactive for further molecule modifications.

Polyglycerols have a large variety of possible chemical architectures: linear, branched, cyclic and hyperbranched, as shown in Figure 1.1 and 1.2. For instance, Cassel *et al*. [6] reported that the number of possible structures corresponding to PG2 and PG3 are 8 and 12 isomeric compounds, respectively. It increases up to 360 isomeric compounds for PG5.

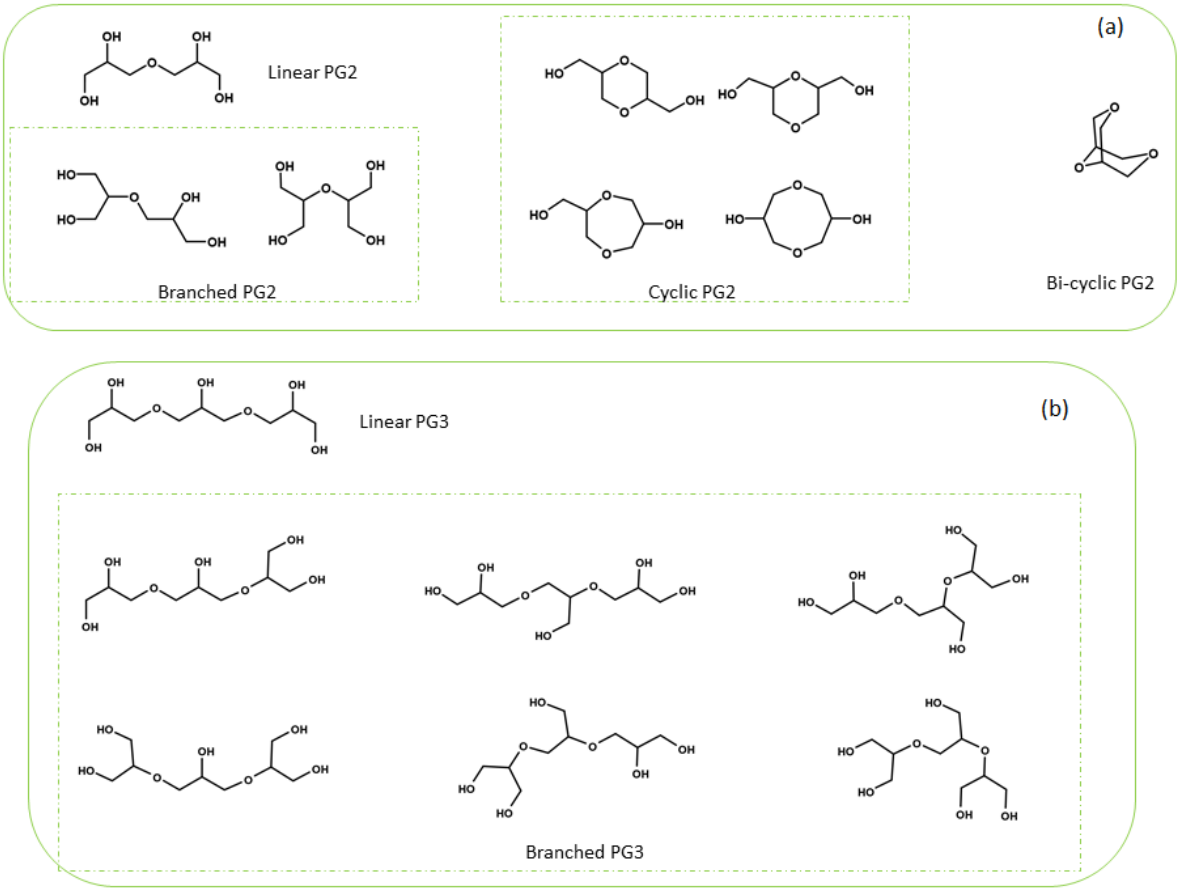

Figure 1.1. Examples of structures for: a) diglycerol (PG2) including linear, branched and cyclic [6], and b) linear and branched triglycerol (PG3) [7].

Hyperbranched PGs (HBPGs) can be divided in two categories based on their molecular weight and consequently their applications: low molecular weight HBPGs (Mw of < 2500 Da) and high molecular weight HBPGs with Mw of 24,000 – 700,000 Da [8, 9]. Biocompatibility and functionality of polyols are functions of the molecular weight and number of hydroxyl ends-groups. For example, a hyperbranched PGs with a molecular weight of 5000 Da could possess 68 hydroxyl ends-groups, which makes it a highly functional material [10, 11]. Therefore, HBPGs have various applications, especially in nanobiotechnology and in nanomedicine [10].

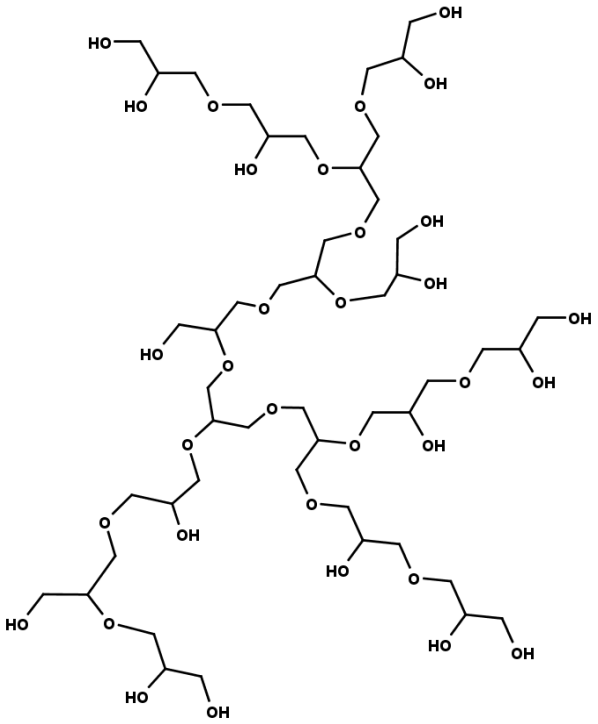

Figure 1.2. Example of a hyperbranched PG16 with a molecular weight of 1202.6 g/mol [12].

Similarly, as shown in Table 1.1, by increasing the molecular weight of the PGs, their properties like viscosity and numbers of hydroxyl groups (*i.e.*, the degree of potential functionalization) also increase.

Table 1.1. Properties of linear polyglycerols commonly available on the market [4, 5].

Name (Abbreviation)	**Molecular weight (g/mol)**	**Number of OH groups**	**Viscosity (mm^2/s) at 50 °C**	**Density (g/cm^3)**	**Hydroxyl value (mg KOH/g)***
Glycerol (G)	92	3	45	1.256 (25 °C)	1830
Diglycerol (PG2)	166	4	287	1.279 (25 °C)	1352
Triglycerol (PG3)	240	5	647	1.2646 (40 °C)	1169
Tetraglycerol (PG4)	314	6	1067	1.2687 (40 °C)	1071
Pentaglycerol (PG5)	388	7	1408	-	1012
Hexaglycerol (PG6)	462	8	1671	-	970
Heptaglycerol (PG7)	536	9	2053	-	941
Octaglycerol (PG8)	610	10	2292	-	920
Nonaglycerol (PG9)	684	11	2817	-	903
Decaglycerol (PG10)	758	12	3199	-	880
Pentadecaglycerol (PG15)	1128	17	4893	-	846

* The number of hydroxyl groups on a polyol is determined by reacting the polyol with acetic acid and then titrating with potassium hydroxide (KOH). The milligrams of potassium hydroxide required to neutralize one gram of the solution is called the hydroxyl value, as discussed in ASTM D4274-11 standard.

Due to their properties, polyglycerols have found a wide range of applications in food, cosmetics, plastics and other industries as we will detail in the following.

1.2 Polyglycerols applications

Currently, as said above, major application of polyglycerols are cosmetics, food industry and pharmaceuticals sectors. In 2015, cosmetics sector dominated other applications while accounting for 47% of the overall volume [13], as shown in Figure 1.3.

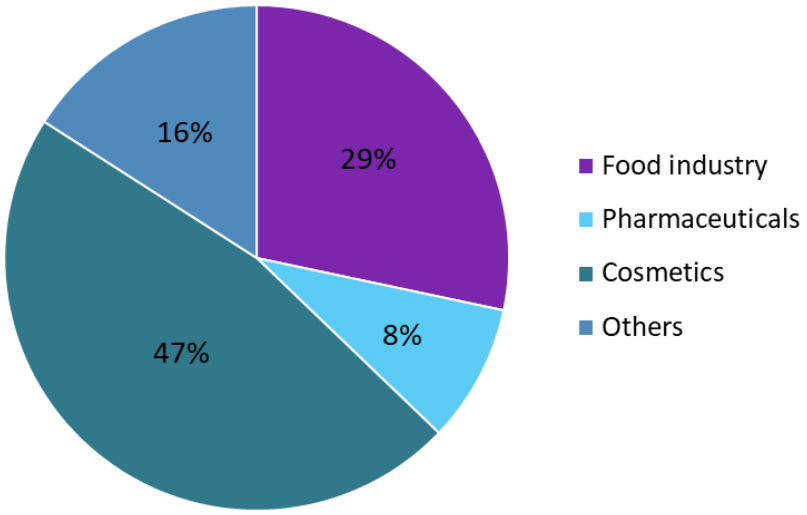

Figure 1.3. Global polyglycerols market distribution by application in 2015 (in volume) [13].

1.2.1 Cosmetics

Diglycerol is widely used in cosmetic formulations as a solvent for fragrances. This short chain PG is non-toxic and has similar properties compared to glycerol but with a lower volatility due to its higher molecular weight (Mw). Moreover, it presents a higher refractive index than glycerol, which is suitable for clear gels. A mixture of diglycerol with menthol also enhance the evaporation, the impact flavour and the longevity of the latter in products such as toothpastes, mouthwashes compared to mixtures with glycerol [5, 14].

Moreover, diglycerol could have applications in cosmetics industry as emulsifier upon conversion to polyglycerol esters to formulate oil/water emulsions for lotions, sunscreens, creams and hair care products as reported by Meyer *et al.* [15] for Evonik Co.

Higher polyglycerols are also attracting interest of cosmetics manufacturers as UV-absorbing polymers. For instance, mixture of polyglycerols containing PG3 to PG12 (free of PG2 and its cyclic forms) with an average molecular weight higher than 500 Da has been utilized to formulate sunscreens and other related products by Johnson & Johnson Co. [16].

1.2.2 Food industry

Linear polyglycerols are widely used in food industry as emulsifiers upon conversion to fatty acid esters, due to their desirable physical characteristics, including a clear appearance at melting point, a desirable Gardner colour, which is a value representing a sample's yellowness measured by UV/VIS spectrophotometer, a mild odour, and a bland taste [5, 17, 18]. Approximately 500,000 metric tons of polyglycerol fatty esters are produced worldwide per year. Sales in the European Union and the United States are estimated to be 200–300 millions € and 225–275 millions USD yearly, respectively [19]. However, local regulations impose certain degrees of polymerization to the food industry; for instance, according to the EU law, PGs for food applications should not contain polymers containing more than 7 condensed glycerol molecules (PG7) [14]. In contrast, PG2 up to PG10 have the approval of U.S. Food and Drug Administration (FDA) [20].

1.2.3 Alternative for PEG

Linear polyglycerols are known as being structurally similar to polyethylene glycol (PEG), which are produced from petro-sourced ethylene oxide. Compared to PEG, the polyglycerols have a higher water-solubility and a slightly better biocompatibility, which makes them a promising and renewable alternative to PEG [15, 21].

1.2.4 Plastic industry

Hyperbranched polyglycerols have already found applications as surfactants in the plastic industry for treating lithographic printing plates and as organic solvents in aqueous inkjet-printing inks to prevent paper deformation. Polyglycerols can be used as performance additives in water-based printing inks due to their higher solubility in water compared to polyesters [3, 20].

1.2.5 Biomedical applications

Both linear and hyperbranched polyglycerols have the potential to be utilized in biomedical applications such as drug delivery, ophthalmic sealant for corneal wounds, anti-bacterial or anti-inflammatory agents [22–26]. Particularly, functionalized HBPGs are of special interest in drug delivery, as shown in Figure 1.4.

However, polyglycerols must meet certain criteria to be used in biomedical applications such as high purity (they must be cyclic compounds-free and have a low coloration [14]).

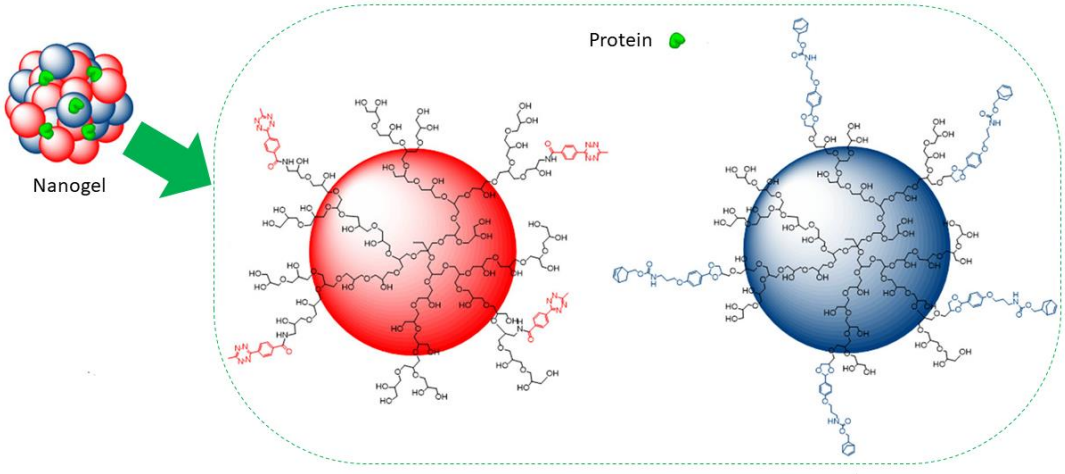

Figure 1.4. A crosslinked *pH*-degradable nanogel, prepared by functionalization of dendritic PGs (adapted from [26]).

1.2.6 Other applications

As the physicochemical properties of polyglycerols can be varied by tuning their structure and degree of polymerization, PGs have many other interesting applications. For instance, diglycerol can be used as an oxygenated fuel additive [27].

Polyglycerols with a degree of polymerization of 3 to 6 have already been used as effective antifoam agents in many industries including food, pharmaceutical, cosmetics, paper, paints and coatings by partial conversion to polyglycerol esters [28, 29].

Polyglycerols with a polymerization degree of 10-20 can be applied as a foam stabilizer for oil fields and coal mines by mixing them with non-ionic surfactants such as ammonia oxide [30].

1.3 Industrial routes for polyglycerols production

Nowadays, polyglycerols manufacturers focus on two methods of production (Figure 1.5):

a) Basic hydrolysis of epichlorohydrin and glycerol
b) Direct polymerization of glycerol in the presence of a strong homogeneous base

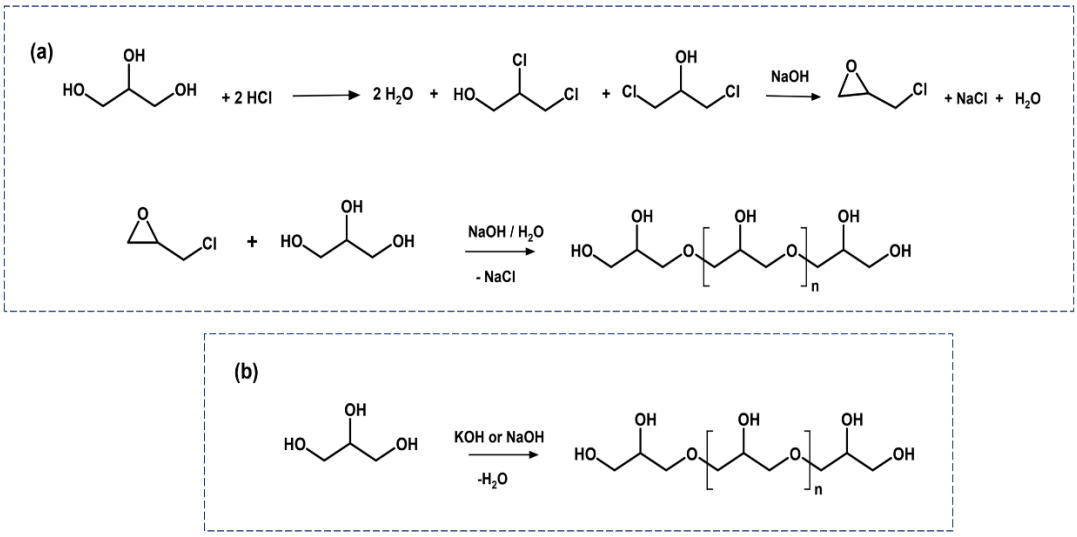

Figure 1.5. Current industrial routes for PGs production, (a) Epicerol® process, with epichlorohydrin and glycidol production from glycerol prior to a basic hydrolysis in presence of glycerol (n = 1-4); (b) Direct polymerization of glycerol using an alkaline homogeneous catalyst (n = 2-10) (adapted from [31, 32]).

The first method, starts from the hydrolysis of epichlorohydrin to glycidol under basic conditions, before the as-formed glycidol is reacted with glycerol or unreacted epichlorohydrin to form diglycerol and higher oligomers as shown in Figure 1.5-a [5]. Since 2011, Solvay has introduced a process for the glycerol-based production of epichlorohydrin, the so-called Epicerol® process, which involves the reaction of glycerol with hydrochloric acid in the presence of Lewis acid catalysts followed by alkaline hydrolysis, as described in Figure 1.5-a [31–33]. However, the overall relative low selectivity, the formation of high amounts of chloride salts (by-products), the need for many intermediate steps, further separation and purification steps [32–34], and most importantly the highly toxic and carcinogenic raw material (epichlorohydrin) are strong disadvantages of this method [2]. In addition, due to side reactions such as dehydration and oxidation reactions, undesired coloured products are formed which leads to a low product quality [5]. Besides, from an industrial point of view, such a process requires an explosion-proof facility, which represents a high capital investment [35].

In the second route (Figure 1.5-b), the polymerization of glycerol is carried out using a strong homogeneous basic catalyst such as KOH or NaOH [17, 18]. However, due to the use of the strong base, cyclic polyglycerols could form and often lead to degradation reactions forming by-products with a dark colour or a strong odour making them non-edible. Thus, bleaching agents such as hydrogen peroxide and sodium hypochlorite must be employed to improve the physical properties of the produced PGs, [17] which is definitely not an environmentally-friendly solution. Using strong alkaline catalyst, such as NaOH and KOH as homogenous catalysts to directly convert glycerol to

PGs, has other disadvantages: (i) the too fast reaction causes difficulty to control the degree of polymerization; (ii) the homogeneous catalyst cannot be recovered from the medium after reaction and hence be reused and (iii) strong bases induce corrosion issues in the industrial equipment.

Concerning the polymerization degree, PGs obtained by the "epichlorohydrin" route, typically do not contain glycerol anymore. For instance, PG3 manufactured by Solvay, contains a minimum of 80% of di-, tri- and tetraglycerol compared to a PGs manufactured by a "catalytic glycerol polymerization" route, which exhibit broader PGs' distributions [36] (Figure 1.6).

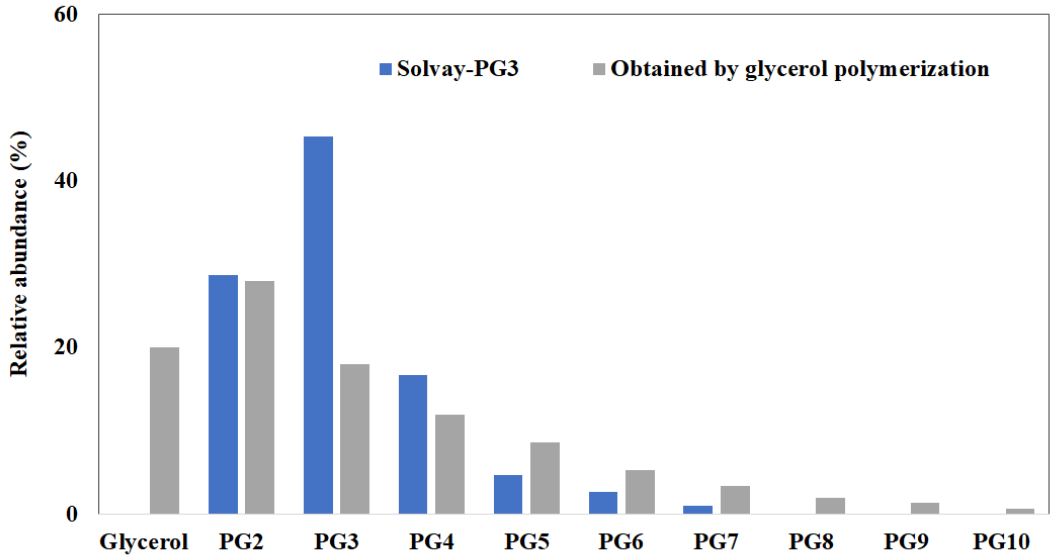

Figure 1.6. Comparison of polyglycerols distributions of Solvay PG3 and PGs obtained from catalytic polymerization of glycerol (average molecular weight = 250 Da) (adapted from [36]).

Besides, polyglycerols, mainly PG2 to PG5, can be synthetized by organic chemistry methods as described by Cassel *et al.* [6]. For instance, for diglycerols, 5 regioisomers out of the 8 possible structures (shown in Figure 1.1), including linear, two branched and two cyclic ones have been synthetized. However, synthetizing the other PGs is limited due to the complexity of the various possible structures that can be formed [6, 37].

1.4 Catalytic polymerization of glycerol

In the literature, glycerol polymerization is referred to as etherification [38–40], self-condensation, oligomerization [41, 42] and polymerization [43]. In this study, we will use the general term *"polymerization"* to refer to the etherification, oligomerization and polymerization. Table 1.2 summarizes the results of the studies on glycerol polymerization over homogenous catalysts.

Table 1.2 . Summary of the conditions used and performances obtained for glycerol polymerization over different homogenous catalysts.

Catalyst	**Temperature (°C)**	**Catalyst loading (wt.%)**	**Reaction time (h)**	**Reaction conditions**	**Glycerol conversion (%)**	**Selectivity to PGs (%)**	**Method used for PGs analysis**	**Reference**
LiOH	240	2	6	Dean–Stark system with a N_2 flow to constantly eliminate the water formed	100	$S_{PG2} = 20$	GC	[44]
K_2CO_3	237	4.16	4	Continuous flow reactor using a microwave heating	45	$S_{PG2} = 45$	GC ESI-MS	[45, 46]
K_2CO_3	250	4.16	4-5	Continuous flow reactor	~50	$S_{PG2} = 43$	GC	[7]
$Al(TFSI)_3$	150	13.2	6	Under static atmosphere	80	$S_{PG2-7} = 90$	GC-FID MALDI-ToF	[47]
LiOH	230 260	0.1	7	Dean–Stark system with a N_2 flow to constantly eliminate the water formed	24 80	$S_{PG2-3} = 100$ $S_{PG2-3} = 68$	GC Hydroxyl value	[48]
KOH NaOH	260-280	2-4	1-4	Continuous N_2 flow to remove formed water	90-95	PG10-25	-	[49]
H_2SO_4	140	4.84	4	Under reduced pressure (26 mbar)	72	-	GPC Hydroxyl value	[50]
H_2SO_4	150	5.2	-	Under vacuum (812 mbar)	-	PG30-PG50	MALDI-ToF	[51]
H_2SO_4	280	14	2	-	90	$S_{PG2-3} < 20$	ESI-MS	[52]
$CsHCO_3$ Cs_2CO_3 CsOH	260	1.85	8	Under atmospheric pressure	64 71 75	$S_{PG2-3} = 35$ $S_{PG2-3} = 64$ $S_{PG2-3} = 58$	GC	[53]

$Ca(OH)_2$	230	0.1	-	Under vacuum	57	S_{PG2-3} = 87	GC	[18]
Na_2CO_3 NaOH	240	2	9	-	76 63	S_{PG2-3} = 93 S_{PG2-3} = 99	GC-FID	[54]
Na_2CO_3	270	3	1	Under atmospheric pressure using a chiller to condense water and a microwave heating	93	S_{PG2-4} = 70	ESI-HRMS	[55]
CsOH	260	2	4	Dean–Stark system with a N_2 flow to constantly eliminate the water formed	90	S_{PG2-3} = 63	GC-FID	[56]
KOH NaOH	260	-	-	Continuous N_2 flow to remove formed water	50-100	-	hydroxyl value	[17]

1.4.1 Homogenous catalysis

Historically, the first route used to produce PGs from glycerol was homogenously-catalyzed by KOH or NaOH at 200-275 °C under CO_2 or N_2 at atmospheric or reduced pressure. Under such conditions, and in the presence of these alkaline catalysts, a wide range of polyglycerols (PG2-PG35) was produced [4, 17, 57].

Further, Garti *et al.* [58] screened the performance of several homogeneous catalysts at 260 °C under inert atmosphere. After 4 h of reaction in presence of 2.5 mol% of catalyst their activity, based on the molar percentage of formed water per glycerol followed the order: K_2CO_3 (94%) ~ Li_2CO_3 (94%) > Na_2CO_3 (92%) > KOH (79%) > NaOH (78%) > CH_3ONa (71%)> LiOH (61%). Under these conditions, both the solubility of the catalysts in the reaction mixture and the catalyst basicity influence the reaction rate. While hydroxides are stronger bases than carbonates, K_2CO_3 was a better catalyst than KOH mainly due to a better solubility of the carbonate in glycerol. For the same reason, the oxides exhibited a lower activity. For instance, the rate of glycerol polymerization (based on mole percent of formed water per glycerol) was lower in the presence of CaO (7%) than of $Ca(OH)_2$ (69%), as shown in Figure 1.7. It should be noted that in some works, oxides and hydroxides of alkali metals were considered as homogeneous catalysts because of their partial dissolution in glycerol, while they are not totally homogenous and could thus have dual catalytic roles by actually catalysing the reaction both homogenously and heterogeneously. This point will be discussed in more details in Section 1.4.3.

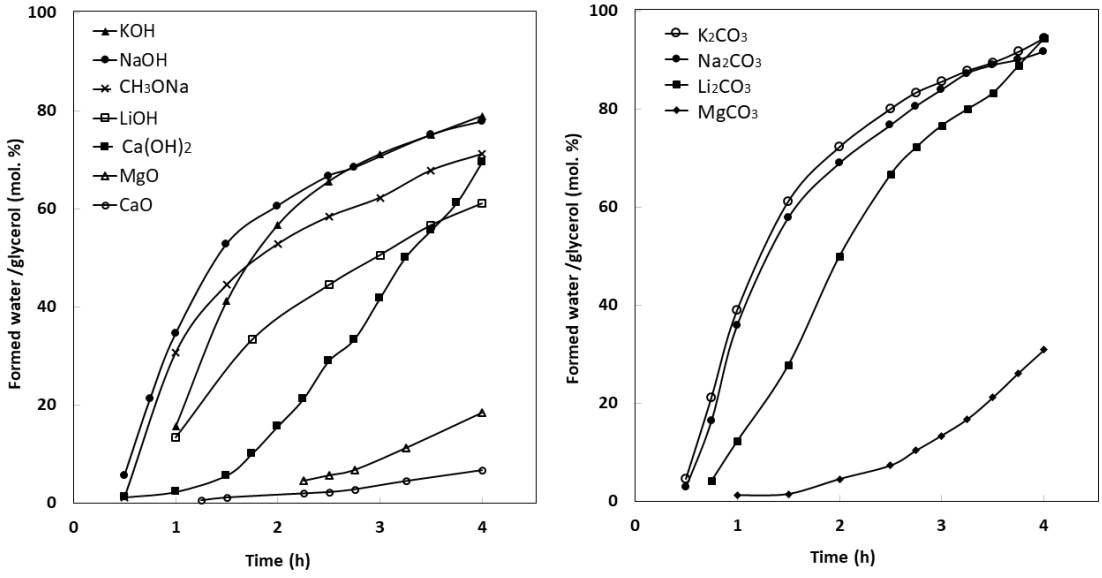

Figure 1.7. Rate of polymerization reactions based on the number of mole of water formed during the reaction, using carbonates and hydroxides or oxides as catalysts (based on data presented in [58]).

However, it should be noted that the authors have not analysed the obtained products, thus, the effect of the type of catalyst and of temperature on the polymerization degree is not clear. For instance, Babayan and Lehman [17] used KOH and NaOH to produce mainly pentaglycerol (PG5). The reaction was carried out at 260 °C in the presence of 2 wt.% of catalysts under vacuum. Although, the reaction was stopped when the collected water reached the theoretical value of 4 moles (approximately 50-100% of glycerol conversion), the obtained polymers have not been identified and the selectivity to PGs is therefore not clearly determined. These catalysts were also applied for esterification of polyglycerols with oils to produce polyglycerols esters [17]. Charles *et al.* [54] have also reported the glycerol polymerization in the presence of 2 wt.% of Na_2CO_3 and NaOH at 240 °C. For 9 h of reaction, glycerol conversions of 76 and 63% with summed selectivities to di and triglycerol of 93 and 99% were obtained for carbonate and hydroxide sodium, respectively. These results are in good agreement with those presented by Garti *et al.* [58], where carbonate was more active than hydroxide.

Bookong *et al.* [55] have also used Na_2CO_3 as a catalyst in reason of its high solubility in glycerol and higher activity than hydroxides (NaOH). For 1 h of reaction, a glycerol conversion of 93% and a selectivity of 70% to PG2-4 were obtained.

Similarly, Len's team has also reported the glycerol polymerization in the presence of 4.16 wt.% of K_2CO_3 at 237 °C [45, 46] where the further increase in reaction temperature was limited due to the heating source (microwave) at 250 °C [7]. They reported a 56% of glycerol conversion after 5 h of reaction with selectivities of 46 and 26% to di and triglycerol, respectively. The maximum degree of polymerization was PG9.

Calcium hydroxide has also been used to produce linear polyglycerols by Lonza Co. [18]. The reaction was performed under vacuum at 230 °C and in the presence of only 0.1 wt.% of catalyst, which made it totally homogenous in these conditions. After 15 h of reaction, 57% of glycerol conversion was obtained with 87% of summed selectivity to di and triglycerol. The maximum degree of polymerization observed was PG6.

The Cs salts, $CsHCO_3$, Cs_2CO_3 and CsOH have also been used for glycerol conversion to diglycerol. These reactions were carried out at a temperature of 260 °C under atmospheric pressure for 8 h. A selectivity of 27% to diglycerol at 75% of glycerol conversion was reached in presence of CsOH [53].

Nosal *et al*. [48] have also reported the glycerol polymerization in the presence of LiOH as catalyst aiming at producing only di and triglycerols by tuning the operating conditions. For 7 h of reaction, glycerol conversions of 24 and 80% with summed selectivities to di and triglycerol of 100 and 68% were obtained from 0.1 wt.% of LiOH at 230 °C and 260 °C, respectively.

Polymerization of glycerol was also studied in the presence of H_2SO_4 as an acidic catalyst at 280 °C. After 2 h of reaction, glycerol conversion reached 90%, while the selectivity to PGs (di, tri and tetra) was less than 20% with many unidentified by-products [52].

Salehpour and Dubé [50] also reported polymerization of glycerol at low temperature (140 °C) under reduced pressure (260 mbar) using H_2SO_4 as catalysts. For 4 h of reaction, the average molecular weight of the obtained polymers was 111400 Da, with 72% glycerol conversion (based on OH groups conversion) for 4.8 wt.% H_2SO_4.

The triflates and triflimidates salts, such as $Al(TFSI)_3$ and $Ga(OTf)_3$, as acidic catalysts have also been used to polymerize glycerol. These reactions were carried out at temperature of 150 °C under static pressure for 6 h with a selectivity of 90% to PGs (di to hepta) at 85% of glycerol conversion in presence of $Al(TFSI)_3$ [47].

Beside the fact that in both acidic and basic homogenous catalytic reactions the reaction rate is high, the lack of control of the glycerol polymerization degree leading to low selectivity, the impossibility to separate the catalyst from the reaction medium and the possibility of acrolein production as a by-product because of glycerol double dehydration, in the presence of acid catalysts, are still issues to be solved [5, 59].

1.4.2 Heterogeneous catalysts

In the last two decades, attention on glycerol polymerization over solid catalysts has been increasing, mainly in reason of the ease of separation by filtration or centrifugation after reaction but also because of their higher selectivity [3]. However, the possibility of acrolein formation in the presence of acid catalysts and instability of the catalysts due to the formation of water in which they are generally partially soluble are still issues to be tackled [50].

Glycerol polymerization over acidic and basic solid catalysts have been investigated using many catalysts groups such as alkali-modified zeolites [60, 61], impregnated basic mesoporous solids based on the MCM-41 family [56], bulk or supported alkaline earth metal oxides [40, 41], or MgAl mixed oxides derived from layered double hydroxides [39, 62].

Rupper *et al.* [40] studied the catalytic effect of alkaline earth metal oxide including BaO, SrO, CaO and MgO with low surface area (< 5 m^2/g) to produce mainly di and triglycerol, aiming at preventing the formation of higher oligomers by performing the reactions at low temperature (220 °C) during 20 h of reaction time. The order of glycerol conversion was reported as follows: BaO ≈ SrO (80%) > CaO (60%) >> MgO (<10%); this order is in accordance with the basicity of these earth metal oxide catalysts, BaO > SrO > CaO > MgO. The authors tuned the surface basicity and Lewis acidity in CaO catalysts and reported that the CaO which possesses the stronger Lewis acidity caused a higher glycerol conversion. However, Lewis acidity is not the sole parameter that could influence the polymerization as MgO possesses the strongest Lewis acidity among this catalyst's series but also the lowest catalytic activity.

As high selectivity towards short chains PGs, including di and triglycerols, was of interest, research groups started to tune and design porous catalysts to orientate the selectivity by the so-called shape-selectivity concept. For instance, when the diglycerol selectivity is favoured, the catalyst pore should be larger than 0.712 and 0.753 nm to be able to form *αα'* and *ββ'* diglycerol isomers, respectively, and to permit the access to glycerol molecules with a size of 0.515 nm [5].

Salehpour and Dubé [61] designed Na-modified microporous zeolites to enhance the shape selectivity toward diglycerol formation. The zeolite structure could suppress the formation of bulky products such as trimer and higher oligomers while diglycerol could form inside the microporous structure of the zeolite. Thus, NaX, NaY and NaBeta were used as catalysts in polymerization reaction at 260 °C. For 8 h reaction time, NaX was the most active catalyst, achieving 50% glycerol conversion with 80% selectivity to diglycerol, followed by NaY and NaBeta, which led to 20% and 10% glycerol conversion, respectively, with 100% selectivity to diglycerol. However, between 4 and 6 h reaction time, Na started to leach out of the zeolite and after 24 h reaction time, the zeolite structure was destroyed. Thus, the highest conversion in the presence of NaX was explained by its lowest stability in the presence of water and highest amount of Na.

García-Sancho *et al*. [39] designed a porous solid catalyst based on Mg/Al mixed oxides from hydrotalcites to tune the shape-selectivity of the glycerol polymerization. The porous structure of these compounds was expected to block and then control reaction selectivity toward desired short chain PGs. These reactions were carried out under batch conditions at 220 °C during 24 h. The authors reported only formation of diglycerol and triglycerol, but the conversion was relatively modest: The highest conversion was 50% over MgAl-Na at near 80% selectivity toward diglycerol, while 100% selectivity was obtained over MgAl-Urea but with only 18% glycerol conversion. They concluded that the lowest the pore diameter of the catalyst, the highest the diglycerol selectivity. However, the low glycerol conversion can be also explained by diffusion limitation of glycerol in small pores of catalyst.

In the same group, MgFe mixed oxides were developed in order to introduce heterogeneous acid sites (Fe^{3+}) to MgO. Polymerization of glycerol was performed over magnesium iron hydrotalcites at 220 °C for 24 h in batch reaction conditions. In these conditions, high diglycerol selectivities of 90% and 100% were obtained over $MgFeO_4$ and $MgFeO_1$, with a glycerol conversion of 41% and 21%, respectively. The authors concluded that the acidity, basicity and porosity of the catalysts contributed to their performances [63].

Besides, Pérez-Barrado [64] also investigated the influence of acidity and basicity of different MgAl and CaAl layered double hydroxides (LDHs) on short chain PGs selectivity. They observed that catalysts with higher acidity (higher number of acidic sites) showed higher conversion (75-96%) and low selectivity to PGs (88% selectivity to acrolein). In contrast, catalysts with less acid sites and higher amounts of medium strength basic sites resulted in lower conversion (24%) and higher

selectivity towards di and triglycerol (100%).

Similarly Sangkhum *et al.* [65] studied the glycerol polymerization in the presence of a Ca-Mg-Al mixed oxide catalyst derived from layered double hydroxide. They reported a PG2 selectivity of 33.2% with a glycerol conversion of 86.2% when the reaction was performed at 230 °C and in presence of 3 wt.% of catalyst for 24 h.

Gholami *et al.* [66] have also investigated the polymerization of glycerol over a $Ca_{1.6}La_{0.4}Al_{0.6}O_3$ mixed oxide catalyst. They obtained a glycerol conversion of 98% with 53% diglycerol selectivity after 8 h of reaction. They concluded that larger pores (average pore size of 18 nm) lead to higher diglycerol selectivity by facilitating the diffusion of glycerol molecules into the mesopores of the catalyst.

Unlike those studies where the product of interest was diglycerol, Bruijnincx's team have synthesized a new catalyst based on CaO in order to obtained higher PGs (> tetra-polyglycerol, PG4+). They used carbon nanofibers (CNF) as a support for CaO to yield larger specific surface areas while the active species (CaO) was mostly unaffected by the presence of the CNF as the interactions between CNF as a support and the active phase were low. The highest conversion was obtained in the presence of 14 wt.% CaO/CNF where glycerol conversion was 100% with 45% selectivity to di, tri and tetraglycerol (PG2-4), at 220 °C for 24 h reaction time [41, 67, 68]. However, since the gas chromatography (GC) method was not able to detect the all formed oligomer, the authors assumed the missing fraction of product (with a 55% of selectivity) could be higher oligomers.

Barros *et al.* have also developed new catalysts in order to obtain short chain PGs. Calcined dolomite, double carbonate of calcium and magnesium ($CaCO_3 \cdot MgCO_3$), and calcined egg shell were utilized to catalyse the polymerization reaction. In the presence of dolomite, glycerol conversion was 90% with selectivity of 55% to PG2-3, respectively at 245 °C for a 24 h reaction time [42]. However, the authors mentioned that the other products (45% of selectivity) that cannot be detected by the applied analytical technique (GC) could be higher oligomer or acrolein. In the same reaction conditions and in the presence of calcined eggshell, glycerol conversion of 100% with 50% selectivity to PG2-3 were obtained [38]. Over both catalysts, increasing the reaction temperature led to an increase of conversion but together with a decrease in di and triglycerol selectivity, probably to the benefit of higher oligomers (PG4+).

More recently, Caputo *et al.* [69] synthetize a catalyst by impregnation of lanthanum (III) on mesoporous sol gel to obtain mostly linear polyglycerol. A conversion of 72 % with selectivities of 30%, 20% and 42% to linear di-, tri- and tetra-oligomers, respectively, and 4% cyclic ones at 240 °C was obtained after 24 h of reaction. However, the conversion decreased to 55 % and 25% after the 2nd and 3rd cycles, respectively, when the catalysts was reused under the same reaction conditions after

recalcination between each step. The authors explained the low conversion observed by the decreased pore sizes after each calcination step, but it seems that La actually leached to the reaction media and the reaction took place only in presence of the support in the 3rd cycle (glycerol conversion of 25%), where the conversion with the sol-gel support was 23 %.

Table 1.3 summarizes the results of the studies on glycerol polymerization over heterogeneous catalysts.

It must be noted that the reaction products have been mainly been analysed by GC techniques in the literature (Table 1.3), while, this analytical method has a detection limitation for the oligomer higher PG4-PG5 [42, 68]. This will be discussed further in Section 1.7. Consequently, as aforementioned, the selectivity to PG4+ was calculated based on the missing fraction of the products that were not detected. Thus, there is not enough precise data on the PG4+ formation for these heterogeneously-catalyzed reactions.

Table 1.3. Summary of the conditions and performances obtained for glycerol polymerization over heterogenous catalysts.

Catalyst	**Temperature (°C)**	**Catalyst loading (wt.%)**	**Reaction time (h)**	**Reaction conditions**	**Glycerol conversion (%)**	**Selectivity to PGs (%)**	**Method used for PGs analysis**	**Reference**
La/sol-gel	240	2	24	Dean–Stark system with a N_2 flow to constantly eliminate the water formed	72	$S_{PG2\text{-}PG3}$ = 54 S_{PG4} = 42	GC-MS LCMS-IT-TOF	[69]
LiOH / Aluminium pillared clay	220	3	3	Under N_2 atmosphere using microwave heating	98	-	HPLC-RI	[70]
7.5 wt.% Ca-MgAl	230	3	24	Dean–Stark system with a N_2 flow to constantly eliminate the water formed	86.2	S_{PG2} = 33.2 S_{PG3} = 36.4	GC-MS GC-FID	[65]
Dolomite (mixed oxide CaO-MgO)	200 245	2	24	Dean–Stark system with a N_2 flow to constantly eliminate the water formed	10 90	$S_{PG2\text{-}PG3}$ = 55 $S_{PG2\text{-}PG3}$ = 45	GC-FID	[42]
Calcined eggshell	220 245	2	24	Under N_2 atmosphere	85 100	S_{PG2} = 35 S_{PG3} = 15	GC-FID	[38]
Duck bones	240	2	12	Dean–Stark system with a N_2 flow to constantly eliminate the water formed	99	-	GC	[44]
14wt.% CaO/CNF	220	2	24	Dean–Stark system with a Ar flow to constantly eliminate the water formed	100	$S_{PG2\text{-}PG4}$ = 45	GC-FID	[68]
MgAl-LDHs – CaAl-LDHs : cHT1	235	2	24	Dean–Stark system with a N_2 flow to constantly eliminate the water formed	24	$S_{PG2\text{-}PG3}$ = 100	GC	[64]

MgAl-LDHs – CaAl-LDHs : cHT2	235	2	24	Dean–Stark system with a N_2 flow to constantly eliminate the water formed	96	$S_{PG2-PG3}$ = 12 $S_{Acroléine}$ = 88	GC	[64]
$MgFeO_4$	220	-	24	Dean–Stark system with a N_2 flow to constantly eliminate the water formed	41	S_{PG2} = 90 S_{PG3} = 10	GC	[63]
$Ca_{1.6}La_{0.4}Al_{0.6}O_3$	250	2	8	Dean–Stark system with a N_2 flow to constantly eliminate the water formed	96.3	$S_{PG2-PG3}$ = 86	GC	[66]
MgAl-Na	220	2	24	Dean–Stark system with a N_2 flow to constantly eliminate the water formed	50	S_{PG2} = 85 S_{PG3} = 15	GC	[39]
$Ca(OH)_2$ $CaCO_3$	140	2.4	~6	Dean–Stark system with a N_2 flow to constantly eliminate the water formed	12 11	-	GPC Hydroxyl value	[50]
$CaO/Ca_{12}Al_{14}O_{33}$	200-250	-	24	Dean–Stark system with a N_2 flow to constantly eliminate the water formed	-	Linear PGs	-	[71]
Zeolite NaX *Zeolite NaY* *Zeolite Na Beta*	260	2	24	Under Ar atmosphere	100 80 50	S_{PG2} = 15 S_{PG2} = 58 S_{PG2} = 90	GC	[61]
MgO BaO-SrO CaO	220	2	20	Dean–Stark system with a Ar flow to constantly eliminate the water formed and ice trap for acrolein	10 80 60	$S_{PG2-PG3}$ = 90	GC	[40]

$Cs_{25}Al(Si/Al:20)$	260	2	20	Dean–Stark system with a N_2 flow to constantly eliminate the water formed	80	$S_{PG2} = 62$ $S_{PG3} = 33$	GC-FID	[56, 72]
Zeolite NaA Zeolite NaZ	200-260	2-5	22	Under N_2 with a reflux condenser and water separator	84.6 90.5	$S_{PG2-PG3} = 62$ $S_{PG2-PG3} = 52$	-	[60]

1.4.3 Dissolution of heterogeneous catalysts

Partial dissolution of CaO-based catalysts generally occurs in the reaction medium and hence a subsequent homogeneous catalysis contribution makes the catalytic system much more complex to understand. As a matter of fact, the formation of colloidal $Ca(OH)_2$ and the leaching of Ca^{2+} in the reaction medium, following Eq (1), has been often reported in glycerol polymerization [40, 41, 56, 61].

$$2CaO + 2H_2O \leftrightarrow Ca(OH)_{2(l)} + Ca^{2+} + 2OH^- \qquad \text{Eq (1)}$$

Ruppert *et al*. [40] measured the total $Ca(OH)_2$ and Ca^{2+} concentration in the reaction medium by inductively coupled plasma (ICP) and also observed the colloidal $Ca(OH)_2$ particles with a size of 50-100 nm by cryo-transmission electron microscopy (TEM). These results showed that the Ca concentration in the reaction medium reached 3-6 wt.% only after 2 h reaction when using calcined-CaO as the catalyst in the polymerization reaction. The authors concluded that the formation of colloidal $Ca(OH)_2$ and leached Ca^{2+} could contribute in polymerization reaction beside solid phase catalyst in the reaction medium. In addition, the colloidal $Ca(OH)_2$ particles could not be separated from reaction mixture and caused a non-transparent mixture (low quality products). Further, this causes catalyst progressive deactivation upon recycling.

Nieuwelink [41] studied the Ca leaching temperature dependency in CaO/CNF with dynamic light scattering (DLS) and conductivity measurements at 100, 150 and 220 °C. Their results indicated that at 100 °C no colloid formation occurs but a large amount of dissolved Ca^{2+} ions was observed in the glycerol mixture. On the other hand, at higher temperatures of 150 and 220 °C, more colloidal formation and less Ca^{2+} ions were observed. This could be linked to the fact that, the polymerization reaction took place at these higher temperatures, then releasing water and hence promoting formation of colloidal $Ca(OH)_2$ according to Eq 1.

The amounts of Ca and Mg leaching from dolomite were also determined by ICP-OES during the glycerol polymerization reaction by Barros *et al.* [42]. According to these authors, 49% Ca and 4% Mg leached into the medium at 245 °C after 24 h of reaction. The authors noted that a homogenous contribution of CaO could play a role on the glycerol conversion, as a significant drop in conversion was observed when dolomite was isolated and reused for a second test.

Cs leaching has also been reported during glycerol polymerization reactions in the presence of Cs-modified zeolites [56]. A lower conversion was observed with reused $Cs_{25}Al$(Si/Al ratio of 20) in comparison with the initial fresh catalyst (60% *vs.* 80%), while both catalysts had similar selectivities to di- and tri-glycerol.

Similarly, for Na-exchanged zeolite catalysts, Na leaching out of the zeolite framework during the first 4 to 8 h of reaction followed by total dissolution of the solid catalysts at 260 °C after 24 h reaction time was also reported by Krisnandi *et al.* [61].

Gholami *et al.* [73] has also reported Ca and La leaching when 20% $Ca_{1.6}La_{0.6}$/MCM-41 was used as a catalyst. A very high glycerol conversion of 91% was observed after 8 h of reaction at 250 °C where suggested a homogenously-catalyzed reactions.

To conclude, several so-called "heterogeneously-catalyzed" reactions were in fact carried out in totally or partially homogeneously-catalyzed conditions, either by dissolution of the catalysts itself or by leaching of active species into the reaction medium. Although, the homogeneous contributions are not very clear, as most often they were not closely studied or even considered. Most of the time the materials used are still classified as solid heterogeneous catalysts. In overall, several advantages and disadvantages can be summarized for homogenous and heterogenous catalysts used in glycerol polymerization reaction (Table 1.4).

Table 1.4. Advantages and disadvantages of different types of catalyst for glycerol polymerization reaction.

Type of catalyst	**Examples**	**Advantages**	**Disadvantages**	**Reference**
Alkaline homogeneous catalysts	KOH NaOH	• High catalytic activity • High degree of polymerization • Short reaction time • Low cost	• Non-recyclable catalysts • Neutralization of the products needed • Equipment corrosion • Difficulty to control the degree of polymerization (i.e. the selectivity)	[2]
Acid homogeneous catalysts	H_2SO_4	• High catalytic activity • Short reaction time	• Non-recyclable catalysts • Neutralization of the products needed • Equipment corrosion • Difficulty to control the reaction • Low selectivity to PGs	[50]
Alkaline heterogeneous catalysts	CaO, BrO, SrO	• Higher selectivity to PGs • Non-corrosive • Recyclable (mostly)	• Slower reaction time • Leaching of catalysts	[40]
Acid heterogeneous catalysts	Mg-Ca-Al	• Non-corrosive • Recyclable	• Slower reaction time • Leaching of catalysts • Higher selectivity to acrolein	[64]

It is clear that alkaline heterogenous catalysts have several advantages over other catalysts including higher selectivity to PGs and non-corrosiveness. Particularly, CaO-based catalysts due to their large availability, lower cost and absence of toxicity in case of leaching into the media, attracted the interest of many research groups as mentioned previously. However, their partial dissolution in glycerol and formation of colloidal $Ca(OH)_2$ from CaO-based catalysts are still issues to be solved.

1.5 Mechanism of glycerol polymerization over alkaline catalysts

The mechanism of polymerization of glycerol over alkaline catalysts comprises two steps: i) deprotonation of a hydroxyl group as a nucleophile, and ii) attack of the as-formed alkoxy anion (glyceroxide ion) on a carbon of another glycerol molecule. However, due to the fact that hydroxyl groups are poor leaving groups, different mechanisms have been proposed to explain the process. For instance, for solid alkaline catalyst such as CaO, MgO, BaO and SrO, it is presumed that a high reaction temperature is required for the formation of PGs by facilitating the leaving of hydroxy group [40]. Another hypothesis was that Lewis acid sites take part in the mechanism through activation of a hydroxyl group as a leaving group (Figure 1.8). However, as aforementioned, the contribution of Lewis acidity in PGs reaction mechanism cannot explain the lowest activity of MgO and the highest activity of BaO and SrO. Moreover, for other catalysts that possess Lewis acid sites such as CaAl layered double hydroxides, the reaction favoured acrolein formation [Table (1.3)].

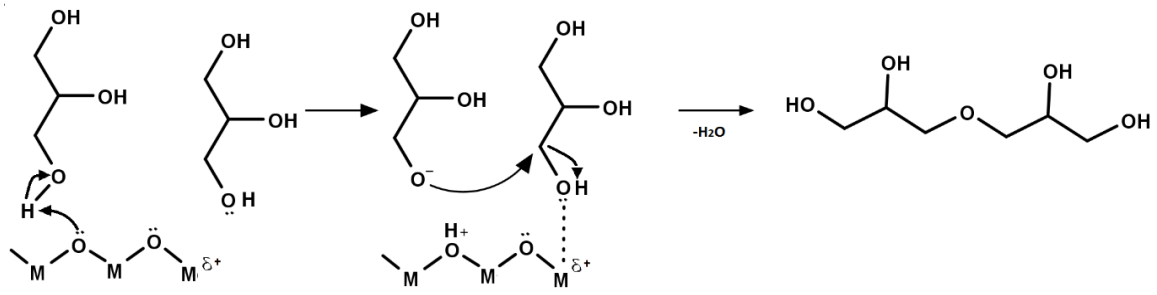

Figure 1.8. Reaction mechanism for glycerol polymerization over earth metal oxides catalysts as proposed by Ruppert *et al.* [40].

Salehpour and Dubé [50] proposed a mechanism for catalysis over $Ca(OH)_2$ suggesting that a protonated glycerol is a better nucleophile that could then attack a second molecule of glycerol, as a weak electrophile, on one of the primary or secondary alcohol groups (Figure 1.9). This mechanism could explain the slower rate of alkaline-catalyzed reaction compared to the acid-catalyzed one, where glycerol becomes a better electrophile due to the $+H_2O$-C bond. Thus, to break the C-O bond and achieve a higher reaction rate, a higher reaction temperature should be applied for alkaline-catalyzed reaction. In this mechanism, calcium ions are also involved by coordinating to the oxygen atoms of

glycerol. This coordination, as the so-called "pseudo-bond", could cause the carbon-oxygen bond of a glycerol molecule to lengthen and thus induce lowering of the energy of the transition state complex. In this mechanism, the $Ca(OH)_2$ should be in homogeneous state to access Ca ions to be involved in the mechanism. Besides, this mechanism could be also assumed for CaO, by Ca leaching into the reaction medium, as aforementioned. Thus, this suggests that the actual mechanism with calcium oxide and hydroxide is actually homogeneous.

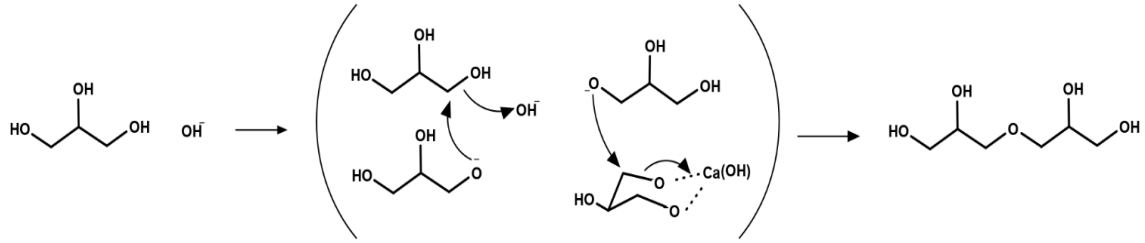

Figure 1.9. Reaction mechanism for glycerol polymerization using $Ca(OH)_2$ as a catalyst, with contribution of Ca in the mechanism, as proposed by Salehpour and Dubé [50].

Martin and Richter [5] suggested that a homogenously alkaline-catalyzed reaction follow a SN2 mechanism as shown in Figure 1.10. Similarly, the protonated glycerol molecule (glyceroxide ion) is a nucleophilic species that attacks the hydroxyl group of glycerol, then forming a water molecule. However, the corresponding cations does not contribute to this mechanism.

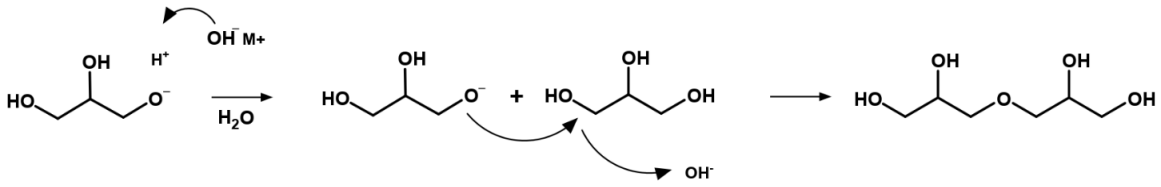

Figure 1.10. Reaction mechanism for homogenously catalyzed glycerol polymerization reaction, as proposed by Martin and Richter [5]

Ionescu and Petrović [43] presumed that the glyceroxide ion could be transformed to glycidol by intramolecular nucleophilic substitution. Then, glycidol, as an intermediate, reacts with the hydroxyl groups of glycerol to form a dimer (Figure 1.11). This is similar to the classical mechanism for formation of polyglycerols by ring opening of glycidol with a fast reaction rate at room temperature (Figure 1.5-a) [5, 74]. However, while it proposes the well-known glycidol ring opening mechanism to produce PGs, it cannot explain the roles of oxides as heterogeneous alkaline catalysts and their slower reaction rate.

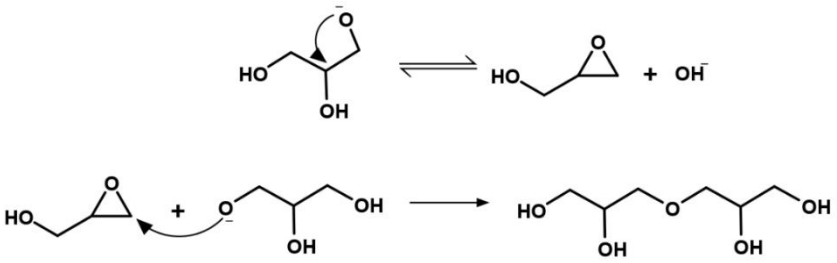

Figure 1.11. Reaction mechanism for alkaline-catalyzed reactions by glycidol formation, as proposed by Ionescu and Petrović [43].

According to all these mechanisms, glycerol polymerization reaction is subjected to a high activation energy, translated with the need of high temperatures to make the reaction possible. The operating conditions actually used will be discussed in the next section.

1.6 Effect of process parameters

A typical glycerol polymerization reaction is a solvent free reaction, where various parameters including temperature, catalyst loading, pressure, atmosphere and, obviously, reaction time could influence the glycerol conversion and the degree of polymerization.

1.6.1 Temperature

According to the literature, temperature plays an important role in the glycerol polymerization reactions catalyzed by both homogenous and heterogeneous catalysts. The studied temperature range for alkaline heterogeneously catalyzed reactions starts from 200 °C to a maximum of 270 °C, as presented in Table 1.3, keeping in mind that the boiling point of pure glycerol is 290 °C under atmospheric pressure and that the decomposition of glycerol could begin before reaching this boiling point [75].

Sangkhum *et al*. [65] studied the effect of temperature on polymerization of glycerol over Ca-MgAl mixed metal oxide as a catalyst. They performed the reaction at 200, 210, 220 and 230 °C and observed, as expected, a significant increase in glycerol conversion from 40% at 220 °C to 86% at 230 °C, while the glycerol conversions were only 5 and 11% at the lower temperatures of 200 and 210 °C, respectively. They also reported a decrease in diglycerol selectivity from nearly 78 to 33% at 220 and 230 °C, respectively.

Gholami *et al.* [66] investigated the effect of temperature on catalytic polymerization of glycerol in the presence of $Ca_{1.6}La_{0.4}Al_{0.6}O_3$ as a catalyst. A significant increase in glycerol conversion from 28.1% at 220 °C to nearly 96% at 260 °C after 8 h reaction was reported, where the yield of PG2 and PG3 was 70%.

Kirby *et al.* [68] also studied the effect of temperature on polymerization of glycerol and coloration of products in the presence of 10 wt.% CaO/CNF. They performed the reactions at the temperatures of 180, 200, 220, 240 and 260 °C and observed glycerol conversions of ~10, ~35, ~55, 80 and 100%, respectively, after 16 h of reaction time. Moreover, they concluded that the highest studied temperature (260 °C) gave rise to the formation of undesired products (dark colour products) like cyclic dimers, acrolein and other dehydration products with a decrease in selectivity to shorter PGs (PG2 and PG3).

Similar results were reported by Barros' team, that observed an increase in glycerol conversion when increasing the temperature from 200 to 245 °C in the presence of egg-shell commercial CaO [38] and calcined dolomite [42]. For instance, the conversion increased from 10% at 200 °C to 80% and 100% at 220 °C and 245 °C, respectively. The diglycerol selectivity decreased with temperature whereas the formation of acrolein increased, and a darker and more viscous product was observed, as shown in Figure 1.12.

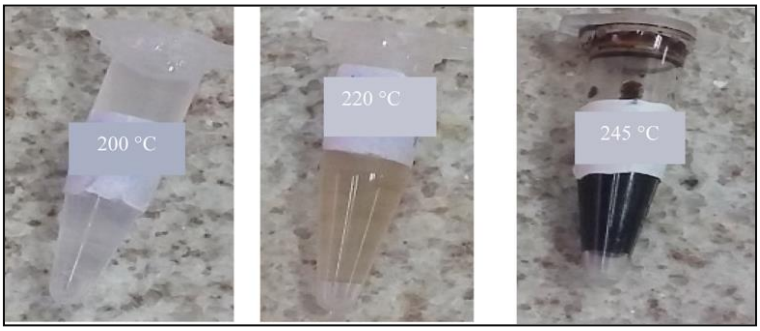

Figure 1.12. Effect of temperature on the transparency of the product of glycerol polymerization in the presence of calcined egg-shell (CaO) [38].

1.6.2 Effect of catalyst loading

Garti *et al.* [58] mentioned that increasing the amount of catalyst can increase the glycerol conversion, further affecting the overall degree of polymerization. Based on the amount of water formed during the reaction, 0.5-1 mol.% of NaOH as a catalyst were proposed for obtaining di- and triglycerols and 4-10 mol.% for higher degree of glycerol polymerization.

Sangkhum *et al.* [65] investigated the effect of Ca-MgAl mixed oxide amount on glycerol polymerization at 220 °C. According to their results, glycerol conversion increased to 20 and 40% in the presence of 2 and 3 wt.% of catalyst, respectively, whereas the glycerol conversion was 6% without catalyst. They reported that increasing the catalyst loading also promoted diglycerol selectivity from 40.4% to 78.3%, respectively (Figure 1.13). However, when the catalyst loading was further increased to 5 wt.%, the glycerol conversion and diglycerol selectivity declined, reaching 27.9% and 42.6%, respectively. They explained this phenomenon by the increase in glycerol conversion and in

the quantity of formed water in the presence of higher amount of catalyst, which might cause back-scission of polyglycerol to glycerol via hydrolysis. However, this explanation is not very convincing since the role of water in an equilibrium reaction would be the same whatever the catalytic system and catalyst amount.

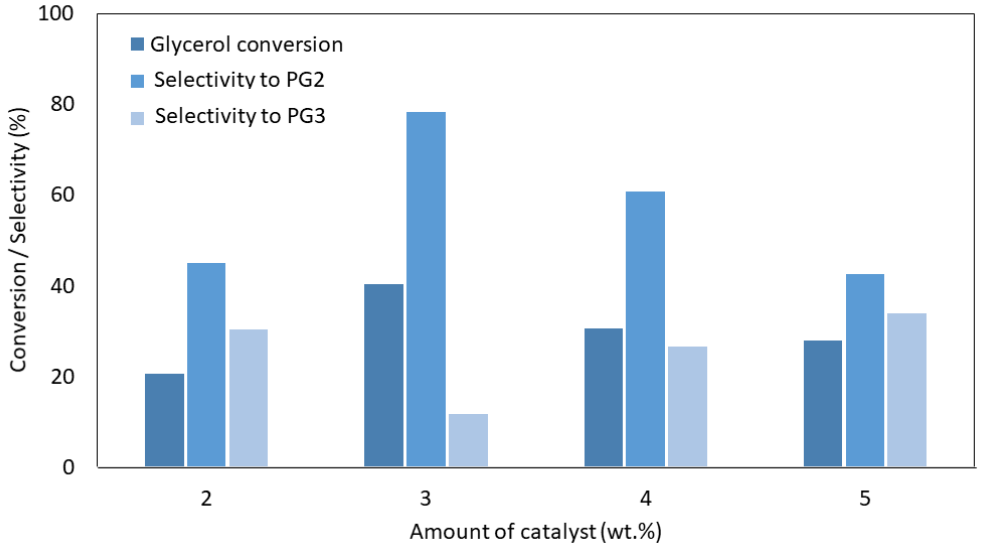

Figure 1.13. Catalytic conversion of glycerol over 7.5 wt. %Ca-MgAl mixed metal oxide at 220 °C for 24 h (adapted from [65]).

Kirby *et al.* [68] studied the effect of CaO, $Ca(OH)_2$ and CaO/CNF loading on glycerol conversion to PGs. According to their results, increasing the amount of CaO from 0.33 mol.% to 3.28 mol% (equivalent to 2 wt.% CaO) had no significant effect on glycerol conversion, while for CaO/CNF, an increase in the amount of catalyst from 0.7 to 2 wt.% induced an increase in conversion from 48% to 76%. They explained this result by homogenous contribution of CaO and $Ca(OH)_2$ in the reaction with complete dissolution of CaO in the reaction mixture at loadings up to 2 wt.% to form $Ca(OH)_2$ (from CaO) and Ca^{2+} species, as previously discussed.

On the other hand, Barros *et al.* [38] reported an increase in the glycerol conversion from 34 to 85 % by increasing the amount of calcined egg shell CaO as a catalyst from 0.5 to 2 wt.% while selectivity to di- and triglycerol decrease from nearly 55 to 43%.

1.6.3 Atmosphere

Traces of oxygen lead to the formation of oxidation products. Therefore, in order to prevent parasite oxidation reactions, glycerol polymerization is preferentially carried out under an inert gas such as N_2 or Ar [58]. However, while recent studies have been mostly carried out under N_2 atmosphere (Table 1.2 and 1.3), a few polymerization reactions were also carried out under CO_2 atmosphere. For instance, Garti *et al.* [58] used both N_2 and CO_2 atmospheres for glycerol polymerization and reported similar production of tetra- and penta-polyglycerol under both conditions. Wilson *et al.* [76] also used sparging of CO_2 to prevent oxidation for glycerol conversion to polyglycerol at 200 °C in the presence of potassium hydroxide. However, the reason behind applying CO_2 have not been clearly explained in these works. We can suppose that it might be linked to the CO_2 Lewis acidic nature, which could contribute to the reaction. However, the impact of CO_2 highly depends on the temperature, solubility of CO_2 in glycerol, concentration of CO_2, pressure and so on [77]. One study also showed the formation of glycerol carbonate from glycerol and CO_2 at 150 °C under 4 MPa in the presence of CeO_2 as a catalyst [78].

Recent studies showed that CO_2 could participate to the catalysts' deactivation. For instance, the effect of CO_2 was studied on glycerol conversion over CaO-based catalysts ($CaO\text{-}SiO_2$) in the gas phase reaction in order to produce lactic acid. Costa *et al.* [79] reported that the initial glycerol conversion was lowered for the reactions carried out under CO_2 compared to N_2 by deactivation of the catalyst by formation of $CaCO_3$. Moreover, many studies kept CaO under nitrogen or used freshly calcined CaO in order to prevent *"deactivation"* of catalyst by contacting with ambient air (reactions with CO_2 and H_2O) and formation of $CaCO_3$ and $Ca(OH)_2$, respectively [40, 41, 80, 81].

Jungermann *et al.* [4] noted that using vacuum at high reaction temperature increased the glycerol conversion by eliminating the formed water from the reaction medium and lead to a narrowing of the range of PGs molecular weight. Although these authors did not mention any values for the applied vacuum and temperature in polymerization reaction, Lemke [16] reported the use of 230 °C and under vacuum of 200 mm Hg where the glycerol boiling point is 243 °C. However, the obtained results have not been compared with results obtained under atmospheric conditions. In practice, in the case of solid catalysts, the polymerization reaction is mainly carried out under atmospheric pressure using a Dean–Stark apparatus with a reflux condenser to continuously remove the water formed during the reaction (as mentioned in Table 1.3).

1.6.4 Reaction time

The polymerization of glycerol in the absence of a solvent and in the presence of a heterogeneous catalyst is a slow reaction because the reactants must diffuse into the porous network of the catalyst in a viscous reaction medium [66]. Consequently, longer reaction times are needed to overcome diffusion resistance and reach higher degrees of polymerization. For instance, Kirby *et al.* [68] studied the composition of reaction mixture during 24 h reaction time at 220 °C in the presence of CaO/CNF. They observed an increase in formation of di- and tri-glycerol during the first 8 h of reaction, and then a progressive decrease of their quantities to the benefit of higher oligomers. Glycerol polymerization reactions catalysed by solids generally take place within 24 h, as shown in Table 1.3.

1.7 Polyglycerols characterization

As said above, glycerol polymerisation can lead to complex mixtures of PGs containing linear isomers coming from the reaction of primary hydroxyls, branched isomers formed from secondary hydroxyls and cyclic isomers resulting from intramolecular condensation of linear and branched ones. [82] Increasing the polymerization degree leads to more and more complex mixtures. Thus, characterization and analysis of such mixtures, even if crucial to evaluate the performances of the studied catalytic processes, are very difficult and generally need the combination of several separations and analysis techniques. Among the different analytical techniques, gas chromatography (GC), high performance liquid chromatography (HPLC) [40, 83, 84], size exclusion chromatography (SEC) [12, 74, 85], electron spray ionization (ESI) [74, 84], matrix-assisted laser desorption ionization (MALDI) and NMR [74] have been mainly reported in the literature to separate and identify polyglycerols.

1.7.1 Gas chromatography (GC)

Gas chromatography using a flame ionisation detector (FID) have been widely used by many researchers to detect polyglycerols in reaction mixtures because it is a relatively simple analytical technique even if, as aforementioned, it has a few limitations. First, polyglycerols higher than PG5 cannot be detected by GC [38, 63, 68, 86] because they are too heavy to be vaporised. Secondly, for a precise GC analysis, a calibration for all the possibly formed PG isomers should be done. For example, the simplest polymer, diglycerol, already consists of three different linear and branched structures and 5 cyclic forms [41]. Moreover, the higher the degree of polymerization, the more complex the chromatogram and the longer the retention times [87].

In addition, silylation of glycerol oligomers is highly recommended for gas chromatographic analysis in order to chemically convert the hydroxyl groups (polar groups) to non-polar groups and make the molecules more volatile so that they can be more easily separated and analysed by GC [5].

1.7.2 High performance liquid chromatography (HPLC)

The separation and analysis of diglycerol (both linear and cyclic) and other PGs up to deca- and undeca-glycerols by HPLC are reported using a refractive index detector (RI) [40, 83]. Crowther *et al.* [84], have also used a liquid chromatograph equipped with an electrospray ionization mass spectrometry (ESI-MS) detector to identify PGs. The only limitation that was noted by the authors is the bad separation of the cyclic isomers (except for cyclic PG2). The summary of the analysis conditions is presented in Table 1.5.

Table 1.5. Summary of operating conditions used in previous works for HPLC-RI analyses.

Column	**Temperature (°C)**	**Eluent**	**Detector**	**Reference**
Waters carbohydrate	n.i.*	Acetonitrile – water (83:17)	RI	[83]
BioRad HPX-87H	60	Acetonitrile – water (50:50)	ESI-MS	[84]
Shimadzu Pathfinder	n.a.	H2O	RI	[40]
C18 Supelcosil	n.a.	-	ESI-MS	[69]

* n.i.: not indicated.

1.7.3 Size exclusion chromatography (SEC)

Size exclusion chromatography with a RI detector (SEC-RID) has been used to determine the distribution of hyperbranched polyglycerols, with a set of three columns: PSS GRAL e4/3/2 [74], PSS Gral column ($10^4/10^4/10^2$ Å porosity) [12] and PSS SDV columns (104/500/50 Å) [12, 85]. The analysis conditions applied in these studies are presented Table 1.6.

Table 1.6. Summary of operational conditions for GPC analysis

Column	**Temperature (°C)**	**Eluent**	**Standard**	**Detector**	**Reference**
PSS Gral ($10^6/10^4/10^2$ Å)	25	DMF (with LiBr)	PS	RI	[85]
PSS Gral ($10^4/10^4/10^2$ Å)	-	DMF (with LiBr)	PEG PS	UV-RI	[12]
PSS SDV (10^4/500/50 Å)	-	TCM-THF	PS	MALLS*	[12]
PSS GRAL e4/3/2	75	DMF (with LiBr)	PS	RI	[74]
PSS SDV e4/3/2 PSS SDV e6/5/4	30	Chloroform	PS	RI	[74]

* Multi angle laser light scattering

It should be kept in mind that SEC-RID gives:

1) a distribution of molecular masses in a given mixture. It means that a monomodal or bimodal distribution represents the existence of one or 2 groups of molecules with a similar range of molecular weights, respectively;
2) the molecular weight obtained is an average and not an absolute one as it based on a calibration curve constructed from molecular weight standards. Thus, the standard for the calibration and the samples should have similar chemical structures.

Nieberle [12] noted that the use of polystyrene (PS) standards may lead to an overestimation of PGs molecular masses due to the different chemical structures. Then, for low molecular weight PGs (up to 3000 Da), polyethylene glycol (PEG) standards are better suited as PGs structurally rather resemble PEG, while for molecular masses between 5000 and 20000 Da, PS standards seem to be more reliable [74, 85, 88].

1.7.4 Electrospray ionization mass spectrometry (ESI-MS)

Electrospray ionization is known to be an effective method to identify substances having high polarity. Electrospray ionization is a soft ionization method. The term *"soft"* indicates that minimum internal energy is transmitted to the analyte during the ionization process [89], so as to preserve the molecular ion without suffering from fragmentation or change in its structure at the source [90, 91].

In ESI, ionization is performed by spraying a sample of the solution to be analysed at atmospheric pressure under the influence of a high electric field resulting in the formation of highly charged droplets. Under these conditions, the droplets break down, forming positive or negative ions (in positive and negative modes, respectively), while moving forward inside the source and their sizes are continuously being reduced as shown in Figure 1.14 [92]. In positive mode, cations, for examples hydrogen ions often just called protons, interact with the droplets or molecules and form new bonds between the cations and the molecules. This produces adduct ions, called cationised molecules with a total mass equal to the mass of the molecule plus the mass of the cation.

One of the advantages of soft ionization methods is the fact that large organic molecules, such as synthetic polymers, that cannot be simply brought into the gas phase and ionized by conventional technique such as gas chromatography can then be detected. Another advantage of soft ionization techniques like ESI and MALDI is their possible coupling with time of flight (ToF) mass analyser. ToF mass analyser enables direct mass spectrometry of mixed polymers by showing the mass spectrum of different molecules in the sample sorted by their mass to charges ratios (*m*/*z*).

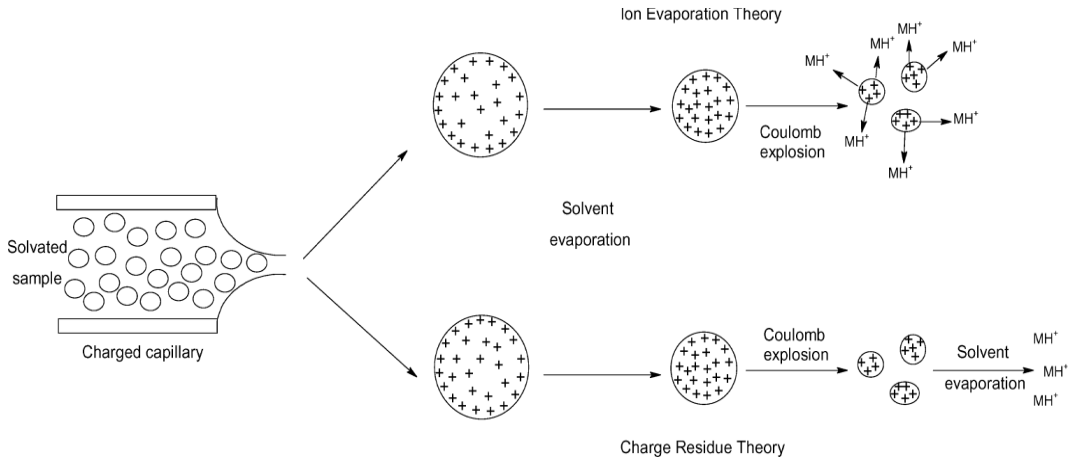

Figure 1.14. A scheme of the ESI mechanism in the positive mode [92].

For instance, tri-, hexa- and deca-polyglycerols from Lonza Co. [84]] and di- and tri-glycerols from Solvay Co. [74] were analysed by ESI-MS, where cyclic and non-cyclic PGs were successfully identified.

While the ESI technique is a very sensitive and precise method to identify various molecules, the identification of diol and triol functional groups such as glycerol is still difficult since the generated molecular ions have too short lifetime to be detected by mass analysis. Thus, the molecular ion peaks are very small or absent in the recorded spectra [93, 94].

1.7.5 Matrix-assisted laser desorption ionization (MALDI)

MALDI is another soft analytical technique for detecting and characterizing organic molecules and synthetics polymers. MALDI-ToF has been used to characterize hyperbranched PGs by [12, 74, 95].

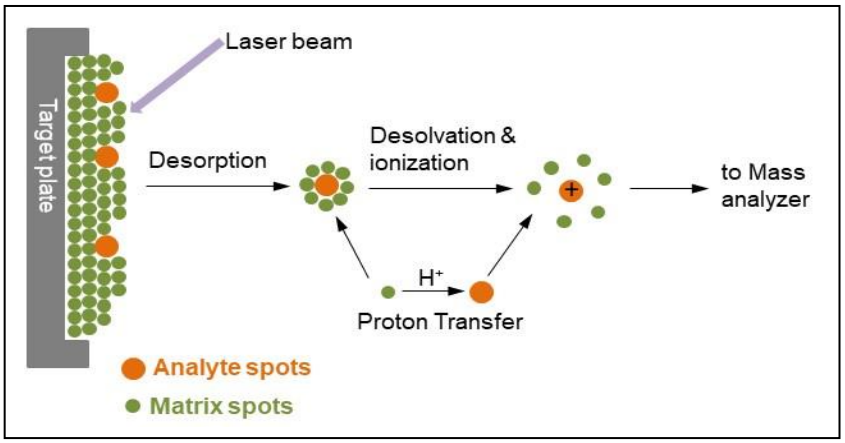

Figure 1.15. A scheme of ionization of molecules by MALDI.

In this technique, a laser absorbing matrix is used to create larger fragile molecules into gaseous ions without fragmentation or decomposition phenomenon [89, 96]. The laser energy is absorbed by the matrix molecules, which are energetically ablated from the surface of the sample, carrying the analyte molecules into the gas phase. During this process, the analytes are ionized by proton transfer from the nearby matrix molecules (single positive charge) as shown in Fig. 1.15 [92, 96].

While MALDI is a sensitive method to analyse polymers, it is limited to identifying the polymers with molecular weight below about 500 Da. Thus, the polyglycerols lower than PG7 are hardly detectable by this technique.

1.7.6 NMR

NMR has been used in many studied to characterize the structure of hyperbranched PGs [9, 12, 85]. On one hand, ^{13}C NMR spectroscopy allows to distinguish between dendritic (D), linear (L13, L14) and terminal (T) units and therefore to calculate the degree of branching (DB) in hyperbranched PGs. In addition, in order to determine the relative amounts of linear, terminal and dendritic subunits, ^{13}C-NMR-spectra of the polymer can be recorded and compared to spectra obtained from suitable model compounds [6, 8, 97]. On the other hand, ^{1}H NMR is reported as being non informative for the analysis of the different structural units with respect to linear, cyclic and branched compounds in PGs' mixtures [74].

1.8 Conclusions

Polyglycerols were shown to be very interesting polyols with a wide range of structures and, accordingly, of applications, particularly in the cosmetics, biomedical and food sectors. PGs are water soluble, biocompatible and highly functional materials. Currently, 52% of PGs market demand is occupied by the short chain PG2 and PG3 (Figure 2). However, PGs with a higher degree of polymerization (PG4 to PG10, namely PG4+) are also of high interest, due to the fact that the possibility of further functionalization is increased by increasing the numbers of available hydroxyl groups in PGs. Thus, in this thesis, we defined our target molecules in two categories, "PG2-3" and "PG4+".

The current industrial methods to produce PGs, like basic hydrolysis of epichlorohydrin, have many disadvantages, such as toxic and carcinogenic starting materials, low selectivity, the formation of high amounts of salts and so on. Using strong alkaline catalyst, such as NaOH and KOH as homogenous catalysts to directly convert glycerol to PGs, has also several disadvantages: fast reaction causes difficulty to control the degree of polymerization; the homogeneous catalyst cannot be recovered from the reaction medium and hence reused and; corrosion issues of the industrial equipment.

Hence, in the last two decades, attention has been paid to the development of a heterogeneously-catalysed process for glycerol direct polymerization over alkaline solid catalysts due to their advantages over alkaline homogeneous and acidic catalysts, such as a better control of the degree of polymerization, the ease of catalyst separation and recycling, as well as being non-corrosive for industrial equipment. Therefore, we aimed at developing a heterogeneous catalytic system to narrow the range of produced polyglycerols which means reaching a highly selective system to PG2-3 or PG4+.

Based on the literature review, alkaline earth oxides such as CaO, BaO and SrO are active catalysts for polyglycerols production and present a lower tendency to form acrolein (by-products). For instance, CaO, SrO, and BaO have shown a conversion of nearly 80% with 90% selectivity to di- and tri-glycerol (PG2-PG3) [40]. 96% of glycerol conversion with 86% selectivity to PG2-PG3 were also reported in the presence of $Ca_{1.6}La_{0.4}Al_{0.6}O_3$ [66].

Moreover, among alkaline earth oxides catalysts, CaO-based catalysts such as CaO, supported CaO on CNF, dolomite (CaO-MgO mixed oxides) and calcined eggshell have shown high catalytic performances with no acrolein formation (Table 1.3 and Figure 1.16). However, these catalysts showed a moderate selectivity to PG2-PG3 and PG4+, probably due to the low reaction temperature. For instance, CaO/CNF exhibited only 45% selectivity to PG2-3 and 55% selectivity to PG4+ at full glycerol conversion.

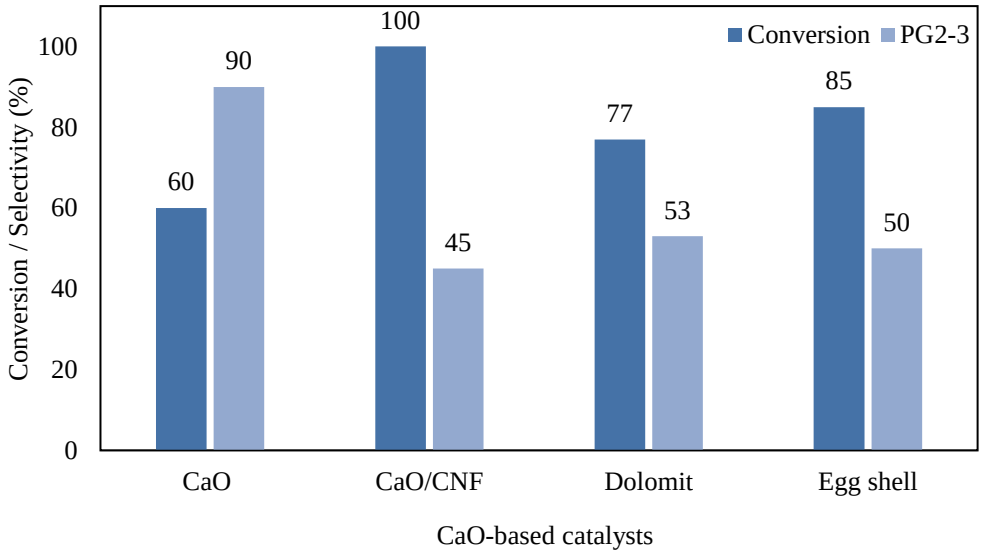

Figure 1.16. Glycerol conversion and selectivity to PG2-PG3 over CaO-based catalysts at 220 °C in the presence of 2 wt.% of various catalysts after 22 h of reaction (Table 1.3).

Furthermore, the catalysts were generally found unstable under polymerization reaction conditions. This is probably due to the water formation during the reaction, which caused a partial dissolution of the solid catalysts and hence a homogenous catalyst's contribution during glycerol polymerization reaction. For, Ca-based catalysts, this homogenous contribution has been reported by many groups in the forms of colloidal $Ca(OH)_2$ and Ca^{2+} [38, 40, 41]. For instance, Barros *et al.* [38] reported that 49% of solid CaO-egg shell became homogeneous (*i.e.*, dissolved in the reaction medium) after 24 h of reaction. Finally, considering, its high catalytic activity, its wide availability, its low cost and its absence of toxicity in case of leaching into the media, Ca-based catalysts could be considered as promising catalysts for glycerol polymerization reactions. However, the homogeneous contribution in the reaction is still a problem to solve.

Besides the catalyst, the operational conditions such as temperature, catalyst amount, atmosphere and reaction time play a very important role on the glycerol conversion and the degree of polymerisation. For instance, Sangkhum *et al.* [65] reported that the glycerol conversion on a 7.5%Ca-MgAl catalyst is doubled when the temperature is increased from 220 to 230 °C. Moreover, the effect of atmosphere has not been well studied in glycerol polymerization catalysed by solid catalysts. Therefore, the temperature, atmosphere and amount of catalyst will be investigated in this work.

Furthermore, in parallel and in order to analyse the complex mixtures of produced PGs containing linear, branched and cyclic isomers, different analytical techniques such as liquid chromatography, electron spray ionization, matrix-assisted laser desorption ionization and NMR will be applied to identify and characterize the produced compounds. In the literature, gas chromatography is the most commonly used method to identify the glycerol polymerization products (Table 1.2 and 1.3). However, this method is not applicable for polyglycerols higher than PG4 and also needs to have a standard for each PG isomers to be identified. On the other hand, electron spray ionization and matrix-assisted laser desorption ionization have been widely used to identify biopolymers and polymers including hyperbranched PGs, based on their molecular weights. Hence, we could benefit from these analytical methods in order to identify the polymerization products.

The overall aim of this thesis is to develop highly selective and stable catalysts for direct glycerol polymerization. Since there are only few reports on the heterogeneous catalytic system with high selectivity to PG4+, we plan to study a Ca-based catalytic system with high performances, in particular a high selectivity to PG4+. According to the literature, the operating conditions, such as temperature and the catalyst amount have a strong influence on the degree of polymerization, thus we will study these parameters in order to improve the PG4+ selectivity of our catalysts. Further, since the reported catalysts in the literature, particularly for PG2-PG3 formation, are almost systematically solubilized during the reaction, we will attempt to develop a more stable Ca-based catalysts able to favour the formation of PG2-3. Therefore, in order to reveal the best Ca-based catalyst, we will first study CaO, $Ca(OH)_2$ and $CaCO_3$. Then the catalytic performances of novel Ca-based catalysts including Ca-diglyceroxide and Ca-hydroxyapatites will be evaluated for this reaction. Moreover, a reliable analytical method will be considered to better identify the PGs obtained after reaction and, consequently, better estimate the selectivity of the tested catalysts.

References

[1] Díaz-Lasprilla, A. M.; Mercado, R. A.; Ramírez-Caballero, G. E. Glycerol Polymerization Degree Effect on the Emulsifying Properties of Polyglycerol Esters. *J. Appl. Polym. Sci.*, **2021**, 50566. https://doi.org/10.1002/app.50566.

[2] Gholami, Z.; Abdullah, A. Z.; Lee, K.-T. Dealing with the Surplus of Glycerol Production from Biodiesel Industry through Catalytic Upgrading to Polyglycerols and Other Value-Added Products. *Renew. Sustain. Energy Rev.*, **2014**, *39*, 327–341. https://doi.org/10.1016/j.rser.2014.07.092.

[3] Hejna, A.; Kosmela, P.; Formela, K.; Piszczyk, Ł.; Haponiuk, J. T. Potential Applications of Crude Glycerol in Polymer Technology–Current State and Perspectives. *Renew. Sustain. Energy Rev.*, **2016**, *66*, 449–475. https://doi.org/10.1016/j.rser.2016.08.020.

[4] *Glycerine: A Key Cosmetic Ingredient*; Jungermann, E., Sonntag, N., Eds.; Cosmetic science and technology series; Dekker: New York, 1991.

[5] Martin, A.; Richter, M. Oligomerization of Glycerol - a Critical Review. *Eur. J. Lipid Sci. Technol.*, **2011**, *113* (1), 100–117. https://doi.org/10.1002/ejlt.201000386.

[6] Cassel, S.; Debaig, C.; Benvegnu, T.; Chaimbault, P.; Lafosse, M.; Plusquellec, D.; Rollin, P. Original Synthesis of Linear, Branched and Cyclic Oligoglycerol Standards. *Eur. J. Org. Chem.*, **2001**, *2001* (5), 875–896. https://doi.org/10.1002/1099-0690(200103)2001:5<875::AID-EJOC875>3.0.CO;2-R.

[7] Galy, N.; Nguyen, R.; Blach, P.; Sambou, S.; Luart, D.; Len, C. Glycerol Oligomerization in Continuous Flow Reactor. *J. Ind. Eng. Chem.*, **2017**, *51*, 312–318. https://doi.org/10.1016/j.jiec.2017.03.020.

[8] Sunder, A.; Mülhaupt, R.; Frey, H. Hyperbranched Polyether−Polyols Based on Polyglycerol: Polarity Design by Block Copolymerization with Propylene Oxide. *Macromolecules*, **2000**, *33* (2), 309–314. https://doi.org/10.1021/ma991191x.

[9] Kainthan, R. K.; Muliawan, E. B.; Hatzikiriakos, S. G.; Brooks, D. E. Synthesis, Characterization, and Viscoelastic Properties of High Molecular Weight Hyperbranched Polyglycerols. *Macromolecules*, **2006**, *39* (22), 7708–7717. https://doi.org/10.1021/ma0613483.

[10] Kainthan, R. K.; Hester, S. R.; Levin, E.; Devine, D. V.; Brooks, D. E. In Vitro Biological Evaluation of High Molecular Weight Hyperbranched Polyglycerols. *Biomaterials*, **2007**, *28* (31), 4581–4590. https://doi.org/10.1016/j.biomaterials.2007.07.011.

[11] Pagliaro, M.; Rossi, M. *The Future of Glycerol*; 2008. https://doi.org/10.1039/9781847558305.

[12] Nieberle, J. Hyperbranched Polyglycerols as Building Blocks for Complex Amphiphilic Structures: Synthesis, Characterization and Applications. PhD thesis, Johannes Gutenberg University Mainz, 2008.

[13] Polyglycerols – Natural Ingredient for Personal Care Products https://grandviewresearchinc.blogspot.com/2018/05/polyglycerols-natural-ingredient-for-personal-care-products.html?utm_source=Social&utm_medium=twitter&utm_campaign=PriyaFCP30May&utm_content=Blog.

[14] Ciriminna, R.; Katryniok, B.; Paul, S.; Dumeignil, F.; Pagliaro, M. Glycerol-Derived Renewable Polyglycerols: A Class of Versatile Chemicals of Wide Potential Application. *Org. Process Res. Dev.*, **2015**, *19* (7), 748–754. https://doi.org/10.1021/op500313x.

[15] Meyer, J.; Friedrich, A.; Foetsch, H.; Springer, O.; Hof, J. M. von; Wenk, H. H. Polyglycerol Esters with a Particular Oligomer Distribution of the Polyglycerol. US9427385B2, August 30, 2016.

[16] Daly, S.; Maitra, P.; Setiawan, B. Sunscreen Compositions Containing a Uv-Absorbing Polyglycerol and a Non-Uv-Absorbing Polyglycerol. US20150320671A1, November 12, 2015.

[17] Babayan, V. K.; Lehman, H. Process for Preparation and Purification of Polyglycerols and Esters Thereof. US3637774A, January 25, 1972.

[18] Lemke, D. W. Processes for Preparing Linear Polyglycerols and Polyglycerol Esters. US6620904B2, 2003.

[19] Hasenhuettl, G. L. Synthesis and Commercial Preparation of Food Emulsifiers. In *Food Emulsifiers and Their Applications*; Hasenhuettl, G. L., Hartel, R. W., Eds.; Springer New York: New York, NY, 2008; pp 11–37. https://doi.org/10.1007/978-0-387-75284-6_2.

[20] Żołek-Tryznowska, Z.; Tryznowski, M.; Królikowska, J. Hyperbranched Polyglycerol as an Additive for Water-Based Printing Ink. *J. Coat. Technol. Res.*, **2015**, *12* (2), 385–392. https://doi.org/10.1007/s11998-014-9643-2.

[21] Thomas, A.; Müller, S. S.; Frey, H. Beyond Poly(Ethylene Glycol): Linear Polyglycerol as a Multifunctional Polyether for Biomedical and Pharmaceutical Applications. *Biomacromolecules*, **2014**, *15* (6), 1935–1954. https://doi.org/10.1021/bm5002608.

[22] Zhang, H.; Grinstaff, M. W. Recent Advances in Glycerol Polymers: Chemistry and Biomedical Applications. *Macromol. Rapid Commun.*, **2014**, *35* (22), 1906–1924. https://doi.org/10.1002/marc.201400389.

[23] Kumari, M.; Prasad, S.; Fruk, L.; Parshad, B. Polyglycerol-Based Hydrogels and Nanogels: From Synthesis to Applications. *Future Med. Chem.*, **2021**, *13* (4), 419–438. https://doi.org/10.4155/fmc-2020-0205.

[24] Salehpour, S.; Zuliani, C. J.; Dubé, M. A. Synthesis of Novel Stimuli-Responsive Polyglycerol-Based Hydrogels. *Eur. J. Lipid Sci. Technol.*, **2012**, *114* (1), 92–99. https://doi.org/10.1002/ejlt.201100049.

[25] Solano-Delgado, L. C.; Bravo-Sanabria, C. A.; Ardila-Suárez, C.; Ramírez-Caballero, G. E. Stimuli-Responsive Hydrogels Based on Polyglycerol Crosslinked with Citric and Fatty Acids. *Int. J. Polym. Sci.*, **2018**, *2018*, 1–8. https://doi.org/10.1155/2018/3267361.

[26] Oehrl, A.; Schötz, S.; Haag, R. Synthesis of PH-Degradable Polyglycerol-Based Nanogels by IEDDA-Mediated Crosslinking for Encapsulation of Asparaginase Using Inverse Nanoprecipitation. *Colloid Polym. Sci.*, **2020**, *298* (7), 719–733. https://doi.org/10.1007/s00396-020-04675-8.

[27] Ayoub, M.; Khayoon, M. S.; Abdullah, A. Z. Synthesis of Oxygenated Fuel Additives via the Solventless Etherification of Glycerol. *Bioresour. Technol.*, **2012**, *112*, 308–312. https://doi.org/10.1016/j.biortech.2012.02.103.

[28] Morlino, N. M.; Sweeny, P. G.; Curham, B. D. Polyglycerol Antifoam Agents in Paper Processing. US5429718A, July 4, 1995.

[29] Nilewski, M.; Favresse, P.; Scharf, A.; Gehrmann, P.; Mettin, T.; Schwan, M.; Springer, O.; Wied, T. Use of Polyglycerol Partial Esters as Defoamers. US9738797B2, August 22, 2017.

[30] Lu, Y. 10-20 Polyglycerol and Production Method Thereof. CN104650340A, May 27, 2015.

[31] Pinto, B. P.; De Araujo Mota, C. J. Developments in Glycerol Byproduct-Based Biorefineries. In *Advances in Biorefineries*; Elsevier, 2014; pp 364–385. https://doi.org/10.1533/9780857097385.1.364.

[32] Milewski, A.; Dydo, P.; Jakóbik-Kolon, A.; Czechowicz, D.; Babilas, D.; Burek, M.; Waśkiewicz, S.; Byczek-Wyrostek, A.; Krawczyk, T.; Kasprzycka, A. Preparation of Triglycerol from Glycerol and Epichlorohydrin at Room Temperature: Synthesis Optimization and Toxicity Studies. *ACS Sustain. Chem. Eng.*, **2018**, *6* (10), 13208–13216. https://doi.org/10.1021/acssuschemeng.8b02817.

[33] Cespi, D.; Cucciniello, R.; Ricciardi, M.; Capacchione, C.; Vassura, I.; Passarini, F.; Proto, A. A Simplified Early Stage Assessment of Process Intensification: Glycidol as a Value-Added Product from Epichlorohydrin Industry Wastes. *Green Chem.*, **2016**, *18* (16), 4559–4570. https://doi.org/10.1039/C6GC00882H.

[34] *Chemical Engineering of Polymers: Production of Functional and Flexible Materials*, 1st ed.; Mukbaniani, O. V., Abadie, M. J. M., Tatrishvili, T. N., Eds.; Apple Academic Press, 2017. https://doi.org/10.1201/9781315365985.

[35] Lemke, D. W.; Nivens, S. Process for Prepapring Polycerol and Mixed Ethers. US20080306211A1, December 11, 2008.

[36] Plasman, V.; Caulier, T.; Boulos, N. Polyglycerol Esters Demonstrate Superior Antifogging Properties for Films. *Plast. Addit. Compd.*, **2005**, *7* (2), 30–33. https://doi.org/10.1016/S1464-391X(05)00359-4.

[37] Len, C.; Delbecq, F.; Cara Corpas, C.; Ruiz Ramos, E. Continuous Flow Conversion of Glycerol into Chemicals: An Overview. *Synthesis*, **2018**, *50* (04), 723–741. https://doi.org/10.1055/s-0036-1591857.

[38] Barros, F. J. S.; Moreno-Tost, R.; Cecilia, J. A.; Ledesma-Muñoz, A. L.; de Oliveira, L. C. C.; Luna, F. M. T.; Vieira, R. S. Glycerol Oligomers Production by Etherification Using Calcined Eggshell as Catalyst. *Mol. Catal.*, **2017**, *433*, 282–290. https://doi.org/10.1016/j.mcat.2017.02.030.

[39] García-Sancho, C.; Moreno-Tost, R.; Mérida-Robles, J. M.; Santamaría-González, J.; Jiménez-López, A.; Torres, P. M. Etherification of Glycerol to Polyglycerols over MgAl Mixed Oxides. *Catal. Today*, **2011**, *167* (1), 84–90. https://doi.org/10.1016/j.cattod.2010.11.062.

[40] Ruppert, A. M.; Meeldijk, J. D.; Kuipers, B. W. M.; Erné, B. H.; Weckhuysen, B. M. Glycerol Etherification over Highly Active CaO-Based Materials: New Mechanistic Aspects and Related Colloidal Particle Formation. *Chem. - Eur. J.*, **2008**, *14* (7), 2016–2024. https://doi.org/10.1002/chem.200701757.

[41] Nieuwelink, A.-E. CaO/CNF for the Oligomerization of Glycerol. Master thesis, Utrecht University, Department of Chemistry, 2015.

[42] Barros, F. J. S.; Cecilia, J. A.; Moreno-Tost, R.; de Oliveira, M. F.; Rodríguez-Castellón, E.; Luna, F. M. T.; Vieira, R. S. Glycerol Oligomerization Using Low Cost Dolomite Catalyst. *Waste Biomass Valorization*, **2018**. https://doi.org/10.1007/s12649-018-0477-5.

[43] Ionescu, M.; Petrović, Z. S. On the Mechanism of Base-Catalyzed Glycerol Polymerization and Copolymerization. *Eur. J. Lipid Sci. Technol.*, **2018**, *120* (6), 1800004. https://doi.org/10.1002/ejlt.201800004.

[44] Ayoub, M.; Sufian, S.; Hailegiorgis, S. M.; Ullah, S.; Uemura, Y. Conversion of Glycerol to Polyglycerol over Waste Duck-Bones as a Catalyst in Solvent Free Etherification Process. *IOP Conf. Ser. Mater. Sci. Eng.*, **2017**, *226*, 012073. https://doi.org/10.1088/1757-899X/226/1/012073.

[45] Nguyen, R.; Galy, N.; Alasmary, F.; Len, C. Microwave-Assisted Continuous Flow for the Selective Oligomerization of Glycerol. *Catalysts*, **2021**, *11* (2), 166. https://doi.org/10.3390/catal11020166.

[46] Nguyen, R.; Galy, N.; Singh, A.; Paulus, F.; Stöbener, D.; Schlesener, C.; Sharma, S.; Haag, R.; Len, C. A Simple and Efficient Process for Large Scale Glycerol Oligomerization by Microwave Irradiation. *Catalysts*, **2017**, *7* (12), 123. https://doi.org/10.3390/catal7040123.

[47] Sayoud, N.; De Oliveira Vigier, K.; Cucu, T.; De Meulenaer, B.; Fan, Z.; Lai, J.; Clacens, J.-M.; Liebens, A.; Jérôme, F. Homogeneously-Acid Catalyzed Oligomerization of Glycerol. *Green Chem.*, **2015**, *17* (8), 4307–4314. https://doi.org/10.1039/C5GC01020A.

[48] Nosal, H.; Nowicki, J.; Warzała, M.; Nowakowska-Bogdan, E.; Zarębska, M. Synthesis and Characterization of Alkyd Resins Based on Camelina Sativa Oil and Polyglycerol. *Prog. Org. Coat.*, **2015**, *86*, 59–70. https://doi.org/10.1016/j.porgcoat.2015.04.009.

[49] Chen, X.; Peng, M. Method for Preparing Polyglycerine with High Degree of Polymerization. CN102532515A, July 4, 2012.

[50] Salehpour, S.; Dubé, M. A. Towards the Sustainable Production of Higher-Molecular-Weight Polyglycerol. *Macromol. Chem. Phys.*, **2011**, *212* (12), 1284–1293. https://doi.org/10.1002/macp.201100064.

[51] Ardila-Suárez, C.; Rojas-Avellaneda, D.; Ramirez-Caballero, G. E. Effect of Temperature and Catalyst Concentration on Polyglycerol during Synthesis. *Int. J. Polym. Sci.*, **2015**, *2015*, 1–8. https://doi.org/10.1155/2015/910249.

[52] Medeiros, M. A.; Araujo, M. H.; Augusti, R.; Oliveira, L. C. A. de; Lago, R. M. Acid-Catalyzed Oligomerization of Glycerol Investigated by Electrospray Ionization Mass Spectrometry. *J. Braz. Chem. Soc.*, **2009**, *20* (9), 1667–1673. https://doi.org/10.1590/S0103-50532009000900015.

[53] Richter, M.; Krisnandi, Y.; Eckelt, R.; Martin, A. Homogeneously Catalyzed Batch Reactor Glycerol Etherification by $CsHCO_3$. *Catal. Commun.*, **2008**, *9* (11–12), 2112–2116. https://doi.org/10.1016/j.catcom.2008.04.007.

[54] Charles, G.; Clacens, J.-M.; Pouilloux, Y.; Barrault, J. Préparation de Diglycérol et Triglycérol Par Polymérisation Directe Du Glycérol En Présence de Catalyseurs Mésoporeux Basiques. *Ol. Corps Gras Lipides*, **2003**, *10* (1), 74–82. https://doi.org/10.1051/ocl.2003.0074.

[55] Bookong, P.; Ruchirawat, S.; Boonyarattanakalin, S. Optimization of Microwave-Assisted Etherification of Glycerol to Polyglycerols by Sodium Carbonate as Catalyst. *Chem. Eng. J.*, **2015**, *275*, 253–261. https://doi.org/10.1016/j.cej.2015.04.033.

[56] Clacens, J.-M.; Pouilloux, Y.; Barrault, J. Selective Etherification of Glycerol to Polyglycerols over Impregnated Basic MCM-41 Type Mesoporous Catalysts. *Appl. Catal. Gen.*, **2002**, *227* (1–2), 181–190. https://doi.org/10.1016/S0926-860X(01)00920-6.

[57] Harris, B. Polyglycerol Esters of Aliphatic Acids of Relatively High Molecular Weight. US2023388, 1935.

[58] Garti, N.; Aserin, A.; Zaidman, B. Polyglycerol Esters: Optimization and Techno-Economic Evaluation. *J. Am. Oil Chem. Soc.*, **1981**, *58* (9), 878–883. https://doi.org/10.1007/BF02672963.

[59] Chai, S.-H.; Wang, H.-P.; Liang, Y.; Xu, B.-Q. Sustainable Production of Acrolein: Investigation of Solid Acid–Base Catalysts for Gas-Phase Dehydration of Glycerol. *Green Chem.*, **2007**, *9* (10), 1130. https://doi.org/10.1039/b702200j.

[60] Harris, E. G.; Hees, U.; Bunte, R.; Hachgenei, J. W.; Kuhm, P. Process for the Production of Oligoglycerol Mixtures of Increased Diglycerol Content. US5349094A, September 20, 1994.

[61] Krisnandi, Y. K.; Eckelt, R.; Schneider, M.; Martin, A.; Richter, M. Glycerol Upgrading over Zeolites by Batch-Reactor Liquid-Phase Oligomerization: Heterogeneous versus Homogeneous Reaction. *ChemSusChem*, **2008**, *1* (10), 835–844. https://doi.org/10.1002/cssc.200800128.

[62] Sivaiah, M. V.; Robles-Manuel, S.; Valange, S.; Barrault, J. Recent Developments in Acid and Base-Catalyzed Etherification of Glycerol to Polyglycerols. *Catal. Today*, **2012**, *198* (1), 305–313. https://doi.org/10.1016/j.cattod.2012.04.073.

[63] Guerrero-Urbaneja, P.; García-Sancho, C.; Moreno-Tost, R.; Mérida-Robles, J.; Santamaría-González, J.; Jiménez-López, A.; Maireles-Torres, P. Glycerol Valorization by Etherification to Polyglycerols by Using Metal Oxides Derived from MgFe Hydrotalcites. *Appl. Catal. Gen.*, **2014**, *470*, 199–207. https://doi.org/10.1016/j.apcata.2013.10.051.

[64] Pérez-Barrado, E.; Pujol, M. C.; Aguiló, M.; Llorca, J.; Cesteros, Y.; Díaz, F.; Pallarès, J.; Marsal, L. F.; Salagre, P. Influence of Acid–Base Properties of Calcined MgAl and CaAl Layered Double Hydroxides on the Catalytic Glycerol Etherification to Short-Chain Polyglycerols. *Chem. Eng. J.*, **2015**, *264*, 547–556. https://doi.org/10.1016/j.cej.2014.11.117.

[65] Sangkhum, P.; Yanamphorn, J.; Wangriya, A.; Ngamcharussrivichai, C. Ca–Mg–Al Ternary Mixed Oxides Derived from Layered Double Hydroxide for Selective Etherification of Glycerol to Short-Chain Polyglycerols. *Appl. Clay Sci.*, **2019**, *173*, 79–87. https://doi.org/10.1016/j.clay.2019.03.006.

[66] Gholami, Z.; Abdullah, A. Z.; Lee, K.-T. Selective Etherification of Glycerol over Heterogeneous Mixed Oxide Catalyst: Optimization of Reaction Parameters. *Chem. Eng. Sci.*, **2013**, *1* (4), 79–86. https://doi.org/10.12691/ces-1-4-6.

[67] Kaiser, A.; Weckhuysen, B. M.; Leinweber, D.; Kirby, F.; Scherl, F. X.; Metz, H. J.; Bruijnincx, P. C. A. Preparation of Polyglycerols. WO2015122770A1, August 20, 2015.

[68] Kirby, F.; Nieuwelink, A.-E.; Kuipers, B. W. M.; Kaiser, A.; Bruijnincx, P. C. A.; Weckhuysen, B. M. CaO as Drop-In Colloidal Catalysts for the Synthesis of Higher Polyglycerols. *Chem. - Eur. J.*, **2015**, *21* (13), 5101–5109. https://doi.org/10.1002/chem.201405906.

[69] Caputo, D.; Casiello, M.; Milella, A.; Oberhauser, W.; Maffezzoli, A.; Nacci, A.; Fusco, C.; D'Accolti, L. Deep Control of Linear Oligomerization of Glycerol Using Lanthanum Catalyst on Mesoporous Silica Gel. *Catalysts*, **2020**, *10* (10), 1170. https://doi.org/10.3390/catal10101170.

[70] Sajid, M.; Ayoub, M.; Yusup, S.; Abdullah, B.; Shamsuddin, R.; Bilad, R.; Chong, C. C.; Aqsha, A. Short-Chain Polyglycerol Production via Microwave-Assisted Solventless Glycerol Polymerization Process Over Lioh-Modified Aluminium Pillared Clay Catalyst: Parametric Study. *Processes*, **2020**, *8* (9), 1093. https://doi.org/10.3390/pr8091093.

[71] Han, Y. H.; Kim, H. R.; Han, I. S.; Choi, H. O.; Kim, H. S.; An, S. Y.; Youn, Y. H. Metal Oxide Catalysts for Etherification, Method for Its Preparation Thereof, and Method for the Production of Linear Polyglycerol Using the Same. WO2010044531A2, April 22, 2010.

[72] Barrault, J.; Clacens, J.-M.; Pouilloux, Y. Methods for Etherifying Glycerol, and Catalysts for Implementing Said Methods. WO2001098243A1, December 27, 2001.

[73] Gholami, Z.; Abdullah, A. Z.; Lee, K. T. Heterogeneously Catalyzed Etherification of Glycerol to Diglycerol over Calcium–Lanthanum Oxide Supported on MCM-41: A Heterogeneous Basic Catalyst. *Appl. Catal. Gen.*, **2014**, *479*, 76–86. https://doi.org/10.1016/j.apcata.2014.04.024.

[74] Barriau, E. Hyperbranched Polyether Polyols as Building Blocks for Complex Macromolecular Architectures. Phd thesis, Johannes Gutenberg University Mainz, 2005.

[75] Cammenga, H. K.; Schulze, F. W.; Theuerl, W. Vapor Pressure and Evaporation Coefficient of Glycerol. *J. Chem. Eng. Data*, **1977**, *22* (2), 131–134. https://doi.org/10.1021/je60073a004.

[76] Wilson, R.; van Schie, B. J.; Howes, D. Overview of the Preparation, Use and Biological Studies on Polyglycerol Polyricinoleate (PGPR). *Food Chem. Toxicol.*, **1998**, *36* (9–10), 711–718. https://doi.org/10.1016/S0278-6915(98)00057-X.

[77] Nalawade, S. P.; Picchioni, F.; Janssen, L. P. B. M. Supercritical Carbon Dioxide as a Green Solvent for Processing Polymer Melts: Processing Aspects and Applications. *Prog. Polym. Sci.*, **2006**, *31* (1), 19–43. https://doi.org/10.1016/j.progpolymsci.2005.08.002.

[78] de Caro, P.; Bandres, M.; Urrutigoïty, M.; Cecutti, C.; Thiebaud-Roux, S. Recent Progress in Synthesis of Glycerol Carbonate and Evaluation of Its Plasticizing Properties. *Front. Chem.*, **2019**, *7*. https://doi.org/10.3389/fchem.2019.00308.

[79] Costa, J. de R. M.; Santos, R. C. R.; Coutinho, L. P.; Silva, O. R.; Barros, H. O.; Freire, V. N.; Valentini, A. CO_2 Role on the Glycerol Conversion over Catalyst Containing CaO-SiO2 Doped with Ag and Pt. *Catal. Today*, **2019**. https://doi.org/10.1016/j.cattod.2019.02.009.

[80] Kouzu, M.; Tsunomori, M.; Yamanaka, S.; Hidaka, J. Solid Base Catalysis of Calcium Oxide for a Reaction to Convert Vegetable Oil into Biodiesel. *Adv. Powder Technol.*, **2010**, *21* (4), 488–494. https://doi.org/10.1016/j.apt.2010.04.007.

[81] Reyero, I.; Arzamendi, G.; Gandía, L. M. Heterogenization of the Biodiesel Synthesis Catalysis: CaO and Novel Calcium Compounds as Transesterification Catalysts. *Chem. Eng. Res. Des.*, **2014**, *92* (8), 1519–1530. https://doi.org/10.1016/j.cherd.2013.11.017.

[82] Barrault, J.; Jerome, F. Design of New Solid Catalysts for the Selective Conversion of Glycerol. *Eur. J. Lipid Sci. Technol.*, **2008**, *110* (9), 825–830. https://doi.org/10.1002/ejlt.200800061.

[83] Naveen Kumar, T.; Sastry, Y. S. R.; Lakshminarayana, G. Analysis of Polyglycerols by High-Performance Liquid Chromatography. *J. Chromatogr. A*, **1984**, *298*, 360–365. https://doi.org/10.1016/S0021-9673(01)92732-3.

[84] Crowther, M. W.; O'Connell, T. R.; Carter, S. P. Electrospray Mass Spectrometry for Characterizing Polyglycerols and the Effects of Adduct Ion and Cone Voltage. *J. Am. Oil Chem. Soc.*, **1998**, *75* (12), 1867–1876. https://doi.org/10.1007/s11746-998-0343-x.

[85] Schubert, C.; Osterwinter, C.; Tonhauser, C.; Schömer, M.; Wilms, D.; Frey, H.; Friedrich, C. Can Hyperbranched Polymers Entangle? Effect of Hydrogen Bonding on Entanglement Transition and Thermorheological Properties of Hyperbranched Polyglycerol Melts. *Macromolecules*, **2016**, *49* (22), 8722–8737. https://doi.org/10.1021/acs.macromol.6b00674.

[86] Gaudin, P.; Jacquot, R.; Marion, P.; Pouilloux, Y.; Jérôme, F. Acid-Catalyzed Etherification of Glycerol with Long-Alkyl-Chain Alcohols. *ChemSusChem*, **2011**, *4* (6), 719–722. https://doi.org/10.1002/cssc.201100129.

[87] De Meulenaer, B.; Van Royen, G.; Vanhoutte, B.; Huyghebaert, A. Combined Liquid and Gas Chromatographic Characterisation of Polyglycerol Fatty Acid Esters. *J. Chromatogr. A*, **2000**, *896* (1–2), 239–251. https://doi.org/10.1016/S0021-9673(00)00391-5.

[88] Luo, X.; Li, Y. Synthesis and Characterization of Polyols and Polyurethane Foams from PET Waste and Crude Glycerol. *J. Polym. Environ.*, **2014**, *22* (3), 318–328. https://doi.org/10.1007/s10924-014-0649-8.

[89] El-Aneed, A.; Cohen, A.; Banoub, J. Mass Spectrometry, Review of the Basics: Electrospray, MALDI, and Commonly Used Mass Analyzers. *Appl. Spectrosc. Rev.*, **2009**, *44* (3), 210–230. https://doi.org/10.1080/05704920902717872.

[90] Leal, R. V. P.; Sarmanho, G. F.; Leal, L. H.; Garrido, B. C.; Carvalho, L. J.; Rego, E. C. P.; Seidl, P. R. Potential of Electrospray Ionization Mass Spectrometry (ESI-MS), Using Direct Infusion, to Quantify Fatty Acid Methyl Esters (FAMEs) in Biodiesel. *Anal. Methods*, **2017**, *9* (26), 3949–3955. https://doi.org/10.1039/C7AY00644F.

[91] Conway, U.; Warren, A. D.; Arthur, C. J.; Gates, P. J. A Study of the Application of Graphite MALDI to the Analysis of Short-Chain Polyethylene Glycols. *Polym. Chem.*, **2021**, *12* (3), 439–448. https://doi.org/10.1039/D0PY01493A.

[92] El-Aneed, A.; Cohen, A.; Banoub, J. Mass Spectrometry, Review of the Basics: Electrospray, MALDI, and Commonly Used Mass Analyzers. *Appl. Spectrosc. Rev.*, **2009**, *44* (3), 210–230. https://doi.org/10.1080/05704920902717872.

[93] Shen, S.; Zhang, F.; Zeng, S.; Zheng, J. An Approach Based on Liquid Chromatography/Electrospray Ionization–Mass Spectrometry to Detect Diol Metabolites as Biomarkers of Exposure to Styrene and 1,3-Butadiene. *Anal. Biochem.*, **2009**, *386* (2), 186–193. https://doi.org/10.1016/j.ab.2008.12.007.

[94] Samame, R. A.; Zu, C.; Knueppel, D. Identification of Vicinal Diols Using a Diagnostic Ion Derived from the Electron Ionization of Orthoester Functional Groups. *Rapid Commun. Mass Spectrom.*, **2020**, *34* (17). https://doi.org/10.1002/rcm.8842.

[95] Nilüfer Solak. Structural Characterization and Quantitative Analysis by Interfacing Liquid Chromatography and/or Ion Mobility Separation with Multi-Dimensional Mass Spectrometry. Phd thesis, university of Akron, 2010.

[96] McEwen, C. N.; Simonsick, W. J.; Larsen, B. S.; Ute, K.; Hatada, K. The Fundamentals of Applying Electrospray Ionization Mass Spectrometry to Low Mass Poly(Methyl Methacrylate) Polymers. *J. Am. Soc. Mass Spectrom.*, **1995**, *6* (10), 906–911. https://doi.org/10.1016/1044-0305(95)00476-T.

[97] Stiriba, S.-E.; Kautz, H.; Frey, H. Hyperbranched Molecular Nanocapsules: Comparison of the Hyperbranched Architecture with the Perfect Linear Analogue. *J. Am. Chem. Soc.*, **2002**, *124* (33), 9698–9699. https://doi.org/10.1021/ja026835m.

Chapter 2

Materials and Methods

2.1 Materials

Calcium oxide and calcium hydroxide were purchased from Alfa Aesar. Glycerol (99% and 99.5% purity), calcium carbonate, calcium nitrate tetrahydrate, $(NH_4)H_2PO_4$, NH_4OH (25-30% solution), ethanol (99.5% purity) and Pluronic® P-123 (Mw~5800 g/mol), molecular sieve adsorbent 5 Å (30-40 mesh) were purchased from Sigma-Aldrich.

The solvents used for ESI-MS analysis were H_2O LiChrosolv® from Merck, methanol and acetonitrile Optima™ (99.9 % purity) from Fisher Chemical. They were all of analytical grade (LC/MS grade). PGs standards including, "polyglycerol 6" (PG6) and "polyglycerol 10" (PG10), were provided kindly by Lonza Co. and "PG2" and "PG3" samples were provided kindly by Dr. Joël Barrault, honorary research director at CNRS.

For MALDI analysis, Trifluoroacetic acid (TFA) and 2,5-Dihydroxybenzoic acid (DHB) were from Sigma-Aldrich and α-Cyano-4-hydroxycinnamic acid (HCCA) was purchased from Tokyo Chemical Industry (TCI).

All the chemicals were used as such without any further purification.

2.2 Catalysts preparation

2.2.1 Calcined CaO

Calcined calcium oxide (CaO) was freshly prepared as described by Ruppert *et al.* [1], performing a high temperature treatment of calcium nitrate tetrahydrate ($Ca(NO_3)_2.4H_2O$) under static air in a calcination oven, where the nitrate salt was heated to 700 °C with a ramp of 10 °C/min for 2 h. Then, freshly calcined CaO was crushed using a mortar and sieved to particle size in the 53 to 100 µm range.

2.2.2 Calcium diglyceroxides

Calcium diglyceroxide (CaDG) was prepared by a modified procedure previously described in the literature [2, 3]. Namely, a mixture of CaO and glycerol (10 : 42 molar ratio) was diluted in an excess of methanol as a solvent and heated to 60 °C for 4 h (Figure 2.1). Then, the obtained yellowish precipitate was washed with methanol to remove unreacted glycerol before the remaining solvent was evaporated under vacuum at 90 °C. We obtained a yield in CaDG of 91 %.

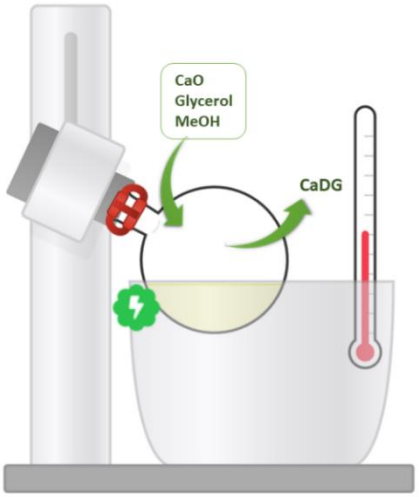

Figure 2.1. Schematic of the CaDG synthesis.

2.2.3 Calcium hydroxyapatites

Hereafter, we describe the methods for synthetizing calcium hydroxyapatites used in this study (Chapter 4).

2.2.3.1 Stoichiometric hydroxyapatite

A stoichiometric hydroxyapatite (noted HAp-S in the following) with the theoretical formula $Ca_{10}(PO_4)_6(OH)_2$ was synthesized by adding dropwise 60 mL of 0.55 M aqueous solution of $Ca(NO_3)_2.4H_2O$ to 200 mL of an aqueous solution of $NH_4H_2PO_4$ (0.099 M) placed under stirring at 70 °C. The pH of the solution was adjusted to 10 prior to mixing by adding a 25-30% NH_4OH aqueous solution (as shown in Figure 2.2). The formed precipitate was centrifuged and washed with milli-Q H_2O several times, before drying at 80 °C for 48 h. Then the obtained white solid calcined at 700 °C with a ramp of 10 °C/min under static air for 4 h.

The HAp-S is formed according to Eq (2.1):

$$10\ (Ca(NO_3)_2.4\ H_2O) + 6NH_4H_2PO_4 + 14NH_4OH \rightarrow Ca_{10}(PO_4)_6(OH)_2 + 20NH_4NO_3 + 52\ H_2O \quad \text{Eq (2.1)}$$

2.2.3.2 Deficient hydroxyapatite

A deficient hydroxyapatite (noted HAp-D in the following) with the theoretical formula $Ca_{8.7}(PO_4)_{4.7}(HPO_4)_{1.3}(OH)_{0.7}$ was synthesized by a method similar to that described in Section 2.2.3.1., but by adding dropwise 60 mL of an aqueous solution of $Ca(NO_3)_2.4H_2O$ (0.55 M) to 200 mL of a $(NH_4)H_2PO_4$ solution with a 0.115 M concentration.

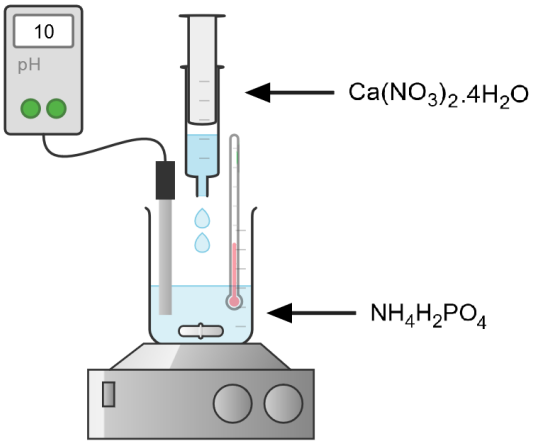

Figure 2.2. Schematic of the set-up used for the synthesis of HAp-S by the precipitation method.

2.2.3.3 Overstoichiometric hydroxyapatite

A Ca-rich hydroxyapatite (noted HAp-R in the following) with the theoretical formula $Ca_{11.62}(PO_4)_6(OH)_{2.62}$ was synthesized by an impregnation method similar to methods described previously in the literature [4, 5].

To synthetize HAp-R, 4.9 g of $Ca(OH)_2$ (0.066 mmol) were mixed in 145 mL of milli-Q H_2O as solvent. The pH of this initial solution was 12.9. Then, 2.32 mL of a 85% of H_3PO_4 solution (0.0341 mmol) was added very slowly to adjust the pH to 4. The slurry mixture was heated at 80 °C for 48 h, before the precipitate was filtered and washed with milli-Q water several times and then dried at 80 °C for 72 h before calcination under static air at 700 °C for 4 h with a ramp of 10 °C/min.

2.2.3.4 P123-hydroxyapatite

P123-hydroxyapatite (noted HAp-CP in the following) was prepared by a modified method described by Mohammad *et al.* [6] by adding 1.68 g of Pluronic P123 to 100 mL of 0.099 M of $(NH_4)H_2PO_4$ aqueous solution. The solution was heated to 70 °C until P123 was fully dissolved. Then, 30 mL of a 0.55 M of $Ca(NO_3)_2.4H_2O$ aqueous solution was added dropwise. The pH of the solutions was adjusted to 10 prior to mixing by adding an appropriate amount of a 25-30% NH_4OH solution. The formed precipitate was centrifuged and washed several times with milli-Q H_2O before final drying at 80 °C for 48 h under static air. Then, the obtained white solid was calcined at 550 °C for 4 h under static air with a ramp of 2 °C/min.

2.2.3.5 Carbonated hydroxyapatite

A carbonated hydroxyapatite (noted HAp-CO in the following) was prepared, using the calcined HAp-S as starting material. 1 g of HAp-S was placed in a glass reactor under CO_2 atmosphere at room temperature and kept for 60 min under these conditions.

2.2.3.6 CaO/HAp

A series of CaO supported on HAp (CaO/HAp) catalysts was prepared by impregnation of $Ca(NO_3)_2.4H_2O$ over deficient HAp (HAp-D), similar to the method described by Yan *et al.* [7] to prepare $CaO\text{-}CeO_2$ supported on HAp. For preparing *x* wt.% CaO/HAp catalyst, the desired amount of $Ca(NO_3)_2.4H_2O$ was dissolved in milli-Q water before mixing with non-calcined Hap-D, as presented in Table 2.1. The slurry solutions were mixed overnight before drying at 80 °C for 12 h and then calcined under static air for 4 h at 700 °C with a ramp of 2 °C/min.

Table 2.1. Weight percentage of loaded CaO (*x*), required amount of Ca nitrate salt and HAp-D for each preparation, theoretical ratio of Ca/P and molecular weight of obtained catalysts.

***x* (wt%)**	**Ca Nitrate (g)**	**HAp-D (g)**	**Ca/P**	**Mw (g/mol)**
5	0.21	0.95	1.6	340.5
10	0.42	0.9	1.76	268.7
30	1.27	0.7	2.63	145.8

2.3 Catalyst characterization

2.3.1 Surface area

The Brunauer-Emmett-Teller (BET) model served as the basis for the measurement of the specific surface area of our materials. N_2 physisorption isotherms at liquid nitrogen temperature were obtained on a TriStar II Plus gas adsorption analyzer (Micromeritics) after outgassing at 130 °C in vacuum for 3 h. The specific surface area was evaluated over the range P/P_0 = 0.05-0.30.

2.3.2 X-ray Photoelectron Spectroscopy (XPS)

X-ray Photoelectron Spectroscopy (XPS) is a quantitative spectroscopic technique that it is widely used for the chemical analysis of the surface layers of catalysts. A typical XPS spectrum plots the number of electrons detected versus their binding energy, where the number of detected electrons is directly related to the amount of element within the XPS sampling volume. To calculate the atomic percentage values, each raw XPS signal was corrected by dividing its signal intensity by a "relative sensitivity factor" (RSF), and normalized over all the elements detected, using the CasaXPS software.

XPS spectra were collected on an Axis UltraDLD Kratos spectrometer using the monochromatic Al Kα radiation (hv = 1486.6 eV) as the excitation source. The calibration of the XPS spectra was made using the carbon C 1s reference peak at 284.8 eV.

2.3.3 X-Ray diffraction (XRD)

X-Ray diffraction patterns of the solid catalysts were recorded on a D8 Discover X-Ray Diffractometer from Bruker using an X-Ray tube in Cu (Kα) radiation (λ = 1.54060 Å). The diffraction angle 2θ was in the 5-70° range with integration steps of 0.01° per second.

2.3.4 Infrared spectroscopy (IR)

Infrared spectroscopy (IR) spectra were recorded on a Fourier transform infrared spectrometer (FTIR), Tensor 37-HTS-XT from Bruker. This technique is used to determine the nature of chemical bonds present in a sample and to characterize the molecular groups to obtain information on the conformation and possible interactions [8]. An MCT (Mercury-Cadmium-Telluride) photoelectric detector cooled by liquid N_2 was used in reflection mode. The spectra were recorded by accumulating 16 scans with a resolution of 4 cm^{-1}. The surface of each sample was flattened before analysis.

2.3.5 Solid state-NMR

The most common technique to get high-resolution NMR spectra is the magic angle spinning (MAS), where the solid sample is rotated very fast about an axis inclined at a "magic" angle θ = 54°44' to the direction of B_0 This technique has been considered as the basis of solid-state NMR. Cross polarization (CP) is routinely used for sensitivity improvement when measuring the SS MAS NMR spectra of spin I = 1/2 nuclei (*i.e.*, ^{13}C). Herein, SS CP-MAS ^{13}C NMR spectra were recorded using a 400 MHz Bruker BioSpin spectrometer equipped with AVANCE-III consoles at spinning rate of 10 Hz for CaGs catalysts.

2.3.6 Elemental analysis

The carbon and hydrogen amount of HAps catalysts were determined using a Thermo Scientific FlashSmart automated analyser. The samples were weighted in tin containers and introduced into the combustion reactor. The reactor was filled with copper oxide followed by wire reduced nickel and maintained at 950 °C and operated with dynamic flash combustion of the sample, where the C and H were detected as CO_2 and H_2O, respectively. The resulted gases were separated on a packed column heated at 60 °C in an oven and detected by a thermal conductivity detector (TCD).

2.3.7 Inductively coupled plasma-optic emission spectroscopy (ICP-OES)

The inductively coupled plasma-optic emission spectroscopy (ICP-OES) is an analytical technique used for quantitative determination of the elements present in a sample. These analyses were performed on a 720-ES ICP-OES from Agilent with axially viewing and simultaneous CCD detection. The quantitative determination of metal content in the catalysts and in the reaction media were made based on the analysis of certificated standard solution (SCP Science). The ICP Expert™ software (version 2.0.4) was used to provide the concentration of Ca and P in liquid samples.

For liquid samples taken from the reaction media, 20 mg were diluted with 4 mL of milli-Q water. To prepare the solid samples, an acid digestion method was applied for total dissolution of catalysts before analysis. Then, 10 mg of each sample were digested with 2 mL aqua Regia (0.5 mL HNO_3 + 1.5 mL HCl) and mixed with a sonification for 15 min and kept overnight at ambient temperature before analysis.

The operating parameters of the instrument were continuously monitored to ensure the maximum performance and reliability of the ICP-OES results. All the analyses were performed 40 min after the spectrometer was turned on to achieve a stable plasma as well as a constant and reproducible sample introduction.

2.3.8 Thermal Analyses

Thermo Gravimetric and Differential Scanning Calorimetry (TGA and DSC) were performed using a Setaram Labsys instrument. A continuous heating was applied from room temperature to 900 °C (for CaGs) and 1100°C (for HAps) with a constant heating rate of 10 °C /min under nitrogen flow.

2.3.9 Scanning electron microscopy (SEM)

To study the morphology of the solid catalysts, scanning electron microscopy (SEM) pictures were recorded on a Hitachi S3600N electron microscope equipped with a Thermo Ultradry EDS detector using an acceleration voltage of 15 kV. The magnification was controlled in the range 30-200 µm.

2.4 Catalytic tests

Several reactors setups were tested to identify the most appropriate one for the glycerol polymerization reaction, notably considering the fact that this reaction is carried out without solvent, in a viscous glycerol-rich medium, in presence of polyglycerols and of a solid catalyst. Herein, the catalytic tests, which were performed either in a Parr® batch reactor (Fig 2.3a) or in a Schlenk-tube reactor (Fig 2.3b), will be detailed below.

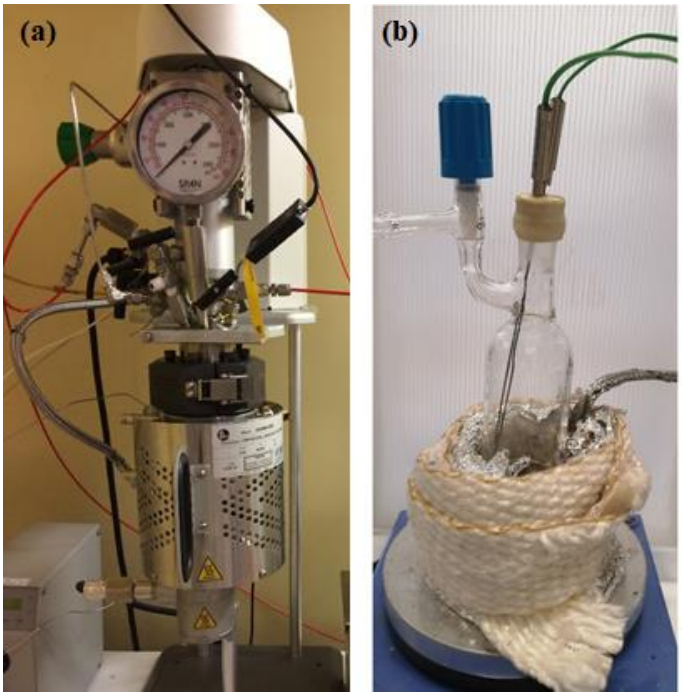

Figure 2.3. a) 50 mL Parr® stainless steel batch reactor and b) 100 mL Schlenk tube reactor.

2.4.1 Parr® batch reactor

A 50 mL Parr® stainless steel batch reactor, equipped with a 4-blades agitator, a thermocouple and a gas injector pipe, was used (Figure 2.3-a). For these experiments, 326 mmol (30 g) of glycerol and a desired amount of freshly calcined calcium oxide (3.2 and 9.6 mol.% based on the number of moles of glycerol) were introduced in the reactor vessel surrounded by a heater. The temperature of reaction was measured by a thermocouple. The experiments were performed under an inert gas (nitrogen or carbon dioxide). In order to remove air, the reactor was purged with N_2 or CO_2 gas up to 10 bar and held for few minutes (3-4 times). The temperature was increased with a rate of approximately 6 °C/min till it reached the desired temperature (210-240 °C).

2.4.2 Schlenk tube reactor

Catalytic tests were performed in a 100 mL Schlenk tube reactor heated by a metallic coil. The inner temperature was controlled by an external heater-controller. The reactor tube was thermally isolated and placed on a stirrer plate during the reaction (Figure 2.3b). To perform the experiments, 218 mmol (20 g) of glycerol and 0.5-3.5 mol.% of catalysts (based on the glycerol number of moles), were introduced in the tube. The temperature was set at the desired value in the range 230-260 °C while stirring was maintained at 1000 rpm. The experiments were performed under N_2 as an inert gas. To remove air, N_2 was flowed through the reactor 30 minutes prior to reaction.

The catalytic tests were performed under vacuum. After the purging by N_2, a 420 mbar vacuum was applied to the reactor. The reactor was placed in a silicon oil bath at 245 °C and the temperature was controlled by a thermocouple placed in the oil bath.

2.4.2.1 Schlenk-tube reactor equipped with an adsorption column

To evacuate the formed water during the reaction, the Schlenk-tube reactor was equipped with an adsorption column, filled with a molecular sieve adsorbent as shown on Figure 2.4. The catalytic tests were carried out in a 100 mL Schlenk tube equipped with a glass column of 30 cm length and 9 mm internal diameter, filled with 6.2 g of molecular sieves adsorbent. The column was packed with adsorbent between two layers of glass wool. For each test 218 mmol (20 g) of glycerol and 2 mol.% of catalyst (based on the number of moles of glycerol) were introduced in the reactor. The reactor was placed in an oil bath at 245 °C and stirred with a magnetic bar at 1000 rpm. The temperature was controlled by a thermocouple placed in the oil bath.

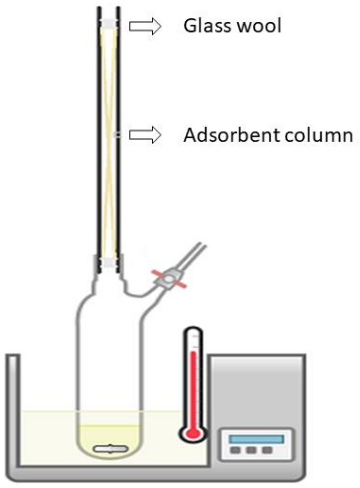

Figure 2.4. Schematic of the Schlenk-tube reactor equipped with an adsorption column.

2.4.3 Carousel

To study the Ca glyceroxides formation, experiments were carried out in 20 mL glass tubes of a Radleys® Carousel reaction station (Figure 2.5). This station is equipped with 12 glass reaction tubes, a stirring hotplate and a cooling system placed on head of the tubes for reflux. To perform the experiments in the carousel's tubes, 8 g (87 mmol) of glycerol and 3.5 mol.% of commercial CaO (based on the number of moles of glycerol) were introduced in each tube, heating set on desired temperature of 230 °C while stirring rate was set at 800 rpm. The temperature was measured individually in each tube by thermocouples. The experiments were performed under N_2 as an inert gas. In order to remove air, N_2 was flowed through the reactors for 30 minutes prior to reaction. The samples were taken out of the reactor station when the temperature reached the desired temperature, namely at 80 °C, 130 °C, 180 °C and 230 °C.

Figure 2.5. A Radleys® Carousel 12-reaction station.

After reactions, the solid catalysts were separated by centrifugation and the liquid phase diluted in a solvent (See details in Section 2.5) to do further analysis.

2.5 Glycerol and polyglycerol analyses

In this thesis, we used several characterization methods for analysing the polyglycerols. Prior to utilizing these techniques to analyse our own reaction products, we used available PGs standards including PG2, PG3, PG6 and PG10 to identify the most suitable analytical techniques among HPLC, SEC, ESI-MS, MALDI-ToF and NMR.

2.5.1 HPLC

High Performance Liquid Chromatography (HPLC) is a form of column chromatography in which a liquid sample or analyte is injected in a solvent (known as the mobile phase) at high pressure through a column filled with chromatographic packing material (the stationary phase).

In order to separate and consequently quantify the glycerol and the reaction products, two different HPLC columns, namely Bio-Rad Aminex HPX-87H and Phenomenex Organic acid H+, were used.

To perform HPLC analyses, 1-5 mg of viscous liquid phase after reaction was diluted in 1 mL of milli-Q H_2O and then filtered to eliminate the solid. The analyses were carried out on a Dionex Ultimate 3000 equipped with a Phenomenex column (organic acid H+) 300 x 7.8 mm with RI detector. The mobile phase used was a 5 mM H_2SO_4 aqueous solution at a flow rate of 0.6 mL/min. The column was maintained at room temperature.

Similar sample preparation was applied, when the HPLC column was changed to a Bio-Rad Aminex HPX-87H column 300 x 7.8 mm. The mobile phase used was a 5 mM H_2SO_4 aqueous solution at a flow rate of 0.5 mL/min. The column was maintained at 60 °C. A typical chromatogram for HPLC-RI using Bio-Rad Aminex column is displayed in Figure 2.6.

A calibration curve was made for glycerol using both columns.

The glycerol conversion was calculated by Equation (2.2) based on the HPLC-RI measurement:

$$Glycerol\ conversion(\%) = 100 * \frac{initial\ mol\ of\ glycerol - mol\ of\ unreacted\ glycerol}{initial\ mol\ of\ glycerol} \quad \text{Eq (2.2)}$$

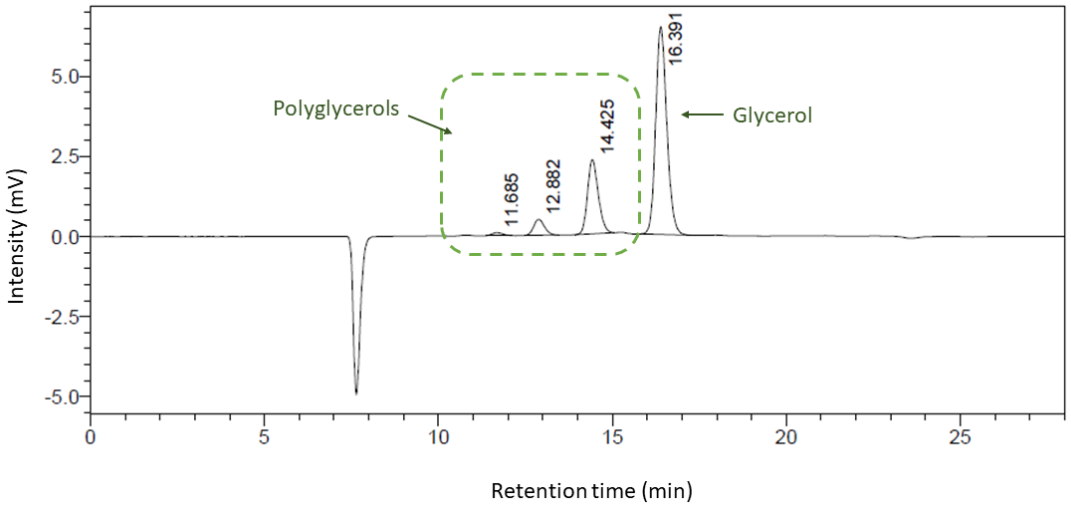

Figure 2.6. Typical chromatogram obtained for HPLC-RI using a Bio-Rad Aminex column.

Further, PG2 and PG3 standards were analysed by these two columns in our laboratory. For PG2, one main peak at 14.4 min and another peak at 12.8 min were observed (see Annex A-Figure A.1), whereas, for PG3, five main peaks at retention times of 10.1, 10.8, 11.6, 12.8 and 14.4 min were observed, whereas the glycerol peak was located at 16.4 min (Fig 2.6). However, the ESI-MS results revealed (see Section 2.5.3 for details) that the PG2 samples actually contained PG2 to PG5, whereas PG3 contained 7 PGs of the PG3-PG6 range. Thus, it was concluded that the separation of all PGs is not possible by HPLC, as it was already suggested in the literature [9]. Therefore, we used the HPLC-RI only to quantify only the amount of glycerol in the reaction mixture.

2.5.2 SEC

Size exclusion chromatography (SEC) analyses was performed by a PSS SECurity SEC instrument equipped with a RI detector. The analyses were performed by PSS GRAM column combination low (3x10 µ GRAM 100 Å, each 8 x 300 mm) with PSS 10 µ GRAM guard column, where the eluent was dimethylacetamide (DMAc) and the standard was polyethylene glycol (PEG) with molecular weights of 329 to 25,300 Da. These analyses were done by Polymer Standards Service (PSS) Co. in Germany for 3 PG samples.

Here, we analysed polyglycerols standards including PG6, PG10 and a catalytic reaction mixture, with a 80% glycerol conversion (see Section B.2.2 for details).

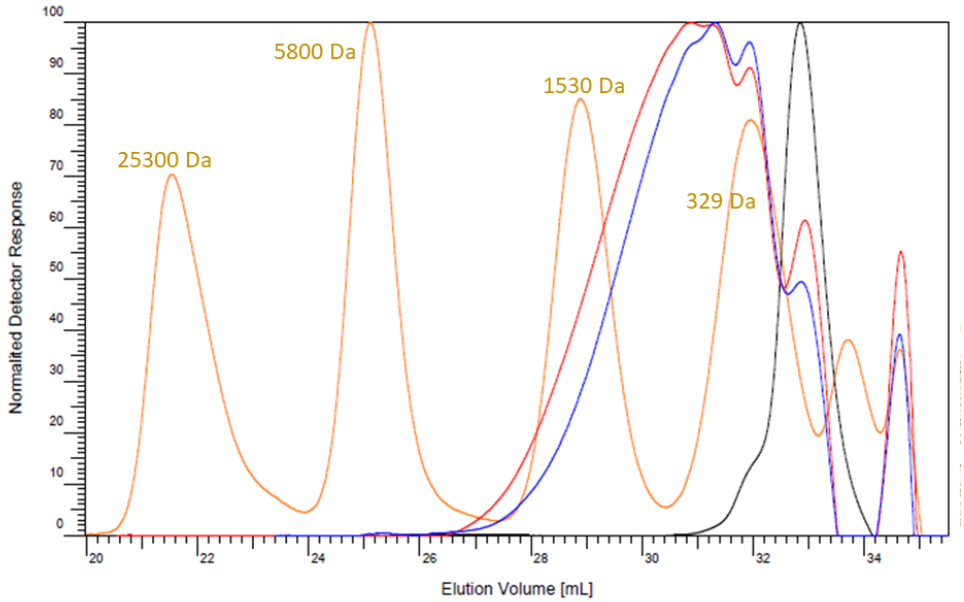

Figure 2.7. Normalized chromatograms of a PG6 standard (blue), a PG10 standard (red), a catalytic reaction mixture (with an 80% glycerol conversion) (black) and a PEG standards (orange).

The three samples' chromatograms and the chromatogram of the PEG standard (with molecular masses equal to 25300, 5800, 1530 and 329 Da) are shown in Figure 2.7. The components of the samples elute after the PEG standards having a molar mass of 5800 Da indicating that their molar masses were lower than this value. For PG6 (Fig 2.7-blue) and PG10 (Fig 2.7-red), 2 peaks were observed, one in the zone lower than 329 Da and another one with four shoulders between ~329 and ~1530 Da, which indicated that the samples have different products distributions.

It is worth mentioning that separation of molecules in SEC analyses is based on hydrodynamic volume and therefore shows a mass distribution in a sample.

2.5.3 Direct infusion ESI-MS

Here, polyglycerols analyses were conducted by direct Electrospray Ionization-Mass Spectrometry (ESI-MS) in a Waters ESI-MS/MS SYNAPT G2-Si HDMS (High Definition Mass Spectrometer) set in the positive ion mode. However, the electrospray ionization mechanism is a very complex method affected by numerous factors such as cone voltage, analyte concentrations, type of solvents and additives [9]. Their adjustment for this study is detailed in Section A.2 of Annex A. Thus, ESI source conditions were set as follows: heated capillary temperature 300 °C, spray voltage 3 kV and capillary voltage 60 V. The mass spectra were acquired in a 50-1800 m/z range and were obtained as an average of 50 scans, each one requiring 0.5 s of acquisition time. The samples diluted in HPLC grade H_2O:methanol (1:1 by vol.) mixture were directly infused into the ESI source at a flow rate of 10 mL/min. Before each set of analysis, the mass spectrometer was calibrated by Sodium formate (NaF) solution in the positive mode.

Taking into account the adjusted parameters, herein, the PG2, PG3, PG6 and PG10 were analysed by direct infusion ESI-MS.

2.5.3.1 Standard analysis

The result of ESI-MS analysis for PG2 standards, showed that PG2 contains linear (or branched) PG2 and PG3 as well as cyclic PG3-5 (Fig 2.8-a), whereas PG3 standard contains linear (or branched) PG3-6 and also cyclic PG4-6 (Fig 2.8-b).

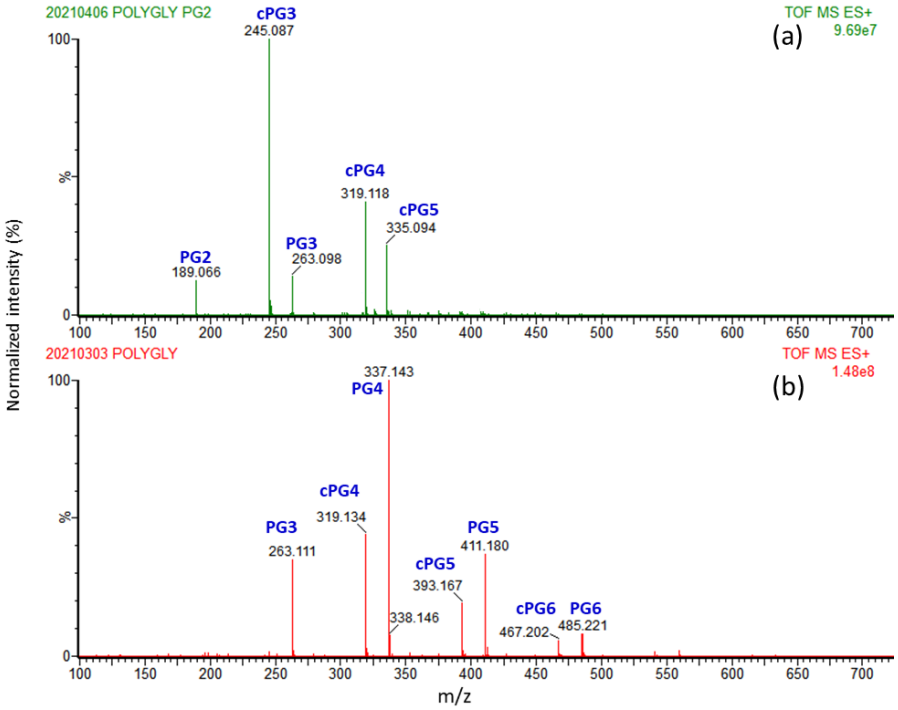

Figure 2.8. ESI-MS spectra for a) PG2 and b) PG3 standards.

Spectra for PG6 and PG10 presented a more complex feature suggesting the presence of several linear (or branched) and cyclic forms. PG6 standard (Fig 2.9a) contains polymers between 245 Da corresponding to $[cPG3+Na]^+$ and PG19 (Fig 2.9a), where the major peak is at 409.1 Da corresponding to $[cPG5+K]^+$. For PG10, the degree of polymerization began from PG3 at 261 Da ($[cPG3+K]^+$) to PG21 (Figure A.2b), where the major peaks observed at 409.1 and 483 Da corresponding to $[cPG5+K]^+$ and $[cPG6+K]^+$, respectively.

Furthermore, observing the peaks at 1463.6 Da (PG19) and 1593.7 Da (PG21) for PG6 and PG10 respectively (Figure A.2) can confirm the sensitivity of ESI-MS techniques.

To better read the ESI-MS spectra, the exact masses for PG2 to PG14, and for their common protonation and cationizations forms are presented in Table A.1.

Finally, the polyglycerol relative selectivity – defined as the ratio of desired oligomers ($PG_{2\text{-}3}$, $PG_{4\text{-}5}$ and PG_{6+}) based on the intensity of total PGs obtained by direct infusion of ESI-MS – was calculated by Eq (2.3):

$$PG_{a-b}\ selectivity = 100 * \frac{Sum\ of\ desired\ PGs\ intensities}{total\ PGs\ intensities} = 100 * \frac{\sum_a^b PG_i}{\sum_2^n PG_i} \qquad \text{Eq (2.3)}$$

Where the *a* and *b* are the number of monomers in PG.

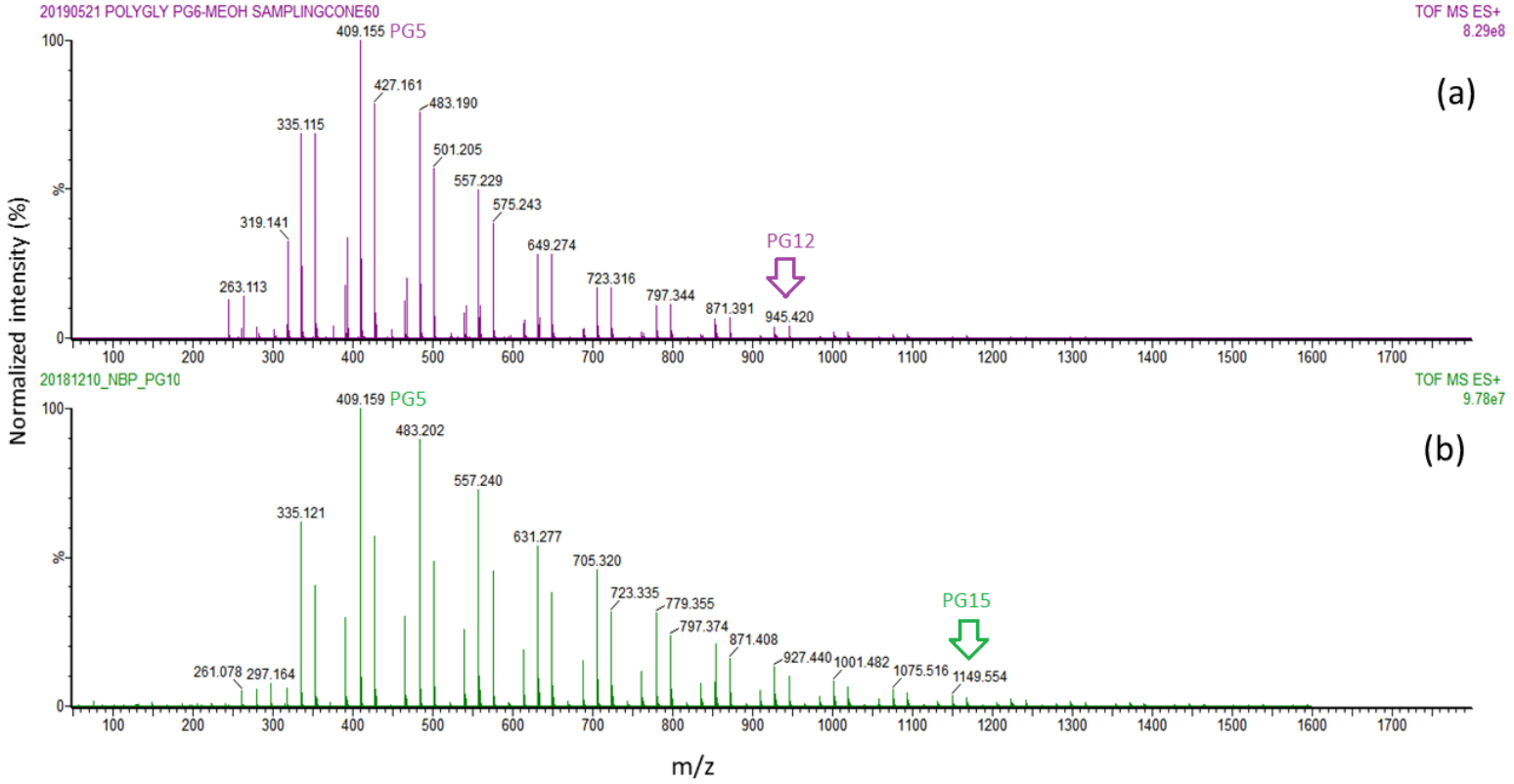

Figure 2.9. ESI-MS spectra for a) PG6 and b) PG10 standards.

2.5.4 MALDI-ToF

In this thesis, the MALDI-ToF MS measurements were performed on an Autoflex Speed Maldi ToF/ToF (Bruker) equipped with a nitrogen laser. Polyethylene glycol (PEG 1000) was used to calibrate the spectra.

We examined the PG6 and PG10 standards using two matrixes: *2,5*-dihydroxybenzoic acid (DHB), and *α*-cyano-*4*-hydroxycinnamic acid (HCCA), as the common matrixes used for MALDI. Matrix solutions were freshly prepared in acetonitrile/H_2O (70/30 v:v) with addition of 0.01% trifluoroacetic acid (TFA) to improve the signal to noise ratio. A sample solution and a matrix solution were poured on a polish stainless steel MALDI target plate.

The results shown in Figure 2.10 present two different PG distributions for PG6 standard (between 400 to 3000 Da), where the major peaks were attributed to PG9 or PG14 when HCCA and DHB were used as matrixes, respectively. Sometimes, a shift in polymerization degree can be observed by using different matrixes [10, 11]. For instance, Conway *et al.* [10] recently showed that the apparent distribution of polyethylene glycols (PEG) (a commonly used standard for MALDI calibration), were changed when 8 different matrixes were used. The other reason for observing a shift in apparent polymerization degree could be due to the fact that when the molecules bound to the cation are very small, it could cause a distortion of the observed molecular weight distribution towards higher masses as reported in the literature [10, 12].

Moreover, PG10 standard was only observed when HCCA was used as the matrix. This observation suggested that HCCA was a better matrix compared to DHB for analysing the PGs. However, as shown in Figure A.4, the polymer peaks were observed from 500 Da and the major peak was attributed to PG9, where the peak between 0 and 500 Da (black dashed in Fig A.4), showing that the matrix caused the analyte (PGs) suppression. It should be noted that “analyte suppression” is a very common issue for MALDI analysis, where caused a detection limitation in the range of molecular masses below 500 Da [10, 13].

From the ESI-MS analyses, we however know that the PG6 and PG10 standards do indeed contain some shorter chain oligomers. It is also possible that the shorter chains are not being detected because they are unable to bind cations present in the sample tightly enough, thus shifting the observed distribution towards higher mass polymer chains. This observation is consistent with previous reports which claimed that the binding energy between the polymer chain and added Na^+ or K^+ cations is too small to survive the MALDI mechanism [10, 14]. Therefore, it can be concluded that MALDI is not a suitable technique to be utilized in the present study.

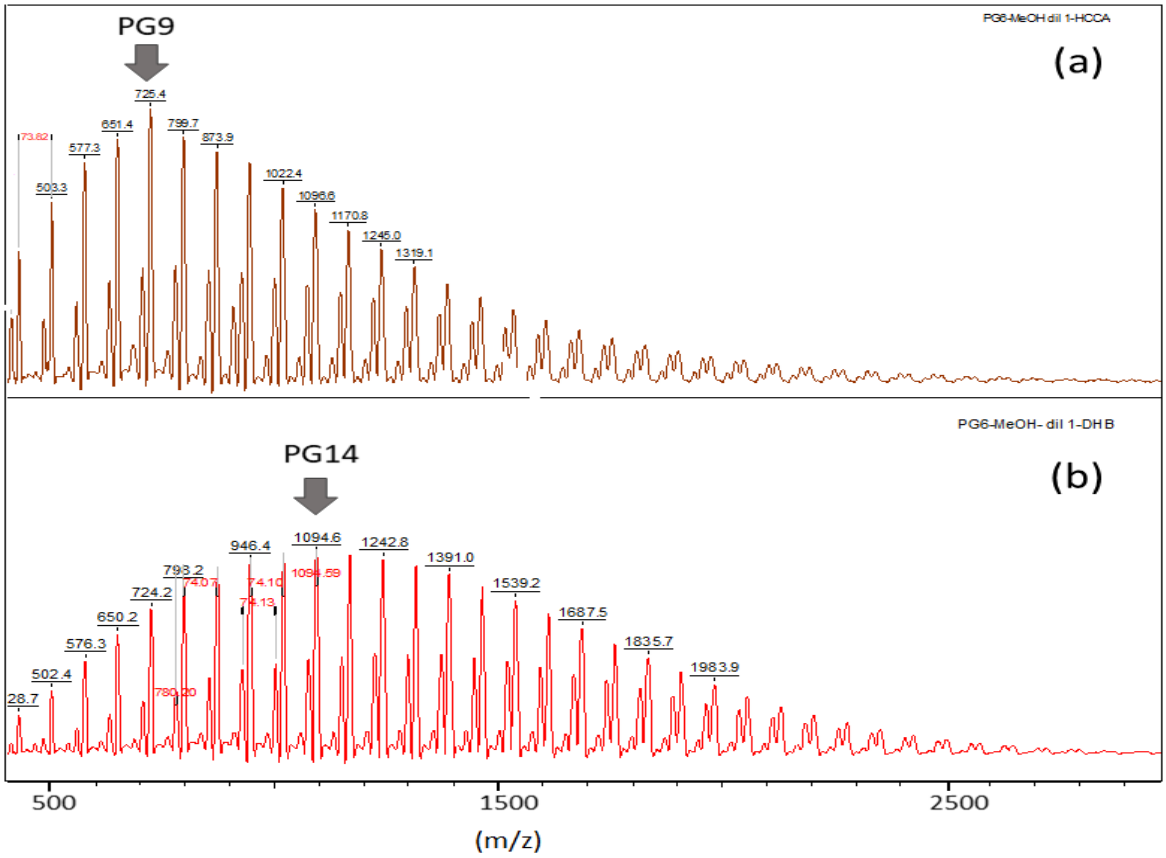

Figure 2.10. MALDI spectra for PG6 standard with a) HCCA and b) DHB as matrixes.

2.5.5 NMR

The NMR experiments were recorded on a Bruker AVANCE II 400 MHz and a Bruker Advance NEO 900 MHz. To prepare the samples, 200 μL of samples were dissolved into 400 μL of H_2O:D_2O (3:1 by vol.) solution.

Glycerol and PGs standards containing PG2, PG3, PG6 and PG10 were analyzed by ^{13}C NMR. For these compounds, the detected peaks' chemical shifts varied in the range of 60 to 85 ppm (Figure 2.11) in agreement with the literature [15, 16].

Based on the glycerol structure (Scheme A.1-1), 2 peaks at 62.7 ppm and 72.1 ppm assigned to -CH_2OH (2 equivalent carbons) and -CH-OH, respectively, were observed by ^{13}C NMR (Fig 2.11). For PG2 standard, 7 peaks at 60.7 ppm, 62.7 ppm, 70.5 ppm, 70.7 ppm, 70.9 ppm, 72 ppm and 81.1 ppm correspond to carbon chain in PGs were observed, which were assigned to linear or branched PG2-3 and cyclic PG3-5, based on the ESI-MS results (shown in Fig 2.8a). Some possible PG2 and PG3 structures that can be present in PG2 standard are shown in Scheme A.1. Besides, the ^{13}C NMR chemical shifts corresponding to these structures, based on the literature [15, 16], are listed in Table A.4.

For the PG2 standard, despite the fact that it contained no glycerol (based on HPLC result, shown in Fig A.1), the chemical shifts at 62.7 ppm 72.1 and 70.5 ppm were assigned to the -CH_2OH and -CH-OH, respectively. For linear PG2 (Scheme A.1-2) and linear PG3 (Scheme A.1-6), the peaks between 70.5-70.9 ppm were assigned to the -CHOH- carbon chain of these structures (2 and 6), as shown in Table A.4. However, the presence of two peaks at 60.7 and 81.1 ppm suggested the presence of branched PG2 (3 and 4) and branched PG3 (8). Moreover, cyclic PG2 (5) is expected to exhibit a peak at 60.7 ppm assigned to -CH_2OH and 2 peaks in the range of 70.5-70.9 ppm corresponding to -CH_2O- and -CHO- of the cyclic carbon chain (Table A.2) [15]. Thus, since cyclic PG2 (5) and a mixture of PG2 (2,3 and 4) possess the same chemical shifts, one cannot conclude on the presence or absence of cyclic PGs in the mixture only based on NMR results.

Moreover, for PG3 standards, 3 supplementary peaks were observed (Fig 2.11) at 68.8 ppm, 69.3 ppm, 79.4 ppm compared to PG2 standards. They were assigned to the carbon chains of branched PG3 (7 and 8) or other branched PG4-6, knowing the fact that for linear PG4-6, likewise to linear PG3 (6), 4 peaks are expected to be observed, assigned to -CH_2OH, -CHOH and -CH_2-O- in these PGs.

The ^{13}C NMR spectra of PG6 and PG10 standards are presented in Fig 2.11. Likewise, the presence of various peaks in the range of 60 to 85 ppm indicates the presence of various PGs structures including linear, branched and cyclic forms. However, it is very difficult to assess the exact structure due to the presence of the same basic units and consequently to the observation of similar chemical shifts.

Hence, it can be concluded that NMR as a sole technique, is not suitable for the analysis of a mixture of various structural units without any separation prior to characterization.

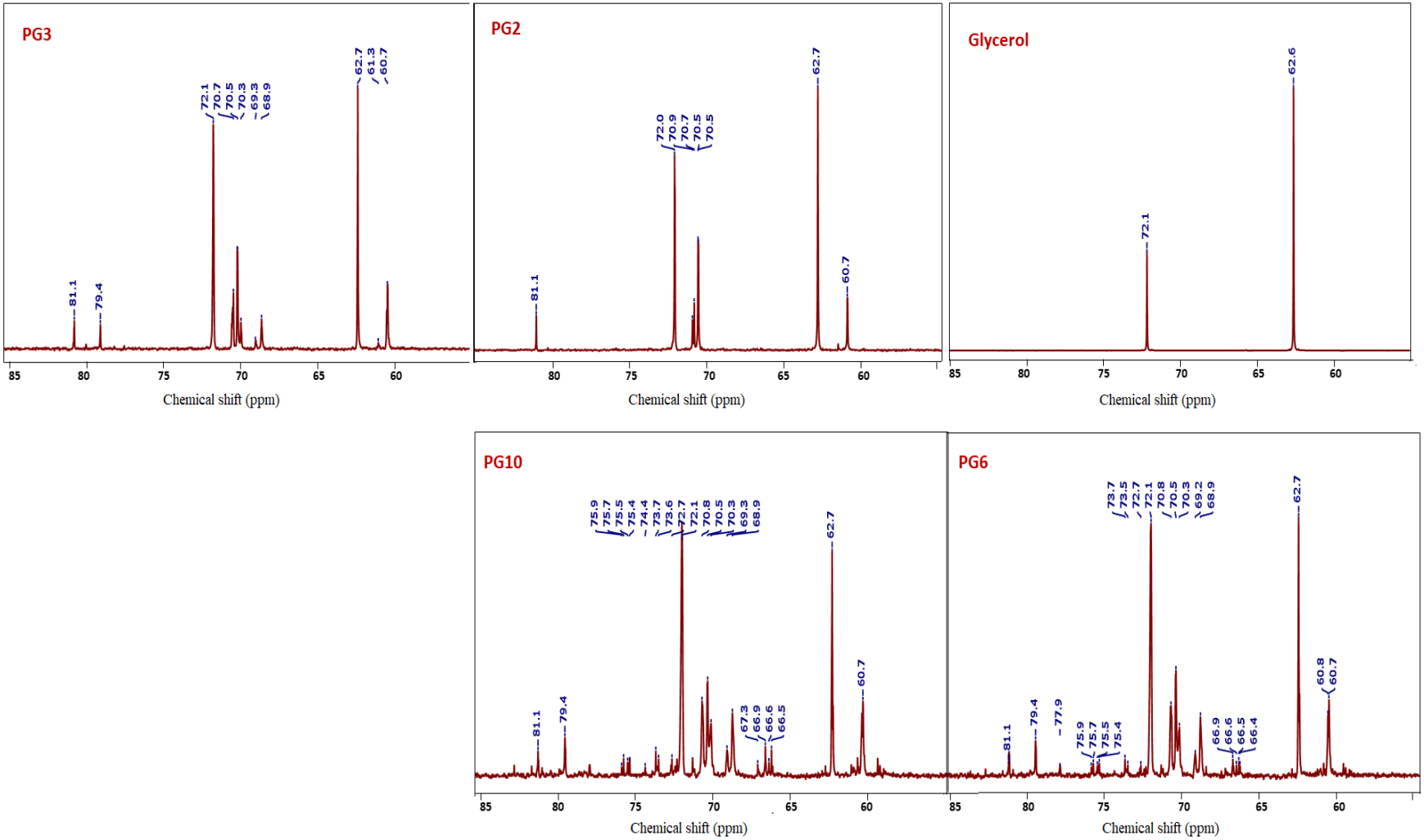

Figure 2.11. ^{13}C NMR spectra for glycerol, PG2, PG3, PG6 and PG10 standards.

2.5.6 Conclusion on polyglycerol analyses

The analytical results for PGs standards indicated that the separation of all PGs is not possible by liquid chromatography methods, neither by HPLC nor by SEC analysis. Nevertheless, it can still provide an information on the presence of polymers in the reaction mixture, besides the fact that HPLC is still a suitable method to detect and quantify the glycerol. Moreover, ESI-MS, as a soft ionization technique, confirmed that PGs samples are a mixture of non-cyclic (linear or branched) and cyclic PGs, based on the polymer's exact mass, whereas, MALDI-ToF, as another soft ionization technique, was not able to detect the polymer with molecular masses lower than 500 Da (corresponds to PGs < pentaglycerol). Our results on PGs standards suggest that ^{13}C NMR could be also used to distinguish between linear and branched structures.

Thus, we decided to choose the HPLC and ESI-MS techniques as the routine methods to analyse glycerol and products.

References

[1] Ruppert, A. M.; Meeldijk, J. D.; Kuipers, B. W. M.; Erné, B. H.; Weckhuysen, B. M. Glycerol Etherification over Highly Active CaO-Based Materials: New Mechanistic Aspects and Related Colloidal Particle Formation. *Chem. - Eur. J.*, **2008**, *14* (7), 2016–2024. https://doi.org/10.1002/chem.200701757.

[2] Kouzu, M.; Hidaka, J.; Wakabayashi, K.; Tsunomori, M. Solid Base Catalysis of Calcium Glyceroxide for a Reaction to Convert Vegetable Oil into Its Methyl Esters. *Appl. Catal. Gen.*, **2010**, *390* (1–2), 11–18. https://doi.org/10.1016/j.apcata.2010.09.029.

[3] Esipovich, A.; Rogozhin, A.; Danov, S.; Belousov, A.; Kanakov, E. The Structure, Properties and Transesterification Catalytic Activities of the Calcium Glyceroxide. *Chem. Eng. J.*, **2018**, *339*, 303–316. https://doi.org/10.1016/j.cej.2018.01.142.

[4] Verwilghen, C.; Rio, S.; Nzihou, A.; Gauthier, D.; Flamant, G.; Sharrock, P. J. Preparation of High Specific Surface Area Hydroxyapatite for Environmental Applications. *J. Mater. Sci.*, **2007**, *42* (15), 6062–6066. https://doi.org/10.1007/s10853-006-1160-y.

[5] Liu, J.; Ye, X.; Wang, H.; Zhu, M.; Wang, B.; Yan, H. The Influence of PH and Temperature on the Morphology of Hydroxyapatite Synthesized by Hydrothermal Method. *Ceram. Int.*, **2003**, *29* (6), 629–633. https://doi.org/10.1016/S0272-8842(02)00210-9.

[6] Mohammad, N. F.; Amiruddin, N. L.; Saleh, S. S. M.; Taib, M. A. A.; Nasir, N. F. M. Effect of Swelling Agent on Pore Properties of Mesoporous Carbonated Hydroxyapatite. *J. Phys. Conf. Ser.*, **2019**, *1372*, 012018. https://doi.org/10.1088/1742-6596/1372/1/012018.

[7] Yan, B.; Zhang, Y.; Chen, G.; Shan, R.; Ma, W.; Liu, C. The Utilization of Hydroxyapatite-Supported CaO-CeO_2 Catalyst for Biodiesel Production. *Energy Convers. Manag.*, **2016**, *130*, 156–164. https://doi.org/10.1016/j.enconman.2016.10.052.

[8] REALCAT http://realcat.ec-lille.fr/en/realcat-techniques-Equipements.html.

[9] Crowther, M. W.; O'Connell, T. R.; Carter, S. P. Electrospray Mass Spectrometry for Characterizing Polyglycerols and the Effects of Adduct Ion and Cone Voltage. *J. Am. Oil Chem. Soc.*, **1998**, *75* (12), 1867–1876. https://doi.org/10.1007/s11746-998-0343-x.

[10] Conway, U.; Warren, A. D.; Arthur, C. J.; Gates, P. J. A Study of the Application of Graphite MALDI to the Analysis of Short-Chain Polyethylene Glycols. *Polym. Chem.*, **2021**, *12* (3), 439–448. https://doi.org/10.1039/D0PY01493A.

[11] Soeriyadi, A. H.; R.Whittaker, M.; Boyer, C.; Davis, T. P. Soft Ionization Mass Spectroscopy: Insights into the Polymerization Mechanism. *J. Polym. Sci. Part Polym. Chem.*, **2013**, *51* (7), 1475–1505. https://doi.org/10.1002/pola.26536.

[12] Shimada, K.; Matsuyama, S.; Saito, T.; Kinugasa, S.; Nagahata, R.; Kawabata, S. Conformational Effects on Cationization of Poly(Ethylene Glycol) by Alkali Metal Ions in Matrix-Assisted Laser Desorption/Ionization Time-of-Flight Mass Spectrometry. *Int. J. Mass Spectrom.*, **2005**, *247* (1–3), 85–92. https://doi.org/10.1016/j.ijms.2005.10.001.

[13] Lou, X.; van Dongen, J. L. J.; Vekemans, J. A. J. M.; Meijer, E. W. Matrix Suppression and Analyte Suppression Effects of Quaternary Ammonium Salts in Matrix-Assisted Laser Desorption/Ionization Time-of-Flight Mass Spectrometry: An Investigation of Suppression Mechanism: MSE and ASE of Quaternary Ammonium Ions in MALDI TOF MS. *Rapid Commun. Mass Spectrom.*, **2009**, *23* (19), 3077–3082. https://doi.org/10.1002/rcm.4224.

[14] Chen, J.-L.; Lee, C.; Lu, I.-C.; Chien, C.-L.; Lee, Y.-T.; Hu, W.-P.; Ni, C.-K. Theoretical Investigation of Low Detection Sensitivity for Underivatized Carbohydrates in ESI and MALDI: Low Sensitivity of Carbohydrates in ESI and MALDI. *J. Mass Spectrom.*, **2016**, *51* (12), 1180–1186. https://doi.org/10.1002/jms.3889.

[15] Cassel, S.; Debaig, C.; Benvegnu, T.; Chaimbault, P.; Lafosse, M.; Plusquellec, D.; Rollin, P. Original Synthesis of Linear, Branched and Cyclic Oligoglycerol Standards. *Eur. J. Org. Chem.*, **2001**, *2001* (5), 875–896. https://doi.org/10.1002/1099-0690(200103)2001:5<875::AID-EJOC875>3.0.CO;2-R.

[16] Barriau, E. Hyperbranched Polyether Polyols as Building Blocks for Complex Macromolecular Architectures. Phd thesis, Johannes Gutenberg University Mainz, 2005.

Chapter 3

Glycerol polymerization over CaGs

*The content of this chapter has been published as an article: N. Ebadi Pour, F. Dumeignil, B. Katryniok, L. Delevoye, B. Revel, S. Paul, Investigating the active phase of Ca-based glycerol polymerization catalysts: On the importance of calcium glycerolate, Molecular Catalysis. 507 (**2021**) 111571. https://doi.org/10.1016/j.mcat.2021.111571.*

3.1 Introduction

As aforementioned in Chapter 1, in the last two decades, attention was paid to glycerol polymerization over alkaline earth oxides-based catalysts such as CaO, BaO and SrO, due to their higher catalytic activity compared to other catalysts [1–3]. Among alkaline earth oxides catalysts, Ca-based catalysts such as CaO, CaO supported on carbon nanofibers [4], dolomite (CaO-MgO mixed oxides), [5] showed higher catalytic activity towards oligomers production. However, all these materials were partially or totally soluble in the reaction media and, consequently, the reactions were supposedly homogeneously catalyzed. Moreover, the higher catalytic activity of CaO has been attributed to the possible *in situ* formation of glyceroxides during the glycerol polymerization reaction [1, 5, 6].

Therefore, based on the literature review, we decided to develop new catalysts based on calcium, which were assumed to act heterogeneously in the glycerol polymerization reaction.

The first catalysts we decided to develop were based on calcium glyceroxides. Ca glyceroxides can be present in various structures, either linear, branched or cyclic (Scheme 3-1). Calcium monoglyceroxides (further noted CaGs), can be described by $Ca(C_3H_6O_3)$ or $Ca(C_3H_7O_3)$ formulae depending on their structure. Calcium diglyceroxides (CaDGs) can be represented by the $Ca(C_3H_7O_3)_2$ or $Ca(C_3H_6O_3)_2$ formulae also depending on their structure. All these compounds are represented in Scheme 3-1. It should be noted that the exact chemical structures of Ca glyceroxides have not yet been reported in the literature, therefore, herein we present possible structures based on the chemical formulas mentioned in the literature.

Note that, in the literature, CaDG is referred generally as Ca glyceroxides [7] or for simplicity Ca glyceroxide [8–10] and calcium monoglyceroxide referred as Ca glycerolate [11]. Thus, to avoid any confusion, in this work, we will use CaG for Ca glycerolate (i.e. monoglyceroxide) and CaDG for Ca diglyceroxide.

It is worth mentioning that calcium glyceroxides such as CaG and CaDG have different applications in the biomedical sector. For instance, calcium glyceroxides have been used as biocidal or sanitising agents by being hydrolysed in water to produce hydroxyl and/or glyceroxide ions, which have anti-microbial properties [12]. CaG was also applied as a calcium supplementation in the pharmaceutical industry [11].

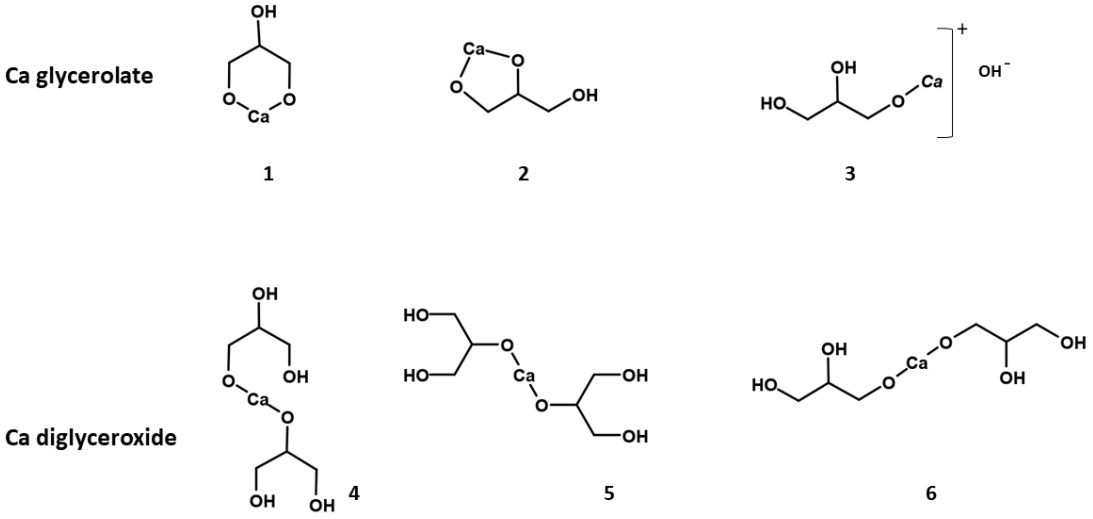

Scheme 3.1. Hypothetical structures of Ca glyceroxides, 1) cyclic CaG with formula $Ca(C_3H_6O_3)$; 2) cyclic-branched CaG with formula $Ca(C_3H_6O_3)$; 3) linear CaG with formula $Ca(C_3H_7O_3)$; 4, 5) branched CaDG and 6) linear CaDG with formula $Ca(C_3H_7O_3)_2$.

Synthesis of Ca-glyceroxides was first reported for a CaO-glycerol system at temperatures from 10 to 150 °C by Grün and Bockish [13] and Fujii and Kondo [14]. Fujii and Kondo [14] reported the formation of 4 types of crystalline glyceroxides at different temperature ranges, namely CaG ($CaC_3H_6O_3$) (Scheme 3.1 (1-3)), CaDG ($Ca(C_3H_7O_3)_2$) (Scheme 3.1 (4-6)), tricalcium octa-glyceroxide ($Ca_3(C_3H_7O_3)_6.(C_3H_8O_3)_2$) and calcium hexa-glyceroxide ($Ca(C_3H_7O_3)_2.(C_3H_8O_3)_4$) from the system of calcium oxide-glycerol (3:100 g:g) at > 100 °C, 40-100 °C, 20-60 °C, < 20 °C, respectively. The authors reported that different Ca crystalline glyceroxides structures can be formed and interconverted depending on the temperature. For instance, calcium hexa-glyceroxide crystal could transform into tricalcium octa-glyceroxide at 18-30 °C, tricalcium octa-glyceroxide to CaDG at 44 °C, while the decomposition of CaDG into CaG was observed in the 130-160 °C temperature range.

Similarly, Taylor *et al.* [11] synthetized CaG ($CaC_3H_6O_3$) as a pharmaceutical product, by heating calcium hydroxide and glycerol above 180 °C in a microwave oven.

Later, Kouzu's group demonstrated that CaDG was formed *in situ* during the transesterification reaction to produce biodiesel starting from CaO as the catalyst precursor, where methanol (present in transesterification reaction) supposedly participates in CaDG formation [15, 16].

The formation of CaDG have been extensively studied in the triglycerides transesterification reaction to produce biodiesel due to the presence of both CaO (as a catalyst for the reaction) and of glycerol (as a co-product of the transesterification reaction) in the reaction media. A typical heterogeneously catalyzed transesterification reaction to produce biodiesel is conducted in the

presence of 1:12 molar ratio of vegetal oil in methanol at 60 °C for 4 h, which results in the formation of fatty acid methyl esters and glycerol. Therefore, the same conditions have been applied to directly synthetize CaDG from glycerol and CaO, however, the glycerol to CaO ratio has not been mentioned. The formation of CaDG under the applied conditions was actually confirmed by XRD analysis [8, 17].

Although CaDG was reported to be an active catalyst for the synthesis of biodiesel by several groups, CaO had slightly higher catalytic activity compared to in situ formed CaDG [15] or CaDG synthesized prior to the reaction [9, 17, 18]. The activity of CaDG was sometimes explained either by its solubility in water and methanol or by the formation of oil-soluble calcium compounds presence in the reaction media [10, 19]. However, there is no clear evidence in the literature on the CaDG solubility under glycerol polymerization reaction conditions. Of course, the operating conditions and the composition of the reaction medium is very different in the polymerization reaction compared to the transesterification reaction.

Despite its role clearly identified in transesterification, to the best of our knowledge no study has been performed so far to elucidate the formation of CaGs during glycerol polymerization reaction. Obviously, the formation of Ca-glyceroxide is also possible in theory during the glycerol polymerization reaction in the presence of CaO. However, only a few studies have actually interpreted their results by the possible formation of Ca-glyceroxides [1, 4–6]. However, Kirby *et al.* [4] reported a higher glycerol conversion to PGs in the presence of synthetized Ca-glyceroxide than in the presence of commercial CaO and $Ca(OH)_2$.

Hence, in this chapter, first we will study the performances of solid Ca-based catalysts, including CaO, $Ca(OH)_2$, $CaCO_3$ and CaDG and compare them to a typical alkaline homogenous catalyst (KOH), and then a characterization study of the catalysts will be presented to investigate the active phase. Finally, based on the characterization of the catalysts and their performances, a mechanism for active phase formation and a mechanism for glycerol polymerization reaction on this type of catalyst will be proposed. To conclude this chapter, the influence of several operating conditions on glycerol polymerization reaction will be studied and discussed.

3.2 Catalysts performances

The catalytic performances of freshly prepared Ca diglyceroxide (CaDG) were evaluated and compared with those of typical Ca-based catalysts mentioned in the literature including commercial CaO (CaO-A), calcined CaO (CaO-C), $Ca(OH)_2$ and $CaCO_3$ and also KOH as a typical homogenous catalyst. The catalytic performances of all these catalysts measured in a standard set of operating conditions are presented in Table 3.1.

CaO-A, CaO-C, $Ca(OH)_2$ and CaDG all showed a glycerol conversion of 22-23 % at 245 °C after 4 h of reaction with a selectivity to diglycerols (linear, branched and cyclic all together) of 13, 13, 8 and 19 %, respectively; whereas the glycerol conversion was lower in the presence of $CaCO_3$ compared to the other catalysts (10%). Higher polyglycerols (PG4+) including tetra, penta- and hexaglycerol were also obtained in the presence of CaO-A, CaO-C, $Ca(OH)_2$ and CaDG.

Table 3.1. Catalytic performances in glycerol polymerization.

Catalyst	**Catalyst amount (wt.%)**	**Glycerol conversion (%)**	**PG2 Selectivity (%)**	**PG3 Selectivity (%)**	**PG4+ Selectivity (%)**
CaO-A	2.13	22	13	32	55
CaO-C	2.13	22	13	32	55
$Ca(OH)_2$	2.8	22	8	37	55
$CaCO_3$	3.8	10	83	17	-
CaDG	8.4	23	19	43	38
*KOH**	1.95	75	0	8	92

*Conditions: 3.5 mol.% of catalyst loading compared to the number of moles of glycerol (*3 mol.% were used for KOH), 245 °C, 4 h of reaction.*

The eye-catching similar catalytic performance observed for CaO, $Ca(OH)_2$ and CaDG suggests that the polymerization reaction was most probably catalyzed by the same *in-situ* formed active phase. Thus, to investigate the actual nature of the working solids, characterizations were performed on the catalysts collected after each reaction. It will be detailed in Section 3.3.

3.2.1 Performances of recycled catalysts

The catalytic performances of the spent catalyst obtained from CaO-C (further noted CaO-R) were assessed upon reutilization in the reaction. The results revealed that, under the same reaction conditions, 47% of glycerol conversion and 70% of selectivity to PG4+ could be reached when CaO-R was used as a catalyst, while conversion and selectivity were only 22% and 55%, respectively, with fresh CaO (Figure 3.1). This increase in performances can be explained by the total dissolution of CaO-R (visually observed) in the new reaction medium where the reaction is then catalyzed homogenously. This dissolution of CaO-R in the 2nd run, which was not observed in the 1st run will be discussed in more details in Section 3.4.

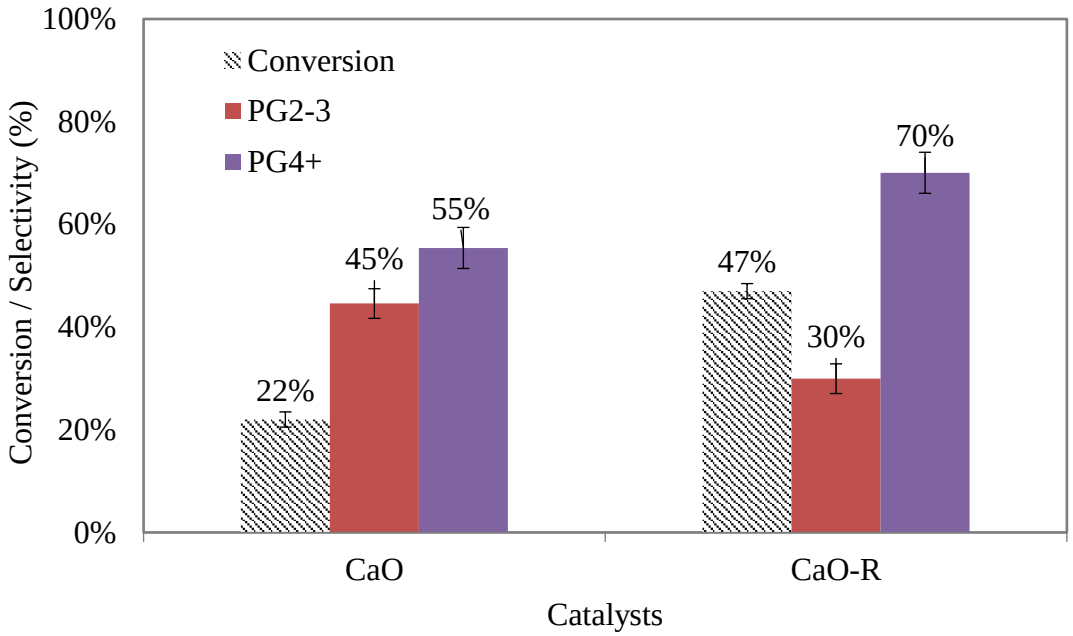

Figure 3.1. Comparison of the catalytic performances of CaO-C and recycled CaO-R catalysts in glycerol polymerization reaction at 245 °C using 3.5 mol.% of catalysts compared to the number of moles of glycerol after 4 h of reaction.

3.2.2 Comparison of the performances with an homogeneous catalyst

KOH as an alkali homogeneous catalyst presented much higher performances than the Ca-based catalysts even using less catalysts (namely, 3 mol.% instead of 3.5 mol.% for the Ca-based catalysts) (Table 3.1). For instance, for CaDG, the glycerol conversion was 23%, while in the same reaction condition, 75% of glycerol conversion was obtained in the presence of KOH. Besides, the activity of KOH was also higher than that of the recycled CaO-R catalyst, considered as a Ca-based homogeneous catalyst (75% *vs.* 47% conversion), where KOH gave 92 % of selectivity to PG4+

(polymerization degree up to PG15) compared to 55% for CaO-R (Figure 3.2). It is obvious that not only the fact that KOH is solubilized in the reaction medium (homogeneous catalyst) but also its high basicity had an impact on glycerol conversion and PGs selectivities. However, the fast reaction rate using KOH made it difficult to control the degree of polymerization leading to a broader distribution of products compared to the one obtained on CaO-R where it was more centered on PG3-5 (Figure 3.2).

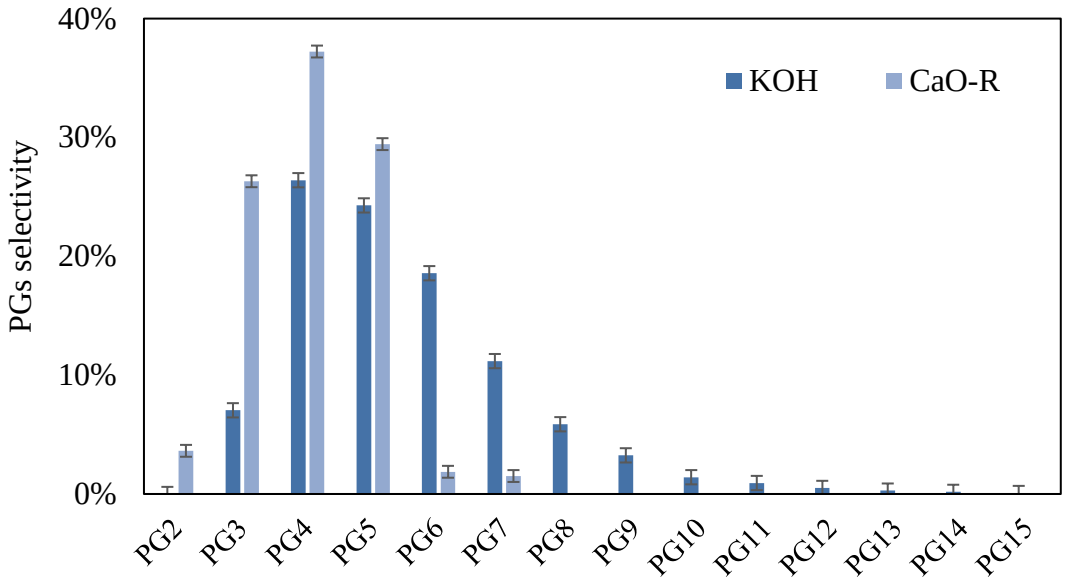

Figure 3.2. PGs distributions for CaO-R (glycerol conversion 23%) and KOH (glycerol conversion 75%)

Hereafter, the characterization of the solid catalysts including CaO, $Ca(OH)_2$, $CaCO_3$ and CaDG, before and after reactions will be discussed, to investigate the actual solid active phase of Ca-based catalysts.

3.3 Catalysts characterization

3.3.1 XRD

First, XRD analyses were carried out on the spent CaO-C (noted CaO-R), $Ca(OH)_2$ (noted CaH-R), $CaCO_3$ (noted CaC-R) and CaDG (noted CaD-R) samples after 4 h of reaction at 245 °C. To verify the structural transformation of the active phase during the reaction, the collected catalysts were analyzed without any intermediate washing and drying steps.

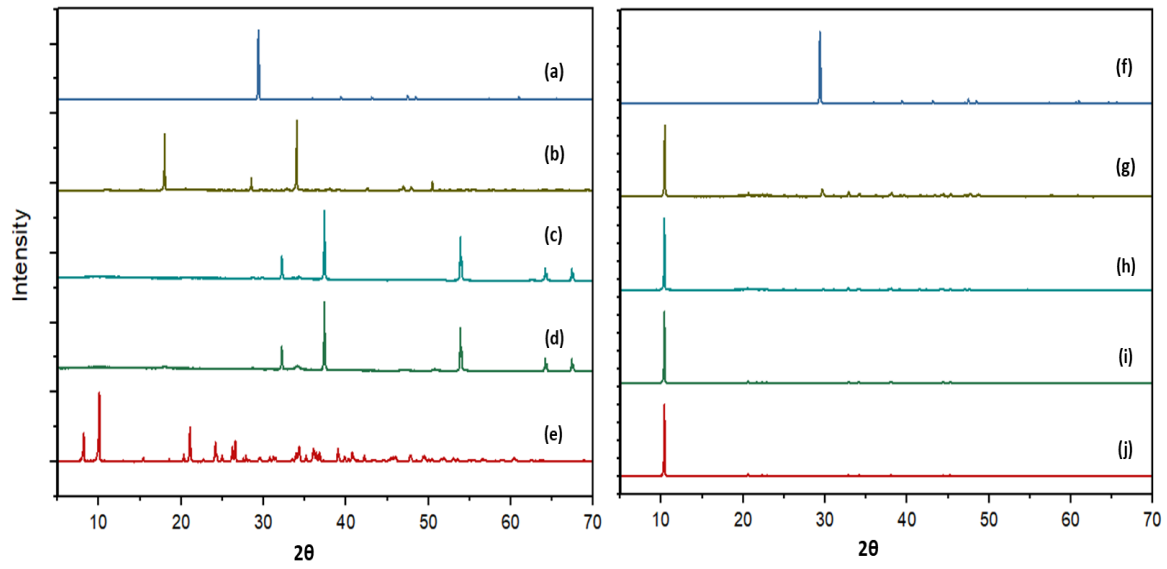

Figure 3.3. XRD patterns of a) $CaCO_3$, b) $Ca(OH)_2$, c) CaO-A, d) CaO-C and e) freshly prepared CaDG (left) and spent catalysts f) CaC-R, g) CaH-R, h) CaO-R(A), i) CaO-R(C) and j) CaD-R (right).

The XRD diffractograms evidenced the structural modification of calcium oxide, calcium hydroxide and CaDG under reaction conditions. Figure 3.3 f-j shows the XRD patterns of the used catalysts. A sharp peak at 2θ = 10.2° (200) (main peak) was observed for CaO-R(A), CaO-R(C), CaH-R and CaD-R after 4 h of reaction. This diffraction pattern was similar to those reported in the literature [11, 14] for CaG with a cubic lattice (001) and also for other crystallized glycerolate metal complexes such as Zn ($Zn(C_3H_6O_3)$) with a cubic lattice (100) [20]. Moreover, no peaks attributed neither to CaO (Figure 3.3 c-d) with 2θ at 32.2, 37.4 and 53.9 (PDF 01-070-4066) nor to Ca hydroxide (Figure 3.3b) with 2θ at 18.14°, 28.7°, 34.2°, and 50.8° (PDF-00-087-0673) were observed for the spent catalysts, suggesting that the latter was quantitively converted to CaG. On the other hand, the XRD pattern of CaC-R (Figure 3.3f) clearly showed that the latter remained in the initial calcite form (PDF-01-071-3699). Thus, these results suggest that the higher catalytic performances in the presence of CaO, $Ca(OH)_2$ and CaDG compared to that of $CaCO_3$ could be attributed to the *in-situ* formation of CaG as an active phase.

It is noteworthy to say that when XRD analyses were carried out on the CaO used samples after washing with ethanol and drying at 80 °C, the diffractograms (not shown here) also revealed the single peak at 2θ = 10.2° corresponding to the CaG structure. This showed that – after all – the washing with ethanol and drying steps did not affect the crystalline structure of CaG.

As a comparison, the XRD pattern of the freshly prepared CaDG is given in Figure 3.3e. It shows 2 main sharp peaks at 2θ = 8.2° and 10.1°, respectively, which is consistent with the theoretical diffractograms of CaDG (PDF-00-021-1544) and with the diffraction pattern reported in the literature for CaDG [17, 18, 21].

Obviously, CaGs begins to form *in situ* when CaO and $Ca(OH)_2$ are introduced in the reaction medium (glycerol), and when the temperature is raised to the reaction temperature (245 °C), as previously reported in the literature (Section 3.1).

3.3.1.1. Temperature effect on *in-situ* CaGs formation

The XRD patterns of the CaO spent catalysts (CaO-R) used at different reaction temperatures, namely 80 °C (noted CaO-R80), 130°C (noted CaO-R130), 180 °C (noted CaO-R180) and 230 °C (noted CaO-R230) are presented in Figure 3.4.

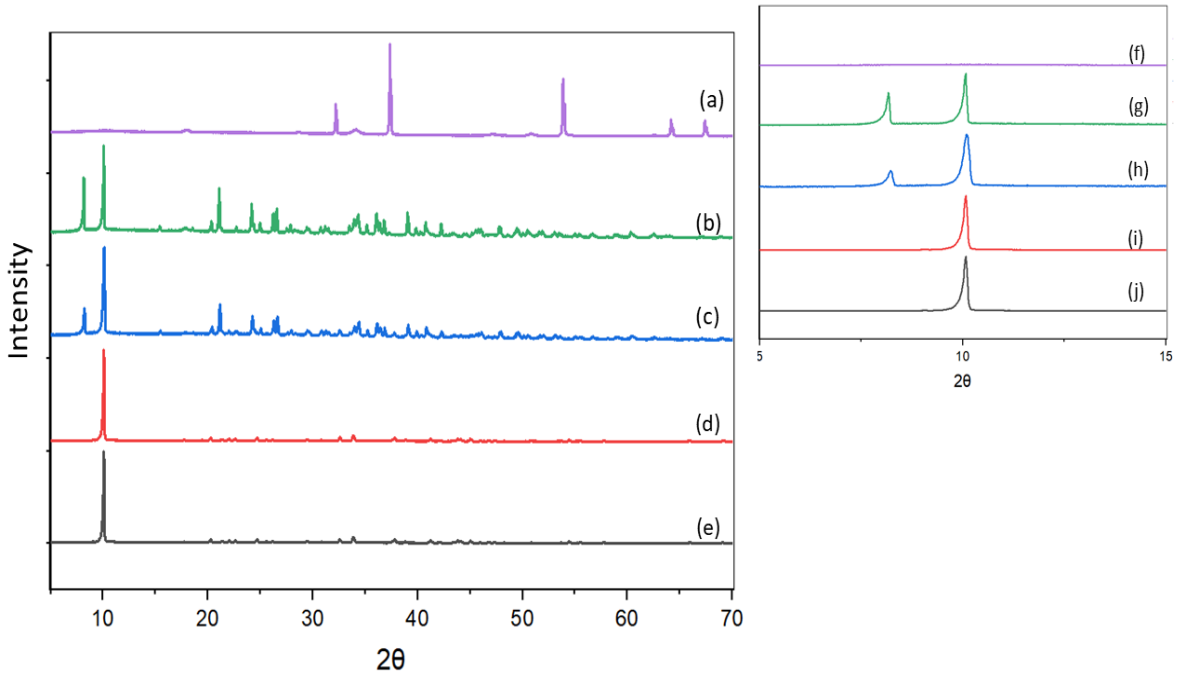

Figure 3.4. XRD patterns of a) fresh commercial CaO; spent CaO catalysts used for a 4 h-reaction at b) 80 °C, c) 130 °C, d) 180 °C and f) 230 °C; and (f-j) zooms of the XRD patterns in the range 2θ = 5-15°.

The diffractogram of CaO-R80 revealed that CaDG was already formed at 80 °C (PDF-00-021-1544) (Fig 3.4.b), as no peaks could be attributed to CaO anymore (PDF 01-070-4066) (Fig 3.4.a)). However, other Ca glyceroxides, such as tricalcium octa-glyceroxide, calcium hexa-glyceroxide and CaG might also be present in the sample, where their smaller peaks could be hidden by the sharp peaks of CaDG. Furthermore, the XRD pattern for CaO-R130 (Fig 3.4c) indicates an increase in the intensity of the peak at $2\theta \sim 10°$ compared to others, more notably relatively to the peak at $2\theta = 8.2°$ attributed to CaDG (Fig 3.4h). This can be explained by the formation of crystalline Ca glycerolate, with a main peak at $2\theta = 10.2°$, from CaDG decomposition, since the interconversion of different CaGs structures with temperature increase is expected according to the literature [14].

A further increase in temperature (180 °C) caused a total decomposition of CaDG to CaG, where only a sharp peak (main peak) of CaG at 2θ =10.2° was observed in the XRD pattern (Fig 3.4d and 3.4i) and no peak attributed to CaDG remained visible. Likewise, the XRD pattern for CaO-R230 (Fig 3.4e and 3.4j) confirmed that CaG is the only phase remaining at 230 °C, i.e. at the temperature where a typical glycerol polymerization reaction begins.

3.3.2 Thermal analyses

TGA was performed on the used catalysts samples to determine the thermal stability of the obtained CaGs, including CaH-R, CaO-R and compared to the freshly prepared CaDG.

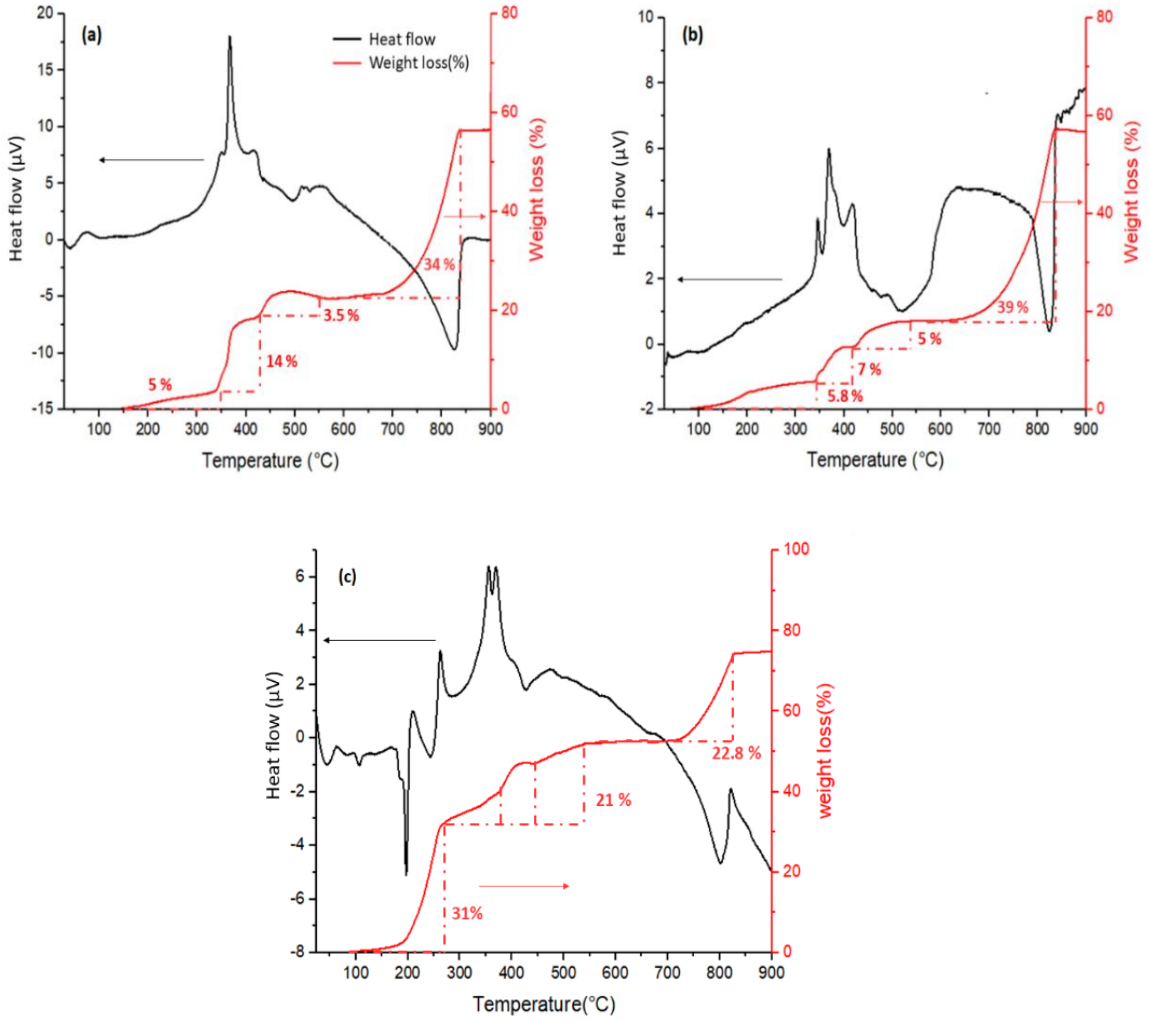

Figure 3.5.TGA–DSC profiles of a) CaO-R, b) CaH-R and c) freshly prepared CaDG.

The TGA curve for CaO-R showed multistep weight loss with a first weight loss of 5 wt.% between 130 and 343 °C, followed by 2 steps of mass losses of 14 wt.% and 3.5 wt.% up to 550 °C. According to the DSC curve, shown in Figure 3.5a, each of these mass losses corresponds to an exothermic peak, which could be attributed to phase transitions of the glyceroxides crystallites. A final weight loss of 34 wt.% was recorded between 550 and 835 °C. The total weight loss of 56.5 wt.% for CaO-R is in good agreement with the theoretical value of 57 % for CaG total decomposition to form CaO plus one molecule of glycerol.

Similarly, the TGA curve for CaH-R (Figure 3.5b) also showed a multistep weight loss with a first weight loss of about 5.8 wt.% between 80 and 140 °C followed by 3 steps of mass loss up to 525 °C (12 wt.%). Three main exothermic peaks in DSC curve between 300 and 500 °C also corresponds to these weight losses. A final weight loss of 39 wt.% was recorded between 525 and 830 °C. The total weight loss of 56.8 wt.% for the CaH-R is very close to the theoretical value of 57 % for the total decomposition of CaG to form CaO plus one molecule of glycerol.

The TGA–DSC profiles of CaDG are shown in Figure 3.5c. Four weight loss steps can be observed. The first step was observed between 100 and 260 °C with a mass loss of 31 wt.%. For this step, the DSC curve showed an endothermic peak, whereby the weight loss was attributed to the partial decomposition of CaDG to CaG when the theoretical weight loss for total decomposition is 41.5% (to form CaG plus one molecule of glycerol). However, Fujii and Kondo [14] reported a decomposition of CaDG to CaG in the range of 130-160 °C; similarly, León-Reina *et al.* [21] observed a peak corresponding to CaDG decomposition between 160 and 200 °C. This variation in the decomposition temperature, reported in the literature and observed in our experiments, could probably be attributed to the presence of different CaDG structures, either linear, cyclic or branched (Scheme 3.1), which can consequently affect the global thermal behavior [22].

Further losses were observed at 260-534 °C with a total loss of 21 wt.%. The final weight loss of 22.8 wt.%, which was recorded between 534 and 830 °C most likely corresponds to the formation of CaO. The total weight loss of 74.4% is very close to the expected one (74.8%) for CaDG total decomposition to CaO and two molecules of glycerol.

3.3.3 ^{13}C Solid State-NMR

The structures of CaO-R and CaH-R were further studied by solid-state ^{13}C SS-NMR. For these compounds, three peaks were observed on the spectra at 67.8 ppm, 70.1 ppm and 74.8 ppm (Figure 3.6a-b).

Based on the CaG structures (Scheme 3.1), for cyclic CaG(1) with a $Ca(C_3H_6O_3)$ formula, 2 peaks corresponding to $-CH_2OCa$ (2 equivalent carbons) and -CH-OH (1 equivalent carbon) are expected to be observed on the ^{13}C NMR spectrum. For CaG (2), 3 peaks corresponding to carbons in $-CH_2OH$, $-CH_2$-OCa and -CH-OCa are expected and for linear CaG(3) with formula of $Ca(C_3H_7O_3)$, also 3 peaks should be observed. Spectra simulations were made with the help of the MestReNova software to try to predict the chemical shifts of carbons in the $-CH_2OH$, $-CH_2$-OCa and -CH-OH groups (Annex B-Fig B.1). This approach is not totally conclusive but, nevertheless, it can be considered that the observed peaks in CaGs (CaO-R and CaH-R) spectra could be either assigned to the $-CH_2OH$ (67.8 ppm), $-CH_2$-OCa (70.1 ppm) and -CH-OH (74.8 ppm) carbon species of glycerol in $Ca(C_3H_7O_3)$ or to $-CH_2OH$ (67.8 ppm), $-CH_2$-OCa (70.1 ppm) and -CH-OCa (74.8 ppm) in CaG (2). Besides, from these spectra it can be concluded that the CaGs are not in their cyclic structure (Scheme 3.1), as only 2 peaks in ^{13}C NMR could be assigned to this structure.

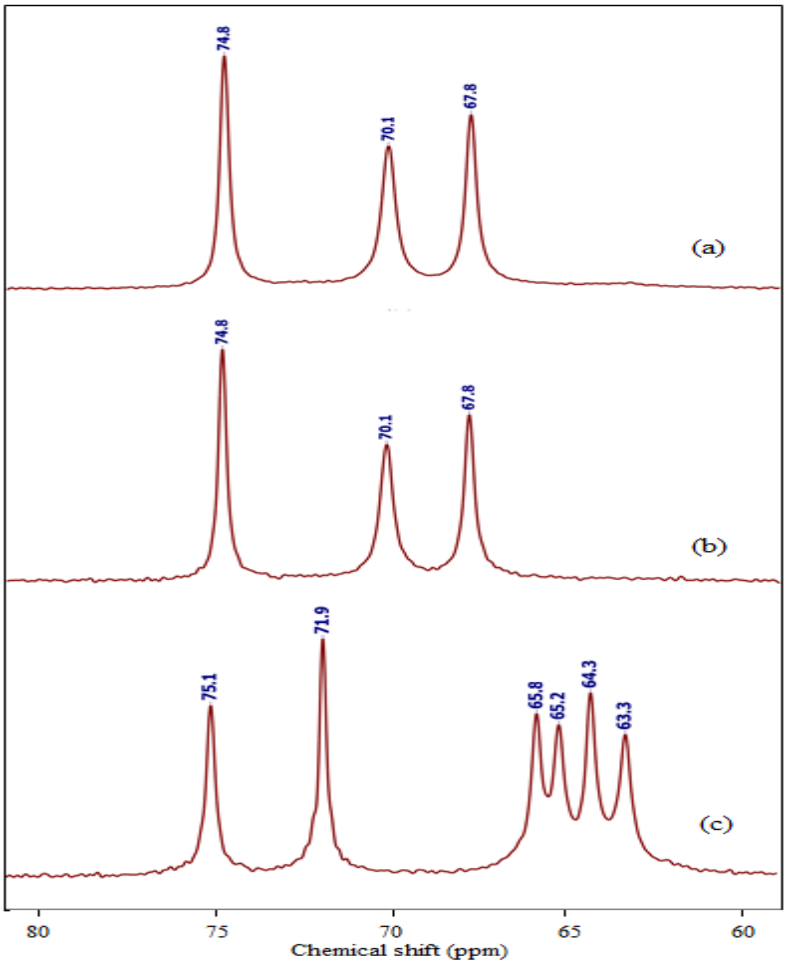

Figure 3.6. ^{13}C SS-NMR spectra of a) CaO-R, b) CaH-R and c) CaDG.

It should also be noted that ^{13}C CPMAS SS NMR is not a quantitative technique, thus, it is difficult to conclude if the CaGs are pure or present as a mixture of two different molecules (CaG(2) and CaG(3)).

Furthermore, for CaDG, six peaks at 63.3, 64.3, 65.2, 65.8, 71.9 and 75.1 ppm were observed in the ^{13}C NMR spectrum (Figure 3.6c). These peaks are characteristic of the carbons of glycerol in the three different structures of CaDG (Scheme 3.1 (4-6)). However, based on the CaDG structures, 6, 2 and 3 peaks are expected to be observed by ^{13}C NMR for CaDG (4), (5) and (6), respectively (Annex B-Fig B.2). Thus, once again due to the fact that ^{13}C CPMAS SS NMR is not a quantitative technique, it cannot be concluded if CaDG is pure CaDG (4) or a mixture of different CaDGs. Nevertheless, similar spectra for CaDG were previously reported by Kouzu *et al*. [23]. It could thus be concluded that CaDG is not present in the *in-situ* formed CaG.

3.3.4 SEM

The morphologies of the catalysts CaO, CaO-R and CaDG were analyzed by SEM (Figure 3.7). Figure 5a shows that CaO-R presented large "potato-shaped" particles with irregularities on the surface (Fig. 7a-left). For CaDG (Figure 3.7b), large particles with an angular rock shape were observed. This is in good agreement with what was previously reported in the literature for CaDG [10, 15]. From Figure 3.7c, it can be seen that calcium oxide is in the form of large agglomerates with outgrowths.

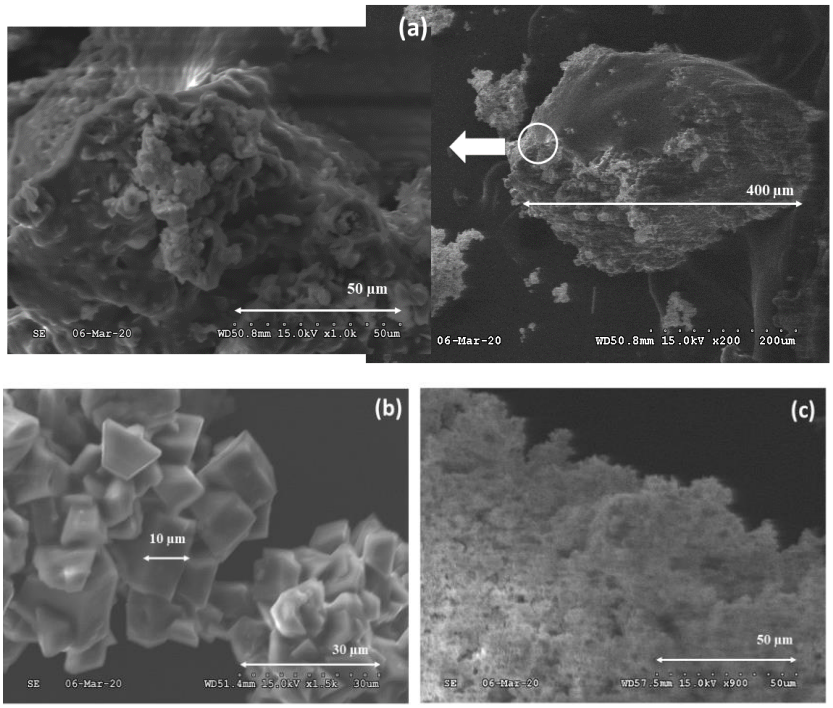

Figure 3.7. SEM analysis of a) CaO-R, b) CaDG and c) CaO samples.

3.3.5 Conclusions on the characterization study

From the XRD results, it can be concluded that CaO and $Ca(OH)_2$ are transformed *in situ* to CaG during the glycerol polymerization reaction. These catalysts also showed a similar thermal behaviour with total weight losses of 56.5 and 56.8 wt.%, respectively for the spent catalysts after test (CaO-R and CaH-R), which match well the theoretical value of 57% when CaG is totally decomposed to form CaO. These results strongly suggest that CaO-R and CaH-R only contain CaGs, but not any CaDG. However, the phase transitions observed between 350 °C and 550 °C for CaO-R and CaH-R suggest that various structures of CaGs were present. Solid-state ^{13}C NMR results were also consistent with XRD and TGA-DSC analyses, confirming that CaO-R and CaH-R contain no CaDG or other Ca glyceroxides suggesting that these samples are mixtures of the CaG(2) and CaG(3) species.

3.4 Mechanisms

3.4.1 Mechanism of CaGs in situ formation

In order to explain the *in situ* formation of CaG we proposed two mechanisms depending on the starting material used:

1) Dissolution-precipitation-crystallization for CaG formation, starting from CaO and $Ca(OH)_2$.
2) CaDG formation and decomposition to CaG.

In the 1st mechanism CaG is formed from CaO (or $Ca(OH)_2$) by a dissolution of the precursor, its conversion in the liquid phase followed by a precipitation step which allow CaG to eventually crystallize.

For the dissolution of CaO (Scheme 3.2-I and 3.2-II) and $Ca(OH)_2$ (Scheme 3.2-III), the Ca cation interacts with the oxygen lone pair of the terminal -OH group in glycerol. In the following, the hydroxyl group of calcium hydroxide (or CaO) abstracts the proton of the as-activated -OH group of glycerol. Consequently, a glycerolate anion and a Ca^{2+} cation are formed which coordinate together with OH^- in a Ca-glycerolate-OH^- complex. When the media is saturated, crystallization takes place, whereby Ca coordinates with more glycerolate anions (Step IV). Besides, colloidal $Ca(OH)_2$ is formed due to the presence of formed water during the reaction , as reported previously by Ruppert *et al*. [1].

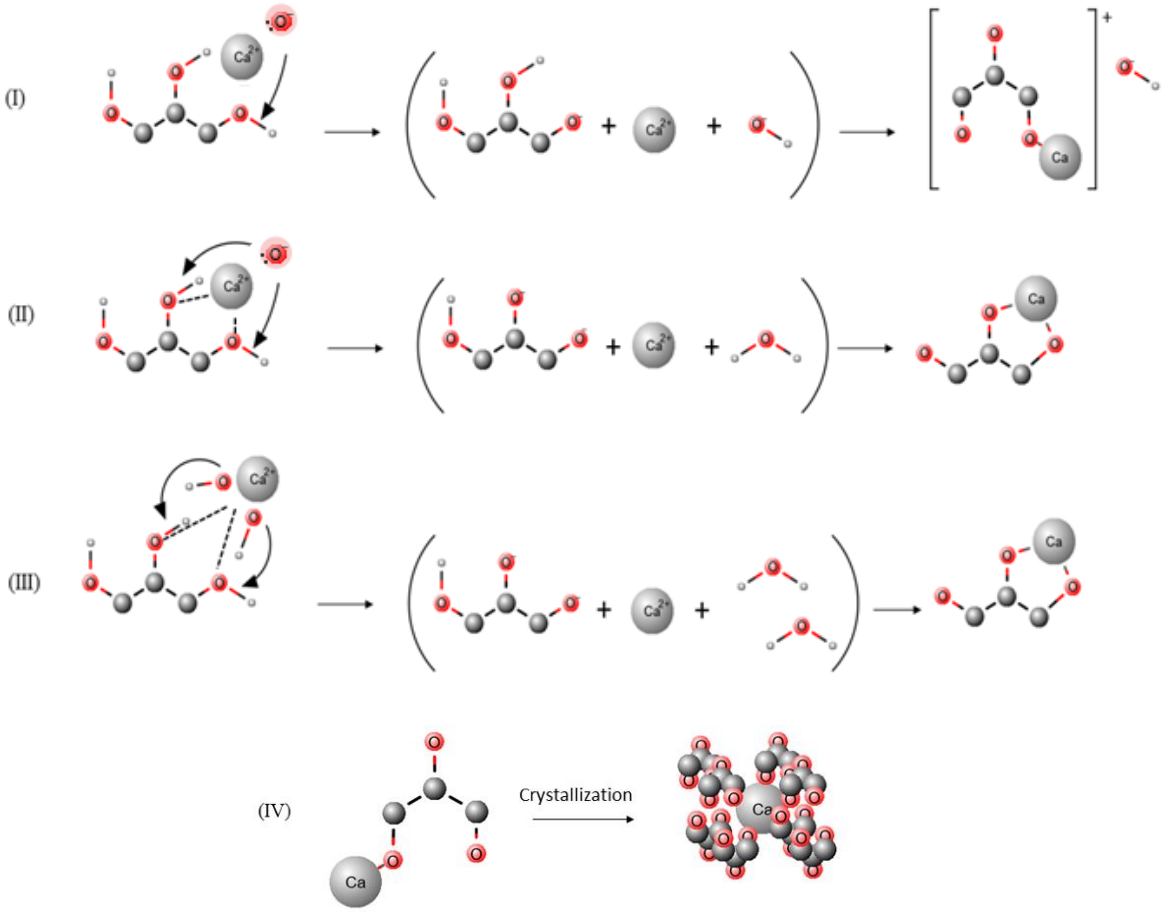

Scheme 3.2. Proposed "*dissolution-precipitation-crystallization*" mechanism for CaG formation.

However, when CaO and $Ca(OH)_2$ are transformed to solid CaG, colloidal $Ca(OH)_2$, Ca^{2+} and hydroxide ions in the liquid phase (Eq. 1-5), an equilibrium takes place between CaG and colloidal $Ca(OH)_2$ (Eq. 4-5).

$$CaO + H_2O \rightarrow Ca(OH)_{2(coll)} \qquad \text{Eq (1)}$$

$$Ca(OH)_{2(s)} \rightarrow Ca(OH)_{2(coll)} \qquad Eq\ (2)$$

$$Ca(OH)_{2(coll)} \rightarrow Ca^{2+} + 2\ OH^- \qquad Eq(3)$$

$$Ca(OH)_{2(coll)} + C_3H_8O_3 \leftrightarrow Ca(C_3H_6O_3) + 2H_2O \qquad Eq\ (4)$$

$$Ca(OH)_{2(coll)} + C_3H_8O_3 \leftrightarrow Ca(C_3H_7O_3)^+ + OH^- + H_2O \qquad Eq\ (5)$$

Finally, a simultaneous dissolution of CaG to Ca ion and intermediate glyceroxide species and its reformation takes place, due to the presence of colloidal $Ca(OH)_2$, as previously described.

Hence, it is clear that after recovering the CaG from the first reaction media, when CaO was the active phase precursor, and during washing step, the colloidal forms of $Ca(OH)_2$ were washed out. Thus, CaG in the fresh media (glycerol) began to solubilize and due to the absence of a protonated oxygen would not be able to reform. This mechanism could also explain why CaG could only form from CaO, $Ca(OH)_2$ and not from $CaCO_3$ due to the presence of protonated oxygens in these compounds.

Scheme 3.3 presents a tentative mechanism for CaG formation during the glycerol polymerization reaction, via the formation of CaDG and its further decomposition to CaG (2nd mechanism).

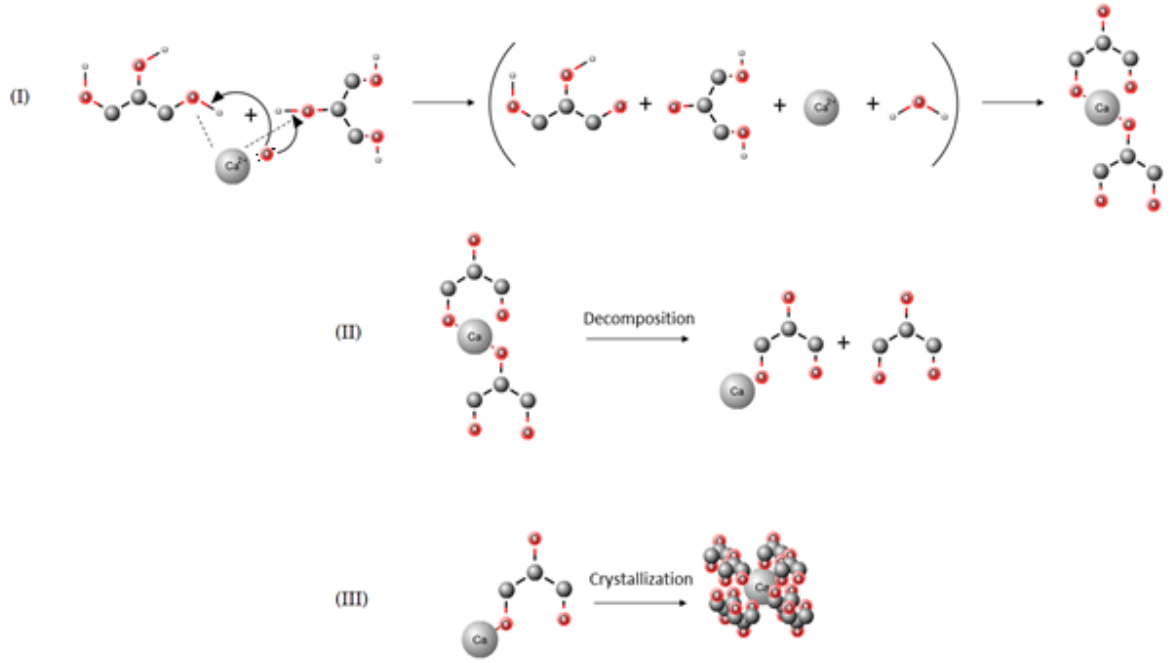

Scheme 3.3. Proposed mechanism for CaG active phase *in situ* formation via CaDG intermediate during the glycerol polymerization reaction.

In the proposed mechanism, CaDG starts to be formed when CaO and glycerol are heated to 80 °C. Then, a further increase in the reaction mixture temperature up to 180 °C causes the decomposition of CaDG to CaG, as it was discussed in details in Section 3.3.1.1 and 3.3.2 of this chapter.

As a matter of fact, CaDG could also form by first, formation of CaG from CaO according to the 1st mechanism and then polymerization of CaDG from CaG, as shown in Eq (6),

$$CaO + 2C_3H_8O_3 \rightarrow Ca(C_3H_7O_3)^+ + OH^- + C_3H_8O_3 \leftrightarrow Ca(C_3H_7O_3)_2 + H_2O \qquad Eq\ (6)$$

where CaG and CaDG can be interconverted depending on the temperature. However, at high temperature (> 180 °C), only CaG remains (See Section 3.3.2).

3.4.2 Mechanism of polyglycerols formation

Upon understanding the CaG formation mechanism, the polyglycerols formation mechanism could be also explained. As also mentioned in Chapter 1, PGs forms in both homogeneously and heterogeneously catalyzed reaction where the precursor catalyst was initially solid due to the solubility of catalysts under these reaction conditions. As aforementioned in the CaG formation mechanism, Ca and hydroxyl ions are present in the reaction medium. Thus, at this stage, the homogenously-catalyzed reaction takes place as described in the literature [24, 25]. On the other hand, the heterogeneously-catalyzed reaction could also take place simultaneously by *in situ* formed CaG. A tentative mechanism of polymerization of glycerol by CaG is presented in Scheme 3.4.

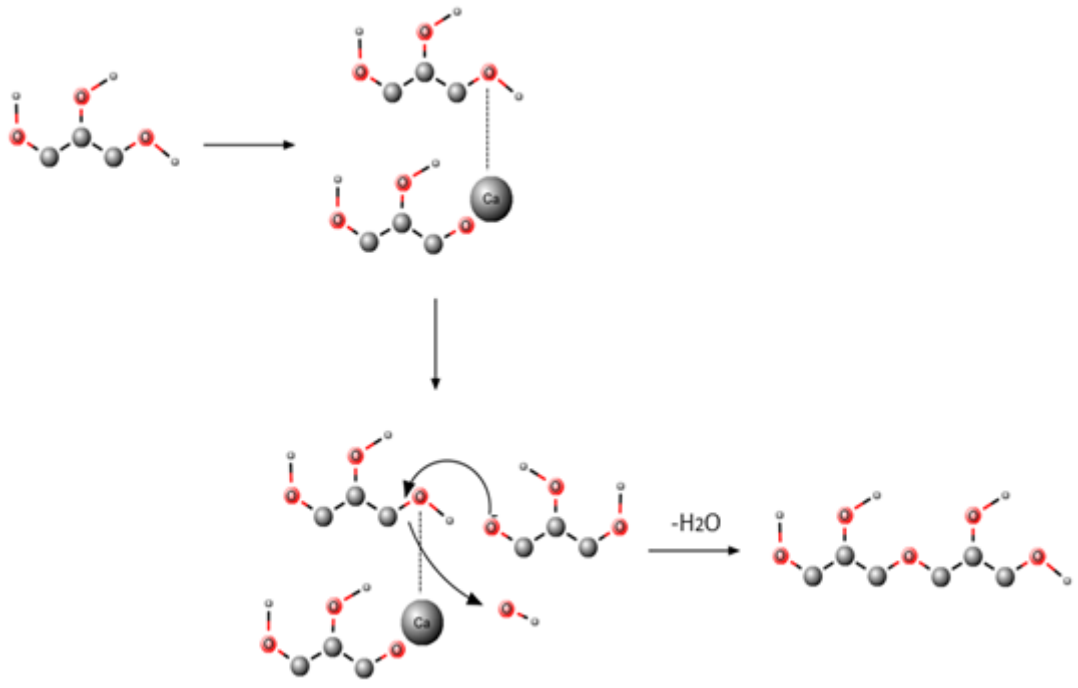

Scheme 3.4. Proposed mechanism for diglycerol formation.

In this mechanism, CaG activates the carbon–oxygen bond of glycerol. By shifting the electron density through the coordination with Ca, the glycerol can be attacked by a glycerolate anion thus removing an hydroxyl group.

It should be noted that in our representation we have chosen the linear CaG structure to simplify the formalization of the mechanism.

So far, the results tend to reveal that the active phase of the Ca-based catalysts presented in this chapter is CaG. However, it has to be noted both CaG and glyceroxide ions participate in PG formation as shown in the mechanism depicted in Scheme 3.4. The use of CaG (CaO-R) was not successful as a heterogeneous catalyst due to its low stability (i.e. high solubility in the reaction medium). Since, CaDG converted to CaG and glyceroxide ion during the reaction, it can promote the PG reaction and it was selected for further studies. Hence, hereafter, the influence of operating conditions on the glycerol conversion and PG4+ selectivity was studied, whereby the stability of CaDG will notably be discussed.

3.5 Influence of the operating conditions

Herein, the effect of operating conditions including temperature, catalyst amount, reaction time and water as a by-product of condensation reaction will be discussed. The range of temperature (230-260 °C), the amount of CaDG as catalyst (0.5 - 3.5 mol. % compared to the number of moles of glycerol) and reaction time (4 - 24 h) were chosen based on the literature review (See Section 1.6 of Chapter 1) and our preliminary results (Section B.2.2 of Annex B). Furthermore, based on the preliminary tests (Annex B-Figure B.3), and in order to avoid to any carbonation of the catalyst, a N_2 atmosphere was used for all the experiments.

3.5.1 Effect of temperature

Herein, catalytic tests were performed in the presence of solid CaDG as a catalyst at the temperature of 230 to 260 °C, while the amount of catalyst kept at the lowest level tested (0.5 mol.%) to individually observe the effect of one independent parameter (temperature) on the reaction.

It is worth mentioning that in general the reaction temperature has a strong influence on catalyst leaching, due *i)* to the solubility of catalyst in glycerol and/or *ii)* to the decomposition of CaDG at higher temperature (> 230 °C), as observed by TGA analyses in Section 3.3.2.

For instance, CaDG proceeds only partially as an heterogenous catalyst when 0.5 mol.% of the catalyst is used at 230 °C (Table 3.2). By increasing the temperature up to 260 °C, it becomes totally soluble in the reaction media, acting then as a homogeneous catalyst. Actually, increasing the

temperature from 230 to 245 °C, the amount of leached Ca increased progressively from 3.99 to 6.02 mg/g as shown in Table 3.2.

Table 3.2. Amount of leached Ca and percentage of remaining solid catalyst based on ICP-OES analyses, after 8 h of reaction in the presence of freshly prepared CaDG as catalyst.

Temperature (°C)	Catalyst concentration (mol.%)	Ca leached (mg/g)	Remaining CaDG (%)
230	0.5	1.57	28
230	2	3.99	54
245	2	6.02	31
245	3.5	9.84	35
260	3.5	13.42	12

As shown in Figure 3.8, an increase of temperature from 230 to 245 °C led to an increase in the glycerol conversion from 16 to 35 %, respectively, after 8 h of reaction. However, at this point, CaDG became totally homogenous at 245 °C, whereas at 230 °C, 28 % of CaDG was still heterogenous in to the reaction medium (Table 3.2). Thus, the higher conversion at 245 °C could be due to both the solubilisation of the catalyst and the higher temperature.

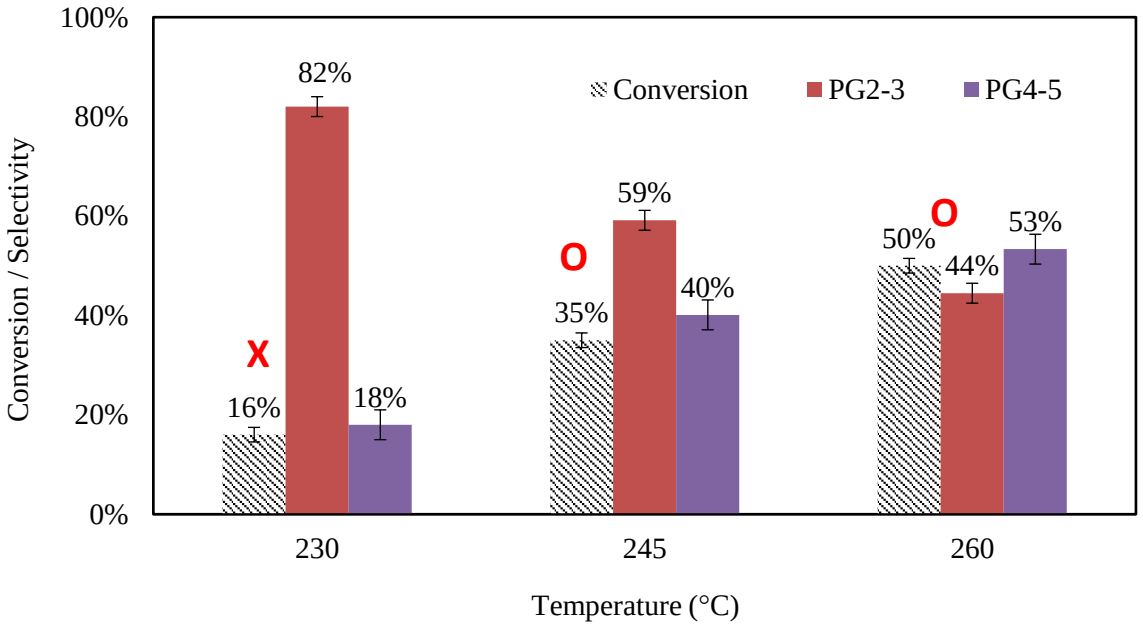

Figure 3.8. Effect of the temperature on the catalytic performances after 8 h of reaction in the presence of 0.5 mol.% of CaDG. Note: X and O represent the partially heterogenous and totally homogenous states of the catalyst, respectively.

Further increasing the reaction temperature to 260 °C enhanced the glycerol conversion to 50 % under the same reaction conditions. However, the reaction proceeds in a totally homogenous phase by complete dissolution of CaDG, which was visually observed after 2 h of reaction only. Hence, once again, this increase in conversion could be due to the fact that the polymerisation reaction needs high temperatures to occur, as reported in the literature, but also to the complete dissolution of the catalyst in the reaction medium.

Temperature had also an influence on the degree of polymerization. The selectivity to PG4+ significantly increased from 18 (at conversion of 16%) to 40 % (at conversion of 35%) at 230 and 245 °C, respectively and reached up to 53 % with 50 % of glycerol conversion at 260 °C, as shown in Figure 3.8. The influence of the temperature on the polymerization degree can be also observed clearly from the ^{13}C NMR results (Annex B-Fig B.5-7). Moreover, at a higher temperature of 260 °C, the ratio of non-cyclic (linear or branched) to cyclic PGs decreased compared to the lower temperature of 230 °C (1.96 *vs.* 2.1), based on the ESI-MS results. Thus, the higher temperature not only caused a higher degree of polymerization but also promoted the formation of cyclic compounds, as also previously reported in the literature [4].

Hence, these results revealed that the temperature has, as expected, a very significant effect on glycerol conversion and consequently polymerization degree. Besides, it has also an important impact on the solubility of the catalyst.

3.5.2 Effect of catalyst concentration CaDG

The influence of the catalyst concentration was studied in the range 0.5 to 2 mol.% compared to the number of moles of glycerol. An increase of the amount of catalyst from 0.5 to 2 mol.% at 245 °C caused a drop in the glycerol conversion from 35 to 23%, but without significant effect on the PG4+ selectivity (41% *vs.* 43%) after 8 h of reaction (Figure 3.9).

Despite the fact that a decrease in conversion when using higher amount of catalyst is generally unexpected, it could be due to the presence of solid material in the reaction media. Actually, the catalyst was totally homogenous when used at lower concentration of 0.5 mol.%, whereby for 2 mol.%, 31% of catalyst remained solid (Table 3.2) in the reaction medium. The presence of solid material in a viscous mixture can cause mass transfer limitations. Therefore, an unexpected decrease in conversion could be observed. Sangkhum *et al*. [6] also reported earlier that a drop in conversion was observed when the amount of solid Ca-Mg-Al mixed oxides was increased.

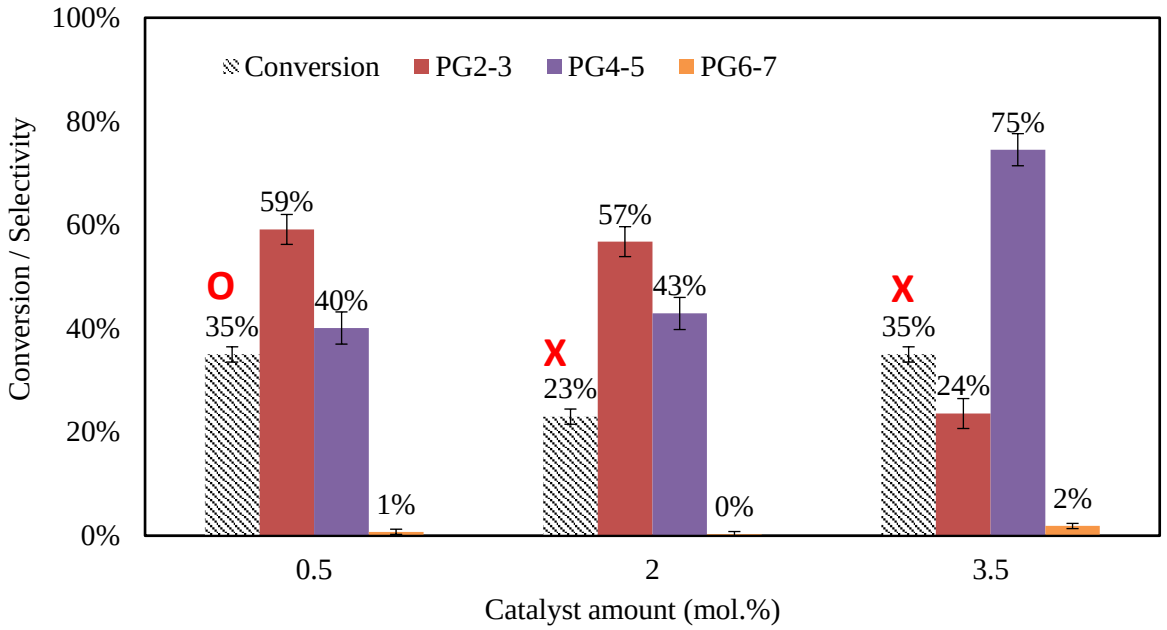

Figure 3.9. Effect of the catalyst concentration on the catalytic performances after 8 h of reaction in the presence of 0.5, 2 and 3.5 mol. % of CaDG compared to the number of moles of glycerol, at 245 °C. Note: X and O represent the partially heterogenous and totally homogenous states of the catalyst, respectively.

Further increasing the amount of catalyst to 3.5 mol.% in the same conditions, caused an increase in glycerol conversion (35%) and PG4+ selectivity (77%), after 8 h of reaction, as shown in Figure 3.9, where 35% of the catalyst remained solid. The observed increase in the glycerol conversion and degree of polymerization by an increase in the amount of CaDG from 2 mol.% to 3.5 mol.%, could be due to *i)* an increase in the amount of leached Ca (6.02 *vs* 9.84 mg/g) or/and *ii)* an increase in the amount of remained solid catalyst (31 % *vs* 35 %) (Table 3.2). However, these effects cannot be distinguished, due to the fact that they occur simultaneously.

Generally speaking, increasing the temperature and amount of catalyst promoted the glycerol polymerization, *i.e.*, higher conversion and higher degree of polymerization.

3.5.3 Effect of reaction time on PG4+ selectivity

The influence of reaction time on the glycerol conversion and degree of polymerization was studied in the presence of 3.5 mol.% of CaDG catalyst at 245 °C.

As shown in Figure 3.10, after the first 4 h of reaction, the relative selectivity to PG2, PG3 and PG4-5 were 19, 43 and 37% respectively at a glycerol conversion of 23%, whereas the selectivity to PG6+ was less than 10%. After 8 h of reaction, the glycerol conversion increased to 35% with a huge drop in PG2-3 selectivity to 22% respectively, to the benefit of PG4-5 (74%). For increased reaction time, PG3 and PG4 gradually decreased from 20 and 40% after 8 h of reaction to 14 and 30% after

22 h of reaction, respectively, whereas PG5 and PG6+ selectivity increased to 30% and glycerol conversion at 70% after 22 h of reaction. As it was expected, both glycerol conversion and polymerization toward PG4+ increased with the reaction time.

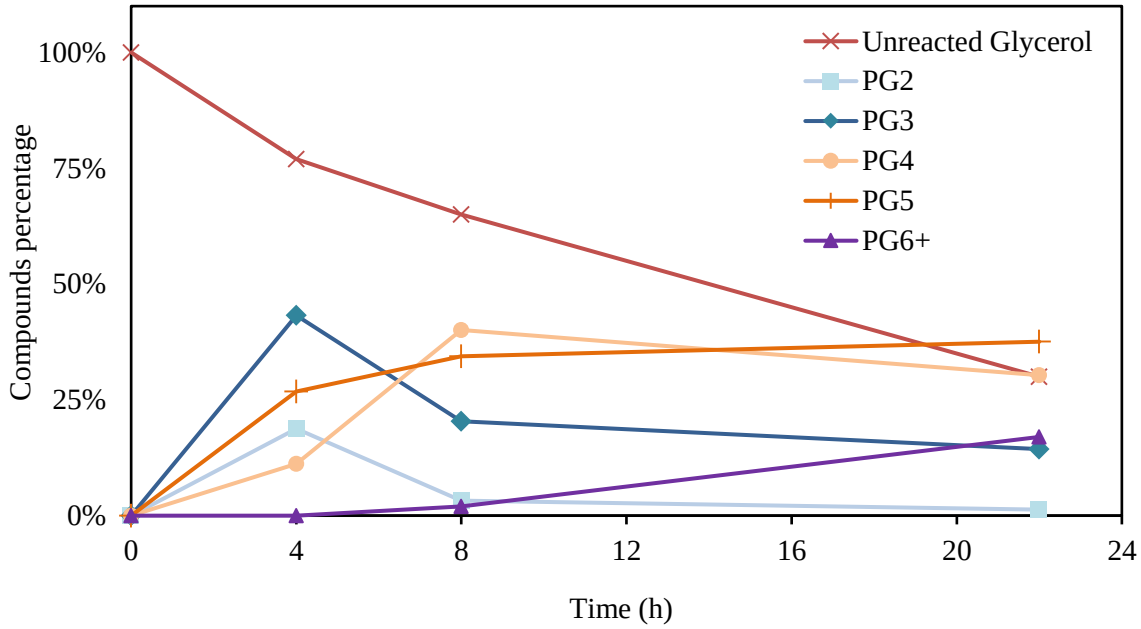

Figure 3.10. Reaction time influence on catalytic performances in the presence of 3.5 mol.% of CaDG, at 245 °C; unreacted glycerol (×), PG2 (■), PG3 (◆), PG4 (●), PG5 (+) and PG6+ (▲).

3.5.4 Water effect

As aforementioned in Chapter 1 (Table 1.2 and Table 1.3), generally the glycerol polymerization reaction is carried out by removing the formed water during the reaction, mainly by utilising a Dean-Stack apparatus or by applying vacuum. Although, it is clear that removing water from the reactor shift the equilibrium to promote glycerol conversion and consequently producing polyglycerols, no study so far has effectively compared the influence of water in the PG reaction.

Thus, the following systems were compared at 245 °C in the presence of 2 mol.% of freshly prepared CaDG. The reaction was performed 22 h in the following conditions :

A. Reaction carried out in a batch reactor under atmospheric pressure.
B. Reaction carried out in a batch reactor under atmospheric pressure by adding H_2O (7 vol.%) prior to reaction.
C. Reaction carried out in a batch reactor equipped with an adsorption column under atmospheric pressure.
D. Reaction carried out in a batch reactor under 420 mbar vacuum.

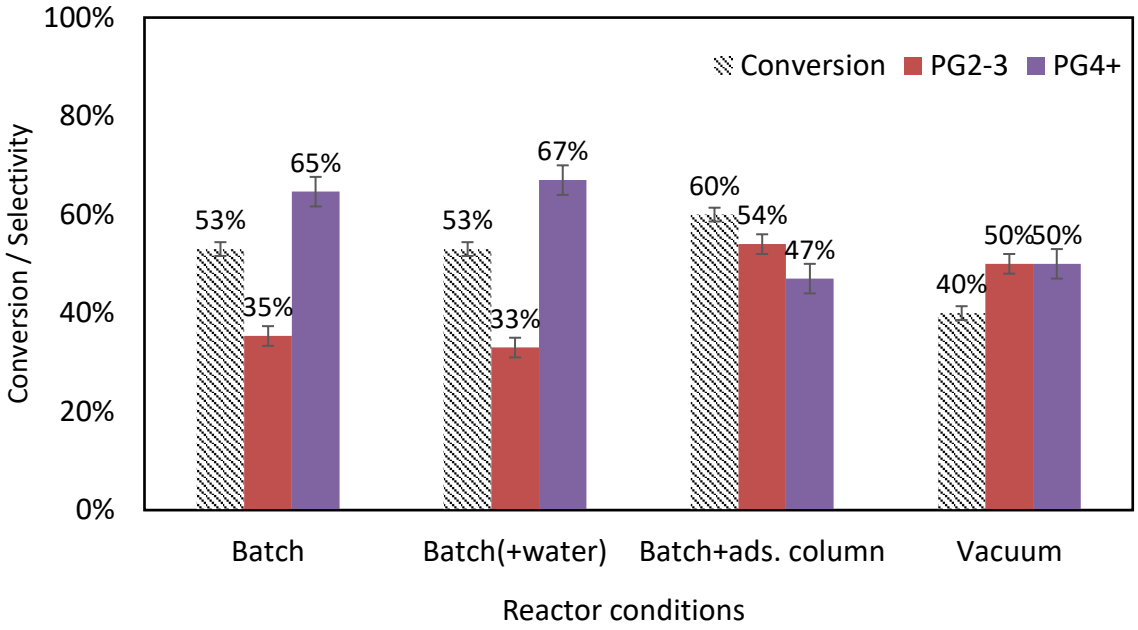

Figure 3.11. Effect of water (addition or elimination) on catalytic performances after 22 h of reaction in the presence of 2 mol.% of CaDG, at 245 °C.

The results surprisingly revealed that the addition of 7 vol.% of H_2O to the system had no impact neither on glycerol conversion nor on the degree of polymerization compared to standard conditions, as shown in Figure 3.11. This could be due to the fact that the added water remained as vapor in the reactor atmosphere due to the high temperature of 245 °C, which can cause a small increase in pressure (not measured) inside the reactor.

Moreover, a glycerol conversion of 60% with a 47% selectivity to PG4+ were obtained when the reaction was performed 22 h in a reactor equipped with an adsorption column (C), whereas in the standard conditions, glycerol conversion and selectivity to PG4+ were 53% and 65%, respectively. This increase in glycerol conversion was expected since water removal should shift the polymerisation reaction forward. Besides, the increase in PG2-3 selectivity (54%) also indicated that water separation promoted the glycerol polymerization to shorter PGs (PG2-3). This increase in PG2-3 formation could be due to the fast termination step in polymerization reaction under these conditions.

On the other hand, a decrease in glycerol conversion (40%) was observed when the reaction was done under vacuum. One should bear in mind that the applied vacuum was not controlled and hence maintained during the 22 h of reaction. Thus, as the reaction began, the formed water gradually increased and the pressure could be higher than 420 mbar (not measured) after 22 h of reaction. Then, so far, under these conditions, water is still present in the reactor atmosphere (not evacuated from the reactor) and can play a role in the vapor-phase equilibrium of H_2O. Hence, applied vacuum influenced on the reaction rate rather than on the equilibrium, probably by decreasing the energy of the initiation step of polymerization. Thus, a higher selectivity to PG2-3 (50%) at lower conversion is also expected.

Afterall, it should be noted again that the catalyst became finally soluble (visually observed) in all applied conditions (A-D) after 22 h of reaction. Thus, one can conclude that the water removal did not prevent the solubilization of the catalyst during the reaction.

Finally, it can be concluded that the reaction with water removal in a reactor equipped with column, had a higher conversion (60%) and higher selectivity to PG2-3 (54%), whereas, the conventional batch reactor, had a higher selectivity to PG4+ (65%) at 53% conversion.

3.6 Conclusions

In this work, the catalytic performances of several Ca-based catalysts were studied. Next to CaO and $Ca(OH)_2$ that have been previously reported in the literature as good catalysts for PGs synthesis from glycerol, CaDG has been assessed as a new catalyst for the glycerol polymerization reaction. The results showed that CaO, $Ca(OH)_2$ and CaDG were transformed to CaG during the reaction and thus exhibited similar catalytic performance. This brings a new insight on the nature of the active phase and on the mechanism of PGs formation.

Moreover, the *in situ* formed catalyst was characterized by XRD, TGA-DSC and solid-state NMR. The XRD analysis confirmed that crystallized spent catalysts are CaG. This is in good agreement with the glycerolate (CaG) patterns already reported in the literature. Besides, while the obtained calcium glycerolate, CaO-R and CaH-R, respectively issued from CaO and $Ca(OH)_2$ showed a similar thermal behavior, namely a total weight loss close to 57 wt.%, which is in very good agreement with the theoretical value for CaG decomposition, the phase transitions observed between 350 °C and 550 °C suggested that Ca glycerolates are present as mixtures of different structures. Furthermore, the SS ^{13}C NMR results confirmed the XRD and thermal analyses and proved that CaG samples most probably consist of mixtures of cyclic-branched CaG(2) and linear CaG(3) and do not contain any cyclic CaG or CaDG. We thus showed that the similarity between catalytic performances of CaO, $Ca(OH)_2$ and CaDG is due to the *in situ* formation of CaG actually acting as the real catalyst. Furthermore, 47% of glycerol conversion was obtained on CaG, vs. 22% on CaO used as the catalyst precursor. This increase in catalytic performances can be explained by a mechanism of CaG *in situ* formation, which comprises the simultaneous dissolution of the catalyst precursors and the precipitation of CaG after recombination of the intermediate with glycerol. A mechanism of glycerol polymerization reaction itself could be subsequently proposed, in which the *in situ* formed CaG and the glyceroxide ion participate in the formation of diglycerol.

Further, the operating conditions were optimized using CaDG as the catalyst to obtain high glycerol conversion and high degree of polymerization. The results revealed that the temperature has a strong influence on both the glycerol conversion and the degree of polymerization.

For instance, increasing the temperature from 230 to 260 °C caused an increased in the selectivity to PG4+ from 18 (at 16% conversion) to 53 % (at 50% conversion) respectively, after 8 h reaction in the presence of 0.5 mol.% of CaDG catalyst. It was also observed that increasing the amount of catalyst from 0.5 to 2 mol.% had no significant effect on the glycerol conversion at 245 °C. However, it promoted the formation of higher degree of PGs. For instance, in the presence of 0.5 and 3.5 mol.% of CaDG, the selectivity to PG4+ increased from 41 to 77 %, respectively, at glycerol conversion of 35 % for both, after 22 h of reaction.

Besides, the results revealed that the water separation from the reactor caused a slightly higher glycerol conversion (60% *vs.* 53%) and a lower selectivity to PG4+ (47% *vs.* 65%), compared to the reaction under an atmospheric condition, while performing the reaction under vacuum caused a decrease in reaction rate.

Therefore, taking into account that a high reaction temperature (260 °C) caused an increase of the catalyst solubility and, consequently, an increase in glycerol conversion and polymerization degree, besides promoting the cyclization of PGs, it can be concluded that the best operating conditions to obtain high catalytic activity toward higher PGs (PG4+), as the target molecules, are 245 °C and 3.5 mol. % of CaDG, where the reaction carried out under atmospheric conditions without water elimination from the reaction medium.

References

[1] Ruppert, A. M.; Meeldijk, J. D.; Kuipers, B. W. M.; Erné, B. H.; Weckhuysen, B. M. Glycerol Etherification over Highly Active CaO-Based Materials: New Mechanistic Aspects and Related Colloidal Particle Formation. *Chem. - Eur. J.*, **2008**, *14* (7), 2016–2024. https://doi.org/10.1002/chem.200701757.

[2] Gholami, Z.; Abdullah, A. Z.; Lee, K.-T. Glycerol Etherification to Polyglycerols Using Ca1+xAl1−xLaxO3 Composite Catalysts in a Solventless Medium. *J. Taiwan Inst. Chem. Eng.*, **2013**, *44* (1), 117–122. https://doi.org/10.1016/j.jtice.2012.09.014.

[3] Anne-Eva Nieuwelink. CaO/CNF for the Oligomerization of Glycerol. Master thesis, Utrecht University, Department of Chemistry, 2015.

[4] Kirby, F.; Nieuwelink, A.-E.; Kuipers, B. W. M.; Kaiser, A.; Bruijnincx, P. C. A.; Weckhuysen, B. M. CaO as Drop-In Colloidal Catalysts for the Synthesis of Higher Polyglycerols. *Chem. - Eur. J.*, **2015**, *21* (13), 5101–5109. https://doi.org/10.1002/chem.201405906.

[5] Barros, F. J. S.; Cecilia, J. A.; Moreno-Tost, R.; de Oliveira, M. F.; Rodríguez-Castellón, E.; Luna, F. M. T.; Vieira, R. S. Glycerol Oligomerization Using Low Cost Dolomite Catalyst. *Waste Biomass Valorization*, **2018**. https://doi.org/10.1007/s12649-018-0477-5.

[6] Sangkhum, P.; Yanamphorn, J.; Wangriya, A.; Ngamcharussrivichai, C. Ca–Mg–Al Ternary Mixed Oxides Derived from Layered Double Hydroxide for Selective Etherification of Glycerol to Short-Chain Polyglycerols. *Appl. Clay Sci.*, **2019**, *173*, 79–87. https://doi.org/10.1016/j.clay.2019.03.006.

[7] Granados, M. L.; Alonso, D. M.; Sádaba, I.; Mariscal, R.; Ocón, P. Leaching and Homogeneous Contribution in Liquid Phase Reaction Catalysed by Solids: The Case of Triglycerides Methanolysis Using CaO. *Appl. Catal. B Environ.*, **2009**, *89* (1–2), 265–272. https://doi.org/10.1016/j.apcatb.2009.02.014.

[8] Kouzu, M.; Hidaka, J.; Wakabayashi, K.; Tsunomori, M. Solid Base Catalysis of Calcium Glyceroxide for a Reaction to Convert Vegetable Oil into Its Methyl Esters. *Appl. Catal. Gen.*, **2010**, *390* (1–2), 11–18. https://doi.org/10.1016/j.apcata.2010.09.029.

[9] Reyero, I.; Arzamendi, G.; Gandía, L. M. Heterogenization of the Biodiesel Synthesis Catalysis: CaO and Novel Calcium Compounds as Transesterification Catalysts. *Chem. Eng. Res. Des.*, **2014**, *92* (8), 1519–1530. https://doi.org/10.1016/j.cherd.2013.11.017.

[10] Esipovich, A.; Rogozhin, A.; Danov, S.; Belousov, A.; Kanakov, E. The Structure, Properties and Transesterification Catalytic Activities of the Calcium Glyceroxide. *Chem. Eng. J.*, **2018**, *339*, 303–316. https://doi.org/10.1016/j.cej.2018.01.142.

[11] Taylor, R. M.; Slade, P. G.; Aldous, G. L. Preparation and Properties of a Glycerolatocalcium Complex. *Aust. J. Chem.*, **1992**, *45*, 1179–1185.

[12] Houseman, R. A.; Venter, A. C. A Method of Reducing the Rate of Degradation of a Biological Material. WO2010106475A2, September 23, 2010.

[13] Grün, Ad.; Husmann, J. Glycerinate der Erdalkalien. *Berichte Dtsch. Chem. Ges.*, **1910**, *43* (2), 1291–1298. https://doi.org/10.1002/cber.19100430221.

[14] Fujii, K.; Kondo, W. Calcium glyceroxides formed in the System of calcium oxide-glycerol. With 4 figures. *Z. Anorg. Allg. Chem.*, **1968**, *359* (5–6), 296–304. https://doi.org/10.1002/zaac.19683590509.

[15] Kouzu, M.; Kasuno, T.; Tajika, M.; Yamanaka, S.; Hidaka, J. Active Phase of Calcium Oxide Used as Solid Base Catalyst for Transesterification of Soybean Oil with Refluxing Methanol. *Appl. Catal. Gen.*, **2008**, *334* (1–2), 357–365. https://doi.org/10.1016/j.apcata.2007.10.023.

[16] Kouzu, M.; Yamanaka, S.; Hidaka, J.; Tsunomori, M. Heterogeneous Catalysis of Calcium Oxide Used for Transesterification of Soybean Oil with Refluxing Methanol. *Appl. Catal. Gen.*, **2009**, *355* (1–2), 94–99. https://doi.org/10.1016/j.apcata.2008.12.003.

[17] Catarino, M.; Martins, S.; Soares Dias, A. P.; Costa Pereira, M. F.; Gomes, J. Calcium Diglyceroxide as a Catalyst for Biodiesel Production. *J. Environ. Chem. Eng.*, **2019**, *7* (3), 103099. https://doi.org/10.1016/j.jece.2019.103099.

[18] Kouzu, M.; Kasuno, T.; Tajika, M.; Yamanaka, S.; Hidaka, J. Active Phase of Calcium Oxide Used as Solid Base Catalyst for Transesterification of Soybean Oil with Refluxing Methanol. *Appl. Catal. Gen.*, **2008**, *334* (1–2), 357–365. https://doi.org/10.1016/j.apcata.2007.10.023.

[19] Sánchez-Cantú, M.; Reyes-Cruz, F. M.; Rubio-Rosas, E.; Pérez-Díaz, L. M.; Ramírez, E.; Valente, J. S. Direct Synthesis of Calcium Diglyceroxide from Hydrated Lime and Glycerol and Its Evaluation in the Transesterification Reaction. *Fuel*, **2014**, *138*, 126–133. https://doi.org/10.1016/j.fuel.2014.08.006.

[20] Reinoso, D. M.; Damiani, D. E.; Tonetto, G. M. Zinc Glycerolate as a Novel Heterogeneous Catalyst for the Synthesis of Fatty Acid Methyl Esters. *Appl. Catal. B Environ.*, **2014**, *144*, 308–316. https://doi.org/10.1016/j.apcatb.2013.07.026.

[21] León-Reina, L.; Cabeza, A.; Rius, J.; Maireles-Torres, P.; Alba-Rubio, A. C.; López Granados, M. Structural and Surface Study of Calcium Glyceroxide, an Active Phase for Biodiesel Production under Heterogeneous Catalysis. *J. Catal.*, **2013**, *300*, 30–36. https://doi.org/10.1016/j.jcat.2012.12.016.

[22] Wall, L. A.; Florin, R. E. Effect of Structure on the Thermal Decomposition of Polymers. *J. Res. Natl. Bur. Stand.*, **1958**, *60* (5), 451. https://doi.org/10.6028/jres.060.046.

[23] Kouzu, M.; Tsunomori, M.; Yamanaka, S.; Hidaka, J. Solid Base Catalysis of Calcium Oxide for a Reaction to Convert Vegetable Oil into Biodiesel. *Adv. Powder Technol.*, **2010**, *21* (4), 488–494. https://doi.org/10.1016/j.apt.2010.04.007.

[24] Martin, A.; Richter, M. Oligomerization of Glycerol - a Critical Review. *Eur. J. Lipid Sci. Technol.*, **2011**, *113* (1), 100–117. https://doi.org/10.1002/ejlt.201000386.

[25] Salehpour, S.; Dubé, M. A. Towards the Sustainable Production of Higher-Molecular-Weight Polyglycerol. *Macromol. Chem. Phys.*, **2011**, *212* (12), 1284–1293. https://doi.org/10.1002/macp.201100064.

Chapter 4

Glycerol polymerization over Ca-based hydroxyapatites

The content of this chapter has been published as an article: N. Ebadi Pour, S. Paul, B. Katryniok, F. Dumeignil, A Highly Stable and Selective Solid Catalyst for Glycerol Polymerization. Catalysts 2021, 11, 1247. https://doi.org/10.3390/catal11101247.

4.1 Introduction

Besides Ca glyceroxides, many types of Ca-rich compounds, particularly derived from organic wastes such as fish scales and animal bones have been successfully used as catalysts [1–4]. In fact, the mineral phase of bones consists of non-stoichiometric calcium hydroxyapatite (HAp). Generally hydroxyapatites, are widely used in biomedicals due to their similarity, from a crystallographic point of view as well as in chemical composition, with human hard tissue such as bones and teeth [5]. Furthermore, due to their interesting properties, such as high thermal stability, very limited water solubility and insolubility in alkaline solutions [6], HAps have also found many applications in catalysis [1–4, 7–9], protein separation [10], and waste-water and soil treatment [6]. Hence, due to these advantages, we decided to study heterogeneous catalysts based on Ca hydroxyapatite for the glycerol polymerization reaction.

A stochiometric HAp (further noted HAp-S) with formula $Ca_5(PO_4)_3(OH)$, usually written as $Ca_{10}(PO_4)_6(OH)_2$, with a Ca/P molar ratio of 1.67, has a hexagonal crystal structure with 44 atoms per unit cell. There are two Ca sites in HAp: i) four Ca(I) sites are surrounded by nine oxygen ions from the surrounding phosphate tetrahedron and ii) six Ca(II) sites are surrounded by six oxygen ions from five phosphate groups and the hydroxyl ion, located in channels with a diameter ranging from 3 to 4.5 Å [11, 12].

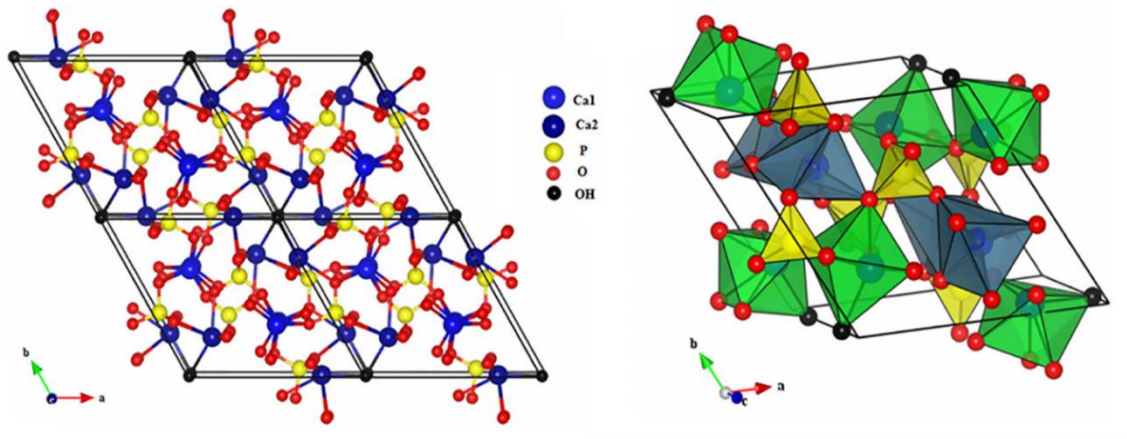

Figure 4.1. Stoichiometric hydroxyapatite unit cell (left) and local environment of Ca in the HAp structure; octahedral ($Ca(I)O_6$), ($Ca(II)O_6$) and tetrahedral (PO_4) (right) [11].

Deficient HAp (non-stoichiometric) hydroxyapatites with Ca/P < 1.67 (further noted HAp-D), are generally represented by the formula $Ca_{10-x}(PO_4)_{6-x}(HPO_4)_x(OH)_{2-x}$ with $0 < x < 1$. Outside this compositional range, the compounds could change to multiphasic mixtures including β-tricalcium phosphate (β-TCP) with a formula of $Ca_3(PO_4)_2$ with Ca/P ratio of 1.5; octacalcium phosphate (OCP)

($Ca_8H_2(PO_4)_6{\cdot}xH_2O$) with a Ca/P of 1.33; calcium hydrogen phosphate ($CaHPO_4$) with a Ca/P of 1 and calcium pyrophosphate (DCP) (β-$Ca_2P_2O_7$) with a Ca/P of 1 [13–15].

Another non-stoichiometric Ca-hydroxyapatite is over-stoichiometric HAp or rich HAp (further noted HAp-R). HAp-R has a Ca/P molar ratio above 1.67. Generally, the excess of Ca in HAp-R could lead to the formation of CaO or $Ca(OH)_2$ on the HAp surface [13].

The structure of HAp can also be changed upon ionic substitution. For instance, Ca^{2+} can be partially substituted by cations like Na^+, K^+, Mg^{2+}, Sr^{2+}, etc. [9, 12, 16–18], and PO_4^{3-} and OH^- can be substituted by CO_3^{2-}, HPO_4^{2-}, SO_4^{2-}, etc. [14, 19, 20]. A common anionic substitution is CO_3^{2-}, as similarly found in the biological HAps [21–23]. CO_3^{2-} can replace *i)* OH^- (A-type) (Eq1), *ii)* PO_4^{3-} (B-type) (Eq. 2) or *iii)* both hydroxyl and phosphate groups (AB-type) in the HAp structure [14, 24]:

i) In A-type substitution, a smaller OH^- is replaced by a larger CO_3^{2-}, where, to keep the charge balance, two OH^- have to be released as shown in Eq (1).

$$Ca_{10}(PO_4)_6(OH)_2 + x\,CO_2 \rightarrow Ca_{10}(PO_4)_6(CO_3)_x(OH)_{2-2x} + x\,H_2O \qquad \text{Eq (1)}$$

Where $0 < x \leq 1$.

ii) In B-type substitution, one or two larger PO_4^{3-} is/are replaced by one or two smaller CO_3^{2-}, where a Ca^{2+} ion or one OH^- ion must be released per phosphate substituted to keep the charge balance:

$$Ca_{10}(PO_4)_6(OH)_2 + x\,CO_2 \rightarrow Ca_{10-x}(PO_4)_{6-x}(CO_3)_x(OH)_{2-x} + x\,H_2O \qquad \text{Eq (2)}$$

Where $0 < x \leq 2$.

iii) And for AB type, presence of HPO_4 is also expected [25]:

$$Ca_{10}\left[(PO_4)_{6-x-y}(HPO_4)_x(CO_3)_y\right]\left[(OH)_{2-(x+y)}(CO_3)_{x+y}\right], \text{ with } 0 < x, y \leq 1$$

Thus, the formulae of the HAp can be modified significantly upon ionic substitutions in their structure and this, of course, consequently modifies their physicochemical and catalytic properties.

Among the various HAp groups mentioned earlier, biological HAp has been studied for transesterification reactions by several groups. For instance, Farooq *et al.* [2] studied a HAp derived from waste chicken bones as heterogeneous catalyst for the transesterification reaction of waste cooking oil for biodiesel production. They reported a biodiesel yield of 89.33% at 5 wt.% of catalyst loading, at a temperature of 65 °C and a reaction time of 4 h. Furthermore, the catalyst was reused for 4 cycles with a biodiesel yield of 79 %, where the recovered catalyst was calcined after each reaction. The decrease of performance observed after each cycle was explained by the deactivation of the

catalyst by deposition of unreacted oil, biodiesel or glycerol on the active sites at the surface of the catalyst.

Furthermore, Yan *et al*. [4] used a HAp derived from pig bones loaded with CaO-CeO_2 for triglycerides transesterification reaction. 30 wt.% CaO-CeO_2/HAp exhibited the highest yield to FAME (91.8%) when 11 wt.% of the catalyst was used at 65 °C for a reaction time of 3 h, whereas the FAME yield was only 83.5 % in the presence of 20 wt.% CaO-CeO_2/Hap used in the same conditions. This increase in catalyst activity was explained by an increase in the basicity of 30%CaO-CeO_2/HAp. Moreover, in terms of catalyst stability, CaO-CeO_2/HAp and HAp were recovered and used for eight cycles where the yield of FAME decreased from 91.8% to 84.4% and from 83.5% to 65%, respectively. The authors explained this decline in catalytic activity by Ca and Cs leaching and by the loss of basic sites from the catalyst surface. For instance, in the first reaction cycle, the concentrations of leached cerium and calcium species were 65 and 100 ppm, respectively, when CaO-CeO_2/HAp was used. However, after 8 cycles, the concentrations of catalyst components (Ca^{2+} and Cs^{4+}) subsequently leached into the product phase decreased to 10 ppm.

With respect to these results, HAps could be envisaged as suitable catalysts for glycerol polymerization, a liquid phase condensation reaction taking place at high temperature. To the best of our knowledge, no study has been performed so far on the catalytic activity of HAps in glycerol polymerization reaction. Therefore, based on the literature review, we decided to develop new catalysts based on calcium hydroxyapatite, which were assumed to act heterogeneously in the glycerol polymerization reaction.

Herein, we prepared, characterized and tested several HAps catalysts to evaluate their catalytic performance in glycerol polymerization reaction. They were classified in three groups:

i) Ca-HAps with various Ca/P ratio (i.e, stoichiometric, deficient and rich HAps).

ii) CaO supported on HAp (CaO/HAp).

iii) Carbonated HAps.

Afterwards, based on the catalyst characterizations and catalytic performances evaluation, the mechanism of deactivation of the catalysts will be studied and discussed.

4.2 Influence of the Ca/P ratio

4.2.1 Catalysts characterization

HAp-D, HAp-S and HAp-R catalysts, prepared as described in Section 2.2.3 of Chapter 2, were characterized by several techniques including BET, XRD, XPS, IR and TGA to study the influence of the Ca/P ratio on their bulk and surface properties.

4.2.1.1 Surface characterization and elemental analysis

The specific surface areas (SSA) of HAp-D, HAp-S and HAp-R were measured using nitrogen adsorption/desorption and the BET model (Table 4.1). The HAp-S with 70.4 m^2/g developed a higher SSA than HAp-D and HAp-R with 19.4 m^2/g and 13.8 m^2/g, respectively.

Moreover, the ICP analysis of the catalysts showed that the atomic Ca/P ratios of bulk HAp-S, HAp-D and HAp-R were 1.66, 1.62 and 1.78 with 36.07 wt.%, 36.16 wt.% and 38.44 wt.% of calcium, respectively (Table 4.1). The difference between the experimental and the theoretical Ca/P atomic ratio for HAp-D (Table 4.1) suggests that other apatites such as β-TCP, OCP and DCP, that are generally expected for a deficient HAp, has not formed (See Section 4.1).

Table 4.1. Surface areas and chemical compositions of the calcined HAps.

Catalyst	BET specific surface area (SSA) (m^2/g)	Theoretical Ca/ P atomic ratio	Experimental Ca/P atomic ratio (ICP)	Ca (wt.%) (ICP)	P (wt.%) (ICP)	C (wt.%)
HAp-D	19.4	1.45	1.62	36.16	17.33	0.108
HAp-S	70.4	1.67	1.66	36.07	16.84	0.111
HAp-R	13.8	1.94	1.78	38.44	17.39	0.8

Some carbon was detected in HAp-D, HAp-S and HAp-R structures. This suggest that atmospheric CO_2 probably absorbed during the synthesis process, as reported also in the literature [13, 14, 26]. However, since the examined samples were calcinated at 700 °C (see Section 2.2.3 of Chapter 2) prior to the elemental analysis, this suggests that a total release of CO_2 could only occur at a higher temperature.

4.2.1.2 XRD

The X-ray diffraction patterns of HAp-S, HAp-D and HAp-R are presented in Figure 4.2 a-c. The characteristic peaks of calcium hydroxyapatite (PDF 04-014-8416) were observed for all these HAps. Moreover, no peaks assign to neither β-tricalcium phosphate (β-TCP) (PDF 00-055-0898); octacalcium phosphate (OCP) (PDF 00-044-0778), nor to calcium pyrophosphate (DCP) (PDF 00-044-0762) were observed (Fig 4.3). In addition, for HAp-R, no other crystalline phase that CaO with 2θ at 32.2°, 37.4° and 53.9° (PDF 01-070-4066) or Ca hydroxide with 2θ at 18.14°, 28.7°, 34.2°, and 50.8° (PDF-00-087-0673) were observed. However, it has to be noted that it is possible that the main XRD peak for CaO at 2θ = 32.2° or $Ca(OH)_2$ at 34.2° is hidden by the intense peaks of HAp-R between 2θ = 31° and 35°.

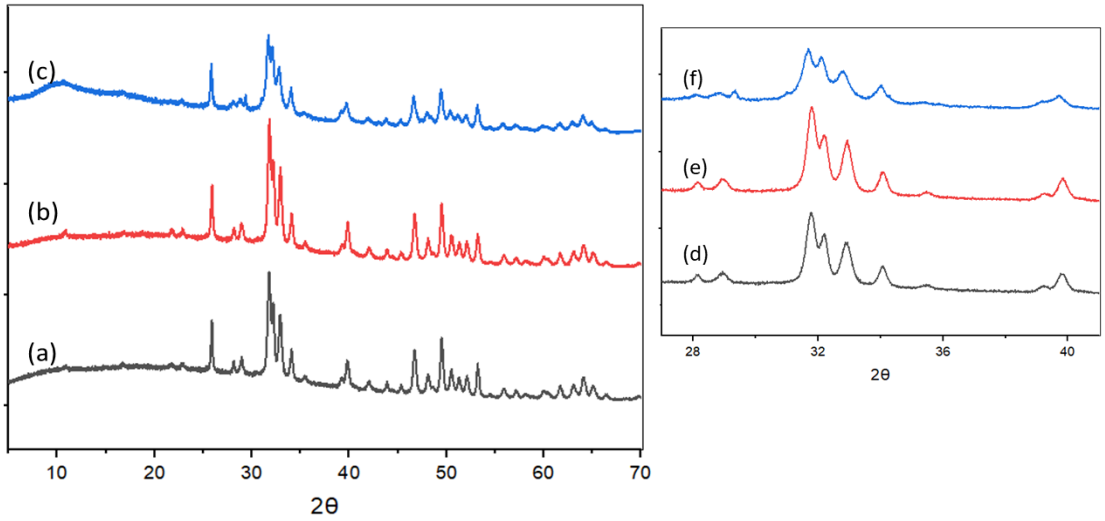

Figure 4.2. XRD patterns of a) HAp-D, b) HAp-S and c) HAp-R; and zooms of the XRD patterns in the range 2θ=27 to 41° for d) HAp-D, e) HAp-S and f) HAp-R.

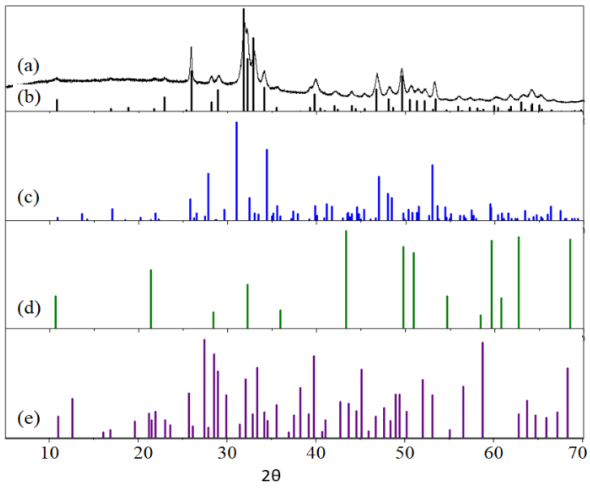

Figure 4.3. XRD patterns of a) HAp-S and the standard PDF cards for b) calcium hydroxyapatite, c) β-TCP, d) OCP and e) DCP.

As shown in Figure 4.2 d-e, the XRD patterns of HAp-S and HAp-D, indicated a better crystallinity compared to HAp-R. Generally, the loss of crystallinity could be due to the variation in maturation time and the synthetizing method [14, 25]. Thus, it is not possible to distinguish the stoichiometric and non-stoichiometric HAps by X-ray diffraction, as also reported in the literature [14, 20].

4.2.1.3 XPS

HAp-D, HAp-S and HAp-R were analyzed by XPS to investigate the catalysts surface compositions, notably the Ca/P ratio and the interactions between the elements present on the surface. The XPS spectra for these catalysts, showed in Figure 4.4, indicate the presence of Ca, P, O and C elements, as it was expected.

The peaks at 284.8 eV, 285.8 eV and 288.6 eV, corresponding to C 1s, were attributed to the organic C (C-C), Ca-OH-C (C-O) and CO_3, respectively (Figure 4.5). The peak at 284.8 eV was used to calibrate the spectra. It has to be noted that a considerable carbon contamination of the HAps' surface can originate from the pump used to the XPS chamber under vacuum. This is generally known as "adventitious carbon" [27].

As shown in Figure 4.5a, for HAp-D and HAp-S, a well-defined doublet with two components Ca $2p_{1/2}$ (347.4 eV) and Ca $2p_{3/2}$ (350.9 eV) is observed, which is attributed to Ca involved in bonds characteristic of HAps [20, 28]. However, the Ca 2p spectrum of HAp-R suggests that the environment of Ca ions on the surface of HAp-R is not similar to that in HAp-S and HAp-D.

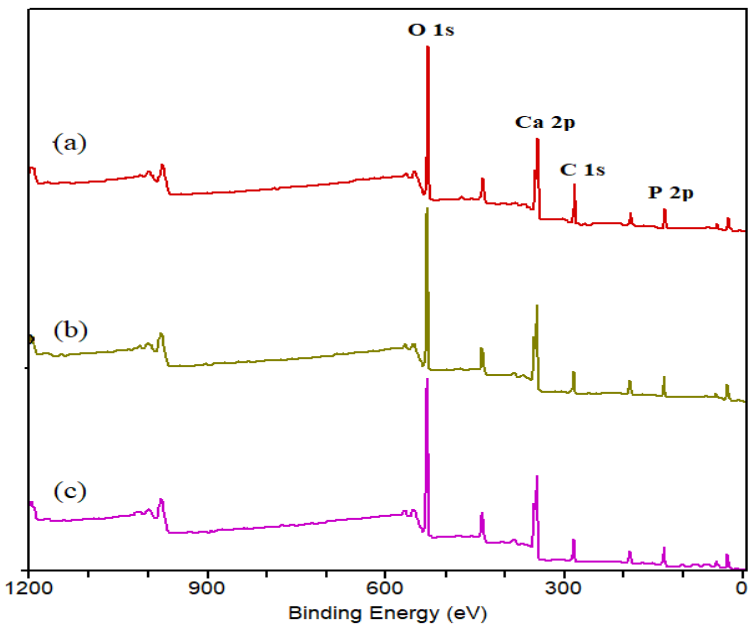

Figure 4.4. XPS spectra of a) HAp-D, b) HAp-S and c) HAp-R.

For all HAps, the O 1s envelope (Fig 4.5c) was fitted with two peaks at 531.1 eV and 532.6 eV, attributed to O-Ca and O-P (or O-H) in the structure of HAps, respectively [28, 29]. It should be noted, although, that the peak assigned to O-C cannot be distinguished in the fitted peaks, however, the presence carbonate peak (288.6 eV) has already confirmed the presence of carbonate on the surface of the HAps.

Table 4.2. Surface chemical compositions (atomic %) of HAp-D, HAp-S and HAp-R (determined by XPS analysis)

Catalyst	**C 1s (%)**	**O 1s (%)**	**Ca 2p (%)**	**P 2p (%)**	**Ca/P (XPS)**
HAp-D	35	43.8	12.4	8.8	1.40
HAp-S	21.7	51.4	15.5	11.4	1.36
HAp-R	22.9	50.9	15.6	10.6	1.48

The atomic percentages in Ca, P, O and C are presented in Table 4.2 for the three catalysts. These values represent the atomic proportions in a surface layer of approximately 10 nm-depth. The Ca/P ratios for HAp-D, HAp-S and HAp-R were 1.4, 1.36 and 1.48, respectively. The lower Ca/P ratios observed on the surfaces of the HAps compared to the bulk ratios determined by ICP (Table 4.1) can be due to the carbonate adsorption on the surface, which caused a change in stoichiometries. This is in an agreement with previous studies [25, 29], and indicates that Ca species are less exposed on the surface.

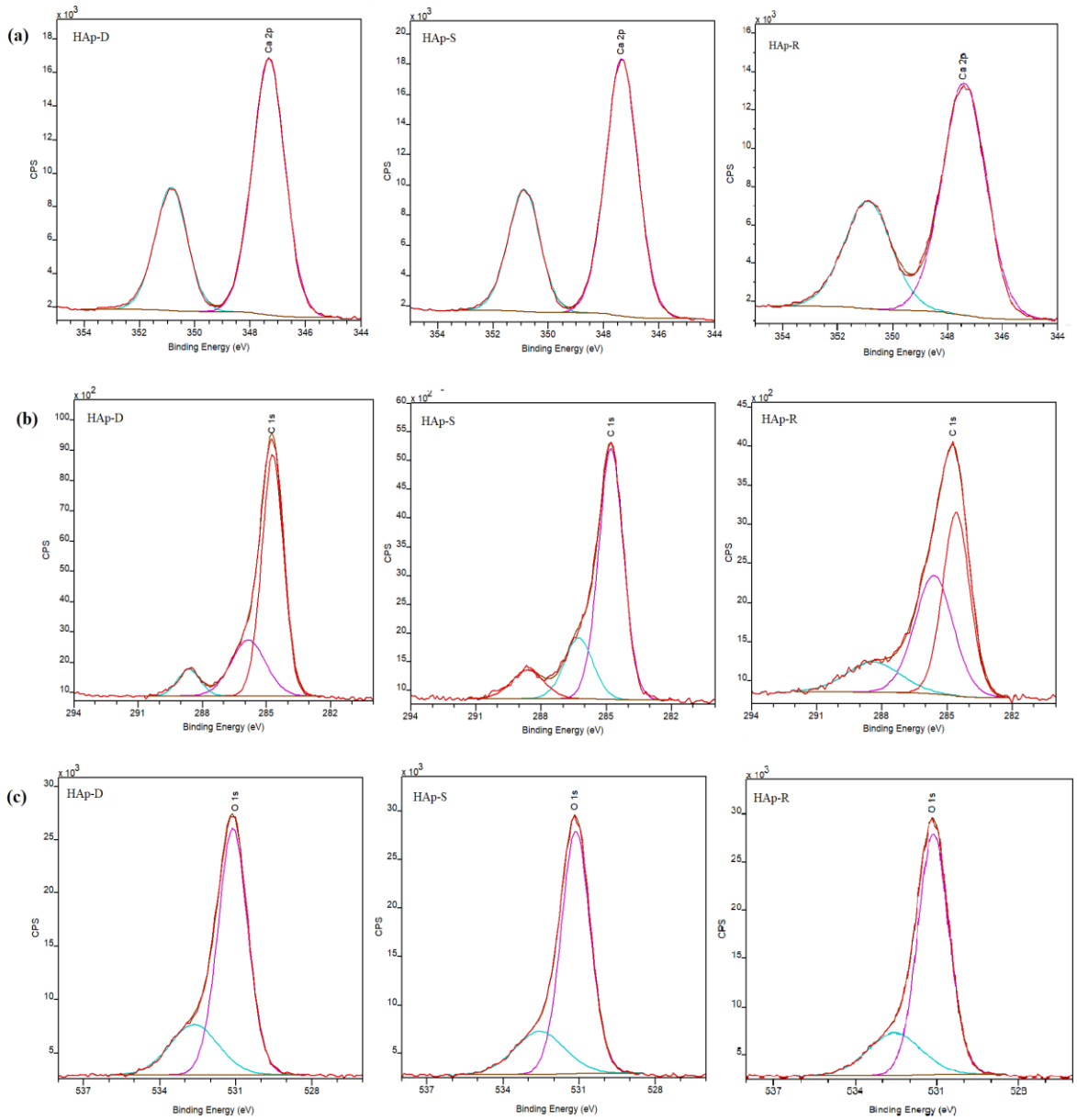

Figure 4.5. XPS spectra of HAp-D, HAp-S and HAp-R for: a) Ca 2p, b) C 1s and c) O 1s.

4.2.1.4 IR analysis

The chemical bonds present in the structures of the HAps were further studied by IR analysis. For HAp-S, HAp-D and HAp-R, the IR spectra confirmed the presence of OH, carbonates and phosphate groups as shown in Figure 4.6.The peak at 3572 cm^{-1} is assigned to the OH groups in the structures of the HAps; whereas the peaks at 652 cm^{-1}, 1084 cm^{-1}, 1173 cm^{-1} and 4 peaks in the region of 1960 to 2220 cm^{-1} are assigned to the vibration of PO_4^{3-} in HAps [14, 25, 26].

Furthermore, the bands in the regions of 1370 cm^{-1} and 1580 cm^{-1} with 4 peaks at 1413 cm^{-1}, 1456 cm^{-1} (A and B-type), 1500 cm^{-1} and 1550 cm^{-1} (A-type) were attributed to carbonate groups [14, 19, 26]. The zooms of the IR spectra in the 800-1800 cm^{-1} region (Fig 4.7 a-b), showed the presence of carbonated groups in all samples but the intensities of the two peaks at 1413 and 1456 cm^{-1} were lower for HAp-D and HAp-S compared to what was observed for HAp-R (Fig 4.7c).

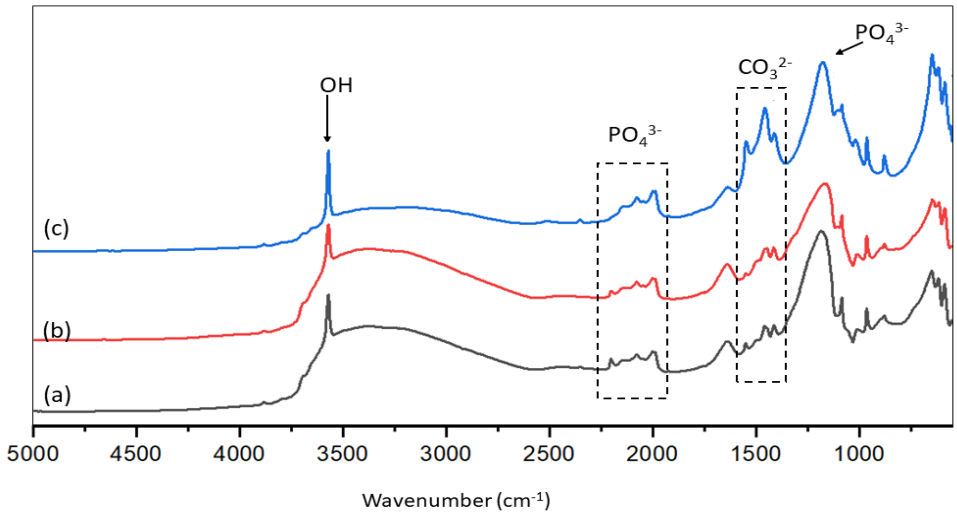

Figure 4.6. IR spectra for a) HAp-S, b) HAp-D and c) HAp-R.

Moreover, three peaks at 878, 963 and 1017 cm^{-1} assigned to HPO_4^{2-} [14, 21, 26] were observed for all HAps (Fig 4.7 (a-c). For the deficient HAp, the presence of HPO_4^{2-} was expected (see Section 4.1). For other HAps, the presence of HPO_4^{2-} can be explained by A and B-type carbonate substitutions as illustrated in (Eq. (3)). Thus, regardless their Ca/P ratios, all the HAps contain PO_4^{3-}, HPO_4^{2-}, CO_3^{2-} and OH^- groups.

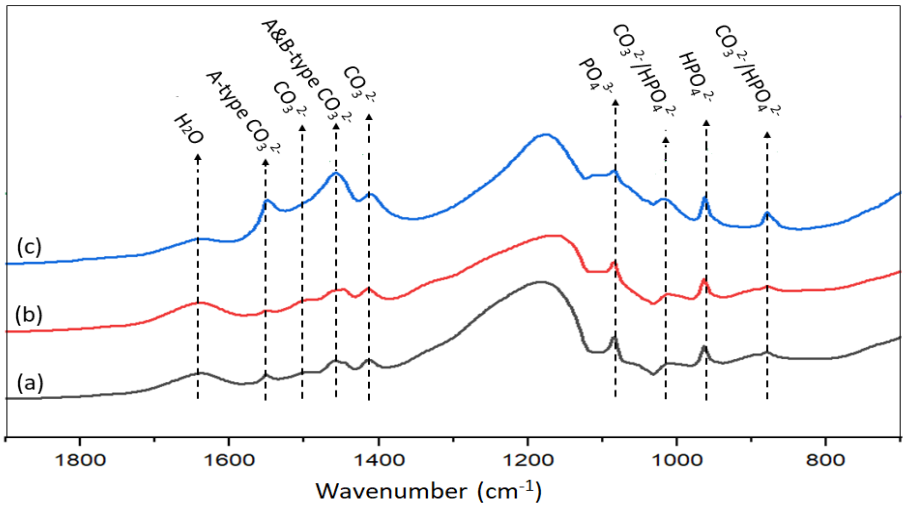

Figure 4.7. Zooms of the IR spectra for a) HAp-S, b) HAp-D and c) HAp-R.

4.2.1.5 Thermal analysis

TGA was performed on the non-calcined HAp-D, HAp-S and HAp-D samples to study their thermal behavior.

The TGA curve for HAp-D showed a total weight loss of 2.02 wt.% between room temperature (RT) and 1100 °C. The first weight loss from RT to 140 °C can be attributed to the release of absorbed H_2O from the sample surface, followed by 2 steps of mass loss of 0.53 wt.% and 0.32 wt.% up to 800 °C (Fig 4.8a), which can be attributed to the release CO_2. The final mass loss of 0.78 wt.% was observed between 800 °C to 1100 °C, where a broad endothermic peak at 957 °C associated with this weight loss was also observed in the DSC curve. This can suggest a phase transition of deficient HAp to stochiometric HAp and TCP. This large broad endothermic peak in the range of 900 to 1100 °C was observed for all the samples.

Similarly, the TGA curve for HAp-S showed a three steps weight lost with a total loss of 5.56 wt.% (Fig 4.8b). The first weight loss (1.81 wt.%) from RT to 214 °C, followed by 2.66 wt.% loss up to 743 °C, suggests the release of H_2O and CO_2 from the sample. The final weight loss of 1.09 wt.% with a corresponding endothermic peak at 919 °C was recorded between 743 °C to 1100 °C, which can be associated with the decomposition of HAp to TCP.

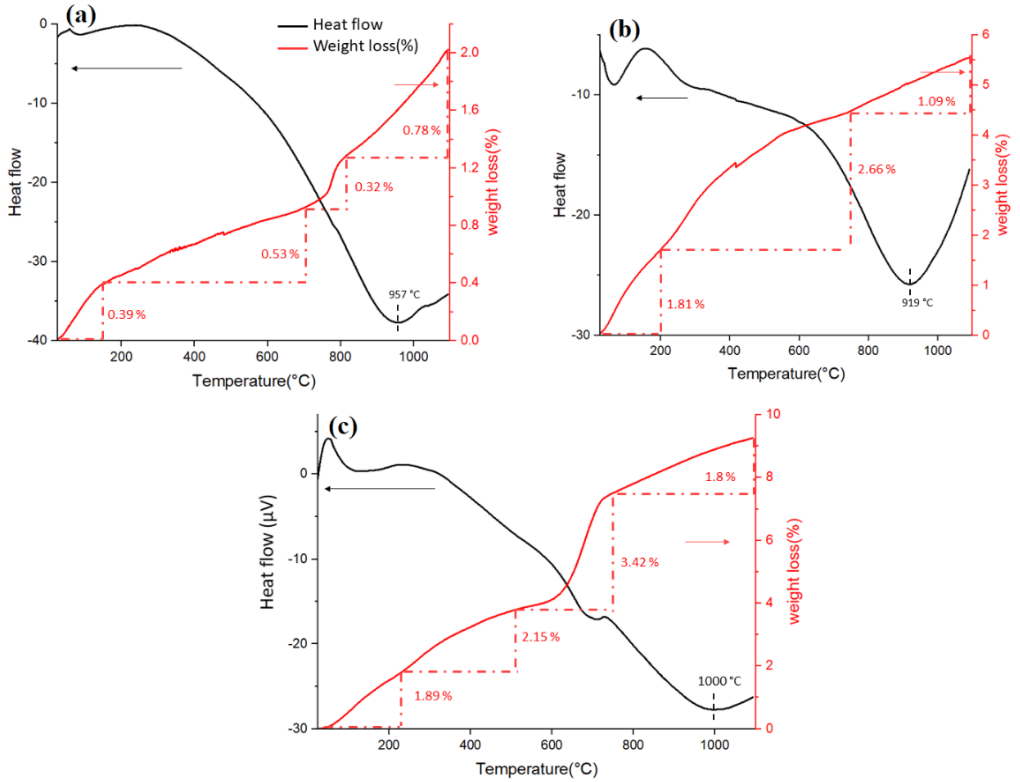

Figure 4.8. TGA-DSC profiles for non-calcined a) HAp-D, b) HAp-S and c) HAp-R.

For HAp-R, the weight lost was observed in 4 steps. First, two mass losses of 1.89 and 2.15 wt.% were recorded between RT and 587 °C, which could correspond to the desorption of H_2O and CO_2 from the surface. A further weight loss of 3.42 wt.% was recorded between 587 and 745 °C. An endothermic peak at 705 °C, which corresponds to this mass loss suggests a decarboxylation of the HAp-R sample at this temperature range. Finally, HAp-R lost 1.8 wt.% when heated up to 1100 °C. This can be similarly attributed to the decomposition of HAp-R to HAp-S, CaO or TCP, as shown in Fig 4.8-c.

4.2.2 Catalytic performances

The catalytic performances of HAp-S, HAp-D and HAp-R were evaluated at 245 °C in the presence of 0.5 mol.% of catalyst (based on the number of moles of glycerol) after 8 h of reaction, as shown in Figure 4.9 (left).

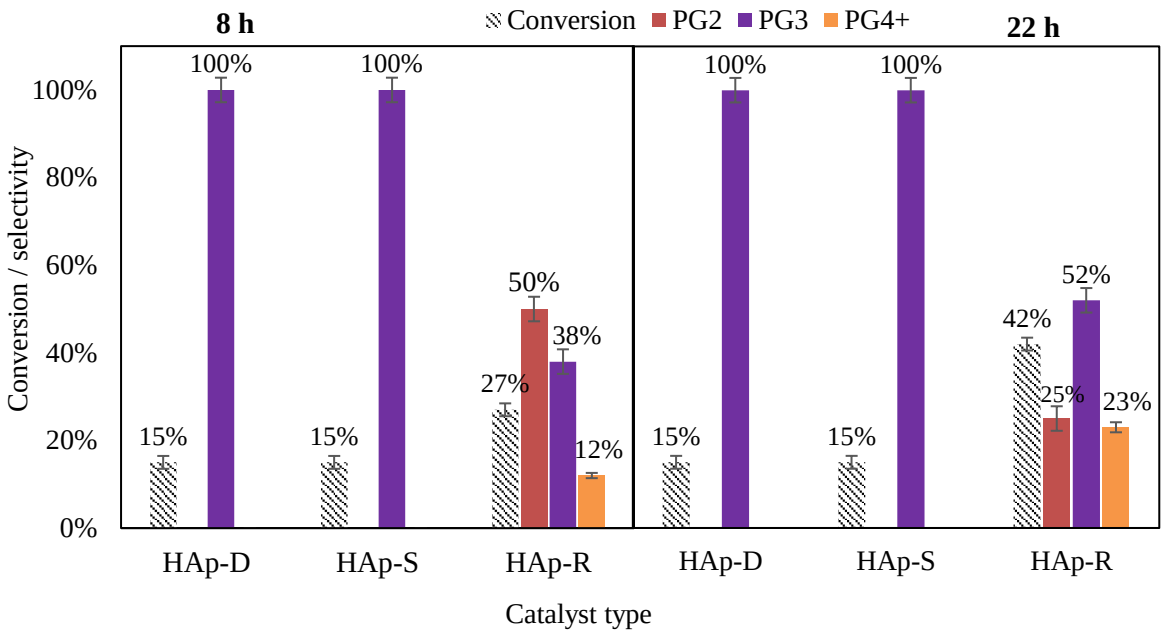

Figure 4.9. Catalytic performances of HAp-D, HAp-S and HAp-R tested at 245 °C after 8 h (left) and after 22 h of reaction (right).

These results showed that HAp-S and HAp-D exhibited the same catalytic performances: 15 % glycerol conversion with 100% selectivity to PG3. More precisely, these catalysts are ultra-selective to only one molecule, which has been identified as cyclic-PG3 by ESI-MS (Figure 4.10a-b). The similar catalytic behavior for these two catalysts could be due to their similar Ca contents, namely 36.07 wt.% for HAp-S and 36.16 wt.% for HAp-D (Table 4.1). The low glycerol conversion of 15% can be explained by the fact that Ca species, as the active site, were less exposed on the surface of catalysts,

as shown by the XPS results (Table 4.2). Surprisingly, the glycerol conversion using HAp-S and HAp-D did not increase when the reaction time was prolonged to 22 h (Figure 4.9 (right)). This could suggest that these catalysts have been deactivated during the first 8 h of reaction. This will be further discussed in Section 4.6.

For the rich hydroxyapatite (HAp-R), a glycerol conversion of 27% with a high selectivity to PG2-PG3 (88%) was also observed after 8 h reaction. Moreover, in contrast to HAp-S, the glycerol conversion increased to 42% with 77% of PG2-PG3 selectivity when the reaction was carried out for 22 h under the same reaction conditions (Fig 4.9 (right)). The higher activity for HAp-R in contrast to HAp-S and HAp-D can be explained by i) higher Ca content on the surface (heterogenous phase) and /or ii) Ca leaching into the reaction media (homogenous contribution). To evaluate both contributions ICP analyses of the reaction medium after test were performed and reported in Table 4.3.

Table 4.3. Amounts of Ca and P leached into the reaction medium (determined by ICP-OES) and percentages of leached calcium when 0.5 mol.% of catalysts was used at 245 °C for 8 h.

Catalyst	**Ca (mg/g)***	**P (mg/g)***	**Leached Ca (%)**
HAp-D	0.19	0.11	1.8
HAp-S	0.06	0.05	0.5
HAp-R	0.37	0.00	3.4

* mg of leached Ca or P /g of reaction mixture

The higher conversion of HAp-R compared to HAp-S or HAp-D (27% vs 15% after 8 h) could be due to the higher Ca/P surface ratio in HAp-R compared to HAp-S (1.48 vs 1.36, Table 4.2). This is due to the presence of a layer of CaO (< 10 nm) on the surface of HAp-R. Thus, the reaction could directly be catalysed by CaO (on the surface). Moreover, the selectivity toward both PG2 (50 %) and PG3 (38%) observed for HAp-R contrasts with what was observed for to HAp-S or Hap-D, which were only selective to PG3 (100 %). This could be explained by the presence of CaO as well.

The increase in the activity of HAp-R might be also attributed to the Ca leaching (3.4 % of Ca) into the reaction medium, which was observed by ICP-OES. When HAp-D and HAp-S were used as catalysts, only 1.8 % and 0.5 % of Ca leached to the reaction media, respectively, after 8 h of reaction (Table 4.3). Since no increase, neither in glycerol conversion nor in PG3 selectivity was observed after 22 h of reaction time in the presence of HAp-D and HAp-S, that could suggest that the leached Ca did not homogeneously contribute to the catalysis of the reaction. If not, the reaction would have continued even if deactivation of the HAp-S and HAp-D solids would have occurred.

It should be also noted that P has not leached in the reaction medium when HAp-R was used as catalyst (Table 4.3). This can be due the fact that leached Ca was due to the solubilization of the CaO present on the surface. On the contrary, for HAp-S and HAp-D, both Ca and P leached in the reaction medium, suggesting a B-type substitution, where both Ca^{2+} and phosphate group can be released to the reaction media (see Section 4.5.1.3).

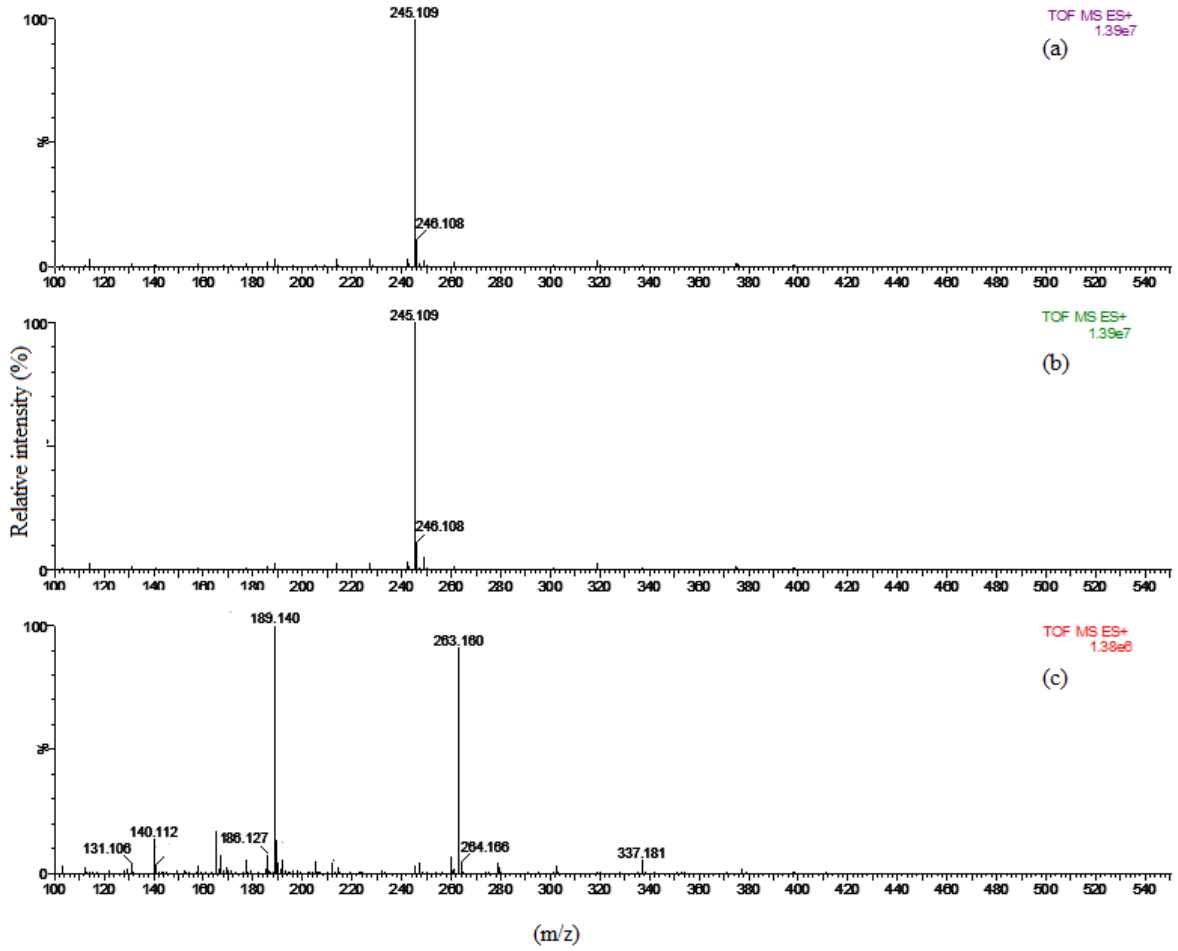

Figure 4.10. ESI-MS spectra of reaction media after 8 h of reaction when a) HAp-D, b) HAp-S and c) HAp-R were used as catalysts at 245 °C.

Furthermore, HAp-R was highly selective to linear PG2-PG3 (as shown in Fig 4.10c), where the peaks at 189.1 and 263.1 Da corresponds to linear PG2 and PG3, respectively (Annex A-Table A.3). The small peak at 337 Da (Fig 4.10c) corresponds linear PG4. It was only observed when HAp-R was used as the catalyst. The peak at 245 Da, observed when HAp-S and HAp-D were used as catalysts, corresponds to cyclic PG3 (Fig 4.10 a-b).

4.2.3 Conclusion

As a short conclusion of this part, it can be said that for all the HAps studied (HAp-S, HAp-D and HAp-R) the formation of calcium hydroxyapatite structures is confirmed and that no other crystalline phase was observed by XRD. Moreover, IR spectra exhibited the characteristic peaks of hydroxyapatite including hydroxyl and phosphate groups for all HAps. In addition to that, the presence of CO_3^{2-} (also confirmed by C analysis) and HPO_4^{2-} groups were also validated.

The XPS spectra for HAp-D, HAp-S and HAp-R confirmed that less Ca was exposed on the surface of these catalysts compared to the bulk. This can be due to the presence of various groups including CO_3^{2-} and HPO_4^{2-}, which changed the surface stoichiometries.

The thermal analysis showed 2 to 10 wt.% of weight loss for these catalysts, which could mainly be attributed to the release of H_2O and CO_2. The TGA results were also in a good agreement with C analysis, where it confirmed that calcination at 700 °C only partially removed the carbonates in the structures of the HAps. Thus, since the results of catalyst characterization confirmed the presence of carbonates in HAps, their effect on the catalyst activity must be studied.

Concerning the catalytic performances, it was showed, on one hand, that both HAp-D and HAp-S exhibited a total selectivity to cyclic PG3 together with a glycerol conversion of 15%. The similar catalytic performances of both catalysts were explained by their similar Ca/P ratios measured by ICP-OES. Moreover, these catalysts also showed a good stability during the glycerol polymerization reaction, where only 1.8 and 0.5 mol.% of the calcium present in HAp-D and HAp-S leached in the reaction media after 8 h of reaction, respectively. However, the absence of difference in the catalytic performances after 8 and 22 h of reaction for these catalysts (Figure 4.9) suggested that they have been deactivated.

On the other hand, a higher glycerol conversion was obtained in the presence of HAp-R (27%), in the same reaction conditions, together with a good selectivity to linear PG2-3 (88%). An increase in the glycerol conversion (42%) with a selectivity of 77% to PG2-PG3, after 22 h of reaction, suggested that catalytic performances could be influenced by the Ca leaching even if 96.5 % of the Ca was still in the solid state, based on the ICP results. The Ca leaching is therefore most probably mainly due to the CaO present on the surface of this rich-HAp.

In addition, leaching of P that was also observed for HAp-D (0.11 mg/g) and HAp-S (0.05 mg/g) (Table 4.3), suggesting that a B-type substitution occurred *in situ* during the reaction, causing both Ca and P leaching to the reaction medium.

So far, HAp-D and HAp-S showed a better stability compared to HAp-R, while HAp-R exhibited a higher glycerol conversion, in the same reaction condition. The three catalysts were highly selective to

PG2-PG3. Thus, an enrichment of HAp-D with calcium could improve the yield to these short chains-PGs. Thus, in next sections, the performances of enriched HAp with Ca (Section 4.3) and the effect of carbonated species on HAp catalyst (Section 4.4) will be investigated.

4.3 Enrichment of HAp by CaO addition

Since, the rich HAp (HAp-R) showed a promising catalytic activity, we decided to enrich HAp-D by addition of CaO to try to improve its performances. Thus, we synthesized and characterized several enriched catalysts further noted *x* wt.% CaO/HAp where *x* is the weight percent of loaded CaO in the range 5 to 30 wt.% and where HAp is always HAp-D.

4.3.1 ICP-OES

The ICP analysis of the 5, 10 and 30 wt.% CaO/HAp contained 37.02, 38.54 and 42.98 wt.% of Ca, respectively. Obviously, the higher amount of Ca led to an increase in the Ca/P ratio for these catalysts, as expected. However, the Ca/P atomic ratio determined by ICP was higher than the theoretical ones. For instance, the theoretical Ca/P ratio for 5 wt.% CaO/HAp was 1.6, whereas, the actual Ca/P was 1.74. Obviously, the differences between the experimental and the theoretical Ca/P atomic ratios in these catalysts originate from the HAp-D support. As aforementioned in Section 4.2.1.1, deficient HAp with theoretical Ca/P ratio of 1.45 had a higher Ca/P ratio of 1.62, which consequently caused an higher Ca/P experimental ratio compared to the theoretical ones for x wt.% CaO/ HAp catalysts (Table 4.4).

Table 4.4. Chemical compositions of the *x* wt.% CaO/HAp catalysts.

Catalyst	**Theoretical Ca/P atomic ratio**	**Experimental Ca/P atomic ratio (ICP)**	**Ca (wt.%)**	**P (wt.%)**
HAp-D (sole)	1.45	1.62	36.16	17.33
5 wt.% CaO/HAp	1.60	1.74	37.02	16.48
10 wt.% CaO/HAp	1.76	1.98	38.54	15.12
30 wt.% CaO/HAp	1.94	2.97	42.98	11.20

4.3.2 XRD

The XRD patterns of HAp-D (bare support) and of HAp-D loaded with 5, 10 and 30 wt.% of CaO are shown in Figure 4.11. For 5 wt.% CaO (Fig 4.11b), no peaks attributed to CaO were observed. That is probably due to the fact that it is well-dispersed on the surface and cannot be detected by XRD.

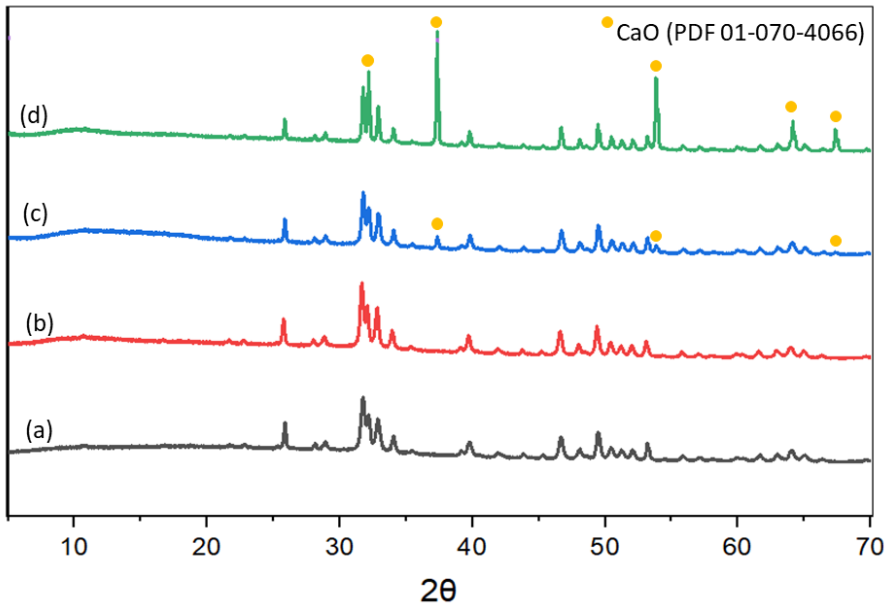

Figure 4.11. XRD patterns of a) HAp-D and b) 5 wt.% CaO/HAp, c) 10 wt.% CaO/HAp and d) 30 wt.% CaO/HAp.

In contrast, for 10, and 30 wt.% CaO/HAp, Fig 4.11 c-d, 5 peaks at 2θ = 32.2°, 37.4°, 53.9°, 64° and 67° attributed to CaO (PDF 01-070-4066) were observed. However, the peaks at 2θ = 32.2° and 64° overlapped with the HAp-D peaks for 10 wt.%CaO/HAp (Fig 4.11-c). Thus, the XRD analysis confirmed the presence of CaO in these catalysts, which was consistent with the elemental analyses.

4.3.3 Catalytic performances

The performances of the *x* wt.% CaO/HAp catalysts were evaluated and compared to HAp-D, pure CaO and a mechanical mixture of of CaO and Hap (5/95 wt.%), using 0.5 mol.% of each catalyst (compared to the number of moles of glycerol) used in the same reaction conditions (245 °C, 8 h).

For 5, 10 and 30 wt.% CaO/HAp, glycerol conversions of 23, 26 and 26% and selectivity to PG2-3 of 67%, 63% and 32% were obtained, respectively (Figure 4.12). The similar glycerol conversion obtained for all the catalysts except sole CaO and HAp-D indicate that glycerol conversion reached a plateau, while the PG2-PG3 selectivity decreased to the benefit of PG4+ polymers by increasing the amount of loaded CaO.

General speaking, an increase of PG4+ selectivity to the expense of PG2-3 selectivity, at a similar level of glycerol conversion could be due to: *i)* a higher amount of solid CaO on the HAp surface (heterogenous phase) or/and *ii)* an increase of the quantity of Ca leached in the reaction medium (homogenous contribution). To evaluate both contributions ICP analyses of the reaction medium after test were performed and reported in Table 4.5.

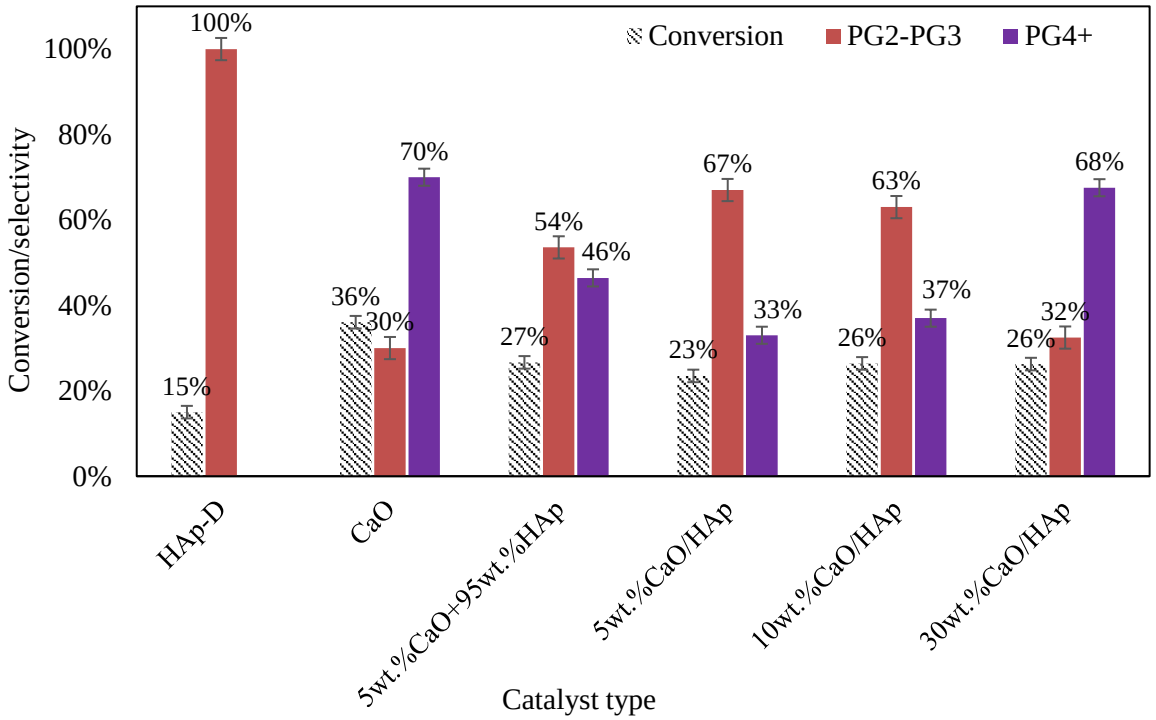

Figure 4.12. Glycerol conversion and selectivities to PGs after 8 h of reaction at 245 °C.

The ICP results shown in Table 4.5 revealed that 3.2 %, 12.2 % and 42.7 % of Ca leached, when the reaction took place in the presence of 5, 10 and 30 wt.% CaO/HAp, respectively. However, it should be noted that the observed leached Ca could originate from CaO and/or HAp. The amount of Ca leaching for 10 and 30 wt.% CaO/HAp were significantly higher than the Ca leached from 5 wt.% CaO/HAp. This result suggests that the effect of the interaction between the support and CaO is reduced by increasing the thickness of the CaO layer on the HAp hence causing a higher leaching for the high loadings.

Furthermore, 5 wt.% CaO/HAp leads to a higher glycerol conversion compared to sole HAp-D (23% *vs* 15%). However, as similarly mentioned for HAp-R (Section 4.2.2), the activity of this catalyst is most likely due to the presence of CaO on the surface. In comparison, sole CaO (0.3 wt.% ~ 0.5 mol.%) showed an higher glycerol conversion, while the selectivity to PG2-PG3 was 30% (Fig 4.12). This could be due to the higher concentration of Ca in the reaction media (100% of leached Ca because CaO is totally solubilized after 0.5 h in the reaction conditions) compared to the reactions which took place in the presence of solid CaO loaded on HAp.

Table 4.5. Ca leached in the reaction medium (determined by ICP) after 8 h of reaction at 245 °C.

Catalyst	**Leached Ca (mg/g)***	**Proportion of Ca in the reaction medium after reaction (%)**
5 wt.% CaO + 95 wt.% HAp	0.51	6.1
5 wt.% CaO/HAp	0.26	3.2
10 wt.% CaO/HAp	0.82	12.2
30 wt.% CaO/HAp	1.75	42.7
Sole CaO	3	100

* mg of leached Ca per g of reaction mixture determined by ICP-OES analyses.

Furthermore, the results also revealed that when CaO and HAp are introduced separately as a simple mechanical mixture into the reaction medium ("5 wt.% CaO + 95 wt.%HAp" sample) instead of using the corresponding 5 wt.% CaO/HAp supported catalyst, it lead to a higher selectivity to PG4+ (46% *vs.* 33%), whereas the glycerol conversions were very close (27% *vs.* 23%). This increase in PG4+ selectivity can be explained by the higher amount of Ca leached from the mechanical mixture compared to what was observed for 5 wt.% CaO/HAp (0.51 *vs.* 0.26 mg/g). More interestingly, the amount of Ca leaching decreased from 6.1% to 3.2 when CaO was supported on the HAp, meaning that CaO is more resistant to leaching and, consequently, caused an improvement in the catalyst stability, when it interacts with the HAp support.

4.3.4 Conclusion

The XRD results confirmed the presence of CaO in 10 and 30 wt.% CaO/HAp, while for 5 wt.% CaO/HAp only the characteristic peaks of hydroxyapatite were observed. However, we should bear in mind that a small amount of CaO well dispersed on the support cannot be observed by XRD. The elemental analysis performed by ICP-OES for solid catalysts confirmed higher Ca/P ratios for these catalysts compared to HAp-D, as expected.

Furthermore, the catalytic performances of these catalysts showed that the highest selectivity to PG2-3 (67%) at 23% of glycerol conversion was obtained when 5 wt.% CaO/HAp was used as catalyst. Moreover, loading a small quantity of CaO on the HAp-D support improves significantly its stability in the reaction conditions, as shown by the decrease by a factor two of the amount of Ca leached after 8 h of reaction.

4.4 Carbonated HAps

Here, we attempted to carbonize the stoichiometric HAp to better understand the influence of the carbonate groups on the catalytic performances. Hap-S was carbonated by two methods: a) by placing the calcined HAp under a CO_2 atmosphere (catalyst further labelled HAp-CO) and b) by adding a polymer (P123) during HAp synthesis (catalyst further labelled HAp-CP).

In the 1st method (HAp-CO), Ca on the surface of HAp was expected to convert to $CaCO_3$ through chemisorption of CO_2. While in the 2nd method (HAp-CP), the carbonization took place at high temperature (700 °C, during the catalyst calcination), by introducing the CO_2 produced from polymer burning (Eq (1)). This method is one of the common method described in the literature to produce carbonated-HAp [30].

4.4.1 Elemental analysis

The ICP analyses showed that the Ca/P atomic ratios of HAp-CO and HAp-CP, were 1.65 and 1.64, that is to say very close to the theoretical expected one of 1.67 (Table 4.6). Moreover, the carbon analysis showed that the amounts of C were 0.19 and 0.22 wt.% for HAp-CO and HAp-CP, respectively. These values are significantly higher than the carbon content in HAp-S (0.11 wt.%) showing that the carbonation process occurred.

Moreover, the carbonated groups in HAp-CO are expected to be $CaCO_3$ on the surface, while in HAp-CP carbonation can also be due to the A-type substitution (replacing the -OH groups). Thus, logically, the Ca contents in these catalysts are very close (Table 4.6).

Table 4.6. Chemical compositions of HAp-CO and HAp-CP

Catalyst	**Theoretical Ca/P atomic ratio**	**Experimental Ca/P atomic ratio (ICP)**	**Ca (wt.%)**	**P (wt.%)**	**C (wt.%)**
HAp-CP	1.67	1.64	36.94	17.50	0.22
HAp-CO	1.67	1.65	37.52	17.64	0.19

Further, XRD and IR analyses were also performed to study the crystalline structures of these catalysts and the formation of carbonate.

4.4.2 XRD

The XRD patterns of HAp-CP and HAp-CO are presented in Figure 4.13. For these catalysts, the characteristic peaks of calcium hydroxyapatite (PDF 04-014-8416) were observed (Fig 4.13). Moreover, no peaks assign to other species, such as β-TCP, OCP and DCP, were observed (see details in Section 4.2.1.2). The HAp-CP spectrum showed a lower degree of crystallinity in the range of 2θ = 30-35°, compared to HAp-CO, but the crystalline structure of HAp remained unchanged by adding carbonate as substituents, which is in good agreement with the literature [11, 31].

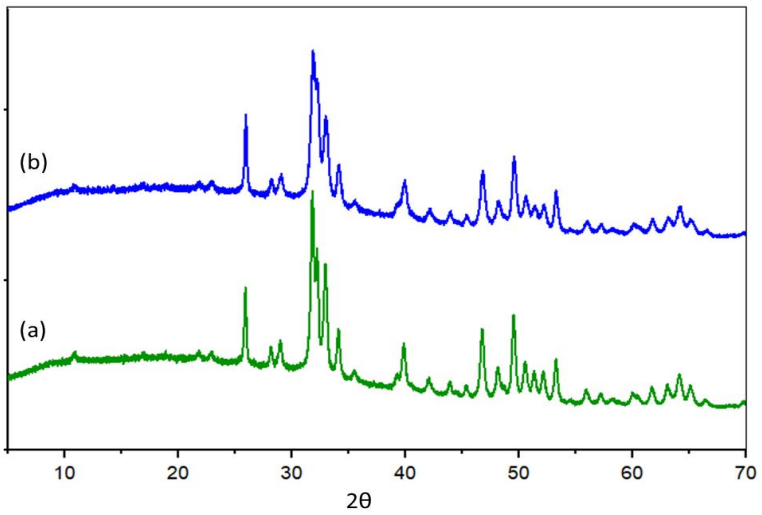

Figure 4.13. XRD patterns of a) HAp-CO and b) HAp-CP.

4.4.3 IR analysis

The chemical bonds of the carbonate groups present in the HAp-CO and HAp-CP structures were further studied by IR analysis. Similarly, as aforementioned in Section 4.2.1.4, the IR spectra confirmed the presence of OH and phosphate groups in these catalysts. Moreover, the intensive bands in the regions of 1370 cm^{-1} and 1580 cm^{-1} indicated the presence of carbonate groups in these catalyst (Figure 4.14).

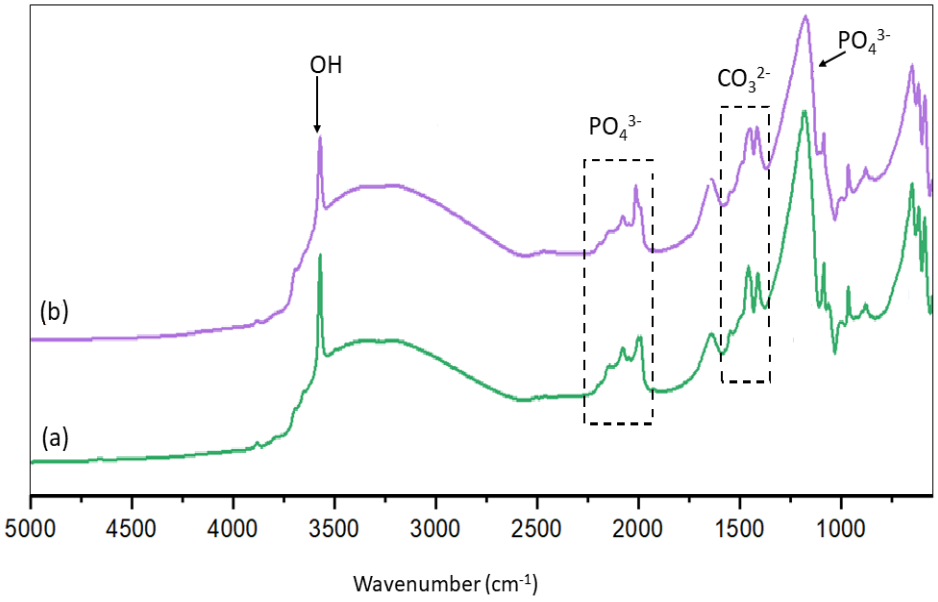

Figure 4.14. IR spectra for a) HAp-CO and b) HAp-CP.

4.4.4 Catalytic performances

The catalytic performances of HAp-CO and HAp-CP, were evaluated at 245 °C in the presence of 0.5 mol.% of catalyst (compared to the number of moles of glycerol) after 8 h of reaction, as shown in Figure 4.15. Surprisingly, the results showed that both HAp-CO and HAp-CP were almost inactive for glycerol polymerization (Fig 4.9).

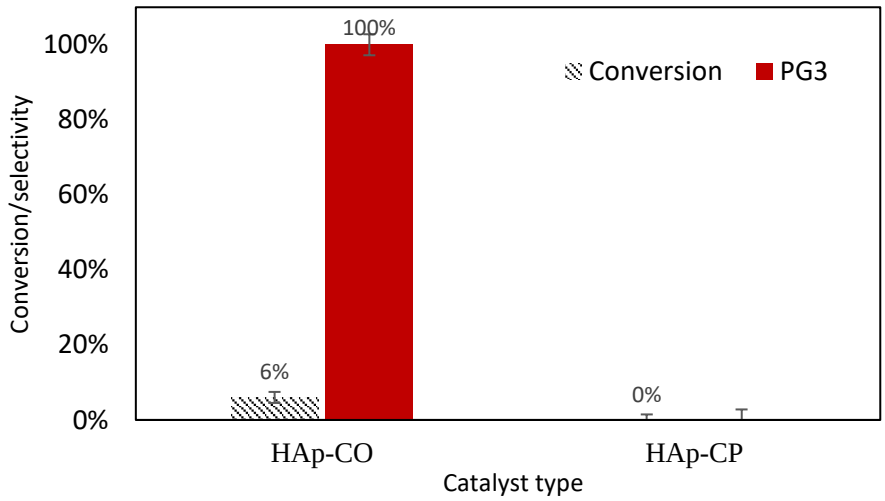

Figure 4.15. Catalytic performances of HAp-CO and HAp-CP after 8 h of reaction at 245 °C.

Since the Ca contents in HAp-CO and HAp-CP are very close (36.94 and 37.52 wt.%, respectively, (Table 4.5)), the loss of catalytic activities for these catalysts must be due to the presence of carbonated groups in their structures (Section 4.3.3). It seems that Ca active sites are totally blocked when transformed by the carbonatation process.

Finally, the catalytic results obtained so far showed that among several HAp-based catalysts, the most promising one is HAp-S, both in terms of selectivity to PG3 and stability (Ca leaching). Hence, hereafter, we have studied the recycling of this catalyst.

4.5 HAp-S recycling tests

The catalytic performances of the spent catalyst obtained from HAp-S were assessed by their reutilization in the same reaction conditions. Here, the spent catalyst was regenerated by washing with two different solvents: 1) water (sample further labelled HAp-W) or 2) ethanol (sample further labelled HAp-Et) (see details in Chapter 2).

For HAp-Et, the catalytic results showed that the recovered catalyst from the 1st run, HAp-Et-1, had a glycerol conversion of 15% with a 100% selectivity to PG3, similar to the fresh HAp-S catalyst used in the same reaction conditions. Moreover, the spent catalysts, HAp-Et-1 and HAp-Et-2, were successfully used in the 2nd and 3rd run reactions, without any loss in activity (Figure 4.16).

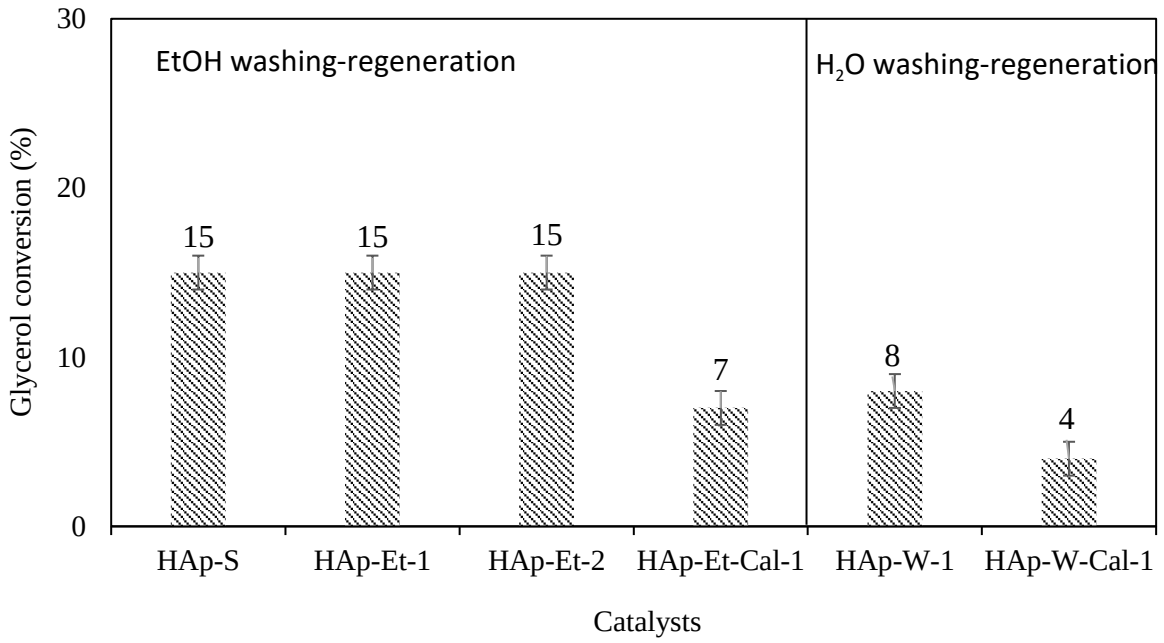

Figure 4.16. Catalytic activity of fresh and recovered HAp-S catalysts washed by EtOH or H_2O, after 8 h of reaction in the presence of 0.5 mol.% of catalyst compared to the number of moles of glycerol at 245 °C.

Moreover, surprisingly, when the HAp-Et-1 was recalcined at 700 °C, prior to the 2nd run reaction, the glycerol conversion decreased from 15 to 7%. Despite the fact that recalcination of spent catalysts were carried out under static air, it probably caused a change in HAp stoichiometry. This could happen by the formation of carbonate groups due to the presence of CO_2 in the oven's atmosphere.

Unlike HAp-Et-1, the spent catalyst washed with water (HAp-W-1) showed a much lower glycerol conversion of 8% compared to HAp-S (15% of conversion) (Figure 4.16). In this case, the decrease in catalytic performance could be due to the formation of hydrated layer on the catalyst surface. Moreover, when the recovered catalyst was recalcined at 700 °C for 4 h, prior to the reaction (HAp-W-Cal-1), it showed a lower performance than HAp-W-1 (4% *vs.* 8%). Hence, similar to HAp-Et-Cal-1, the catalyst recalcination caused deactivation.

Therefore, to understand the deactivation phenomenon, further characterization of spent catalysts was needed, which will be further discussed.

4.5.1 Characterization of the spent catalysts

4.5.1.1 BET surface areas and carbon analysis

For the spent catalyst washed by EtOH (HAp-Et), the BET analyses showed a decrease in the surface area for HAp-Et-1 (36.6 m^2/g) and HAp-Et-2 (38 m^2/g) compared to HAp-S (73.68 m^2/g). The C contents increased for HAp-Et-1 (1.96 wt.%) and HAp-Et-2 (2.38 wt.%) compared to HAp-S (0.11 wt.%), as presented in Table 4.7.

Table 4.7. Specific surface areas and carbon compositions of fresh HAp-S and spent catalysts.

Name	**BET** **Specific surface area (m^2/g)**	**C** **(wt.%)**
HAp-S	73.6	0.11
HAp-W-1	38.3	2.13
HAp-Et-1	36.6	1.96
HAp-Et-2	38	2.38
HAp-Et-Cal-1	60	0.37

These results suggest that a carbon deposition (probably coming from PGs and glycerol) occurs on the catalyst surface during the reaction which caused a significant decrease in the specific surface areas of the recovered catalysts. However, it had no effect on the catalyst performances. Moreover, the recalcination of the catalyst partially removed the C in HAp-Et-Cal-1, as expected.

The higher amount of carbon in HAp-W-1 compared to HAp-Et-1 (2.13 wt.% *vs* 1.96 wt.%) confirmed that regenerating catalyst by ethanol was more efficient than with water.

4.5.1.2 XRD

The XRD patterns of HAp-Et and HAp-W are presented in Figure 4.15. For these catalysts, the characteristic peaks of calcium hydroxyapatite (PDF 04-014-8416) were observed (Fig 4.15). The XRD results revealed that crystalline structure of recovered HAps, including HAp-Et-1, HAp-W-1 and HAp-Et-Cal-1, remained unchanged after reaction and washing or calcination.

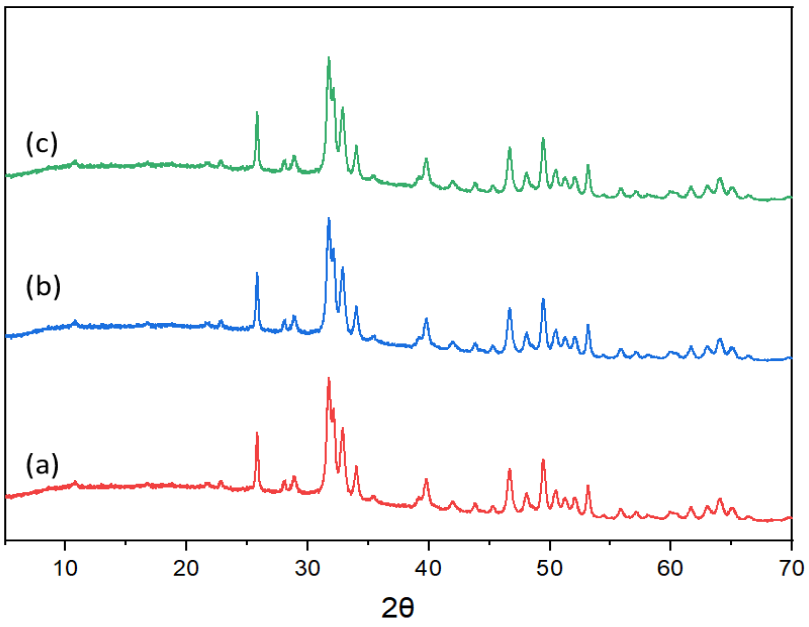

Figure 4.17 XRD patterns of a) HAp-Et-1, b) HAp-W-1 and c) HAp-Et-Cal-1.

Further, these catalysts were also analysed by IR to study the carbon bonds present in the spent catalysts.

4.5.1.3 IR

The IR spectra of spent catalysts, including HAp-Et-1, HAp-W-1, HAp-W-Cal-1 are shown in Fig 4.16 b-d. Similarly to HAp-S (Fig 4.16a), the peaks assigned to OH^-, to phosphate groups and to carbonate groups (between 1377 cm^{-1} and 1580 cm^{-1}) were observed for all the recovered HAps (see Section 4.2.1.4). However, the intensity of the peaks at 1413 cm^{-1}, 1456 cm^{-1} (A and B-type) attributed to carbonate significantly increased, for the spent catalysts compared to HAp-S, in the following orders: HAp-S << HAp-Et-1< HAp-W-1< HAp-W-Cal-1.

Besides, two peaks observed at 2880 cm^{-1} and 2940 cm^{-1} (Fig 4.16 b,c) were attributed to the C-H bonds in spent HAps. C-H bonds were detected because of the presence of glycerol and/or PGs in the samples. This assumption is supported by the fact that these peaks disappeared after recalcination of the spent catalyst (HAp-Et-Cal-1) (Fig 4.16d).

Furthermore, the peak at 3400 cm^{-1} (3000-3500 cm^{-1}), attributed to H_2O became more intense for non-calcined spent catalysts, (HAp-Et-Cal-1<< HAp-Et-1< HAp-W-1), which suggests that the catalysts became hydrated during reaction. As water is formed by the polymerization reaction this observation is logical.

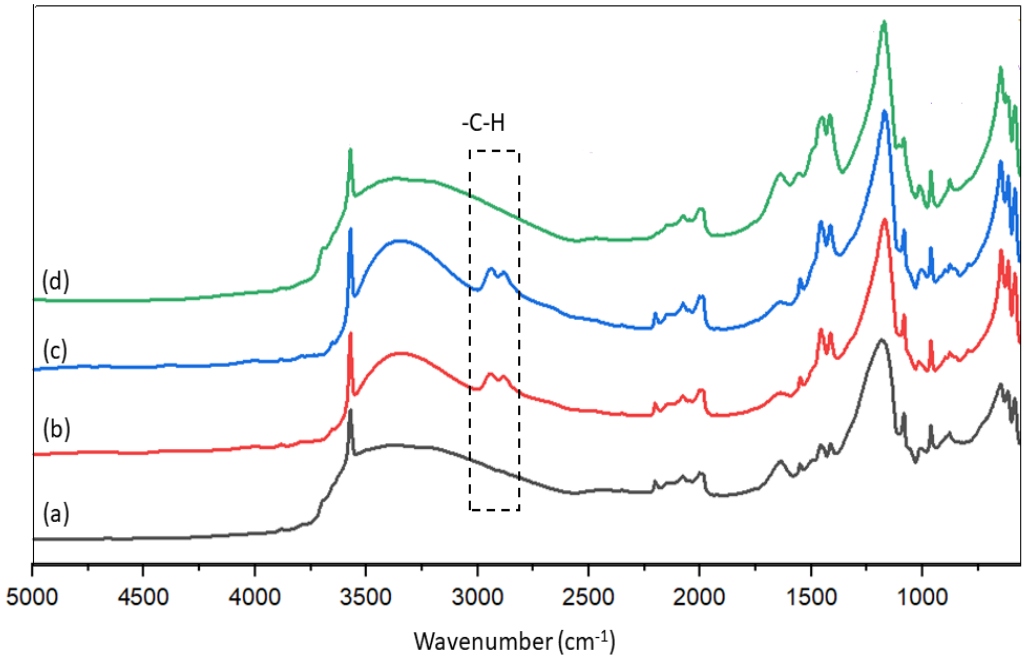

Figure 4.18. IR patterns for a) fresh HAp-S, and b) HAp-Et-1, c) HAp-W-1, and d) HAp-Et-Cal-1 spent catalysts.

4.5.2 Conclusion

The results of the recycling experiments showed that the spent catalyst washed by EtOH (HAp-Et) was successfully reused 3 times with a constant glycerol conversion of 15% (100% selectivity to PG3). In contrast, HAp-W washed with water lost half of its activity when reused for a 2nd run of reaction (7% *vs*. 15%). This suggests that the catalyst is deactivated upon hydration.

Furthermore, the IR and C analyses confirmed that the catalysts after reaction became carbonized by formation of CO_3^{2-} and -CH groups. In addition, IR and C analyses showed that the -CH groups are removed after recalcination of catalyst (HAp-Et-Cal-1).

The catalytic tests showed that the -CH groups had no effect on the catalytic activity when regenerated catalysts were reused without any further thermal treatment. On the contrary, -CH groups could convert to CO_3^{2-} under calcination treatment then leading to the decrease of the catalyst activity.

4.6 Deactivation mechanisms

Herein, based on the results of the catalytic tests and catalyst characterization study, we propose some mechanisms for the HAps deactivation.

In brief, the HAps can be deactivated due to the following reasons:

i. Physical deposition of glycerol and/or reaction products/polymers on their surface;
ii. Interaction of H_2O with Ca^{2+} on the surface;
iii. Chemisorption of glycerol and/or PGs on catalytic sites.

These three hypotheses were examined by performing supplementary experiments.

4.6.1 Physical deactivation

As aforementioned in Section 4.2.2, HAp-D and HAp-S were deactivated after 8 h of reaction. Here, we assumed that the formed PGs can poison the catalyst surface by physical interaction with the catalyst. This hypothesis was examined by performing a reaction with HAp-S as the catalyst in the presence of 3 wt.% of a PG3 standard. In this case, no glycerol conversion was observed. This result proved that the catalyst's surface was poisoned by PGs (as illustrated in Scheme 4.1).

However, when the spent catalyst was regenerated by EtOH, the PGs layer was washed out and the catalyst recovered its activity (see Section 4.5.1).

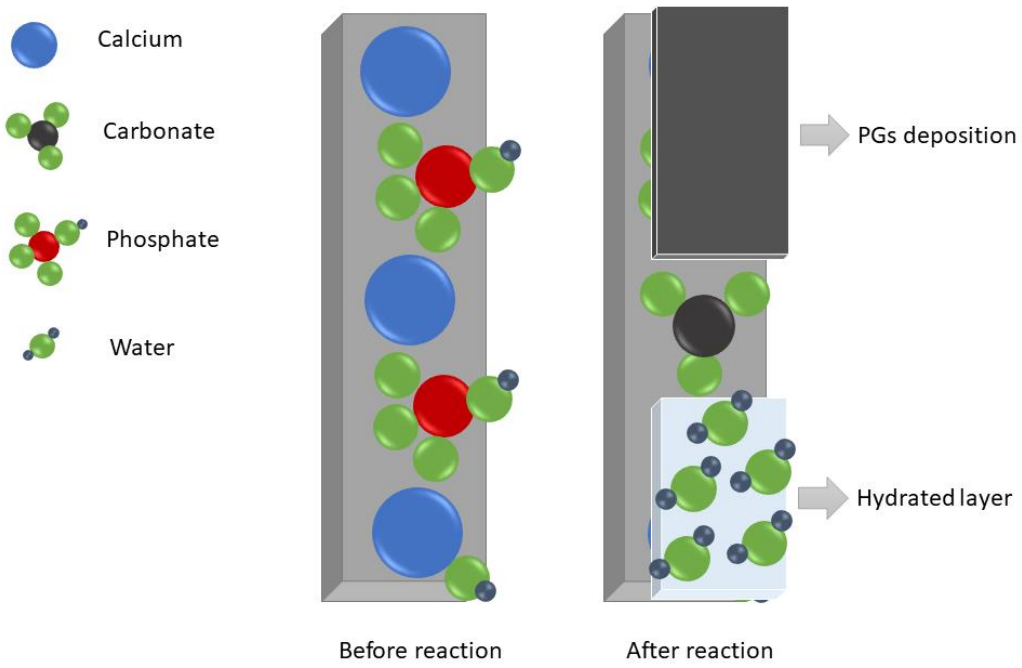

Scheme 4.1. Schematic of the surface of HAp before reaction (left) and after reaction upon poisoning by PGs layer, water layer and carbonate substitution (right).

4.6.2 Water deactivation

This hypothesis of water deactivation was assessed by performing a reaction in the presence of 0.5 wt.% of extra water in the reaction medium. The results revealed that the catalytic activity dropped to 5% of glycerol conversion (*vs.* 15%). Moreover, when H_2O was used to regenerate the spent catalyst (see Section 4.5), the catalyst's surface became more hydrated, as shown by the IR analysis (Fig 4.18), which consequently caused a drop in the activity.

Thus, H_2O can strongly interact with Ca^{2+} ions and form a hydrated layer on the surface including inside the porous network. This phenomena has already been reported in the literature [32–35].

4.6.3 Deactivation by chemisorption

In addition to physical deactivations, the catalyst can be also deactivated by chemisorption of glycerol/ PGs. In fact, the carbonation probably changed the Ca nature through $CaCO_3$ formation. As aforementioned in Chapter 3, $CaCO_3$ had a low conversion compare to other catalysts (see Section 3.2 of Chapter 3). Thus, that could happen for the same reason.

For instance, the lower catalytic performances of carbonated catalysts, HAp-CO and HAp-CP, compared to HAp-S, where they had similar Ca/P ratios measured by ICP, proved that the carbonatation caused deactivation.

Moreover, the -CH bonds on the spent catalysts (Fig 4.18 b-c) can also deactivate the catalysts upon the conversion to carbonate during calcination ($CaCO_3$ formation). For instance, the catalytic performances of HAp-Et decreased when it was recalcined under static air (HAp-Et-Cal), where -CH bonds were removed after thermal treatment and converted to CO_3^{2-}. This phenomenon was confirmed in IR analysis (Fig 4.16 d), where the intensity of carbonate peaks was increased by removing the -CH peaks.

4.7 Main conclusions

In this chapter, several Ca-based catalysts, classified in three groups, were assessed for glycerol polymerization:

a) Ca-based HAp
b) A deficient hydroxyapatite (HAp-D) loaded with different amounts of CaO: *x* wt.% CaO/HAps
c) Carbonated HAps

In the first group, HAp-D, HAp-S and HAp-R, with different theoretical Ca/P ratios were studied. These catalysts were characterized by XRD, IR, XPS, TGA-DSC and ICP-OES. The elemental analysis showed that HAp-D and HAp-S had close Ca/P ratios of 1.62 and 1.66, respectively, while HAp-R had a higher Ca/P ratio of 1.78. XRD analysis confirmed that these catalysts had the crystallized structure of Ca hydroxyapatite, despite the difference in their theoretical Ca/P ratios. Furthermore, the XPS analysis showed that the Ca/P ratios on the surface of the catalysts were lower than those in the bulk (measured by ICP) meaning that less Ca was exposed at the surface of the catalysts.

Furthermore, IR analysis brought a new insight on the structures of the HAps. It confirmed the presence of CO_3^{2-} and HPO_4^{2-}, besides, PO_4^{3-} and OH^- groups in their structure. The intensity of the carbonate groups peaks were in a good agreement with carbon analysis, and were ranked as follows: HAp-R (0.8 wt.%) >> HAp-S (0.111 wt.%) ~ HAp-D (0.108 wt.%).

Further, the catalytic tests showed that HAp-D and HAp-S exhibited similar performances, 15% of glycerol conversion with a total selectivity to PG3 (100%) at 245 °C after 8 h of reaction. HAp-R also exhibited a good selectivity to linear PG2-PG3 (88%) at 27% of glycerol conversion in the same conditions.

The same catalytic performances of HAp-D and HAp-S can be explained by their similar atomic Ca/P ratio, as observed by ICP and XPS characterizations. Higher catalytic activity of HAp-R was explained by a higher atomic Ca/P ratio than HAp-S and the higher quantity of Ca leached into the

reaction medium (homogeneous contribution).

In the 2nd group of catalysts, HAp-D used as a support was enriched by loading CaO on its surface. First, the catalysts were characterized by XRD and ICP-OES. The XRD results confirmed the presence of CaO in 10 and 30 wt.% CaO/HAp, which was in a good agreement with ICP results. ICP results also proved that 5, 10 and 30 wt.% CaO/HAp had higher Ca/P ratios of 1.74, 1.94 and 2.97, respectively, compared to the HAp-D support (1.62).

Then, the catalytic results showed that similar glycerol conversions were obtained in the presence of 5, 10 and 30 wt.% CaO/HAp, under the same reaction conditions, while the selectivity to PG2-3 decreased with the increase in the Ca concentration. Moreover, the ICP analysis for the reaction media, confirmed that Ca actually leached into the reaction media, where it can cause a simultaneous homogeneous catalysis. However, 5 wt.% CaO/HAp, for which the amount of leached Ca was the lowest, exhibited the best selectivity toward PG2-PG3 (67%) of the CaO/HAps catalysts series. Most importantly the catalyst stability improved by loading a small amount of CaO on the HAp.

For HAp-CO and HAp-CP carbonated HAps, 6% and 0% of glycerol conversion were obtained, respectively. The XRD spectra for these catalysts confirmed the formation of Ca-hydroxyapatite. This was in an agreement with ICP analysis, which showed the atomic Ca/P ratios of 1.65 and 1.64 for HAp-CO and HAp-CP, respectively. Moreover, the IR analysis confirmed the presence of carbonate bonds in HAp-CO and HAp-CP structures. We thus assumed that the decrease in the catalytic activities of carbonated catalysts is due to the carbonate formation (mostly in $CaCO_3$ form), which led to deactivation of catalyst. As also similarly observed in Chapter 3, where $CaCO_3$ showed a lower catalytic activity compered to CaO (Table 3.1)

Further, based on our results, we proposed and examined three mechanisms that could explain the catalyst deactivation:

i) Physical deposition of PGs, *ii)* water deactivation and *iii)* chemisorption of polymers on catalytic sites.

Finally, the results suggested that HAps were mostly deactivated by the presence PGs and water during the PG reactions.

Thus, it can be concluded that among the HAp-based catalysts discussed in this chapter, HAp-S, HAp-D and rich HAps, including HAp-R and 5 wt.% CaO/HAp, are the most promising solid catalysts for the glycerol polymerization reaction, in respect to their high stability and high selectivity to PG2-PG3 (Table 4.8). Actually, carbonated HAps lost their activity through carbonization and 10 and 30 wt.% CaO/HAp were found unstable because of an important Ca leaching in the reaction medium.

Table 4.8. Glycerol conversion, PG2-PG3 selectivity and percentages of leached calcium when 0.5 mol.% of catalysts is used at 245 °C for 8 h.

Catalyst	Conversion (%)	PG2-3 Selectivity (%)	Ca leaching (%)
HAp-S	15	100	0.5
HAp-D	15	100	1.8
HAp-R	27	88	3.4
5 wt.% CaO/HAp	23	67	3.2

References

[1] Chinglenthoiba, C.; Das, A.; Vandana, S. Enhanced Biodiesel Production from Waste Cooking Palm Oil, with NaOH-Loaded Calcined Fish Bones as the Catalyst. *Environ. Sci. Pollut. Res.*, **2020**, *27* (13), 15925–15930. https://doi.org/10.1007/s11356-020-08249-7.

[2] Farooq, M.; Ramli, A.; Naeem, A. Biodiesel Production from Low FFA Waste Cooking Oil Using Heterogeneous Catalyst Derived from Chicken Bones. *Renew. Energy*, **2015**, *76*, 362–368. https://doi.org/10.1016/j.renene.2014.11.042.

[3] Gupta, J.; Agarwal, M.; Dalai, A. K. Marble Slurry Derived Hydroxyapatite as Heterogeneous Catalyst for Biodiesel Production from Soybean Oil. *Can. J. Chem. Eng.*, **2018**, *96* (9), 1873–1880. https://doi.org/10.1002/cjce.23167.

[4] Yan, B.; Zhang, Y.; Chen, G.; Shan, R.; Ma, W.; Liu, C. The Utilization of Hydroxyapatite-Supported CaO-CeO2 Catalyst for Biodiesel Production. *Energy Convers. Manag.*, **2016**, *130*, 156–164. https://doi.org/10.1016/j.enconman.2016.10.052.

[5] Wei, G.; Ma, P. X. Structure and Properties of Nano-Hydroxyapatite/Polymer Composite Scaffolds for Bone Tissue Engineering. *Biomaterials*, **2004**, *25* (19), 4749–4757. https://doi.org/10.1016/j.biomaterials.2003.12.005.

[6] Ibrahim, M.; Labaki, M.; Giraudon, J.-M.; Lamonier, J.-F. Hydroxyapatite, a Multifunctional Material for Air, Water and Soil Pollution Control: A Review. *J. Hazard. Mater.*, **2020**, *383*, 121139. https://doi.org/10.1016/j.jhazmat.2019.121139.

[7] Li, X.; Sun, L.; Zou, W.; Cao, P.; Chen, Z.; Tang, C.; Dong, L. Efficient Conversion of Bio-Lactic Acid to 2,3-Pentanedione on Cesium-Doped Hydroxyapatite Catalysts with Balanced Acid-Base Sites. *ChemCatChem*, **2017**, *9* (24), 4621–4627. https://doi.org/10.1002/cctc.201701332.

[8] Matsumura, Y.; Moffat, J. Catalytic Oxidative Coupling of Methane Over Hydroxyapatite Modified with Lead. *Catal. Lett.*, **1993**, *17* (3–4), 197–204. https://doi.org/10.1007/BF00766142.

[9] Silvester, L.; Lamonier, J.-F.; Lamonier, C.; Capron, M.; Vannier, R.-N.; Mamede, A.-S.; Dumeignil, F. Guerbet Reaction over Strontium-Substituted Hydroxyapatite Catalysts Prepared at

Various (Ca+Sr)/P Ratios. *ChemCatChem*, **2017**, *9* (12), 2250–2261. https://doi.org/10.1002/cctc.201601480.

[10] Ajish, P.; Alex, X. Removal of Protein Aggregates from Biopharmaceutical Preparations Using Calcium Phosphate Salts. WO2011156073A1, December 15, 2011.

[11] Fihri, A.; Len, C.; Varma, R. S.; Solhy, A. Hydroxyapatite: A Review of Syntheses, Structure and Applications in Heterogeneous Catalysis. *Coord. Chem. Rev.*, **2017**, *347*, 48–76. https://doi.org/10.1016/j.ccr.2017.06.009.

[12] Zilm, M. E.; Chen, L.; Sharma, V.; McDannald, A.; Jain, M.; Ramprasad, R.; Wei, M. Hydroxyapatite Substituted by Transition Metals: Experiment and Theory. *Phys. Chem. Chem. Phys.*, **2016**, *18* (24), 16457–16465. https://doi.org/10.1039/C6CP00474A.

[13] Raynaud, S.; Champion, E.; Bernache-Assollant, D.; Thomas, P. Calcium Phosphate Apatites with Variable Ca/P Atomic Ratio I. Synthesis, Characterisation and Thermal Stability of Powders. *Biomaterials*, **2002**, *23* (4), 1065–1072. https://doi.org/10.1016/S0142-9612(01)00218-6.

[14] Diallo-Garcia, S. Hydroxyapatites, Un Système Basique Atypique Modulable Par La Synthèse : Vers l'identification Des Sites Actifs. Phd thesis, Université Pierre-et-Marie-Curie, 2012.

[15] Ruiz-Aguilar, C.; Olivares-Pinto, U.; Aguilar-Reyes, E. A.; López-Juárez, R.; Alfonso, I. Characterization of β-Tricalcium Phosphate Powders Synthesized by Sol–Gel and Mechanosynthesis. *Bol. Soc. Esp. Cerámica Vidr.*, **2018**, *57* (5), 213–220. https://doi.org/10.1016/j.bsecv.2018.04.004.

[16] Kannan, S.; Ventura, J. M. G.; Lemos, A. F.; Barba, A.; Ferreira, J. M. F. Effect of Sodium Addition on the Preparation of Hydroxyapatites and Biphasic Ceramics. *Ceram. Int.*, **2008**, *34* (1), 7–13. https://doi.org/10.1016/j.ceramint.2006.07.007.

[17] Cacciotti, I. Cationic and Anionic Substitutions in Hydroxyapatite. In *Handbook of Bioceramics and Biocomposites*; Antoniac, I. V., Ed.; Springer International Publishing: Cham, 2015; pp 1–68. https://doi.org/10.1007/978-3-319-09230-0_7-1.

[18] Kannan, S.; Ventura, J. M. G.; Ferreira, J. M. F. Synthesis and Thermal Stability of Potassium Substituted Hydroxyapatites and Hydroxyapatite/β-Tricalciumphosphate Mixtures. *Ceram. Int.*, **2007**, *33* (8), 1489–1494. https://doi.org/10.1016/j.ceramint.2006.05.016.

[19] Mohammad, N. F.; Amiruddin, N. L.; Saleh, S. S. M.; Taib, M. A. A.; Nasir, N. F. M. Effect of Swelling Agent on Pore Properties of Mesoporous Carbonated Hydroxyapatite. *J. Phys. Conf. Ser.*, **2019**, *1372*, 012018. https://doi.org/10.1088/1742-6596/1372/1/012018.

[20] Silvester, L.; Lamonier, J.-F.; Vannier, R.-N.; Lamonier, C.; Capron, M.; Mamede, A.-S.; Pourpoint, F.; Gervasini, A.; Dumeignil, F. Structural, Textural and Acid–Base Properties of Carbonate-Containing Hydroxyapatites. *J Mater Chem A*, **2014**, *2* (29), 11073–11090. https://doi.org/10.1039/C4TA01628A.

[21] Von Euw, S.; Wang, Y.; Laurent, G.; Drouet, C.; Babonneau, F.; Nassif, N.; Azaïs, T. Bone Mineral: New Insights into Its Chemical Composition. *Sci. Rep.*, **2019**, *9* (1), 8456. https://doi.org/10.1038/s41598-019-44620-6.

[22] Wu, S.-C.; Hsu, H.-C.; Hsu, S.-K.; Tseng, C.-P.; Ho, W.-F. Effects of Calcination on Synthesis of Hydroxyapatite Derived from Oyster Shell Powders. *J. Aust. Ceram. Soc.*, **2019**, *55* (4), 1051–1058. https://doi.org/10.1007/s41779-019-00317-7.

[23] CHAPTER 1. Biological Apatites in Bone and Teeth. In *Nanoscience & Nanotechnology Series*; Royal Society of Chemistry: Cambridge, 2015; pp 1–29. https://doi.org/10.1039/9781782622550-00001.

[24] Resende, N. S.; Nele, M.; Salim, V. M. M. Effects of Anion Substitution on the Acid Properties of Hydroxyapatite. *Thermochim. Acta*, **2006**, *451* (1–2), 16–21. https://doi.org/10.1016/j.tca.2006.08.012.

[25] Silvester, L. Synthesis of Higher Alcohols from Ethanol over Hydroxyapatite-Based Catalysts, Lille University, 2013.

[26] Koutsopoulos, S. Synthesis and Characterization of Hydroxyapatite Crystals: A Review Study on the Analytical Methods. *J. Biomed. Mater. Res.*, **2002**, *62* (4), 600–612. https://doi.org/10.1002/jbm.10280.

[27] Miller, D. J.; Biesinger, M. C.; McIntyre, N. S. Interactions of CO2 and CO at Fractional Atmosphere Pressures with Iron and Iron Oxide Surfaces: One Possible Mechanism for Surface Contamination? *Surf. Interface Anal.*, **2002**, *33* (4), 299–305. https://doi.org/10.1002/sia.1188.

[28] Gomes, G. C.; Borghi, F. F.; Ospina, R. O.; López, E. O.; Borges, F. O.; Mello, A. Nd:YAG (532 Nm) Pulsed Laser Deposition Produces Crystalline Hydroxyapatite Thin Coatings at Room Temperature. *Surf. Coat. Technol.*, **2017**, *329*, 174–183. https://doi.org/10.1016/j.surfcoat.2017.09.008.

[29] Sheikh, L.; Tripathy, S.; Nayar, S. Biomimetic Matrix Mediated Room Temperature Synthesis and Characterization of Nano-Hydroxyapatite towards Targeted Drug Delivery. *RSC Adv.*, **2016**, *6* (67), 62556–62571. https://doi.org/10.1039/C6RA06759J.

[30] Nowicki, D. A.; Skakle, J. M. S.; Gibson, I. R. Faster Synthesis of A-Type Carbonated Hydroxyapatite Powders Prepared by High-Temperature Reaction. *Adv. Powder Technol.*, **2020**, *31* (8), 3318–3327. https://doi.org/10.1016/j.apt.2020.06.022.

[31] Madupalli, H.; Pavan, B.; Tecklenburg, M. M. J. Carbonate Substitution in the Mineral Component of Bone: Discriminating the Structural Changes, Simultaneously Imposed by Carbonate in A and B Sites of Apatite. *J. Solid State Chem.*, **2017**, *255*, 27–35. https://doi.org/10.1016/j.jssc.2017.07.025.

[32] Bolis, V.; Busco, C.; Martra, G.; Bertinetti, L.; Sakhno, Y.; Ugliengo, P.; Chiatti, F.; Corno, M.; Roveri, N. Coordination Chemistry of Ca Sites at the Surface of Nanosized Hydroxyapatite: Interaction with H_2O and CO. *Philos. Trans. R. Soc. Math. Phys. Eng. Sci.*, **2012**, *370* (1963), 1313–1336. https://doi.org/10.1098/rsta.2011.0273.

[33] Prakash, M.; Lemaire, T.; Caruel, M.; Lewerenz, M.; de Leeuw, N. H.; Di Tommaso, D.; Naili, S. Anisotropic Diffusion of Water Molecules in Hydroxyapatite Nanopores. *Phys. Chem. Miner.*, **2017**, *44* (7), 509–519. https://doi.org/10.1007/s00269-017-0878-1.

[34] Corno, M.; Rimola, A.; Bolis, V.; Ugliengo, P. Hydroxyapatite as a Key Biomaterial: Quantum-Mechanical Simulation of Its Surfaces in Interaction with Biomolecules. *Phys. Chem. Chem. Phys.*, **2010**, *12* (24), 6309. https://doi.org/10.1039/c002146f.

[35] Tanaka, H.; Chikazawa, M.; Kandori, K.; Ishikawa, T. Influence of Thermal Treatment on the Structure of Calcium Hydroxyapatite. *Phys. Chem. Chem. Phys.*, **2000**, *2* (11), 2647–2650. https://doi.org/10.1039/b001877p.

Chapter 5

General conclusions and perspectives

The main purpose of this PhD was to develop heterogeneous catalytic systems for direct polymerization of glycerol to obtain selectively PG2-PG3 or PG4+. Based on the literature review, alkaline earth oxides, particularly Ca-based catalysts, such as CaO and $Ca(OH)_2$, were identified as the most promising catalysts for glycerol polymerization reactions, due to their low cost, wide availability, absence of toxicity, high catalytic activity and high selectivity, either to PG2 and PG3, at low temperature (230 °C), or to PG4+ at higher temperatures (> 245 °C).

However, a key issue identified for these catalysts is their stability, i.e. their partial or total dissolution in the liquid medium under reaction conditions (namely, high temperature >230 °C, medium rich in glycerol and presence of water formed by the condensation reactions) transforming them into homogeneous catalysts which is not what is aimed at in this work.

Furthermore, a huge gap in knowledge exists in the PGs analysis. In fact, the most commonly used methods to analyse PGs so far was gas chromatography (GC), which is only able to detect PGs up to PG4 and not any cyclic PGs (even if there are smaller than PG4). Therefore, in the previous literature on that subject, most of the time the missing fraction of products were assumed to be cyclic PGs, while it could also have been polymers higher than PG4 (PG4+). Hence, this issue in the PGs analysis could have led to an underestimation of the polymerization degrees which have been previously reported in the literature.

Based on these critical points, we have attempted in this thesis to *i)* develop a selective heterogeneous catalyst to yield PG4+; *ii)* develop a stable and selective heterogeneous catalyst to yield PG2-PG3 and *iii)* find a reliable analytical technique to analyse the mixtures of PGs obtained after reaction.

In the first step, the catalytic performances of Ca diglyceroxide (CaDG) were compared to those of CaO, $Ca(OH)_2$ and $CaCO_3$, as typical Ca-based catalysts reported in the literature. Our results revealed that the catalytic performances of CaO, $Ca(OH)_2$ and CaDG were similar, in the same reaction conditions. These results strongly suggested an *in situ* formation of an identical active phase. Actually, characterizing the spent catalysts we showed that CaG was the real active phase formed *in situ* from CaO, $Ca(OH)_2$ and CaDG, playing the role of precursors. Furthermore, we explained the *in situ* formation of CaG by two proposed mechanisms: *i)* Dissolution-precipitation-crystallization for CaG formation, starting from CaO and $Ca(OH)_2$; and *ii)* CaDG formation and its further thermal decomposition to CaG. Based on these mechanisms, CaG could form directly from CaO and $Ca(OH)_2$ or by previous formation of CaDG followed by its decomposition to CaG. More importantly, the study the mechanism of CaG formation helped us to better understand the mechanism of glycerol polymerization when the CaG is the active phase.

However, although CaG was the active phase for the glycerol polymerization reaction, it became

totally homogeneous in the reaction medium during the first few hours of the reaction. CaDG showed a higher *stability* (i.e. a higher insolubility) compared to CaG under the same reaction conditions. This high stability of CaDG was expected, according to the proposed mechanism for CaG formation. Thus, CaDG was selected as a potential solid stable catalyst for further experiments.

It was found that temperature has a huge influence on the catalytic activity of CaDG. The glycerol conversion and selectivity to PG4+ were both increased by increasing the temperate from 230 °C to 260 °C, confirming that the reaction has an high activation energy. However, high temperature (260°C) also caused the formation of cyclic PGs and consequently led to the coloration of the reaction mixture (yellowish to brown), which is not desirable for PGs' applications. The parameters that affect the cyclization and coloration were further investigated to obtain the best conditions where the catalyst has a high activity and the reaction mixture are preferably colourless.

Taking into account all these points, CaDG proved to have the best catalytic performances toward higher PGs with 77% selectivity to PG4+ (at 35% glycerol conversion), at 245 °C in presence of 3.5 mol. % of catalyst. However, under these conditions, 65% of CaDG was solubilized after 8 h of reaction. Thus, it can be concluded that despite its high catalytic activity and selectivity to PG4+, its stability under the reaction conditions is still an unsolved issue, as we targeted a purely heterogenous catalyst in this project.

In another part of this work, HAp-based catalysts including HAp-S, HAp-R and 5 wt.% CaO/HAp were shown to have a very high selectivity to PG2-3 and also a higher insolubility compared to CaDG. When 0.5 mol.% of HAp-S and HAp-R were used as catalyst at 245 °C, only 0.5 % and 3.4 % of Ca were leached to the medium, respectively, while 100 % of Ca leached to the reaction medium when CaDG was used under the same reaction conditions. Thus, it can be concluded that HAp-based catalysts have generally a higher stability than CaG-based catalysts in the same reaction conditions.

In addition, HAp-S showed very interestingly a total selectivity to PG3 (100%, at 15% glycerol conversion) at 245 °C when 0.5 mol.% of this catalyst was used for 8 h of reaction time. Unfortunately, the HAp-S was finally deactivated due to the presence of PGs and water in the reaction mixture. Therefore, improving the operating conditions is crucial to avoid the HAp deactivation and improving its activity. Further, the study the mechanism of PG3 formation on the HAp-S can bring a new insight to better control the PG formation on this kind of heterogenous catalysts.

HAp-R and 5 wt.% CaO/HAp, as Ca-rich HAps, showed a glycerol conversion of 27 % and 23% with a good selectivity to PG2-3 (88% and 67%), respectively. More interestingly, our results revealed that loading CaO on the HAp, significantly decrease the amount of Ca leaching. Thus, tuning the amount of Ca in the Ca-rich HAp and also the synthesis protocol could probably improve the catalyst's activity, stability and PGs selectivity as well.

Another important part of this work was to find a reliable analytical technique that is able to detect all the PGs formed (including non-cyclic and cyclic ones). Among the advanced analytical techniques tested in this PhD, direct infusion ESI-MS was found to be the best. However, there are still a few obstacles to overpass to be able to perform a real complete quantification of all the products present in the reaction medium. For instance, glycerol is not detected and pure polyglycerols standards are needed to do the calibration.

For the continuation of the project, it would also be important to find a suitable separation method of the used catalyst after reaction. Indeed, one challenge of using an heterogenous catalyst for glycerol polymerization reaction, is its separation from a highly viscous solventless reaction mixture. This implies the dilution of the reaction mixture by 10 to 20 times with a solvent (generally ethanol) followed by centrifugation. Obviously, the PGs' recovery can be performed by a method such as vacuum evaporation for instance but it is not energy- and time-efficient and it also would bring the question of the advantage of using an heterogenous catalyst (i.e., the ease of the separation of the catalyst from the medium where the reaction occurs).

Improving the stability of CaGs (CaG and CaDG), as selective catalysts to PG4+ would be important. Hence, in future studies, it could be tried to support CaGs on HAp to increase the stability of the active phase while keeping its high selectivity to PG4+.

Moreover, in order to get an easier separation of the catalyst from the medium, "ceramic-hydroxyapatite" in the form of pellets could be tested. It could then hugely ease the recovery of the catalyst after use. Therefore, synthetizing ceramic-HAp, characterizing and testing them, including their stability, under glycerol polymerization reaction would be of high interest.

Annex A

A.1 HPLC-RI

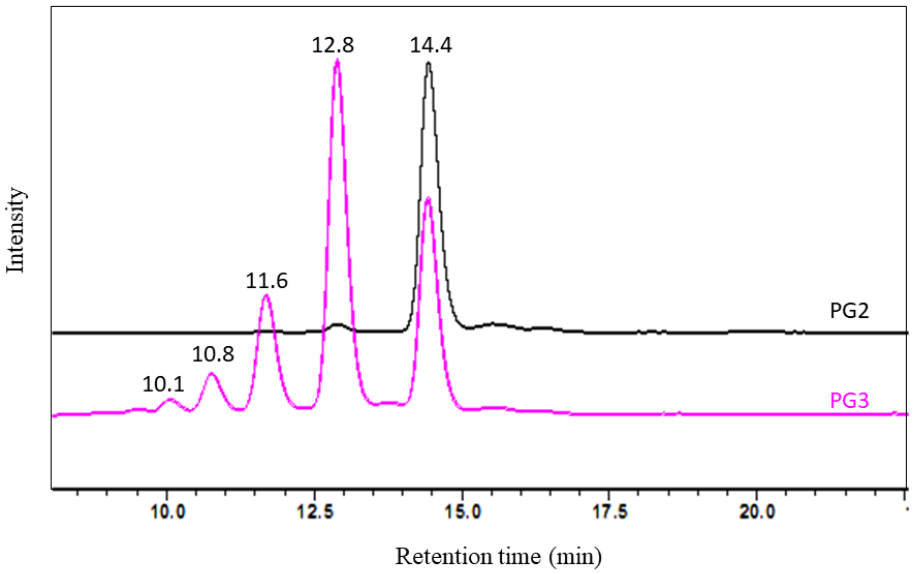

Figure A.1.PG2 (black) and PG3 (pink) standards HPLC-RI chromatograms obtained using a Bio-Rad Aminex column.

A.2 Direct infusion ESI-MS

Herein, we studied the parameters including solvent type, cone voltage and additives that could have an influence on the ESI analysis before analysing the PGs standards composition.

A.2.1 Solvent effects

Solvent properties such as volatility, surface tension, viscosity, conductivity, ionic strength, dielectric constant, electrolyte concentration and pH could affect the ESI process by altering the charge state distribution of the analytes [1]. Among the possible solvents, H_2O, methanol and acetonitrile are the most widely used ones in ESI. H_2O and MeOH have low dielectric constants, which lead to better sensitivity, and MeOH has higher volatility resulting on higher ion intensity. However, each solvent or combination of them and their effects on the ESI process also depend on the analyte properties [1]. While our results revealed that the samples diluted in a mixture of MeOH : H_2O (1:1 v:v) and ACN : H_2O (1:1 v:v) had similar ion intensity peaks for PGs, considering the high solubility of polyglycerols in these solvents we decided to choose MeOH : H_2O (1:1 v:v) solution, due to its volatility. Therefore, all the samples were diluted in a MeOH : H_2O (1:1 v:v) solution prior to analysis.

A.2.2 Effect of cone voltage

Typical cone voltage parameters for ESI is in the region of 10 to 60 V [2]. Herein, cone voltages of 20, 60 and 120 V were applied for PG6. As shown in Figure A.3., at cone voltages of 20 and 60 V, the major PG detected in the PG6 sample is actually PG6, while an increase in cone voltage to 120 V changed the main detected polyglycerol to PG9 (Fig A.2-c). This increase in the apparent PG degree of polymerization was also reported for PG6 and PG10, previously [2] when the cone voltage from 80 to 100 V was increased. This could be explained by the fact that the cone voltage reduces the incidence of ion clusters. Thus, in a high cone voltage such as 120 V, ion clusters have more internal energy and they are prone to aggregate in large clusters. Therefore, further analyses were performed at a cone voltage of 60 V.

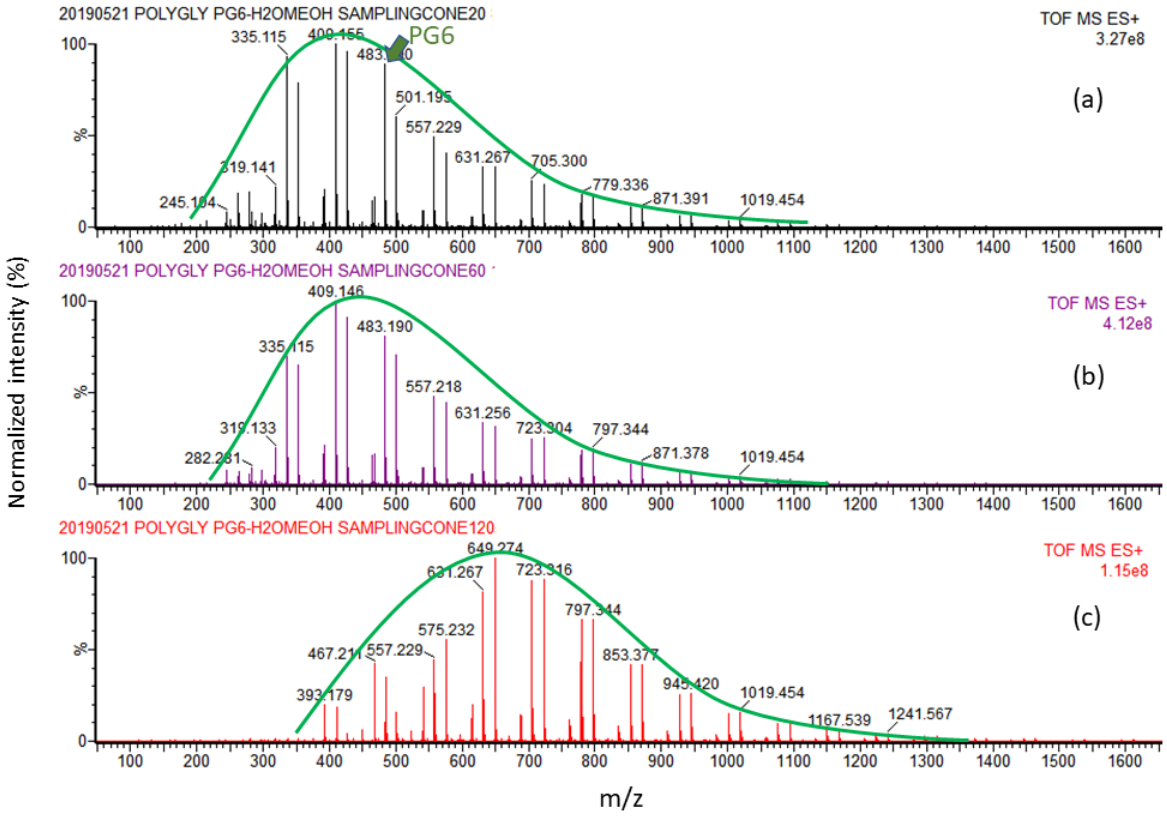

Figure A.2. PG6 distribution with cone voltage of a) 20V, b) 60V and c) 120 V.

A.2.3 Adduct ions and additives

Another important parameter is the use of additives that can cause the formation of adducts. Crowther *et al*. [2] reported that the most stable adduct ions for polyglycerols were formed with Li^+ and Na^+ (highest total ion current) while adducts ions with H^+, K^+, Rb^+ and Cs^+ had lower ion intensity and therefore formed relatively unstable adduct ions. Besides, the formation of NH_4^+ was reported by addition of ammonium acetate, ammonia and methylamine as additives to the solvent [3]. The size of the molecules and their polarity can also affect the formation of adduct ion by certain cation. For instance, small oligomer like diglycerols are hardly observed with K^+, Rb^+ and Cs^+[2].

However, among these adduct ions, we identified that $[M+H]^+$ and $[M+Na]^+$ are the most common forms of ions in ESI-MS, even without addition of additives to the solvent. These ions could arise from impurities (even from HPLC grade or glassware and sample vials) [1, 3]. In general, there is no rule for adduct formation. For example, Ma and Kim [4] suggested the suppression of Na adduct formation by adding 0.1 mol% of additives such as acetic acid and formic acid (as a source of protons) in analysing steroids, while we observed intense peaks of $[M+Na]^+$ even by adding formic acid.

So far, it can be concluded that type of solvent and addition of acid to promote protonation had no significant affect on the PGs analyses by ESI-MS. While the higher cone voltage of 120 V caused an overestimation of the polymerization degree. Thus, to have a reproducible analysis, the same conditions were applied for analysing the samples: 1:1 v:v of MeOH : H_2O as solvent, sampling cone voltage of 60 V and no addition of additives.

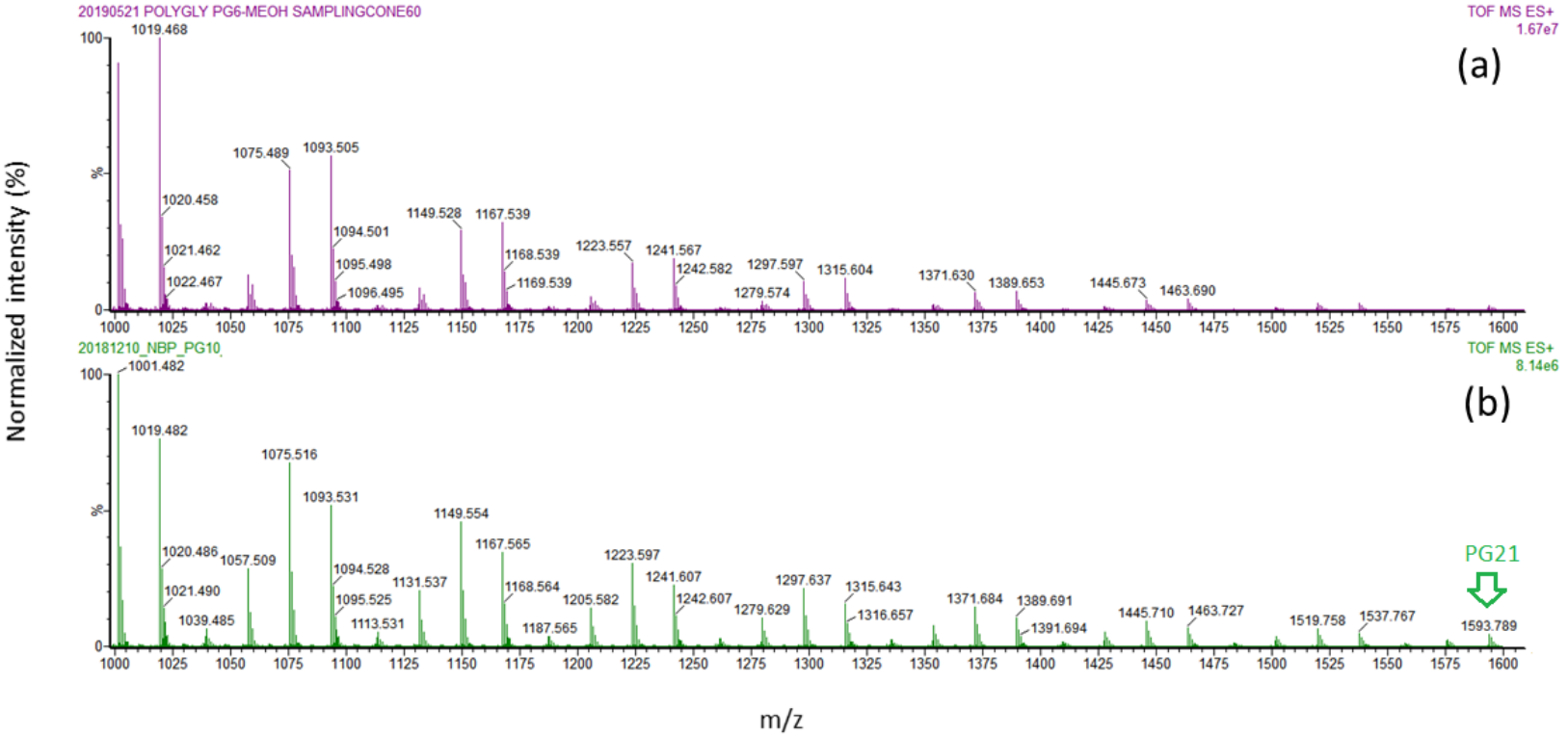

Figure A.3. ESI-MS spectra for a) PG6 and b) PG10 standards, focused on the area from 1000 to 1600 Da.

Annex A

Table A.1.Exact masses of linear, cyclic and bicyclic PG1 to PG14 and of their most common adducts ions (in g/mol (Da)).

	Linear				Cyclic				Bicyclic		
	Exact Mass	$(M+2H)^{2+}$	$(M+Na)^{+}$	$(M+K)^{+}$	*Exact Mass*	$(M+2H)^{2+}$	$(M+Na)^{+}$	$(M+K)^{+}$	*Exact Mass*	$(M+2H)^{2+}$	$(M+Na)^{+}$
Glycerol	92.09	47.04	115.07		-	-	-		-	-	-
PG2	166.08	84.04	189.06	205.17	148.06	75.03	171.04	187.15	130.05	66.02	153.03
PG3	240.12	121.06	263.10	279.21	222.10	112.05	245.08	261.19	204.09	103.04	227.07
PG4	314.15	158.07	337.13	353.24	296.14	149.07	319.12	335.23	278.12	140.06	301.10
PG5	388.19	195.09	411.17	427.28	370.18	186.09	393.16	409.26	352.16	177.08	375.14
PG6	462.23	232.11	485.21	501.32	444.21	223.10	467.19	483.30	426.20	214.10	449.18
PG7	536.26	269.13	559.24	575.35	518.25	260.12	541.23	557.34	500.23	251.11	523.21
PG8	610.30	306.15	633.28	649.39	592.29	297.14	615.27	631.38	574.27	288.13	597.25
PG9	684.34	343.17	707.32	723.43	666.32	334.16	689.30	705.41	648.31	325.15	671.29
PG10	758.38	380.19	781.36	797.46	740.36	371.18	763.34	779.45	722.34	362.17	745.32
PG11	832.41	417.20	855.39	871.50	814.40	408.20	837.38	853.49	796.38	399.19	819.36
PG12	906.45	454.22	929.43	945.54	888.43	445.21	911.41	927.52	870.42	436.21	893.40
PG13	980.49	491.24	1003.47	1019.58	962.47	482.23	985.45	1001.56	944.46	473.23	967.44
PG14	1054.52	528.26	1077.50	1093.61	1036.51	519.25	1059.49	1075.60	1018.49	510.24	1041.47

A.3 MALDI

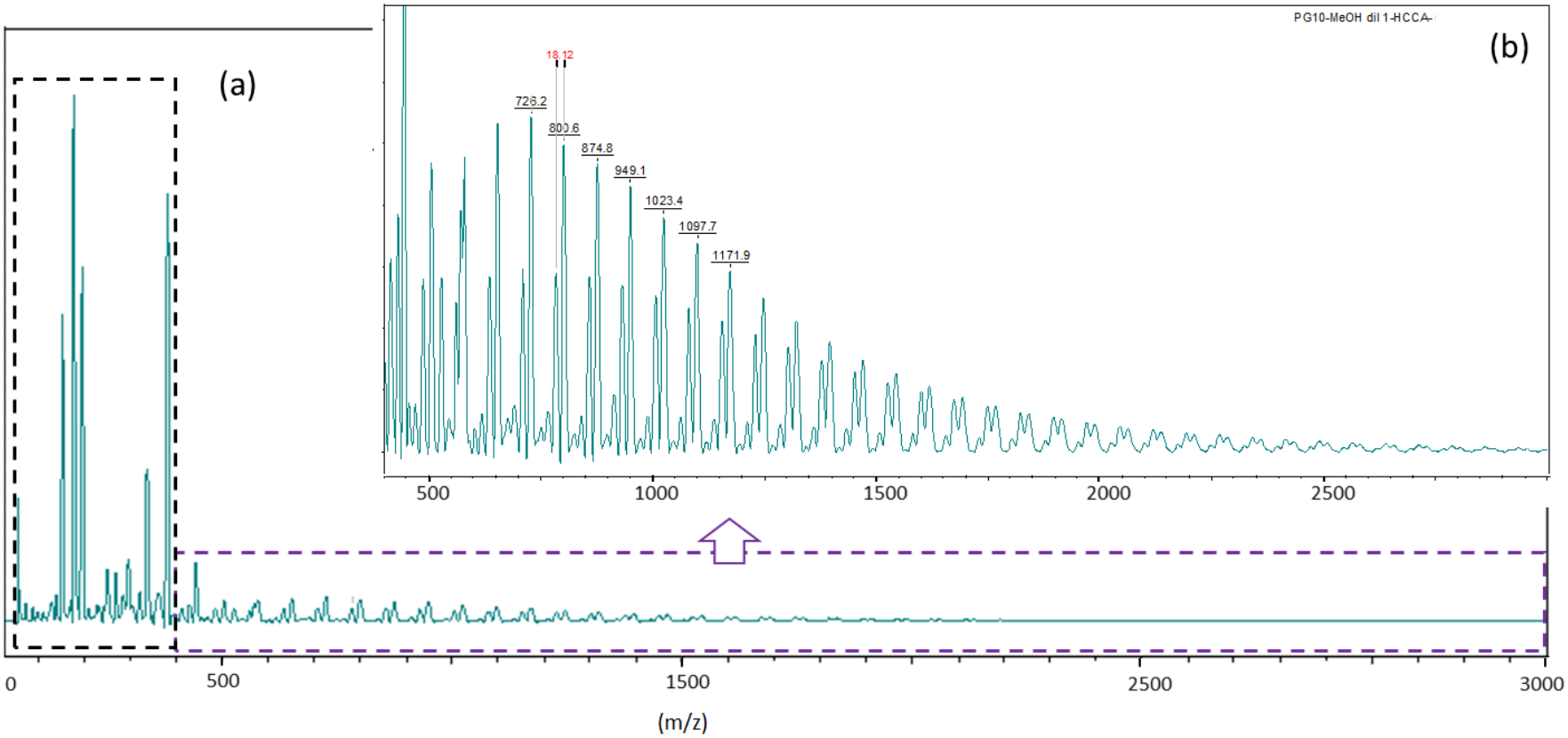

Figure A.4. MALDI spectra for PG10 standard with HCCA as matrix.

A.4 NMR

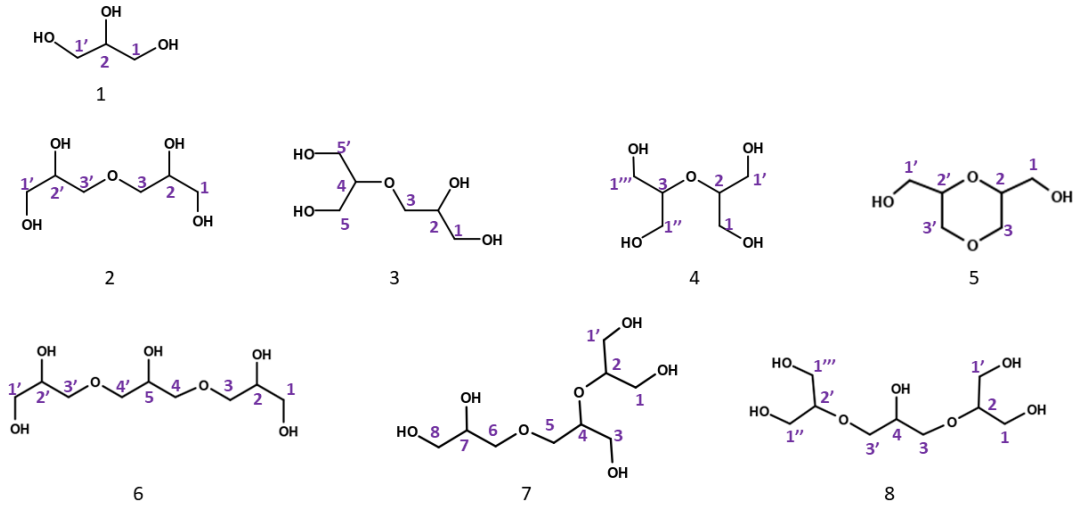

Scheme A.1. Glycerol, diglycerols and triglycerols structures.

Table A.2. ^{13}C NMR chemical shifts of glycerol and PG2, PG3

	-CH_2OH	Chemical shift (ppm)	-CHOH-	Chemical shift (ppm)	-CH_2-O-	Chemical shift (ppm)	-CH-O-	Chemical shift (ppm)
1	C1, C1′	62.7	C2	72.1				
2	C1, C1′	62.7	C2, C2′	70.5-70.9	C3, C3′	72.1		
3	C1 C5, C5′	62.7 60.7	C2	70.5-70.9	C3	70.5-70.9	C4	81.1
4	C1, C1′, C1″, C1‴	60.7					C2, C3	81.1
5	C1, C1′	62.7			C3, C3′	70.5-70.9	C2, C2′	70.5-70.9
6	C1, C1′	62.7	C2, C2′ C5	70.5-70.9 70.5-70.9	C3, C3′, C4, C4′	72.1		
7	C1, C1′ C3, C8	60.7 62.7	C7	70.5-70.9	C5, C6	70.5-72.1	C2, C4	79.4-81.1
8	C1, C1′, C1″, C1‴	60.7	C4	68.9-70			C2, C2′	81.1

References

[1] Kostiainen, R.; Kauppila, T. J. Effect of Eluent on the Ionization Process in Liquid Chromatography–Mass Spectrometry. *J. Chromatogr. A*, **2009**, *1216* (4), 685–699. https://doi.org/10.1016/j.chroma.2008.08.095.

[2] Crowther, M. W.; O'Connell, T. R.; Carter, S. P. Electrospray Mass Spectrometry for Characterizing Polyglycerols and the Effects of Adduct Ion and Cone Voltage. *J. Am. Oil Chem. Soc.*, **1998**, *75* (12), 1867–1876. https://doi.org/10.1007/s11746-998-0343-x.

[3] Kruve, A.; Kaupmees, K. Adduct Formation in ESI/MS by Mobile Phase Additives. *J. Am. Soc. Mass Spectrom.*, **2017**, *28* (5), 887–894. https://doi.org/10.1007/s13361-017-1626-y.

[4] Ma, Y.-C.; Kim, H.-Y. Determination of Steroids by Liquid Chromatography/Mass Spectrometry. *J. Am. Soc. Mass Spectrom.*, **1997**, *8* (9), 1010–1020. https://doi.org/10.1016/S1044-0305(97)00122-0.

Annex B

B.1 ^{13}C SS NMR

With the help of the MestReNova software, the ^{13}C-NMR spectra for the compounds represented on Scheme 3.1 (1-3) were simulated (Figure B.1 (a-c)). Accordingly, 2 peaks were predicted at 65.96 ppm and 65.2 ppm for cyclic CaG (1) corresponding to -CH_2OCa and -CH-OH, respectively (Fig B.1-a). For CaG (2), 3 peaks at 60.7, 66.3, 75.2 ppm corresponding to -CH_2OH, -CH_2-OCa and -CH-OCa, respectively (Fig B.1-b), were predicted. For the linear CaG (3), 3 peaks at 64.17, 68.67, 70.99 ppm corresponding to -CH_2OH, -CH_2-OCa and -CH-OH (Fig B.1-c) were predicted. Obviously, NMR simulation techniques help to get insights on the structures of the molecules by an estimation of the NMR spectrum but is not expected to provide the exact chemical shifts for a given molecule [1].

Thus, we can tentatively assign the peaks observed in the experimental CaG spectrum to the -CH_2OH (67.8 ppm), -CH_2-OCa (70.1 ppm) and -CH-OH (74.8 ppm) carbons in glycerol in CaG (2) and CaG (3), where 3 peaks are predicted for them.

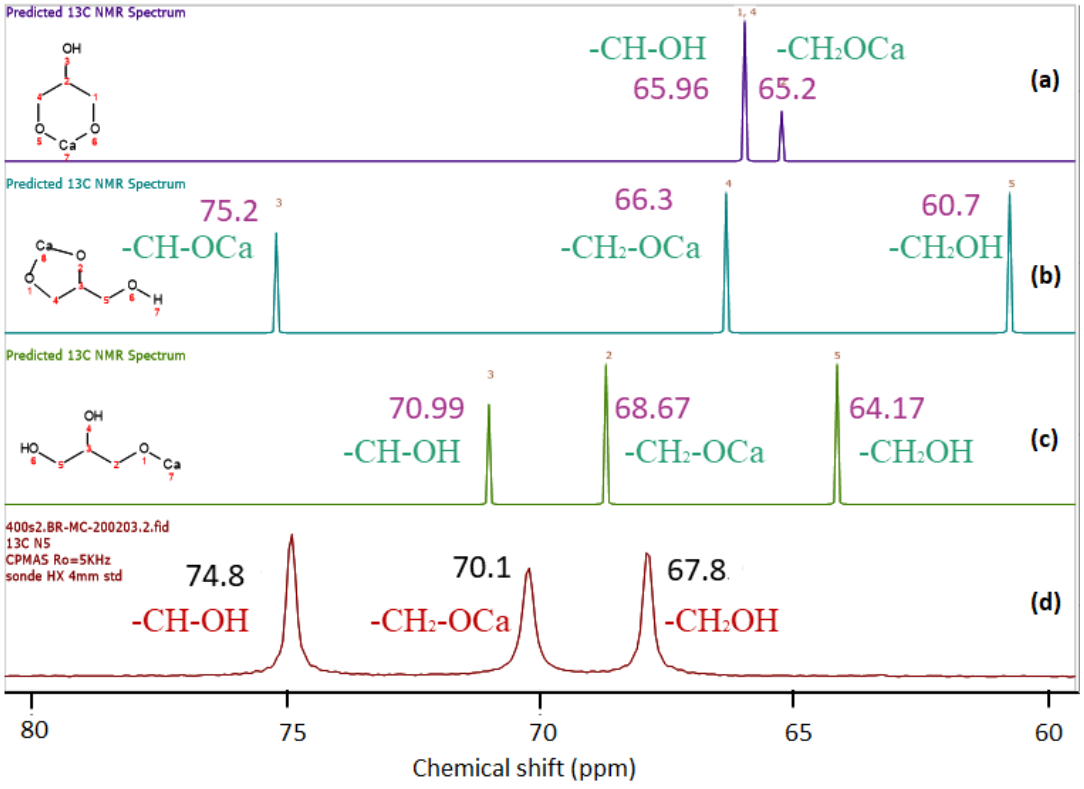

Figure B.1. ^{13}C NMR spectra in the range from 60 to 80 ppm for a) predicted CaG (1), b) predicted CaG (2), predicted CaG (3) and d) spent catalyst from CaO (CaG-O).

Furthermore, for freshly prepared CaDG, six peaks were observed in the ^{13}C NMR spectrum (Figure B.2-d). These peaks are characteristic of carbon atoms in the glycerol backbone in the three different structures of CaDG (Scheme 3.1 (4-6)), like also mentioned in Section 3.3.3 (Chapter 3).

The ^{13}C-NMR spectra for the compounds represented on Scheme 3.1 (4-6) were simulated (Fig B.2 (a-c)), whereby 5 peaks were predicted at 61.3, 63.9, 66.8, 70.5 ppm and 75.1 ppm for CaDG (4) corresponding to -CH_2OH, -CH_2OH, -CH_2-OCa ,-CH-OH and -CH-OCa, respectively (Fig B.2-a). For CaDG (5), 2 peaks were predicted at 61.3 and 75.1 ppm corresponding to -CH_2OH and -CH-OCa, respectively (Fig B.3-b). For the linear CaDG (6), 3 peaks at 63.9, 66.8 and 70.5 ppm corresponding to -CH_2OH, -CH_2-OCa and -CH-OH (Fig B.2-c), respectively, were predicted.

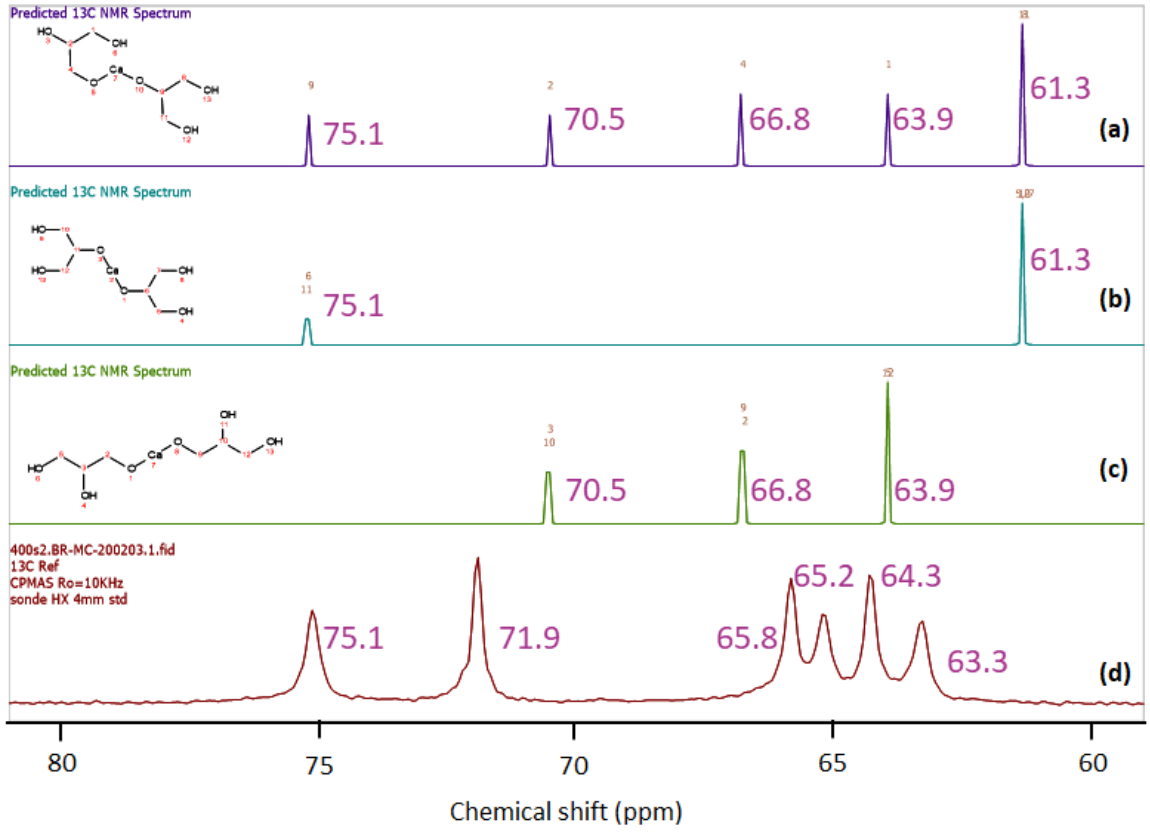

Figure B.2. ^{13}C NMR spectra in the range from 60 to 80 ppm for a) predicted CaDG (4), b) predicted CaDG (5), predicted CaDG (6) and d) freshly prepared CaDG.

B.2 Catalytic performances of CaO

At the beginning of this thesis, we attempted to reproduce the results presented in the literature. We examined the performances of CaO, as a typical Ca-based catalyst reported in the literature, in several operating conditions, including atmosphere, temperature and catalyst concentration. Hereafter, are reported the performances observed using CaO under various reaction conditions.

B.2.1 Atmosphere effect

As previously mentioned in Chapter 1 (Section 1.6.3), the use of an inert gas such as N_2, He or CO_2 during glycerol polymerization reaction has been reported. Thus, here, we examined N_2 and CO_2 as a potential atmosphere for the reaction in the presence of CaO as the catalyst.

Catalytic tests were carried out in the presence of 3.2 mol.% (based on the number of moles of glycerol) freshly calcined CaO in a Parr batch reactor to investigate the effect of the gas atmosphere on the glycerol polymerization. Two reactions were performed at 230 °C under 10 bar of N_2 or CO_2 for 24 h. The results show that the glycerol conversion is significantly lower in the presence of pressurized CO_2 (45%) compared to pressurized N_2 (80%), with a total selectivity to PG2-PG3. This decrease in conversion could be due to the *in situ* formation of $CaCO_3$ from CaO in the presence of CO_2 during the reaction as detected by X-ray diffraction (XRD). The XRD pattern of the catalyst after reaction under CO_2, with sharp peaks at $2\theta \approx 28°$, 36°, 39°, 43° and 49°, confirmed the formation of calcium carbonate (Fig B.3-b). On the contrary, the XRD pattern of the spent CaO after reaction under N_2 exhibited CaG characteristic peaks (Fig B.3-c). Thus, it can be concluded that CO_2 cannot be used as an inert gas for the glycerol polymerization reaction.

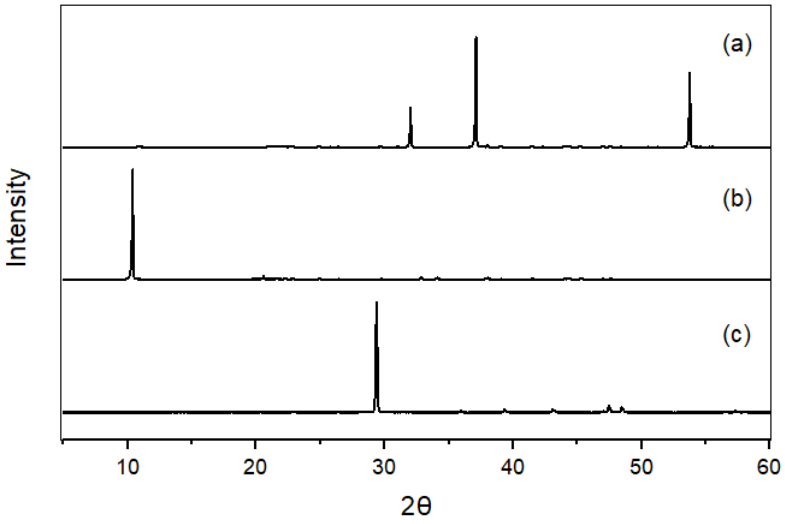

Figure B.3. XRD patterns for a) freshly calcined CaO and spent catalysts after reaction using b) N_2 and c) CO_2.

B.2.2 Design of experiments using CaO as a catalyst

In order to find the best set of standard operating conditions for glycerol polymerization, a design of experiments (DoE) was scheduled. 8 experiments were done using a two-level factorial (2^3) DoE for three parameters: temperature, amount of catalyst and pressure under N_2 atmosphere. The designed experiments and the obtained conversion after 18 h are shown in Table B.1, where A, B and C are the temperature (°C), amount of catalyst (mol.% compared to the number of moles of glycerol) and pressure (bar), respectively; and R_1 (standing for Response 1) is the glycerol conversion (%) and R_2 (Response 2) is the selectivity to PG4+:

Table B.1. Factorial design (2^3) DoE comprising 3 parameters and 2 levels

Run	A Temperature (°C)	B Catalyst Concentration (mol. %)	C Pressure (bar)	R1 Glycerol conversion (%)	R2 Selectivity to PG4+ (%)
1	210	9.6	10	14	0
2	210	3.2	1	3	0
3	240	3.2	1	54	67
4	210	9.6	1	14	0
5	240	3.2	10	68	54
6	240	9.6	10	80	66
7	240	9.6	1	77	78
8	210	3.2	10	4	0

R_1 was considered in a first approach to interpret the DoE results. It revealed that the temperature (A) has, as expected, the most significant effect on glycerol conversion, while pressure (C) has the lowest impact (Fig B.4-a). For instance, the glycerol conversion significantly increased from 3% to 54% by an increase of temperature from 210 to 240 °C, in the presence of 3.2 mol.% CaO under atmospheric pressure (Runs 2 and 3 in Table B.1), while, the glycerol conversion only slightly increased (from 54% to 68%) when the reaction took place under 10 bar of N_2 compared to the atmospheric condition at 240 °C in the presence of 3.2 mol.% catalyst (Runs 3 and (in Table B.1).

The catalyst concentration has a positive effect on glycerol conversion (Fig B.4-a), but does not have a significant impact on the second response R_2 (PG4+ selectivities) as shown in Fig B.4-b. Moreover, as shown in Figure B.4-c, the highest conversion was obtained, as expected, at the highest temperature and using the highest amount of catalyst.

Besides, it was obvious from the results, shown in Table B.1 that the catalytic activity of CaO is negligible at low temperature (210 °C), which could be due to the fact that the PG reaction required high activation energy, *i.e.*, higher temperatures. Thus, we decided to consider a higher temperature range (230 to 260 °C) for further experiments. Moreover, despite the fact that an increase in the CaO concentration from 3.2 mol.% to 9.6 mol.% (equal to 6 wt.%) had no significant impact on glycerol conversion, we decided to examine lower ranges for catalysts' amounts (0.5 to 3.5 mol.%) for further experiments.

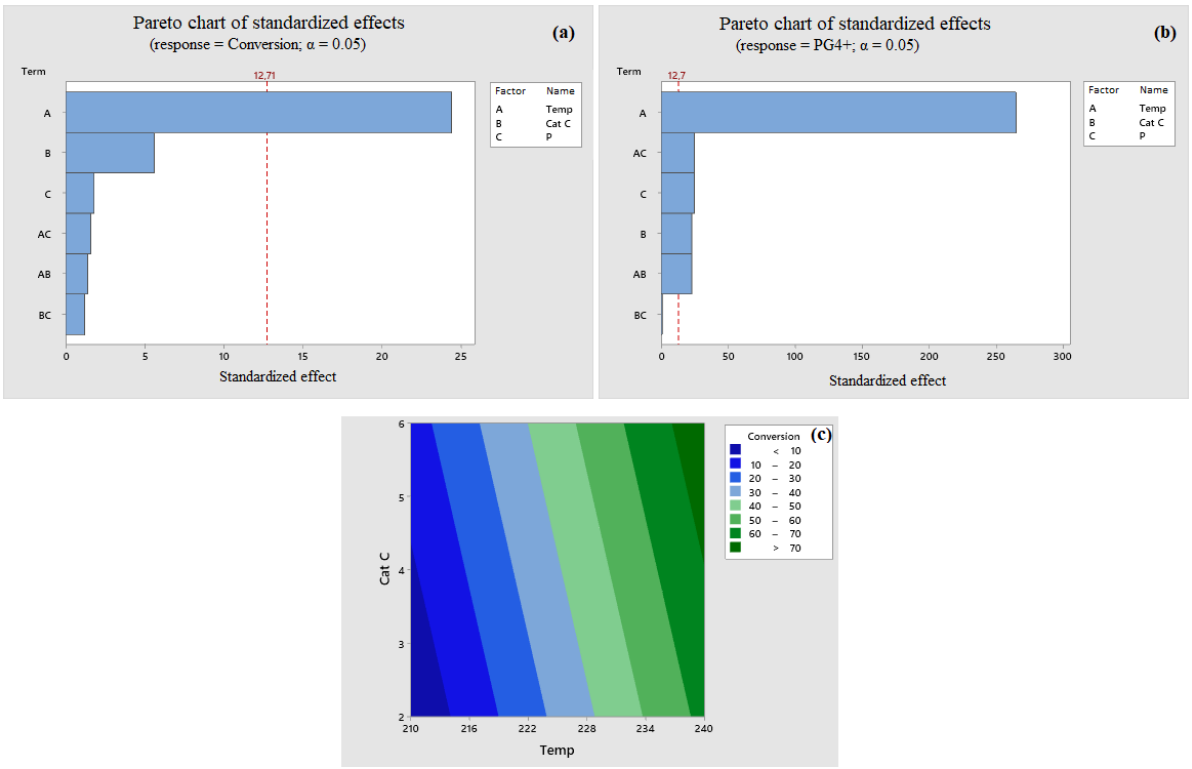

Figure B.4.Pareto chart showing the effect of temperature (°C) (A), amount of catalyst (wt.%) (B) and pressure (bar) (C) on a) R_1: glycerol conversion, b) R_2: PG4+ selectivity and c) effect of temperature and amount of catalyst on conversion.

B.3 Liquid phase ^{13}C NMR

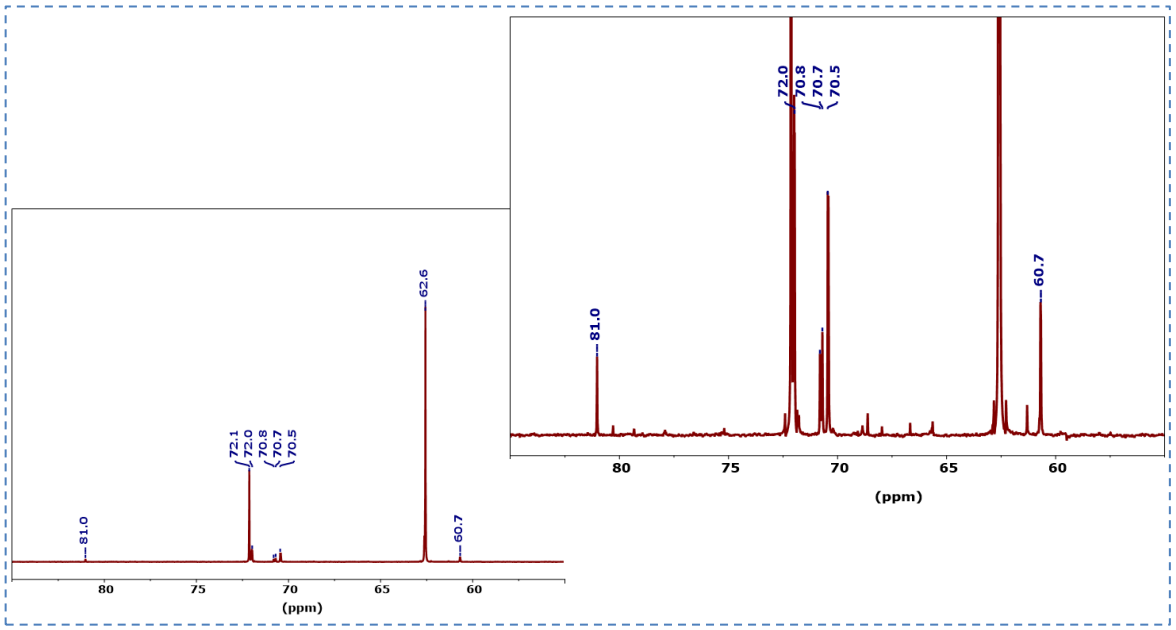

Figure B.5. ^{13}C NMR spectrum of the reaction mixture after 8 h at 230 °C in the presence of 0.5 mol.% CaDG

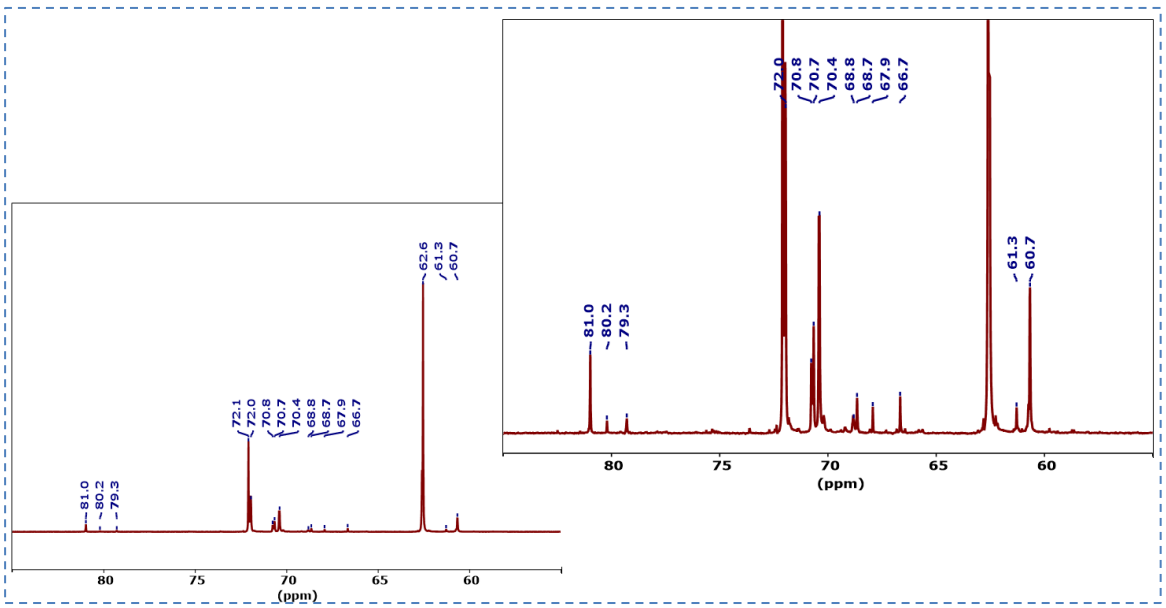

Figure B.6. ^{13}C NMR spectrum of the reaction mixture after 8 h at 245 °C in the presence of 0.5 mol.% CaDG

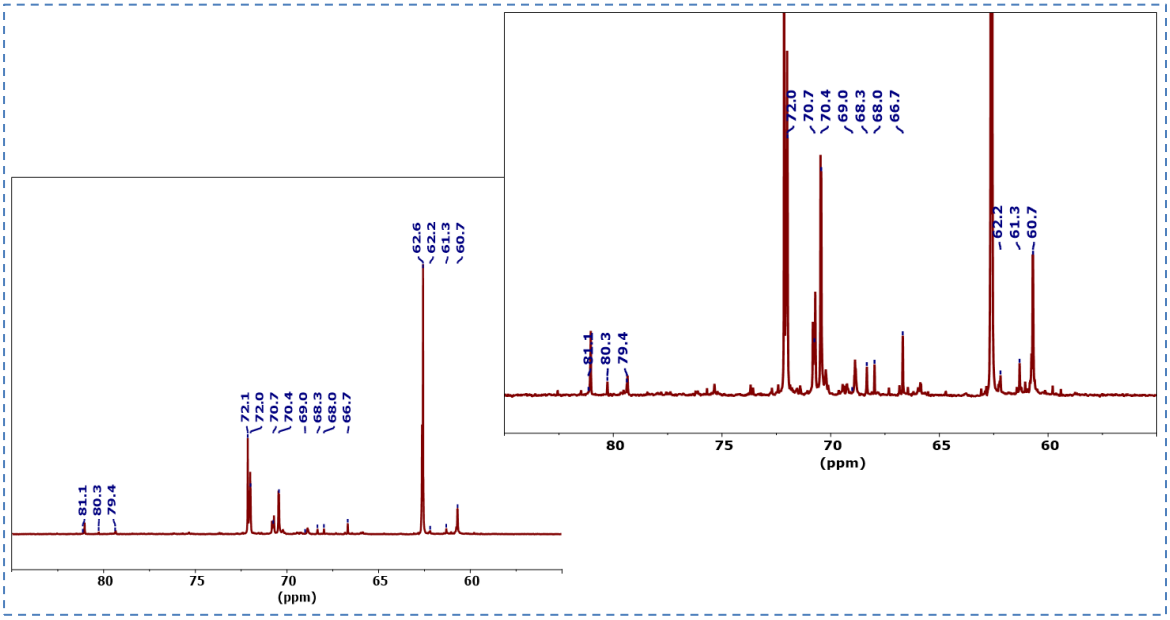

Figure B.7. ^{13}C NMR spectrum of the reaction mixture after 8 h at 260 °C in the presence of 0.5 mol.% CaDG.

The ^{13}C NMR spectra for 3 reaction liquid mixtures obtained at 230 °C (Fig B.5), 245 °C (Fig B.6) and 260 °C (Fig B.7), showed that the chemical shifts of the peaks varied in the range of 60 to 85 ppm, which is in good agreement with PGs standards (Figure A.9). According to Table A.4, the peaks at chemical shifts of 62.6 and 72.1 ppm, are common between glycerol and linear PGs, whereas the signals in the range of 60.7-62.2 ppm, 66.8-72 ppm and 79-81 ppm confirmed the presence of branched and cyclic PGs, but are not distinguishable as discussed previously in Chapter 2. Nevertheless, the increasing intensity of these peaks with the reaction temperature suggested an increase in the polymerization degree.

Reference

[1] Toukach, F. V.; Ananikov, V. P. Recent Advances in Computational Predictions of NMR Parameters for the Structure Elucidation of Carbohydrates: Methods and Limitations. *Chem. Soc. Rev.*, **2013**, *42* (21), 8376–8415. https://doi.org/10.1039/C3CS60073D.

Titre: Développement de systèmes catalytiques à base de Ca pour la polymérisation sélective de glycérol

Les polyglycérols (PGs) sont des polyols biocompatibles hautement fonctionnels présentant de nombreuses applications industrielles. Environ 50 % de la demande concerne le di- et le tri-glycérol (PG2-3), principalement pour les cosmétiques, et les autres 50 % la fraction tétra- à déca-glycérol (PG4-10), principalement pour l'industrie alimentaire. La croissance de la demande en PGs biosourcés incite les chercheurs à développer de nouveaux catalyseurs pour la polymérisation du glycérol. Au cours des deux dernières décennies, une grande attention a été accordée aux systèmes à base de Ca, en raison de leurs bonnes performances catalytiques, de leur grande disponibilité et de l'absence de toxicité. Toutefois, ces catalyseurs présentent jusqu'alors une sélectivité modérée. Un autre problème des catalyseurs hétérogènes, non résolu à ce jour, est lié à leur instabilité due à une dissolution partielle dans le milieu réactionnel. Ainsi, l'objectif de cette thèse est de développer des catalyseurs hétérogènes à base de Ca qui soient stables, hautement actifs pour convertir le glycérol et hautement sélectifs, soit en PG2-3, soit en PG4-10.Nous avons d'abord étudié pour cette réaction le diglycéroxyde de Ca (CaDG), CaO, $Ca(OH)_2$ et $CaCO_3$. Les catalyseurs ont été analysés par DRX, RMN du ^{13}C à l'état solide et ATG-ACD. La DRX a montré la présence, après test, de glycérolate de calcium (CaG) dans les catalyseurs dérivés de CaO, $Ca(OH)_2$ et de CaDG. Ceci a été corroboré par les résultats des analyses ATG-ACD. La RMN du ^{13}C a montré que le CaG est un mélange de ses formes linéaire $Ca(C_3H_7O_3)$ et cyclique ramifiée $Ca(C_3H_6O_3)$. Le CaG est la phase active solide réelle qui est formée *in situ* à partir de CaO, de $Ca(OH)_2$ ou de CaDG, précurseurs du catalyseur. Deux mécanismes de formation de CaG sont proposés : a) dissolution de CaO et de $Ca(OH)_2$, suivie de la formation de CaG et de sa précipitation/cristallisation et b) formation de CaDG et décomposition progressive en CaG. CaDG étant directement converti en CaG et en ion glycéroxyde pendant la réaction, il peut promouvoir la formation des PGs. Ainsi, l'effet sur les performances catalytiques de la température de réaction, la quantité de catalyseur, le temps de réaction et la présence d'eau, a été étudié. Les produits de la réaction ont été analysés par spectrométrie de masse (ESI-MS). Le CaDG a montré la plus grande sélectivité en PG4-10 (84%) à 70% de conversion du glycérol, à 245 °C après 22 h de réaction en présence de 3.5 mol.% de catalyseur. Cependant, l'analyse ICP du milieu réactionnel a montré que 70% du CaDG était alors en phase liquide. Néanmoins, en raison du faible coût, de l'absence de toxicité et de la très haute sélectivité en PG4-10, le CaDG peut être considéré comme un catalyseur prometteur pour la polymérisation du glycérol. Enfin, pour tenter de développer un système sélectif pour la production de PG2-3, des catalyseurs à base d'hydroxyapatite de calcium (HAp) ont été synthétisés, caractérisés et testés. Ils sont divisés en trois groupes : *i)* les HAp déficientes, stochiométriques et riches en Ca, *ii)* les HAp enrichies en CaO (CaO supporté sur HAp) et *iii)* les HAp carbonatées. Tous ces solides ont été caractérisés par DRX, IR, XPS, ATG-ACD et ICP-OES. Parmi eux, l'HAp stochiométrique (rapport Ca/P=1,67) s'est montrée hautement sélective en PG3 (100%) à 15% de conversion du glycérol. De plus, l'HAp riche en Ca (rapport Ca/P=1,78) et le catalyseur à 5 % poids de CaO sur HAp ont également présenté une sélectivité élevée en PG2-3 à 245 °C après 8 h en présence de 0,5 % molaire de catalyseur : 88 % et 67 % (à 27 % et 23 % de conversion), respectivement. Plus important, ces catalyseurs sont très stables dans les conditions de réaction (moins de 5% de lixiviation du Ca). Au contraire, les HAps carbonatées ont une très faible activité. Enfin, nous avons prouvé que les HAps peuvent être désactivées par la présence d'eau et de polymères.

Mots cléfs: Polyglycérol, Polymérisation catalytique, Catalyse hétérogène, Calcium, Glycérol.

Title: Development of Ca-based catalytic systems for the selective polymerization of glycerol

Polyglycerols (PGs) are biocompatible and highly functional polyols with a wide range of applications in many industries. About 50% of the demand in PGs concerns di- and tri-glycerol (PG2-3), mainly for cosmetics, and the other 50% tetra- to deca-glycerol (PG4-10), mainly for food industry.The increase of the demand for bio-based PGs encourages researchers to develop new catalytic systems for glycerol polymerization. In the last two decades, much attention was paid to alkaline earth oxides-based catalysts, particularly Ca-based catalysts, due to their high catalytic performances, their wide availability and the absence of any toxicity. However, Ca-based catalysts showed, up to now, a moderate selectivity to PG2-3 or to PG4-10. Another issue for heterogenous catalytic systems, which is unsolved so far, is their instability due to partial dissolution in the reaction medium. Thus, the purpose of this PhD is to develop Ca-based heterogeneous catalysts which are stable, highly active to convert glycerol and highly selective, either to PG2-3 or to PG4-10. First, we investigated for this reaction calcium diglyceroxide (CaDG) and other Ca-based catalysts including CaO, $Ca(OH)_2$ and $CaCO_3$. The catalysts were analyzed by XRD, solid-state ^{13}C-NMR and TGA-DSC analyses. XRD evidenced the presence of calcium glycerolate (CaG) in the spent catalysts when starting from CaO, $Ca(OH)_2$ and CaDG. This was corroborated by TGA-DSC results. Further, the ^{13}C-NMR results showed that CaG is a mixture of its linear form $Ca(C_3H_7O_3)$ and its cyclic-branched form $Ca(C_3H_6O_3)$. As a main outcome, we showed that CaG is the actual *solid* active phase, which is formed *in situ* from CaO, $Ca(OH)_2$ or CaDG playing the role of catalyst precursors. Two mechanisms for the CaG formation were proposed: *a)* the dissolution of CaO and $Ca(OH)_2$, the formation of CaG and its precipitation followed by crystallization and *b)* the formation of CaDG and its gradual decomposition to CaG. Since CaDG is directly converted to CaG and a glyceroxide ion during the reaction, the effect of operating conditions on the catalytic performances, including the temperature, the amount of CaDG used, the reaction time and the presence of water, was investigated. The reaction products were analysed by electron spray ionization-mass spectrometry (ESI-MS). CaDG showed the highest selectivity to PG4-10 (84%) at a glycerol conversion of 70%, at 245 °C in the presence of 3.5 mol.% of catalyst after 22 h of reaction. However, the ICP analysis of the reaction medium showed that 70 % of CaDG was dissolved in the liquid phase under these conditions. Still, considering the low cost, the absence of any toxicity and the high selectivity to PG4-10 of CaDG, this species is considered as a promising catalyst for glycerol polymerization. To try to develop a selective catalytic system for PG2-3, several calcium hydroxyapatite (HAp)-based catalysts have been synthetized, characterized and tested for glycerol polymerization reaction. These catalysts were divided in three groups; *i)* Ca-based HAps including Ca-deficient, stochiometric and Ca-rich HAps, *ii)* HAp enriched with CaO (CaO supported on HAp) and *iii)* carbonated HAp. The catalysts were characterized by XRD, IR, XPS, TGA-DSC and ICP-OES analyses. Among them the stochiometric HAp with a Ca/P ratio of 1.67 was highly selective to PG3 (100%) at 15% glycerol conversion. Moreover, rich-HAp with a Ca/P ratio of 1.78 and 5wt.% CaO/HAp catalysts also exhibited a high selectivity to PG2-3, 88% (at 27% conversion) and 67 % (at 23% conversion), respectively, at 245 °C after 8 h of reaction in the presence 0.5 mol.% of catalyst. Most importantly, these heterogeneous catalysts were highly stable under reaction conditions as shown by ICP-OES analyses (less than 5 % of Ca leaching). In contrast, the carbonated-HAps showed a very low catalytic activity (below 6% of glycerol conversion). Finally, we proved that HAps can be deactivated by the presence of water and polymers.

Key words: Polyglycerol, catalytic polymerization, Heterogeneous catalysis, Calcium, Glycerol.